-Combination of Advanced Oxidation Processes with biological treatment for the remediation of water polluted with herbicides-

Memòria presentada per na Mª**José Farré Olalla** a l´ Escola de Doctorat i Formació Continuada i al Departament de Química de la Universitat Autònoma de Barcelona, per optar al Grau de Doctora en Química.

Univesitat Autònoma de Barcelona
Bellaterra, June 2007

Dr. José Peral Pérez Professor Titular del Departament Química de la Universitat Autònoma de Barcelona,

CERTIFICO:

Que la Llicenciada en Química MªJosé Farré Olalla ha realitzat la tesis titulada "Combination of Advanced Oxidation Processes with biological treatment for the remediation of water polluted with herbicides" al Departament de Química de la Universitat Autònoma de Barcelona sota la meva direcció per optar al grau de Doctora en Química.

I per que així consti, signo el present certificat a Bellaterra el 13 de abril del 2007.

José Peral Pérez

INDEX

Acknowledgments

This work has been supported by European Commission (CADOX project, EVK1-CT-2002-00122), Spanish Government (MEC, project CTQ2005-02808) and CICYT (project PPQ2002-04060-C02-01). I also want to thank Makhteshim Agan España S.A., Aragonesas Agro S.A and the WWTP from Manresa.

I would like to express gratitude to the Green Chemistry and Photocatalysis group from the Universitat Autònoma de Barcelona for giving me the opportunity to carry out a doctoral project. In particular, I would like to thank my thesis director Dr. José Peral for the supervision, attention and help received. I also want to thank particularly Dr. Xavier Domènech in recognition of his effort to achieve a "sustainable environment" of work in the group, beyond the knowledge and experience shown. In addition, I am grateful to Dr. Stephan Brosillon for accepting and guiding me during my stay at l´ Ecole Nationale Supérieure de Chimie de Rennes. Moreover, I would like to thank Dr. José Antonio Ayllón and Dr. Julián Carrera for their help with the revision of some parts of the final manuscript. Also I thank Dra. Alba Eustaquio for the chromatography lessons received and Albert Guisasola for the respirometry assessment. Last but not least, I owe big thanks to Julia García for her continuous aid, for introducing me to SBR technology and biological analyses as well as, in collaboration with Dr. Ivan Muñoz and Nilbia Ruiz, for their help with the LCA studies presented in this thesis.

I would also express thanks to; Dra. Maribel Franch, David Gutiérrez, Ana Serra, Marc Estruga, Marc Campillo, Dani Calvo, Juan Manuel Ramírez, Xavi Batlle, Neus Vilà, Meritxell Bartés, Nuria Crivillers, Raquel Rios, Noemí Parraga and other colleagues that have been close to me inside this "green world" during these four years for their help, patience and support. A particular thank is to Rosa Calzada for making easier and funnier the bureaucratic stuff.

Finally, a very special "thank you" goes to my family and friends for being there whenever I need them. Among them, I want to especially thank Cristian.

MªJosé

To my parents and my sister. . .

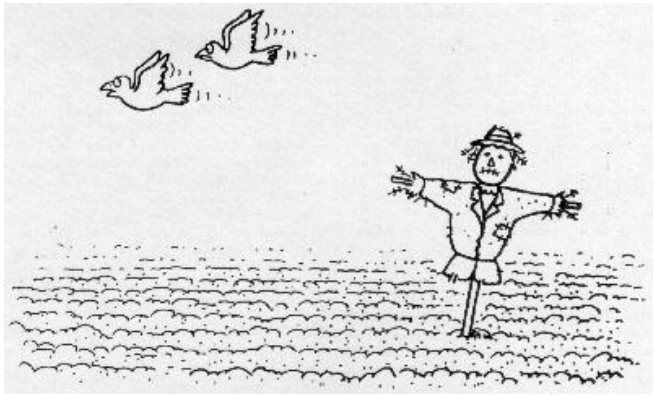

Why do they want the scarecrow if we are scared enough with their herbicides…..

Foreword

Water is an irreplaceable basic principle for life. This natural resource is a factor of subsistence for the human beings as well as a fundamental element for social welfare. Nevertheless, although water is one of the most abundant resources on the planet, still 1100 million people (i.e., 18% of the world's population) have no access to safe drinking water and 2600 million people (i.e., 42% of the world's population) have no access to improved sanitation. The main reason is that 97.5% of the water in the planet is located in the sea; therefore it is excessively salty for direct use as drinking water. 70% of the remaining 2.5%, that is fresh water, is locked in the icecaps and glaciers. 20% is confined to remote areas, and much of the rest arrives at the wrong time and place causing natural disasters. Thus, only less than 1% of the world's fresh water resources are ready for human use.

The problem with regard to the water requirement is not only related to its supply, but also to its demand. Globally, domestic use represents 10% of the world's fresh water ready for human use. This demand is estimated to increase about 50% in the next two decades, mainly due to the predicted growth in the global population from 6500 million today to 7900 million by 2025. Apart from the domestic needs, the local requirement is divided mainly into industrial and agricultural demand. Industrial water use represents 20% of the world's fresh water ready for human use. In this ever-increasing sector, the water cycles are generally open. The industry extracts water from aquifers, from surface water or the public drinking water net and then, after being used for industrial needs, it is discharged as wastewater. On the other hand, water required for agriculture, which corresponds to the highest percentage of world's fresh water ready for human use (i.e., 66%), is increasing even faster. This rise is mainly due to extensive irrigation programmes necessary to fulfil the increasing population's needs and to sustain the industrial agriculture of the "Green Revolution". Apart from that, 4% of the world's fresh water is evaporated directly from reservoirs.

The water quality is the last but not least factor to consider when discussing water shortage. The non-biodegradable anthropogenic pollution discharged in the water systems deteriorates the water quality and, consequently, the removal of pollutants at source is of imminent necessity. Due to all the aspects mentioned, water shortage is one of the most worrying problems for this millennium. *"Reducing by half the proportion of people without*

sustainable access to safe drinking water" as well as *"integrate the principles of sustainable development into country policies and programmes and reverse loss of environmental resources"* are part of the 7th UN millennium development goal.

The unbalanced ratio between water supply and water demand, as well as the water quality deterioration, mean it is important to develop new operating systems that guarantee the optimization of the use of this natural resource. One particular proposition to reach equilibrium is to relieve the water shortage by utilizing regenerated wastewaters. Regenerated wastewater is water that after being used is treated and disinfected for subsequent re-use. As mentioned above, the industry sector uses approximately 20% of the total water ready for human use, most of it is used in cooling, washing or rinsing processes. In those cases, the utilization of regenerated wastewater is highly relevant. Regenerated wastewater can be also an attractive proposition for agricultural water necessities. Both, the industrial and agricultural optimization of water, could contribute to the improvement of the environmental quality as well as to the improvement of public water supply. One example of innovative technology to regenerate wastewater is the so-called Advanced Oxidation Processes (AOP) which can be optimised by combining with biological treatments.

The aim of this work is to bring new insights into the general problem of water quality improvement by finding new ways of treating water polluted with different herbicides. The work has been divided in four chapters: *Introduction, Materials and Methods, Results and Discussion and Concluding Remarks.*

The Introduction reviews and describes the Advanced Oxidation Processes used in this work, the biological treatment, the natural interferences found in wastewater, and some different strategies used to assess the efficiency of the coupling of chemical and biological treatments. In addition, the environmental impacts associated to this strategy have been evaluated by means of Life Cycle Assessment methodology. Thus, a brief introduction to this environmental assessment tool has been also included. The Materials and Methods chapter has been added to the memory in order to facilitate repetition of the methods and guide further work in this field, as well as to allow the reader to understand all the experiments carried out. The Results and Discussion chapter is presented as a compendium of four publications.

Degradation of some biorecalcitrant pesticides by homogeneous and heterogeneous photocatalytic ozonation

Chemosphere 58 (2005) 1127-1133.

Biodegradability of treated aqueous solutions of biorecalcitrant pesticides by means of photocatalytic ozonation

Desalination 211 (2007) 22-33.

Assessment of photo-Fenton and biological treatment coupling for Diuron and Linuron removal from water

Water Research 40 (2006) 2533-2540.

Combined photo-Fenton and biological treatment for Diuron and Linuron removal from water containing humic acid

Journal of Hazardous Materials *in press.*

Two more works accepted for publication are included in Annexe 1.

Evaluation of the intermediates generated during the degradation of Diuron and Linuron herbicides by the photo-Fenton reaction

Accepted for publication in Journal of Photochemistry and Photobiology A: Chemistry.

Life cycle assessment for the removal of Diuron and Linuron herbicides from water using three environmental friendly technologies

Accepted for publication in Environmental Technology.

The theoretical framework, the methods used, as well as the results and conclusions extracted from these works are included in the main body of the thesis.

Annexe 2 includes data not shown in the publications and necessary to demonstrate the quality of the presented results.

Glossary of symbols and abbreviations

A	acceptor molecule; absorbance
AEP	Aquatic Eutrophication Potential
AOP	Advanced Oxidation Process
AP	Acidification Potential
ARD	Abiotic Resource Depletion
ASM 1	Activated Sludge Model nº1
b	energy of Langmuir sorption constant ($L \cdot mg^{-1}$); path length (cm)
BOD	Biochemical Oxygen Demand ($mg \cdot L^{-1}$)
C, c	concentration
C_A	TOC value in the test mixture three hours after the beginning of Zahn-Wellens test ($mg \cdot L^{-1}$)
C_{AB}	TOC value of the blank measured three hours after the beginning of the Zahn-Wellens test ($mg \cdot L^{-1}$)
CAS	Chemical Abstracts Service registry number
C_B	TOC value of the blank at time of sampling in Zahn-Wellens test ($mg \cdot L^{-1}$)
$C_{desorbed}$	TOC concentration corresponding to the blank ($mg \cdot L^{-1}$)
C_e	equilibrium TOC concentration ($mg \cdot L^{-1}$)
COD	Chemical Oxygen Demand ($mg \cdot L^{-1}$)
C_o	TOC content of HA in solution without biomass ($mg \cdot L^{-1}$)
$C_{solution}$	TOC concentration in solution ($mg \cdot L^{-1}$)
C_{sample}	TOC concentration corresponding to the sample ($mg \cdot L^{-1}$)
C_T	TOC value in the test mixture at time of sampling in Zahn-Wellens test ($mg \cdot L^{-1}$)
D	donor molecule
DO	Dissolved Oxygen ($mg \cdot L^{-1}$)
D_t	percentage of biodegradation
E^0	Redox Potential (V)
e^-_{cb}	photoexcited electron in the conduction band
EC_{50}	toxicity Effective Concentration ($mg \cdot L^{-1}$)
E_g	Band gap (eV)
EI	Electron Impact
ESI	Electro Spray Ionization
EU	European Union
FATP	Freshwater Aquatic Toxicity Potential
GS	Gas Chromatography
GWP	Global Warming Potential
h^+_{vb}	hole in the valence band
HA	humic acid
HILIC	Hydrophilic Interaction Liquid Chromatography
HPLC	High Performance Liquid Chromatography
HRT	Hydraulic Retention Time (days)

HTP	Human Toxicity Potential
$h\nu$	photon
IC	Inorganic Carbon; Ion Chromatography
IC_0	control initial Luminescence Intensity
IC_{15}	Luminescence Intensity after 15 minutes bacteria-control contact
%INH	percentage of Inhibition
IT_0	initial Luminescence Intensity
IT_{15}	Luminescence Intensity after 15 minutes bacteria-toxic contact
k	reaction rate constant
K	equilibrium rate constant
k_1	rate constant of first-order sorption (min^{-1})
k_2	rate constant of second-order sorption ($g \cdot mg^{-1} \cdot min^{-1}$)
K_F	Freundlich adsorption capacity ($mg \cdot g^{-1}$)
K_{ow}	octanol-water partition coefficient
L	ligand
LC	Liquid Chromatography
LC_{50}	Lethal Concentration
LCA	Life Cycle Assessment
LMCT	Ligand to Metal Charge Transfer
MAEP	Marine Aquatic Ecotoxicity Potential
MRM	Multi Residual Monitoring
MS	Mass Spectroscopy
MW	Molecular weight
n	Freundlich intensity constant
NDIR	Non-Dispersive Infrared gas analyzer
NHE	Normal Hydrogen Electrode
NOM	Natural Organic Matter
NP-HPLC	Normal Phase High Performance Liquid Chromatography
ODP	Ozone Depletion Potential
OUR	Oxygen Uptake Rate ($kg \cdot m^{-3} \cdot s^{-1}$)
$OUR_{endogenous}$	OUR related to cellular maintenance ($kg \cdot m^{-3} \cdot s^{-1}$)
$OUR_{exogenous}$	OUR related to the consumption of organic matter ($kg \cdot m^{-3} \cdot s^{-1}$)
$OUR_{herbicide}$	herbicide Oxygen Uptake Rate ($kg \cdot m^{-3} \cdot s^{-1}$)
OUR_{st}	standard sample Oxygen Uptake Rate ($kg \cdot m^{-3} \cdot s^{-1}$)
Ox	oxidant species
p.a	pro analysis
POP	Photochemical Oxidation Potential
PVC	polyvinyl chloride
pzc	point of zero charge
Q^0	maximum adsorption capacity Langmuir constant ($mg \cdot g^{-1}$)
q_e	equilibrium sorption capacity ($mg \cdot g^{-1}$)
q_t	adsorbed grams

RP-HPLC	Reverse Phase High Performance Liquid Chromatography
Red	reducing species
S_o	concentration of dissolved oxygen ($mg \cdot g^{-1}$)
SBR	Sequencing Batch Reactor
S_s	easy biodegradable substrate
SRT	Sludge Retention Time
T	temperature (^oC)
t	time
t_c	contact time (min)
TC	Total Carbon ($mg \cdot L^{-1}$)
TEP	Terrestrial Ecotoxicity Potential
TOC	Total Organic Carbon ($mg \cdot L^{-1}$)
TSS	Total Suspended Solids ($g \cdot L^{-1}$)
UPLC	Ultra Performance Liquid Chromatography
UV	Ultraviolet radiation
UVA	Ultraviolet A radiation
V	volume
V_L	volume of liquid phase (m^3)
VSS	Volatile Suspended Solids ($g \cdot L^{-1}$)
w	weight
W_A	weight of dried residue and dried filter (g)
W_B	weight of dried filter (g)
W_C	weight of residue and filter after ignition (g)
WFD	Water Framework Directive
WWTP	Wastewater Treatment Plant
X_h	biomass
X_p	inorganic matter
X_s	hardly biodegradable organic matter
λ	irradiation wavelength (nm)
ε	molar absortivity ($L \cdot mol^{-1} \cdot cm^{-1}$)

TABLE OF CONTENTS

CHAPTER 1
INTRODUCTION

1. Water pollution by herbicides and conventional wastewater treatments

Plants are able to produce natural poisonous chemicals in order to prevent the attack of insects and predators. Based on this effect, a preventive strategy has been developed to take advantage of a more productive agriculture by using synthetic compounds. This preventive scheme is based on the general use of pesticides to avoid pests proliferation and on the specific utilization of herbicides to control non-desirable weeds. The employment of chemicals to control weeds started in 1932 with 4-6-dinitro-o-cresol [1]. Then, after the Second World War the industry based on the production of synthetic chemicals for crop protection appeared with the commercialization of 2,4-dichlorophenoxiacetic (2,4-D,1945) and 4-chloro-2-methylphenoxiacetic (MCPA,1946) acids [2]. After that, when the ureas (1950), the triazines (1955) and the bipyridiniums (1960) were available, the use of herbicides became a usual practice [1].

Herbicides represent a risk factor for human health and the environment because they are difficult to degrade and toxic compounds that generally end up in aquatic sources, where they can persist for long periods. Apart from lixiviates coming from agricultural fields, a common source of highly polluted effluents containing herbicides are wastewaters from manufacturing plants and unused solutions coming from herbicide containers or agricultural equipment. Consequently, the remediation of water polluted with herbicides has received much attention in the last decades. Nonetheless, herbicides are only an example of anthropogenic pollution. In general, the material progress of modern societies has generated a vast range of toxic or non biodegradable compounds of synthetic nature, such as pharmaceuticals, personal care products, dyes, etc., that also contribute to increase the level of pollution in aquatic ecosystems [3].

Fortunately, the increasing social and political concern about environment preservation has engendered a stricter water quality control by regulating hazardous pollutant emissions. Currently, in the European Union, Europe Directive 2000/60/CE [4] has stressed the necessity to adopt measures against water contamination in order to achieve a progressive reduction of pollutants by treating wastewater.

Briefly, conventional wastewater treatments involve mechanical, biological, physical and chemical processes. After filtration and elimination of particles in suspension, biological treatment

is the most suitable method to eliminate organic matter from solution. Biological treatments are well recognized and relatively economical. Regrettably, as mentioned above a vast range of synthetic organic compounds are non biodegradable or toxic for which conventional wastewater treatment, based on a microbiological activity, is not feasible.

Physical treatments include methods such as coagulation, flocculation, sedimentation, flotation, filtration, adsorption onto activated carbon, and air striping. These physical methods are losing acceptance since their main drawbacks are the transfer of pollutants from the liquid phase to a new phase instead of their elimination [5]. Thus, physical wastewater treatment methods require post-treatments to remove the pollutant from the newly contaminated environment, enhancing in this way operational costs and diminishing effective viability.

Chemical treatments include the application of chlorine, chlorine dioxide, peracetic acid, and permanganate among others to oxidize organic matter. Nevertheless, occasionally the combination of oxidants with the original toxic compounds may generate more toxic substances that aggravate the environmental problem. Thermal methods, which can be also included in this classification, may imply high quantities of energy and can also release to the air more hazardous compounds [6]. Among the chemical processes, the so-called Advanced Oxidation Processes (AOPs) appear to be a promising field of study due to the effective complete mineralization of organic contaminants under mild conditions. Individual applications of AOP, combination of different AOPs and the combination of AOP with biological treatment have been proposed as effective and suitable methods for the remediation of wastewaters.

2. Advanced Oxidation Processes (AOPs) for wastewater treatment

Advanced Oxidation Processes (AOPs) are chemical oxidation techniques able to produce in situ reactive free radicals, mainly the hydroxyl radical (HO·), by means of different reacting systems. The concept was originally established by Glaze et al. [7] as "oxidation processes which generate hydroxyl radical in sufficient quantity to affect water treatment". As shown in Table 1.1, the standard redox potential of this powerful radical is very high when comparing with other reactants involved in wastewater treatments. Thus, HO· is a non selective oxidant that is able to oxidize a wide range of organic molecules with rate constants usually in the order of 10^6-10^9 $M^{-1}·s^{-1}$ [8, 9].

Table 1.1 Standard potential of several oxidant species [10].

Species	E^0 (V vs NHE)
HO·	2.80
O_3	2.07
H_2O_2	1.78
HO_2·	1.70
ClO_2	1.57
HOCl	1.49
Cl_2	1.36

(T=25 ºC)

Oxidation reactions that produce radicals tend to be followed by additional oxidation reactions between the radical and other species until stable oxidized products are formed. The oxidation reactions of hydroxyl radical with organic compounds are well known [8, 9, 10]. These are electrophilic reactions that occur principally by H abstraction from C-H, N-H, or O-H bonds, or by HO addition to C=C bonds or to aromatic rings (Equations 1.1-1.3). Also the hydroxyl radical can react with organic matter by electron transfer processes as seen in Equation 1.4.

$$HO^{\cdot} + R\text{-}H \rightarrow H_2O + R^{\cdot} \qquad (1.1)$$

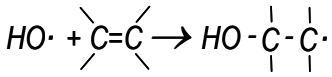

(1.2)

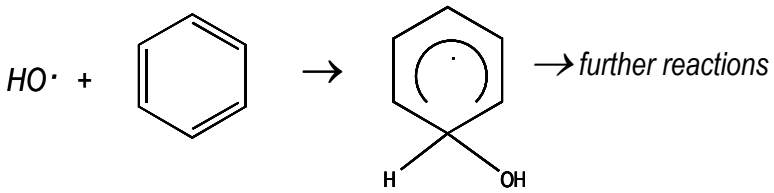

(1.3)

$$HO^{\cdot} + RX \rightarrow [RX]^{+\cdot} + HO^{-} \qquad (1.4)$$

At the end, the reaction of hydroxyl radical with organic pollutants leads to the complete mineralization to CO_2 , H_2O and minority inorganic ions as Cl^-, NO_3^-, NH_4^+, SO_4^{2-}, etc.

When treating wastewater, it must be considered that besides organic matter in solution, inorganic ions are also present. These inorganic species can be initially contained in the wastewater as well as can be produced during the mineralization of organic pollutants. Therefore, these must be considered because when existing at relative high concentration, inhibition of pollutants abatement may be observed [11, 12, 13, 14]. This inhibition is probably due to a general scavenging of hydroxyl radicals apart from specific effects depending on each AOP system, as catalyst precipitation or adsorption onto the active sites of the heterogeneous catalyst (discussed later in the manuscript). Due to the high reactivity of hydroxyl radicals, they are able to react with inorganic ions in the media as Cl^-, HCO_3^- and HPO_4^{2-}, leading to the formation of anion radicals like $[ClOH]^{-}\cdot$, $CO_3^{-}\cdot$ and $HPO_4^{-}\cdot$ that are less reactive than the hydroxyl radical. This leads to a reduction of the efficiency of pollutants abatement, as said before. Moreover, natural organic matter (NOM) in solution, such as humic acids, may also act as hydroxyl radical scavengers. This effect will be discussed later in Section 5 of this introduction.

Apart from these general undesirable scavenging effects, the complete mineralization of most of the organic matter is possible when the hydroxyl radical is the main oxidant species present in solution. This is one of the main advantages of this sort of processes since other chemical oxidation techniques mostly yield the partial oxidation of target compounds and, as explained before, the generation of new hazardous compounds is possible. Generation of small

amounts of residues, the applicability when there are low concentrations of pollutants, and the possibility of coupling with biological systems are other important advantages of AOPs [15, 16]. The possibility of coupling with biological systems is of special interest in order to solve the main disadvantage associated to all AOP, which is their high related operational cost when working as wastewater treatment [15].

AOPs can be classified by considering the phase where the process takes place. Hence, homogenous or heterogeneous processes can be differentiated. AOPs classification can also consider the different possible ways of hydroxyl radical production. In this way, photochemical and non-photochemical processes can be distinguished. Table 1.2. classifies some of the most important AOPs into photochemical and non-photochemical processes.

Table 1.2 Classification of some AOPs as photochemical and non-photochemical processes [16].

Non-photochemical processes	Photochemical processes
Ozonation in basic media (O_3/ HO^-)	O_3/UV ($\lambda \leq 320$ nm)
O_3/H_2O_2	H_2O_2/UV ($\lambda \leq 300$ nm)
O_3/Ultrasound	O_3/H_2O_2/UV ($\lambda \leq 320$ nm)
H_2O_2/Ultrasound	Photocatalytic ozonation ($\lambda \leq 320$ nm)
Electron Beam	Heterogeneous photocatalysis (TiO_2/UV) ($\lambda \leq 400$ nm)
Fenton (Fe^{2+}/H_2O_2)	Water photolysis in ultravacuum (UVV) ($\lambda \leq 190$)
Electro-Fenton	Photo-Fenton (Fe^{2+}/H_2O_2/UV) ($\lambda \leq 550$ nm)
	Photoelectro-Fenton($\lambda \leq 550$)

2.1. Photochemical Advanced Oxidation Processes

Photochemical Advanced Oxidation Processes refers both, to AOPs that need photons to initiate the oxidation process, and non-photochemical AOPs that increase their efficiency when working with artificial or natural radiation. Photochemical AOPs are particularly appropriate when treating wastewater containing compounds that do not absorb the incoming radiation. Otherwise the quantum efficiency can decrease by competitive absorption when treating compounds with high absorbtivity.

The AOPs considered in this experimental work are photo-Fenton, TiO_2-photocatalysis, ozone/UV, photo-Fenton/ozone and, finally TiO_2-photocatalysis/ozone. As seen in Table 1.2, these photochemical processes require radiation of wavelengths higher than 300 nm. Since the natural solar radiation arriving to the earth´s surface comprises wavelengths from 300 to 3000 nm, their direct use as photon source has been already recognized [17, 18, 19]. The production of artificial light is highly-priced, thus the operational costs associated with these processes can be substantially reduced by using sunlight as the driving force. The reduction of operational cost by using natural solar light is a general advantage of all the AOPs described in this work [15], although the superior efficiency of the photo-Fenton reaction in most of the research in this field has been previously demonstrated [20].

The first part of this thesis compares the mineralization efficiency of photo-Fenton, TiO_2-photocatalysis, ozone/UV, photo-Fenton/ozone, and TiO_2-photocatalysis/ozone for the degradation of some specific herbicides in aqueous phase (i.e., publications 1 and 2). The rest of the work has been based on the photo-Fenton process (i.e., publications 3, 4, and unpublished results presented in Annexe 1). For that reason the photo-Fenton process has been more extensively described in this introduction.

2.1.1. Photo-Fenton process

The so-called photo-Fenton process involves the reaction of ferrous ions (catalyst) and hydrogen peroxide (oxidizing agent) under UV/visible radiation to form active oxidant species, mainly hydroxyl radical, which oxidize organic compounds when they are present in aqueous solution.

Compared to other oxidants, hydrogen peroxide is not expensive, not dangerous, easy to handle and poses no lasting environmental threat since it readily decomposes to water and oxygen. In addition, iron is also reasonably priced, safe and environmentally friendly because iron is the second most abundant metal and the fourth most abundant element on the earth after oxygen, silicon and aluminium [21]. Such an easy and economical mode to generate hydroxyl radicals has promoted this oxidation method for wastewater treatment. Another important advantage of the photo-Fenton process is the inexistence of mass transfer limitations due to its

homogeneous catalytic nature. The most important drawback of the photo-Fenton process, as explained later, is the necessity of pH adjustment.

2.1.1.1. Principles of photo-Fenton chemistry

Dark reactions (Fenton and Fenton-like processes)

At the end of XIX century, Henry J. Fenton reported that H_2O_2 could be activated by iron salts to oxidize tartaric acid [22]. After that, in 1934 Haber and Weis [23] proposed that, under dark conditions, the hydroxyl radical was responsible for this oxidation process according to Equation 1.5.

$$Fe^{2+} + H_2O_2 \rightarrow Fe^{3+} + HO^- + HO^{\cdot} \qquad k=40\text{-}80\ M^{-1}\cdot s^{-1} \qquad (1.5)$$

This reaction is known as the Fenton process and the bimolecular rate constant of Fenton reaction in acidic solutions at 25 ^oC was later assigned by different researchers [24, 25]. After production, hydroxyl radicals can be scavenged by reacting with another Fe^{2+} (Equation 1.6) or they may react with an organic compound as explained in Section 2 (Equations 1.1-1.4).

$$Fe^{2+} + HO^{\cdot} \rightarrow Fe^{3+} + HO^- \qquad k=2.6\text{-}5.8\cdot 10^8\ M^{-1}\cdot s^{-1} \qquad (1.6)$$

Since the Haber and Weis report, different efforts have been made to understand the complete chemistry of the Fenton processes. Although controversy about the real mechanism of Fenton reaction is still present, this introduction attempts to give a brief overview of the most important contributions to the chemistry of this process. Two main reaction pathways were first proposed in the literature. In 1951, Barb et al. [26, 27], supporting the Haber-Weis theory, reported a radical mechanism for the decomposition of H_2O_2 in acidic solution in the dark and in the absence of organic matter. In 1959 Kremer and Stein published some works based on an ionic mechanism [28, 29]. In 1975 Walling published a paper which proved the radical mechanism in acidic media [30]. More recently, some authors have reported that the hydroxyl radical is not the only oxidizing agent, but also some type of high-valent iron-oxo intermediates, mainly ferryl ion (Fe^{4+}), are responsible for the direct attack to organic matter [31, 32]. Indeed, the difficult

analysis of the oxidant species involved in this complex process has impeded the determination of a unique degradation pathway. Nevertheless, the evidence of a high yield of organic matter mineralization seems to indicate that the most important oxidant species is the hydroxyl radical. The traditional accepted radical mechanism for the Fenton reaction is shown through Equations 1.5 to 1.13 [21] where the listed rate constants have been reported by Sychev and Isaak [33]. Concerning this mechanism, it must be noted that the most abundant iron species in water are ferric (Fe^{3+}) and ferrous (Fe^{2+}) ions. In absence of other complexing substances, these ions form octahedral complexes with six water or hydroxide ligands, depending on the pH [34]. For simplicity, through the mechanism, Fe^{2+} and Fe^{3+} are taken to represent all species present in solution for each oxidation state and ligands have been omitted.

$$Fe^{2+} + H_2O_2 \rightarrow Fe^{3+} + HO^- + HO^{\cdot} \qquad k=40\text{-}80\ M^{-1}\cdot s^{-1} \qquad (1.5)$$

$$Fe^{2+} + HO^{\cdot} \rightarrow Fe^{3+} + HO^- \qquad k=2.6\text{-}5.8\cdot 10^{8}\ M^{-1}\cdot s^{-1} \qquad (1.6)$$

$$Fe^{3+} + H_2O_2 \rightarrow Fe^{2+} + HO_2^{\cdot} + H^+ \qquad k=1\text{-}2\cdot 10^{-2}\ M^{-1}\cdot s^{-1} \qquad (1.7)$$

$$Fe^{2+} + HO_2^{\cdot} \rightarrow Fe^{3+} + HO_2^- \qquad k=0.72\text{-}1.5\cdot 10^{6}\ M^{-1}\cdot s^{-1} \qquad (1.8)$$

$$Fe^{3+} + HO_2^{\cdot} \rightarrow Fe^{2+} + O_2 + H^+ \qquad k=0.33\text{-}2.1\cdot 10^{6}\ M^{-1}\cdot s^{-1} \qquad (1.9)$$

$$HO^{\cdot} + HO^{\cdot} \rightarrow H_2O_2 \qquad k=5\text{-}8\cdot 10^{9}\ M^{-1}\cdot s^{-1} \qquad (1.10)$$

$$HO^{\cdot} + H_2O_2 \rightarrow HO_2^{\cdot} + H_2O \qquad k=1.7\text{-}4.5\cdot 10^{7}\ M^{-1}\cdot s^{-1} \qquad (1.11)$$

$$HO_2^{\cdot} + HO_2^{\cdot} \rightarrow H_2O_2 + O_2 \qquad k=0.8\text{-}2.2\cdot 10^{6}\ M^{-1}\cdot s^{-1} \qquad (1.12)$$

$$HO^{\cdot} + HO_2^{\cdot} \rightarrow H_2O + O_2 \qquad k=1.4\cdot 10^{10}\ M^{-1}\cdot s^{-1} \qquad (1.13)$$

Equations 1.7 and 1.9 are also called Fenton-like reactions. The Fenton-like process generates ferrous ion which in the presence of excess of H_2O_2 is readily transformed giving ferric ion [35]. Nevertheless, this process is the rate limiting step in the catalytic iron cycle. Thus, the

iron cycling takes place, with approximately constant ferric ion concentration, traces of ferrous ion and a constant hydroxyl radical production.

Moreover, as explained in the previous section, in the presence of organic matter the electrophilic reaction of hydroxyl radical with organic compounds leads to the formation of organic radicals (Equations 1.1-1.3) that can also react either forming dimers, or with ferrous and ferric ions as follows [21]

$$2R^{\cdot} \longrightarrow RR\ (dimer) \qquad (1.14)$$

$$R^{\cdot} + Fe^{2+} \longrightarrow R^{-} + Fe^{3+} \qquad (1.15)$$

$$R^{\cdot} + Fe^{3+} \longrightarrow R^{+} + Fe^{2+} \qquad (1.16)$$

On the other hand, a direct reaction between iron species and some specific compounds providing an alternative Fenton-like pathway, has been observed. It has been reported that quinones or hydroquinones structures react with ferric ion through Equations 1.17 and 1.18 [36].

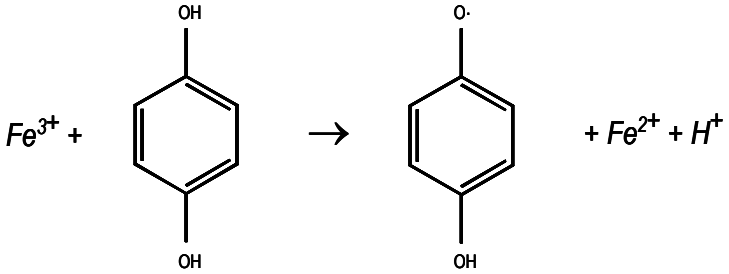

(1.17)

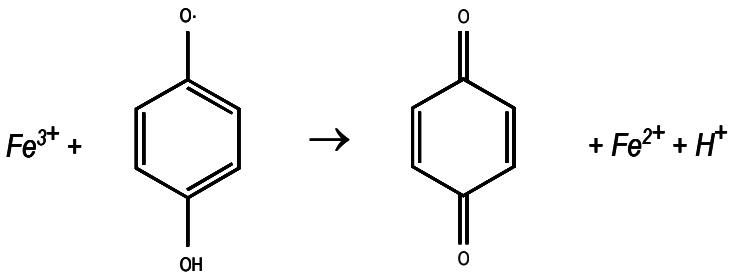

(1.18)

This reaction between ferric ion and quinones is of special interest to this work because they are generally generated along the mineralization process of aromatic compounds before ring opening (the herbicides selected for this study are aromatic compounds).

Considering pH operational conditions, the Fenton-like reaction is pH-dependent, contrary to what happens with the Fenton reaction. When pH increases more than 2.5-3.5, depending on the iron concentration and temperature, the ferric ion precipitates in amorphous ferric oxyhydroxides forming a red brown sludge that can co-precipitate organic compounds and that produces technological troubles [37]. For that reason, the optimum pH for the Fenton process has been determined as slightly below 3.

Photoassisted reaction (photo-Fenton process)

Ferric ion complexes at pH below 3 are highly photoactive. These complexes undergo ligand-to-metal charge transfer (LMCT) excitation, to give ferrous ion and an oxidized ligand as follows [38, 39]

$$Fe^{3+}(L^{-})_n + h\nu \rightarrow Fe^{2+}(L)_{n-1} + L_{ox}^{\cdot} \qquad (1.19)$$

This is the base of the so-called photo-Fenton process that typically gives faster rates and a higher degree of mineralization than the Fenton reaction. This efficiency increase is explained because the reduced ferrous ion needed in the Fenton reaction is recovered and reacts with the hydrogen peroxide in excess to produce more HO· (Equation 1.15) and because oxidation of the ligand may lead to further degradation of target compounds [35, 40]. Specifically, at pH below 3, in absence of other ligands, the most abundant Fe^{3+}-hydroxy complex present in solution is $Fe(HO)^{2+}$ which absorbs radiation from 300 nm until 410 nm, decomposing as shown in Equation 1.20 [35]. In this way, pH=2.8 has been recurrently proposed as optimum pH for the photo-Fenton reaction [32, 35].

$$[Fe(HO)]^{2+} + h\nu \rightarrow Fe^{2+} + HO^{\cdot} \qquad (1.20)$$

When other ligands, different from hydroxyl-ligands, are present in solution ferric ion can also form complexes and undergo photoreduction. Indeed, the Fe^{3+}-complex has different light absorption properties depending on the ligand. Therefore, photoreduction may take place with different quantum yield and at different wavelengths. One example to be noted is the complexing of ferric ion with carboxylic acids because the latter are generally by-products generated during the mineralization process. Fe^{3+}-oxalate complex is a well known photoactive example that has been commonly used as a chemical actinometer [41]. This complex has much higher quantum yields than Fe^{3+}-hydroxo complexes, thus it is more efficiently photodegraded under visible radiation (up to 550 nm) regenerating ferrous ion through Equation 1.21 [42]. In fact, the addition of oxalate has been often proposed to increase the photo-Fenton efficiency as a degradation process [43].

$$[Fe(C_2O_4)_3]^{3-} + h\nu \longrightarrow Fe^{2+} + 2C_2O_4^{2-} + C_2O_4^{-}\cdot \qquad (1.21)$$

Fenton and photo-Fenton reactions are inhibited by inorganic ions. Although the effect of hydroxyl radical scavenging by some inorganic ions has been highlighted in the previous section, the effect of inorganic ions presence when using Fenton related processes must be considered in more detail. In particular, ferric ion forms complexes with phosphate that are quite insoluble in neutral or mildly acidic solution [12]. Moreover, sulphate, chloride and fluoride inhibit the process because these ions reduce the reactivity of ferric ion through coordination to form less reactive complexes [12, 21, 26, 35, 44].

Finally, much effort has been done to determine the optimum reactants concentration ratio when mineralizing organic matter by means of the photo-Fenton reaction. Typical ranges are 1 part iron per 5-25 parts of hydrogen peroxide (w/w) [45]. This imprecise information about operational conditions of photo-Fenton reaction is a result of the undefined pathway involved in the process depending on the nature of the ligands and reactive species, as commented before. Moreover, the optimum reactant ratio depends on the specific features of the system, such as the reactor design and the light source characteristics. Thus, an optimization process must be always considered because an excess of reactant concentration may inhibit the mineralization process. Apart from the direct reaction between ferrous ion and hydroxyl radical (see Equation 1.6), when considering the Fe^{4+}-oxo intermediate, a reaction between the excess of ferrous ion with ferryl ion that interferes with the formation of the hydroxyl radical has been proposed [46]

$$H_2O_2 + Fe^{2+} \rightarrow [FeO]^{2+} + H_2O \quad (1.22)$$

$$[FeO]^{2+} + Fe^{2+} + H^{+} \rightarrow [Fe(HO)]^{2+} + Fe^{3+} \quad (1.23)$$

$$[Fe(HO)]^{2+} + H^{+} \rightarrow Fe^{3+} + H_2O \quad (1.24)$$

Furthermore, the presence of en excess of H_2O_2 would deplete the valuable hydroxyl radicals by forming $HO_2\cdot$ that are less reactive than the former (Equation 1.11) [47].

2.1.1.2. Application of photo-Fenton to wastewater treatment

Although the Fenton reaction was discovered in 1894 [22], until the beginning of the 1990s only few examples of its use as a wastewater treatment were suggested [48]. From then, the number of scientific articles on applications of Fenton and photo-Fenton chemistry to wastewater treatment has increased exponentially over the years.

Among the main applications of this degradation system, the treatment of waste streams from dye manufacture [47, 49] and paper pulp bleaching effluents have been widely studied [50, 51]. The elimination of toxic and non biodegradable herbicides has been also considered as a response to the necessity of the elimination of this kind of persistent compounds mainly in the industrial manufacturing or for the treatment of unused solutions [52, 53, 54]. The treatments of wastes generated at wine distilleries [55], olive mill production plants [56], landfill leachates [57], surfactants [58], photographic developer wastes [59], and many other industrial activities whose effluent wastes contain toxic or non biodegradable compounds, have been studied and reported during the last two decades.

Despite the great deal of work devoted to these processes, scanty indications have been found about their industrial applications [15]. Nevertheless, a first commercial wastewater treatment plant, based on a solar photo-Fenton process, devoted to the removal of herbicides from polluted effluents when recycling herbicides containers has been installed in Spain [60].

The main drawbacks of Fenton and photo-Fenton as a wastewater treatment system are mainly related to the need for pH control and the problem of sludge generation, as explained before. In order to solve these weaknesses, Fenton and photo-Fenton modified technologies where iron is used as heterogeneous catalyst, have been developed [61, 62, 63].

2.1.2. Other Advanced Oxidation Processes

2.1.2.1. Heterogeneous photocatalysis

Heterogeneous photocatalysis involves the process taking place at the interfacial boundary between a catalyst surface and a liquid media. The catalyst used in this process generally is a solid semiconductor whose irradiation promotes the generation of radical species, mainly hydroxyl radical, capable of mineralizing the organic pollutants present in wastewaters.

Among the different semiconductors reported in the literature, TiO_2 is the most stable, efficient and promising material. TiO_2 exists mainly in two natural different crystal structures: rutile and anatase. Both structures consist of titanium centres surrounded by six oxygen atoms that occupy the corners of TiO_6 distorted octahedrons, and differ by the distortion of each octahedron and by the assembly model of the octahedral chain [64], as seen in Figure 1.1.

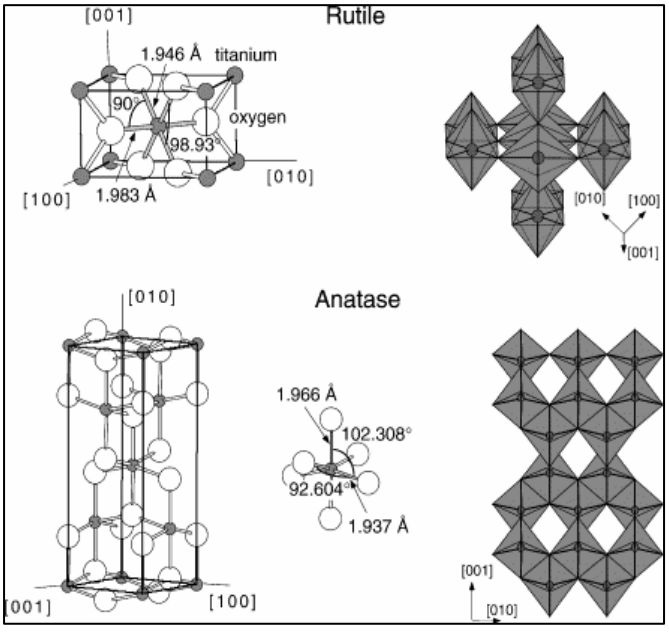

Figure 1.1. Bulk structures of rutile and anatase polymorphs [65]

The commercial catalyst TiO_2 Degussa P-25, which has a particular allotropic form consisting of 80% anatase and 20% rutile, is considered as a standard material for photocatalysis [66]. This catalyst gives the best results in pollutants mineralization, mainly as a result of synergistic effects in the interaction between the two different polymorphs [67].

Besides near UV radiation for the activation of the economical and non toxic TiO_2, the system only needs water and oxygen for the production of hydroxyl radicals, therefore the addition of new oxidants to the reaction bulk is not necessary. In addition, it can work at both acid and basic pH conditions and can be reused although its progressive deactivation has been observed [68]. Regrettably, apart from the deactivation process, the main drawback associated to this process is the low quantum yields of light adsorption and the low efficiency when comparing with other AOPs [66]. Furthemore, the secondary operations required (filtration or coagulation) when recovering the catalyst after use, are another important drawback of this method. A possible solution is the fixation of the catalyst onto some inert substrate. Unfortunately, several problems like mass transfer limitations, decrease of photocatalytic process performance, and higher incidence of catalyst deactivation phenomena appear with such a catalyst configuration [69].

2.1.2.1.1. Principles of heterogeneous TiO_2-photocatalysis chemistry

Fujishima and Honda marked the beginning of a new era in heterogeneous photocatalysis when they discovered in 1972 the photocatalytic splitting of water on TiO_2 electrodes [70]. Then, Carey et al. [71] reported the photocatalytic degradation of biphenyl and chlorobiphenyls in the presence of titanium dioxide. Since then, many applications using the TiO_2/UV process have been investigated.

As explained above, in general heterogeneous photocatalysis implies the utilization of a semiconductor. This kind of material can act as sensitizer for light-induced redox processes due to its electronic properties [72]. It means that the catalyst absorbs a photon and, after excitation, interacts with the ground state of an adsorbed compound. To fully understand the properties of semiconductors it is necessary to describe the band theory. In this theory, at 0 K, a perfect crystal of a semiconductor material possesses a group of very close and filled electronic states (valence

band), a void energy region where no energy levels are available and, at higher energies, another group of close and empty electronic states (conduction band). The void region which extends from the top of the filled valence band to the bottom of the vacant conduction band is called the band gap (E_g). When TiO_2 is photoexcitated with radiation having energy equal to or greater than E_g, an electron is promoted from the valence band to the conduction band, thus a conduction band electron (e^-_{cb}) and a valence band hole (h^+_{vb}) pair are generated (Equation 1.25). TiO_2 band gap energy is estimated as $3.23 \geq E_g \geq 3.02$ eV, depending on its allotropic form, thus the process requires irradiation of wavelengths below 400 nm [73].

$$TiO_2 + h\nu \longrightarrow h^+_{vb} + e^-_{cb} \qquad (1.25)$$

After the generation of the electron-hole pair, the charge carriers either recombine in the bulk of the particle with the release of heat (non irradiative process), or migrate to the particle surface where they can also recombine or can react with adsorbed substances according to the redox potential of each adsorbate. If the redox potential is appropriate for a thermodynamically allowed reaction, an electron transfer proceeds towards acceptor molecules (A), whereas a positive photohole is transferred to a donor molecule (D) as shown in Figure 1.2.

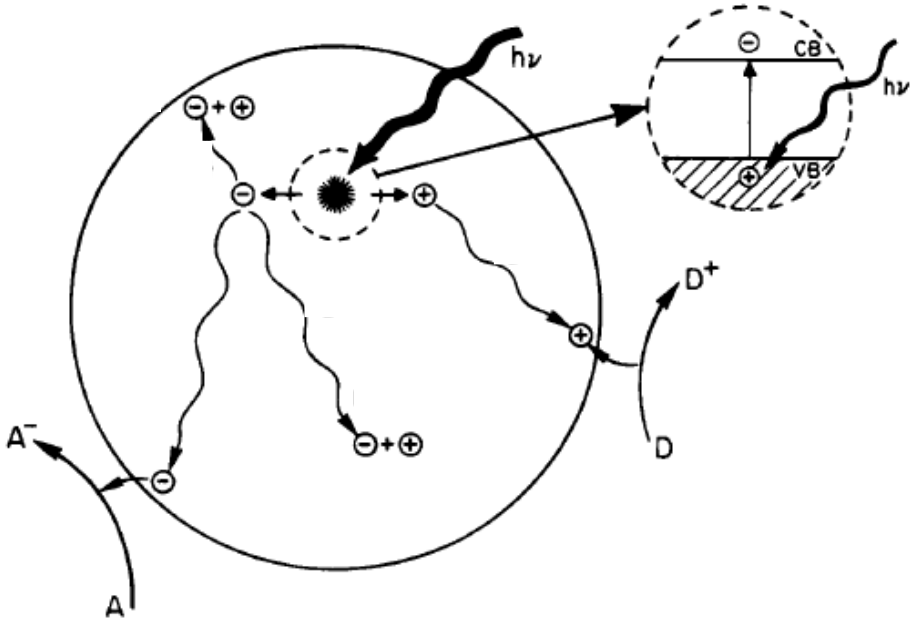

Figure 1.2. Schematic photoexcitation in a TiO_2 particle followed by deactivation events [19]

Figure 1.3. attempts to give more detailed information about the processes that take place in the surface of the TiO_2 catalysist.

Charge-carrier trapping	Characteristic times
$e^-_{cb} + >Ti(IV) \longrightarrow >Ti(III)$	10 ns
$e^-_{cb} + >Ti(IV)OH \leftrightarrows >Ti(III)OH$	100 ps
$h^+_{vb} + >Ti(IV)OH \longrightarrow >Ti(IV)OH^{+\cdot}$	10 ns
Charge-carrier recombination	
$e^-_{cb} + >Ti(IV)OH^{+\cdot} \longrightarrow >Ti(IV)OH$	100 ns
$h^+_{vb} + >Ti(III)OH \longrightarrow >Ti(IV)OH$	10 ns
Interfacial charge transfer	
$>Ti(IV)OH^{+\cdot} + D \longrightarrow >Ti(IV)OH + D^{+\cdot}$	100 ns
$e^-_{tr} + A \longrightarrow >Ti(IV)OH + A^{-\cdot}$	very slow (ms)

Figure 1.3. Time domains of the electron transfer processes involved in TiO_2 heterogeneous photocatalysis [66]

As seen in Figure 1.3, the recombination of electrons and holes occurs quickly (i.e., 100 ns for electron recombination and 10 ns for hole recombination). If a recombination process does not occur, the captured electrons remain as >Ti(III) or as >Ti(III)OH and the holes remain as >Ti(IV)-$OH^{+\cdot}$. Under conventional operating conditions (i.e., aerobic conditions), the electron reduces adsorbed $O_{2(ads)}$ to the superoxide radical anion $O^{-\cdot}_{2(ads)}$ [72]. The reduced species may experience further electron transfer processes or chemical reactions, involving water and pollutant species over the surface or, otherwise, in the bulk of the solution, after undergoing desorption [74].

On the other hand, there are two mechanisms coexisting for the oxidation of organic matter. The first one involves the direct oxidation of adsorbed organic matter by a valence band hole (h^+) to produce the corresponding organic radical [75], while the second assumes the

generation of hydroxyl radicals from adsorbed hydroxyl groups or water molecules. After that, the organic species can react with the hydroxyl radical either at the catalyst surface or in the solution bulk [66]. This mechanism is efficient when electron-hole recombination process is minimised. The role played by molecular oxygen in the reduction of this recombination is well known since oxygen is an efficient conduction band electron trap [19].

The pH influences the surface properties of the semiconductor. For TiO_2, at pH higher than approximately 6 the surface becomes negatively charged and the opposite for pH lower than 6. At pH of about 6 (the point of zero charge -pzc-) the catalyst surface is, on average, neutral [76]. Although changes in the rate of photocatalyitc activity from one end of the pH range to the other are usually small [77], the adsorption properties change depending on the experimental conditions. Thus, the photocatalytic reaction rate of target compounds can be substantially altered due to ions sorption to the active sites of the catalyst [78].

Finally, the rates of heterogeneous photocatalytic degradation processes normally increase with the catalyst loading until a certain upper limit where the whole catalyst surface is illuminated. The optimum catalyst loading value depends on the particular characteristics of the photocatalytic system, like the reactor design or the type of light source. Nevertheless, this value generally is comprised within the range 0.8 and 2.5 $g \cdot L^{-1}$ [68].

2.1.2.2. Ozonation

Ozone, which is generally produced in situ by a high-voltage electric discharge process in presence of air or oxygen, is a powerful oxidant (electrochemical oxidation potential of 2.07 V vs NEH opposed to 2.8 V vs NEH for hydroxyl radical). The chemistry involved in the formation of ozone is represented as follows

$$O_2 + energy \rightarrow O^{\cdot} + O^{\cdot} \qquad (1.26)$$

$$O^{\cdot} + O_2 \rightarrow O_3 \qquad (1.27)$$

The mechanism of the reaction between ozone and dissolved organic substances has been described by Hoigné and co-workers [11, 79, 80]. Briefly, two mechanisms of attack of ozone to the organic molecule can be distinguished in water depending on the pH: a slow, direct and highly selective attack of molecular ozone takes place at low pH (generally with molecules of high electronic density), whereas free radicals from ozone decomposition react fast and non-selectively at high pH. The AOP definition implies the presence of hydroxyl radicals, thus ozone is considered as an AOP when working at high pH. At this pH, hydroxyl radicals are generated by means of reaction between O_3 and HO^- ions as follows [80, 81, 82]. Kinetic constants have been measured at 20 ^oC.

$$O_3 + HO^- \rightarrow O_2 + HO_2^- \qquad k=70\ M^{-1}\cdot s^{-1} \qquad (1.28)$$

$$HO_2^- + O_3 \rightarrow HO^\cdot + O^-_2{}^\cdot + O_2 \qquad k=2.8\cdot 10^6\ M^{-1}\cdot s^{-1} \qquad (1.29)$$

$$O^-_2{}^\cdot + O_3 \rightarrow O^-_3{}^\cdot + O_2 \qquad k=1.6\cdot 10^9\ M^{-1}\cdot s^{-1} \qquad (1.30)$$

$$pH \leq 8 \quad O^-_3{}^\cdot + H^+ \leftrightarrows HO_3^\cdot \qquad (1.31)$$

$$HO_3^\cdot \rightarrow HO^\cdot + O_2 \qquad k=1.4\cdot 10^5\ M^{-1}\cdot s^{-1} \qquad (1.32)$$

$$pH \geq 8 \quad O^-_3{}^\cdot \leftrightarrows O^{-\cdot} + O_2 \qquad (1.33)$$

$$O^{-\cdot} + H_2O \rightarrow HO^\cdot + HO^- \qquad k=10^8\ M^{-1}\cdot s^{-1} \qquad (1.34)$$

$$HO^\cdot + O_3 \rightarrow HO_2^\cdot + O_2 \qquad k=10^8\text{-}2\cdot 10^9\ M^{-1}\cdot s^{-1} \qquad (1.35)$$

Due to its high reactivity towards microorganisms and dissolved organic matter, ozone has been widely used for disinfection and purification of water [82]. Although ozone technology for water treatment is well established and proven, the production of this oxidant requires large amounts of electrical energy and initial economic invesment (i.e., the ozonisator, the abatement system for residual ozone and in general the construction materials to prevent corrosion). Thus, the high operational costs generally associated to this process are the main drawback of this

technology [15]. Moreover, phase mass transfer limits its efficiency, and diffusers, venturis, and contact towers are required [83]. Another important disadvantage of ozonation is the high ozone/product required ratio (i.e., 5:1 [16]) for the achievement, when possible, of a complete mineralization process. Also, low degradation rate constants are obtained when treating some specific compounds such as acids, alcohols and low molecular weight organochlorine compounds [84, 85].

In order to provide larger ozonation efficiency, as well as to optimize economic requirements, new methods such as the hydrogen peroxide addition to the ozone system, irradiation with ultraviolet light or both have been investigated. Moreover the combination of ozone with other AOPs like heterogeneous photocatalysis and photo-Fenton have been also proposed, and will be discussed later.

2.1.2.2.1. Principles of ozone/UV chemistry

In order to increase the hydroxyl radical production in the ozonation system, the irradiation with UV light was explored by Peyton and Glaze [86]. The radiation with UV light to aqueous ozone solution produces hydrogen peroxide as follows

$$O_3 + h\nu + H_2O \rightarrow H_2O_2 + O_2 \qquad (1.36)$$

H_2O_2 is a weak acid, powerful oxidant and unstable compound that initiates the decomposition of ozone by means of a chain mechanism which is represented as follows [87, 88].

$$H_2O_2 \leftrightarrows HO^-_2 + H^+ \qquad (1.37)$$

$$HO^-_2 + O_3 \rightarrow O^-_3 + HO_2^{\cdot} \qquad k=2.8\cdot10^6\ M^{-1}\cdot s^{-1} \qquad (1.38)$$

$$HO_2^{\cdot} \leftrightarrows O_2^{-} + H^+ \qquad (1.39)$$

$$O_2^{-}{}^{\cdot} + O_3 \rightarrow O_3^{-}{}^{\cdot} + O_2 \qquad k=1.6\cdot10^9\ M^{-1}\cdot s^{-1} \qquad (1.40)$$

$$O_3^{-}\cdot + H^{+} \leftrightarrows HO_3\cdot \qquad (1.41)$$

$$HO_3\cdot \rightarrow HO\cdot + O_2 \qquad k=1.4\cdot10^{5}\ M^{-1}\cdot s^{-1} \qquad (1.42)$$

$$O_3 + HO\cdot \rightarrow O_2 + HO_2\cdot \qquad k=1.1\cdot10^{5}\ s^{-1} \qquad (1.43)$$

Ultraviolet lamps must emit radiation at 254 nm for an efficient ozone photolysis [87]. Nevertheless, the ozone spectrum is extended over 330 nm (see Figure 1.4), thus the possibility of using a less energetic lamp can be considered. Indeed, previous research has demonstrated that ozone photolysis may occur until 320 nm by means of a UVA-black light lamp or natural solar radiation [18].

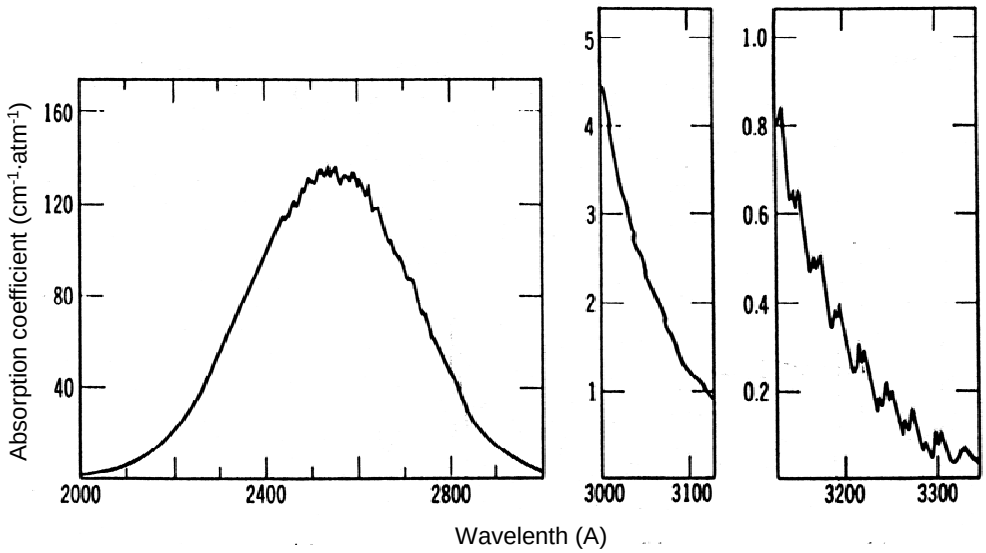

Figure 1.4. Ozone absorption spectra [89]

Apart from ozone/UV or ozone/H_2O_2 combination, the coupling of ozone with photo-Fenton or TiO_2-photocatalysis can efficiently increase the mineralization yield of the oxidation process. This effect is explained in the following sections.

2.1.2.2.2. Principles of photo-Fenton/ozone chemistry

As explained in the previous section, ozonation achieves limited mineralization of organic compounds when used as a wastewater treatment. In 1972 Hewes and Davinson reported that the presence of Fe^{2+}, Mn^{2+}, Ni^{2+} or Co^{2+} sulphate during ozonation of wastewaters induced an increase of TOC removal as compared to single ozonation [90].

The efficiency increase in the mineralization process when coupling photo-Fenton and ozone systems is entirely due to the increase in hydroxyl radical generation. When $Fe^{2+}/H_2O_2/UV/O_3$ is applied as wastewater treatment, different reactions occur in the solution bulk. On one side, $H_2O_2/UV/O_3$ increases the production of hydroxyl radical by means of a chain reaction mechanism following Equations 1.36 to 1.43 as explained in Section 2.1.2.2.1. On the other hand, production of hydroxyl radicals by the photo-Fenton reaction can also occur as explained in Section 2.1.1.1.

Moreover, ferrous ion is oxidized by ozone. Different mechanisms of oxidation of ferrous ion to ferric ion by ozone have been reported. A first mechanism was proposed by Hart et al. [91]. This mechanism described the transference of an electron from the reduced metal to ozone, forming ferric ion and the radical ion O^{-}_{3} and then the formation of hydroxyl radical. Afterwards, Nowell and Hoigné [92] suggested that the hydroxyl radical was not an intermediate in the reaction of ferrous ion with ozone and assumed a mechanism involving an oxygen-transfer from ozone to ferrous ion. More recently, Logager et al. [93] based on those previously proposed mechanisms suggested that in acidic solutions ferrous ion directly reacts with O_3 to generate the intermediate [FeO^{2+}]. This species evolves to hydroxyl radical as follows. Kinetic constants are measured at 25 ^{o}C.

$$Fe^{2+} + O_3 \rightarrow [FeO]^{2+} + O_2 \qquad k = 8.2 \cdot 10^{5}\ M^{-1} \cdot s^{-1} \qquad (1.44)$$

$$[FeO]^{2+} + H_2O \rightarrow Fe^{3+} + HO^{\cdot} + HO^{-} \qquad k = 1.3 \cdot 10^{-2}\ s^{-1} \qquad (1.45)$$

This mechanism has been used to describe the organic matter mineralization increase detected when using the coupled photo-Fenton/ozone system in publication 1.

2.1.2.2.3. Principles of TiO_2-photocatalysis/ozone chemistry

Another alternative to increase the production of hydroxyl radicals in the ozonation system is photocatalytic ozonation by adding TiO_2 to the solution and irradiating with UV light.

The TiO_2-photocatalysis combined with ozone can increase the rate of mineralization due to the increment of hydroxyl radicals production. When $TiO_2/UV/O_3$ is applied as wastewater treatment, different reactions occur in the solution bulk. On one side, UV/O_3 increases the production of hydroxyl radical by means of a chain reaction mechanism following Equations 1.36 to 1.43 as explained in Section 2.1.2.2.1. On the other hand, production of hydroxyl radicals may occur by the reaction of adsorbed H_2O molecules with the photogenerated holes at the illuminated TiO_2 particle as explained in Section 2.1.2.1.1. [94].

Finally, the synergistic effect of combining both techniques must be considered. Different mechanisms have been proposed in the literature. The first one, proposed that adsorbed O_3 molecules can react with photogenerated electrons at the TiO_2 particle as follows [95]

$$O_3 + e^- \rightarrow O^-_3 \cdot \qquad (1.46)$$

$$O^-_3 \cdot + H^+ \rightarrow HO \cdot + O_2 \qquad (1.47)$$

In consequence, the presence of dissolved ozone in the irradiated TiO_2 aqueous suspensions decreases the electron-hole recombination (see Section 2.1.2.1.1.), increasing the efficiency of the photocatalytic process [94]. This mechanism has been used to explain the increase of TOC removal when reporting the elimination of herbicides in publication 1.

More recently, Kopf et al. [96] proposed an electron transfer from TiO_2 to the oxygen molecule to form $O^-_2 \cdot$ radical, then this radical reacts with ozone to give $HO \cdot$ radicals as follows

$$O_3 + O^-_2 \cdot \rightarrow O^-_3 \cdot + O_2 \qquad (1.48)$$

$$O^-_3 \cdot + H^+ \rightarrow HO \cdot + O_2 \qquad (1.49)$$

In conclusion, as explained for photo-Fenton/ozone, the efficiency of TiO_2-photocatalysis/ozone is increased due to an enlargement of the hydroxyl radical production. Nevertheless, both coupled technologies still have disadvantages related to the high operational costs involved in ozonation.

2.1.2.3. Application of other AOPs to wastewater treatment

Many applications of AOPs for the treatment of wastewaters have been reported in the literature since the late 1980s when this nomenclature was established by Glaze et al. [7]. Illustrative examples of photo-Fenton application to wastewater treatment have been shown in Section 2.1.1.2. The last publications concerning TiO_2-photocatalysis and ozonation as wastewater treatments include the remediation of wastewaters polluted with dyes [97, 98], pesticides [53, 73], pharmaceuticals [99], etc. Also the treatment of wastewater from olive mills [56, 100] and from paper industry by means of AOPs has been reported [51, 101]. Beyond the mineralization of chemical pollutants in wastewater, ozone has been extensively used to kill bacteria and other microorganisms. More recently TiO_2-photocatalysis has been used to produce the same effects with remarkable success [102]. In particular, it is noteworthy the use of TiO_2 to eliminate pathogenic agents in water sources from sunny regions of isolated rural communities of less-favoured countries, where the required equipment to produce ozone is not available [103].

The integration between ozone and photo-Fenton or TiO_2-photocatalysis is currently under discussion and fewer applications are reported. These are mainly related to the treatment of cellulose bleaching effluents [104], textile effluents [105, 106] and water containing short chain organic acids [107]. The success of more economical and sustainable technologies for wastewater treatment, such as photo-Fenton and TiO_2-photocatalysis, has eclipsed the development of such combined technologies.

3. Biological wastewater treatment

Biological treatment is the most common, economically and environmentally attractive method used for wastewaters remediation in comparison with other physical and chemical treatments [5]. There are two main categories of conventional microbial-based systems for the remediation of wastewater: aerobic and anaerobic treatment [108]. The former is completed in the presence of oxygen whereas the anaerobic treatment is executed in absence of oxygen. This work is based on aerobic wastewater treatments since it is the most rapid, easy to carry out and effective degradation method for the majority of pollutants [109].

3.1. Principles of aerobic biological wastewater treatment

Aerobic wastewater treatments are primarily based on the bacteria´s capability of assimilating biodegradable organic matter present in a polluted effluent.

Bacteria can be classified on the basis of the way they obtain carbon for their development. Autotrophic organisms obtain carbon from inorganic sources, whereas heterotrophic organisms require organic matter as a food source. Most heterotrophic organisms obtain energy through the use of energy stored in chemical bonds, while autotrophic bacteria can also obtain energy from the light through photosynthesis. Thus, autotrophic bacteria can be classified as chemotropic and phototrophic, respectively [110].

Among the different variants of aerobic wastewater treatment, activated sludge process is the most popular biological treatment [108]. The concept is simple and configuration consists of an aerated reactor where microorganisms grow by assimilating the contaminants in the wastewater. The solids are settled out in a separated clarifier or in the same reactor, depending on the configuration (explained later in the text), and are re-used to consume more contaminants. The complex microbial community used in this process is known as activated sludge and is mainly composed of aerobic heterotrophic bacteria. Their mean chemical composition can be considered as $C_8H_{15}O_4N$ [111], although other formulas have been estimated in the literature [110, 112]. Aerobic heterotrophic bacteria obtain carbon and energy as a result of oxidative processes

of organic matter in the presence of oxygen leading to the growth of the microbes and the release of oxidized products. This process can be represented through Equations 1.50 and 1.51 [110].

$$\textit{Organic matter} + O_2 + \textit{bacteria} \longrightarrow CO_2 + H_2O + \textit{other oxidized products} + \textit{energy} \quad (1.50)$$

$$\textit{Organic matter} + \textit{bacteria} + \textit{energy} \longrightarrow \textit{new bacteria cells} \quad (1.51)$$

In absence of organic matter, bacterial oxygen consumption continues as a result of a progressive auto-oxidation process of the cellular mass known as endogenous respiration. To explain this phenomenon, different models of general active sludge behaviour have been defined by the International Water Association (IWA). Figure 1.5 shows a simple approximation of the activated sludge behaviour that is known as Activated Sludge Model nº1 (ASM 1) [113].

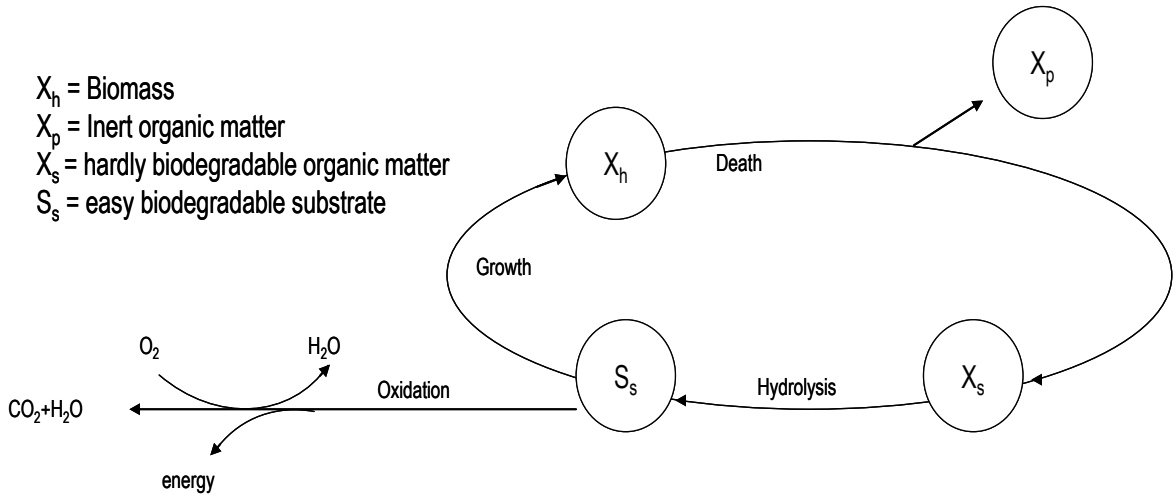

Figure 1.5. Activated Sludge Model nº1 for activated sludge [113]

As seen in Figure 1.5, once the biomass dies, it is divided into inert organic matter (X_p) and biodegradable organic matter (X_s) that after hydrolysis can be used endogenously for the cellular maintenance through the above process known as endogenous respiration. Nevertheless, the amount of biomass generated by means of endogenous respiration is lower that the amount of dead biomass. For that reason, the biomass population will disappear in absence of organic substrate [114].

Although activated sludge is mainly composed of aerobic heterotrophic bacteria, fungus, protozoa and other minority microorganisms can also be present. In addition, a limited number of autotrophic microorganisms exist in the consortia that obtain energy by oxidizing ammonia to nitrate in a process known as nitrification [110].

Apart from organic matter, oxygen, and nitrogen, microorganisms also require a range of nutrients to grow such as phosphorous and trace elements (i.e., mainly potassium, sodium, calcium, magnesium, chloride and iron). Otherwise, the cellular growth can slow down or stop. These elements must be present at a given ratio in order to give a suitable growth. Many industrial effluents are nutrient deficient, thus mainly nitrogen and/or phosphorous must be added. The ratio at which nutrients should be supplied is contentious, with COD : N : P ratios of 100 : 20 : 1 [115], 250 : 7 : 1 [116] and 100 : 10 : 1, and trace sulphur [117] quoted in the literature.

Beyond nutrient requirements, other factors can affect the effectiveness of biological treatment such as the nature of organic matter and the environmental conditions. The information about the former is essential since toxic and non biodegradable compounds can not be assimilated by the biomass without the presence of specific previously adapted microorganisms [118]. On the other hand, pH and temperature are other environmental factors affecting biodegradability. Moreover, metabolic reactions occur faster at optimum pH, usually defined as 6-8, and optimum temperature defined between 25 and 33 ^{o}C [108].

As mentioned previously, in the activated sludge process, organic matter is removed from solution by biological metabolism, oxygen is consumed by the organisms and new cell mass is synthesised. Based on an average data that cover a large variety of wastewater substrates, an excess sludge production of 0.55 mg per mg COD consumed during the wastewater treatment has been considered [119]. This sludge production excess is the main drawback of biological treatment since a posterior management is required prior to its disposal. The goals of sludge treatment are to stabilize, to reduced odours, to remove some of the water, to decompose some of the organic mater and to kill disease causing organisms. A typical sludge treatment involves thickening, dewatering, and stabilization process followed by a main disposal method (i.e., incineration, agricultural land application or landfill disposal) [120].

3.2. Basic types of aerobic biological systems for wastewater treatment

A fundamental classification of biological systems can be completed by considering the aggregation state of the biomass. Thus, there are basically two types of biological wastewater treatment technologies, suspended growth and immobilised growth biological systems.

Suspended growth biological systems rely on mixing to keep microorganisms in suspension, and to ensure that they are in continuous contact with as much substrate as possible. In the immobilised growth configurations, microorganisms are attached to a solid medium and the wastewater passes over the medium as a film. Immobilised growth biological systems are advantageous compared to suspended growth systems when treating wastewater with a high concentration of pollutants, because with this kind of reactors a higher cellular density is possible [108]. Moreover, it has been demonstrated that immobilized microbial systems greatly improve bioreactor efficiency; for instance, increasing process stability and tolerance to shock loadings, allowing higher treatment capacity per biomass unit and generating relatively less biological sludge [121]. Nevertheless, the quantification of biomass is not possible when using immobilised growth reactors. Therefore, since the concentration of the treated effluent used in this work was low and the characterization of biomass was desired, suspended growth systems were used to assess biodegradability.

Among the common types of suspended growth configurations based on activated sludge technology, continuous flow and batch systems are the most utilized. The batch operation is the oldest type and a modern version of this configuration is called Sequencing Batch Reactor (SBR) [108]. Research on SBRs began in the 1970's [122], although in 1914 Arden and Lockett already designed reactors based on the principles of the SBR technology [123]. This work has used SBR to evaluate the biological treatment of target effluents.

Briefly, the activated sludge continuous flow process consists of a biological reactor coupled to a solids capture device, such as clarifier or solid separator, to remove the biomass. After separation, the biomass is pumped back into the biological reactor to maintain a high concentration of microorganisms. Thus, the obtained effluent is free of biomass in a space-oriented system. Contrary, in the SBR system biomass separation occurs in the biological reactor and not in a separate clarifier. Globally, SBR works under non-steady state conditions with unit

operations that involve appropriate aeration and decantation steps based on a fill-and-draw cyclic operation in the same reactor [124, 125].

Basically, all SBR have five phases in common (Figure 1.6), which are carried out in a sequence as follows:

1. Fill: Raw wastewater is added to the reactor and mixed with the biomass held in the tank.
2. React: The metabolic biological reactions, which are responsible for the compsumption of organic matter in presence of oxygen, are carried out under controlled conditions.
3. Settle: Aeration and mixing are stopped and the sludge is separated from the supernatant.
4. Draw: Supernatant or treated effluent is removed.
5. Idle: This is the time between cycles. This last period consists in an initiative process where the excess of sludge is eliminated. Since idle is not a necessary phase, it is sometimes omitted.

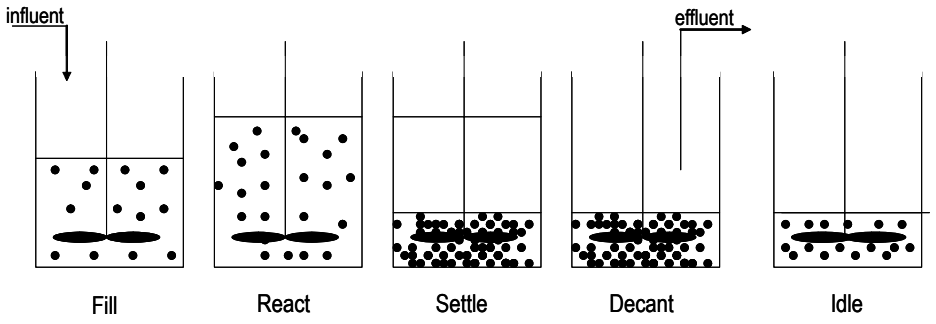

Figure 1.6. Typical sequence operation during one cycle of the SBR process.

The most remarkable advantages of this type of technology when comparing with conventional activated sludge continous flow process include the suitability for simple automatization and manual control reduction, the easy managing of unexpected effects like bad settling (i.e., sludge bulking control), the lower economic cost, and the greater operation flexibility. Moreover, the operation in the fill-and-draw model prevents the washed out of biomass, thus diminishing the necessity of further separation [122].

4. Coupling AOP with biological systems for wastewater treatment

Fundamentally, the biodegradability of a chemical compound refers to its potential for biodegradation. When biological treatment can not completely eliminate pollutants from wastewater (i.e., biorecalcitrant compounds), alternative removal strategies must be considered. The biorecalcitrant character of a chemical compound can be due to the lack of the microbial capacity to assimilate the molecule, or due to its toxicity for microorganisms. Toxicity is described as the irreversible deleterious response of a biologic system to a chemical compound that seriously disrupts metabolic functions or produces death.

Occasionally, after biomass acclimation with the hazardous chemical the biotreatment can be finally achieved [126, 127, 128]. Acclimation is defined as the biomass acquisition of degradation capacity as time proceeds. For a mixed culture, one explanation for acclimation can be the selection of specialized microorganisms [129, 130, 131]. Indeed, it has been demonstrated after much scientific investigation related with microbial biodegradation, that under specific biotreatment (i.e., absence or presence of oxygen, pH, temperature, nutrient medium, etc.) all chemicals are potentially biodegradable. Nevertheless, when speaking in terms of pollution control, wastewater biodegradability refers to its potential for biodegradation under conventional biological treatments.

Concerning wastewater treatment, AOPs are alternative remediation techniques for toxic and non biodegradable hazardous substances. Many examples of non-biodegradable and toxic wastewaters have been proven to lose their toxicity as well as to increase their biodegradability upon a chemical treatment before total mineralization has been achieved [132]. In this way, the coupling between AOP and biological treatments can be used to achieve degradation of target pollutants in a proper economical and environmental way, since operational costs of biological treatment are normally lower than the ones of chemical treatment. The main objective of this coupling is to modify the structure of pollutants by transforming them into less toxic and easily biodegradable intermediates by means of an AOP. Then, the subsequent mineralization can be achieved in an easier and shorter time with the biological treatment [133]. Focusing on this strategy, Sarria et al. [133] developed a general scheme that can be used to plan a combined AOP and biological process for wastewater treatment.

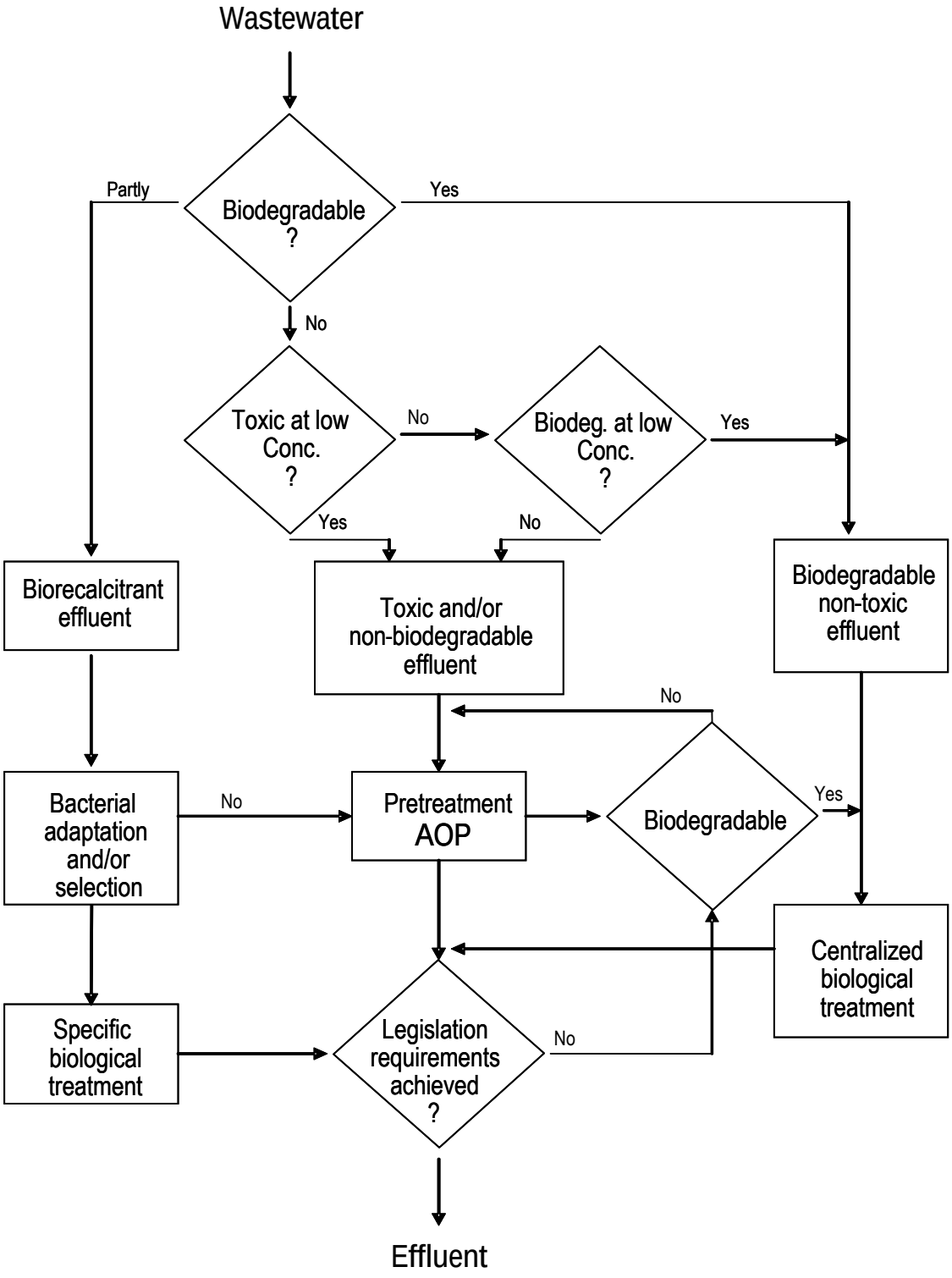

Figure 1.7. General strategy of wastewater treatment [133]

As seen in Figure 1.7, wastewater can be classified as biodegradable, non biodegradable and partially biodegradable. When treating biodegradable wastewater containing relatively small concentrations of recalcitrant compounds (i.e., partly biodegradable), two tactics can be followed. As seen in Figure 1.7, Sarria et al proposed a bacterial adaptation to remove the small non biodegradable fraction of wastewater. Additionally, an inverse strategy can be followed [132]. This means that conventional biological pretreatment can be initially used to remove the biodegradable fraction of wastewater and after that, a chemical treatment can oxidize the remaining refractory fraction. In addition, the biological activity of a bacteria consortium occasionally leads to the formation of some biorecalcitrant or toxic metabolites that may stop the degradation process. In these cases, biological-chemical-biological treatment can solve the problem [132, 134, 135]. The model compounds used in this work are toxic and non biodegradable (i.e., herbicides), therefore only a chemical pre-treatment by means of AOP followed by a biological process has been considered.

When working with a combined chemical and biological process, some practical aspects must be taken into consideration. On the one hand, chemical oxidants and the bioculture can not mix because the chemical oxidants used can cause damaging effects to the microorganisms. Also detrimental effects can be produced by an excessively acid pH. For that reason, pH adjustment to approximately 7 is necessary because acid chemically treated effluents are generally produced due to both, the generation of acid species in the oxidation process, and the required acid pH conditions of some AOPs.

On the other hand, large oxidation times are not necessary when coupling both treatments because excessive chemical oxidation, that generally implies high electrical and chemical reactant consumptions, may result in highly oxidized products possessing little metabolic value for the microorganism [132]. Nevertheless, the solution resulting from the photo-treatment should be free of toxic and non biodegradable compounds. In this way, the assessment of the biodegradability and toxicity along the chemical process is necessary to determine an optimum pretreatment time that guarantees the success of the coupled system. This assessment is widely discussed in Section 6 of this introduction.

4.1. Application of AOP-biological coupled systems to wastewater

Studies that first attempted the strategy of combining chemical and biological processes for wastewater treatment before 1995 were extensively reviewed by Scott and Ollis [132]. Large molecules such as soluble polymers, oils, herbicides and specific industrial effluents were enclosed in the first investigations reported by combining biological treatment with ozone/UV [136], ozone/H_2O_2 [136], Fenton´s reagent [137] and TiO_2-photocatalysis systems [138] among others. From 1990´s until now much effort has been done to develop this strategy. Different chemical techniques, among them the AOPs, have been reported to be efficient when coupling with aerobic or anaerobic biological cultures to treat wastewater. Moreover, a microorganism consortium or a pure microbial culture, acclimated or non-acclimated can be also used in the biological process enhancing, in this way, the possibilities of obtaining an effective removal of contaminants. Sarria et al. [139] presented an overview of works published between 1998 and 2002.

Recently, some works based on the coupled AOP-biological system have been reported demonstrating the applicability of this strategy. Most of the papers published within the last four years (2003-2007) and based on the coupling between AOP and aerobic biological treatment are presented in Table 1.3, based on the structure proposed by Scoot and Ollis [132]. The proposed systems mainly include ozone, ozone/UV, ozone UV/H_2O_2, TiO_2-photocatalysis, Fenton and photo-Fenton. On the other hand wastewaters under study come mostly form textile (azo-dyes) and pesticides contaminated effluents. Finally, the most used methods to assess biodegradability are the evaluation of BOD_5/COD ratio, Zahn Wellens test, COD and TOC abatement in the subsequent biological reactor, and oxygen uptake rate (OUR). Moreover, much of these works also evaluate the potential toxicity by means of different techniques. All these strategies needed to assess the potential biocompatibility of the phototreated effluents are discussed in Section 6 of this introduction.

Finally, it is also important to highlight the first industrial scale application of an oxidative pre-treatment (photo-Fenton or ozone) coupled to an aerobic immobilized biomass treatment located in Villaricos (Spain) for the treatment of salt water polluted with α-methylphenylglycine [140].

Table 1.3. Studies utilizing AOP coupled to aerobic biological treatment for the degradation of biorecalcitrant compounds. (Grade corresponds to the effectiveness for combined oxidation studies, + modest increase, ++ dramatic increase, - adverse effect.)

Authors	Chemicals Degraded	Concentration	Chemical Oxidation Scheme	Measure of biodegradability	Grade
Lapertot M. et al. [52,141]	pesticides	30 mg·L^{-1}	photo-Fenton	Zahn Wellens	++
Essam T. et al. [142]	chlorophenols	50 mg·L^{-1}	UV/TiO_2, UV/H_2O_2, UV/TiO_2/H_2O_2	COD removal	++
Suarez-Ojeda M.E. et al. [143]	o-cresol wastewater	COD=9500 mg·L^{-1}	Catalytic Wet Air Oxidation	respirometry COD removal	++
Al Momani F. et al. [144]	2,4-dichlorophenol	100 mg·L^{-1}	photo-Fenton	BOD/COD	+
García A. et al. [145]	carbaryl	0.05-0.01 g·L^{-1}	UV/TiO_2	activated sludge respirometry	++
Azadeh A. and Mehrab M.[146]	methyl tert-butyl ether	30 mg·L^{-1}	UV/TiO_2	COD removal	-
Kajitvichyanukul P and Suntronvipart N [147]	hospital wastewater	COD=1350 mg·L^{-1}	photo-Fenton	BOD_5/COD	++
Lafi W. K. and Al-Qodah Z. [148]	pesticides	1000 mg·L^{-1}	O_3/UV	COD removal	++
Tantak N. P. and Chaudhari S. [149]	azo-dyes	50 mg·L^{-1}	Fenton	COD removal	++
Wiszniowski J. et al. [150]	landfill leachate	COD=500 mg·L^{-1}	UVC/TiO_2	activated sludge respirometry	++
Maldonado M.I. et al. [151]	α-methylphenylglycine	500 mg·L^{-1}	ozone	Zahn Wellens	++
García-Montaño J. et al. [152, 153]	azo-dyes	250 mg·L^{-1}	photo-Fenton	BOD_5/COD and respirometry	++
Sudarjanto G. et al. [154]	azo-dyes	COD=100 mg·L^{-1}	UV/H_2O_2	COD removal	++
Gökçen F. and Özbelge T.A. [155]	azo-dyes	1000 mg·L^{-1}	ozone	BOD_5/COD and COD removal	+
Mohanty S. et al. [156]	H-acid	500 mg·L^{-1}	TiO_2	COD removal BOD	+
Contreras S. et al. [157]	2,4-dichlorophenol	-	ozone	TOC removal	++
Al Moami F. et al. [158]	2,4-dichlorophenol	100 mg·L^{-1}	photo-Fenton	BOD_5/COD TOC removal	+
Lopes de Morais J. et al. [57]	landfill leachate	COD=5200 mg·L^{-1}	photo-Fenton and H_2O_2/UV	BOD_5/COD	++
di Laconi C. et al. [159]	tannery wastewater	-	ozone	-	++
Alaton I.A. [160]	penicillin formulation wastewater	COD=615 mg·L^{-1}	ozone and O_3/H_2O_2	BOD_5/COD	+
Fongsatitkul P. et al. [161]	textile wastewater	COD=1047 mg·L^{-1}	Fenton	COD removal	++
In-Ock K. et al. [162]	leachate	COD=920 mg·L^{-1}	UV/H_2O_2	BOD_5/COD	+
Contreras S. et al. [163]	2,4-dichlorophenol	100 mg·L^{-1}	ozone	BOD_5/COD and TOC removal	+

5. Natural interferences in wastewater treatment: humic acids

When polluted water is of natural origin, natural organic matter (NOM) can also be present in solution. Thus the assessment of the wastewater remediation process in presence of such compounds is of practical interest.

Humic substances are typically the major component of NOM in water supplies. They constitute 30-50% of the dissolved organic carbon of NOM in surface waters [164] and generate a carbon concentration that generally ranges from 3 to 20 $mg \cdot L^{-1}$ [165]. Humic substances are derived from soil and are also produced within natural waters and sediments by chemical and biological processes such as the decomposition of plants, algae and microbial material [166]. The elucidation of the complex composition of humic acid has been one of the most important tasks of humus chemistry and many scientists have worked on it. It is known that humic acid is basically composed by phenolic, carbonylic, and carboxylic groups. An empirical formula of $C_{72}H_{43-95}O_{30}N_4 \cdot 0\text{-}38H_2O$ for the basic structures has been proposed [167]. Furthemore, Fukushima and Tatsumi [168], recently published the elemental composition of different natural and commercial samples. The elemental composition for the humic acid used in the present work, purchased from Aldrich, is 51.5% C, 4.8% H, 0.9% N, 37.4% O, 3.3 % S and 2.1% ash.

When treating wastewaters containing humic acid by means of different photochemical AOPs, several observations have been reported. It has been suggested that humic substances can act as sensitizers that produce reactive intermediates such as singlet oxygen, superoxide anion, hydrogen peroxide, solvated electrons or peroxylradicals of humic substances in triplet states [169]. All these species may enhance the efficiency of the degradation process [170, 171].

However, some negative effects on the degradation rates of wastewaters containing humic acid have been also published. The process efficiency can be affected not only by the scavenging of hydroxyl radical by humic acid [172,173] but also because this substance can act as a photon trap [171, 174]. Zepp et al. [175] proposed that the phenolic groups present in the humic substances are responsible for such efficiency reduction.

Furthermore, the adsorption of organic matter onto the humic acid surface has been also investigated [176]. Hence, when evaluating the treatment of water polluted with humic acid, the assessment of pollutants depletion by adsorption onto humic acid surface can not be omitted.

Finally, humic acids can be degraded by intense UV photolysis (i.e, 450 W high-pressure mercury vapour lamp, 500 W xenon short arc lamp, etc. [177,178]).

In the present work the effect of humic acids has been investigated in both, the chemical and the biological treatment. The effect that humic acid has on live biomass form a WWTP must be considered. It is well known that humic acid is an example of a biorecalcitrant non toxic polymeric compound, but it is strongly adsorbed onto the biomass when both are in solution. It has been previously reported that biosorption of humic acid onto live biomass is described by Freundlich isotherms [179] which depicts a monolayer adsorption on a solid surface characterized by an asymmetrical energy distribution (see Chapter 2, Section 4 for bioadsorption studies). The Freundlich isotherm equation is

$$q_e = K_F C_e^{1/n} \qquad (1.52)$$

Where q_e is the amount of humic acid adsorbed per gram of biomass, C_e the equilibrium concentration of humic acid in solution and K_F and $1/n$ are isotherm constants that can be considered as an indicator of adsorption capacity and intensity, respectively [180].

6. Analytical assessment for coupling AOPs with biological treatment

When treating organic matter by means of an AOP, oxidized by-products are generated along the mineralization process. Therefore, the success of the coupling between AOPs and biological treatment may be guaranteed by assessing the potential impact of generated by-products to the biomass.

Biodegradability and toxicity of the generated by-products can be evaluated either by ecotoxicological tests, or by chemical characterization to define the effluent nature. In recent decades, a number of alternative tests have been proposed and applied for the rapid evaluation of biological damage in the environment. Some alternatives for assessing biodegradability and toxicity as well as some chemical analyses based on chromatographic methods are discussed in this section.

6.1. Acute toxicity testing

Toxicity can be classified as acute (short-term, high dose), chronic (long-term, low dose), or subchronic (intermediate-term, high or low-dose). As said previously, when discussing in terms of pollution control, wastewater biodegradability refers to its potential for easy biodegradation under conventional biological treatments. Thus the assessment of acute toxicity is necessary to predict a possible coupling between chemical and biological systems.

Classical bioassays to assess acute toxicity, which involve fish-lethality assays, are too laborious to be widely applicable [181]. Nevertheless, modern, sensitive, straightforward and cost-effective methods are currently well developed and available to establish the toxicity of compounds for aquatic organisms.

Acute toxicity tests using invertebrates, plants, and algae have been used in aquatic risk assessment studies. One of the most common invertebrate toxicity tests uses the crustacean invertebrate species Daphnia magna [182]. The inhibition of growth or mobility after hours or days is used in this test as the indicator of toxicity. Recently, biosensors have been also used to test

toxicity. This method is interesting because of the possibilities of mass production, ease of use, fast response and adaptability to on-line monitoring [183]. Finally, toxicity tests based on bacteriological metabolic activity when faced with a potential toxic compound are also widely used. Several bio-assays using pure bacteria have been standardized and can be classified according to the measured parameter as growth or bacteria multiplication inhibition. Different toxicity tests based on these principles have been revised by Farré and Barceló [181].

The test used in this experimental work is based on the inhibition of the bioluminescence bacteria Vibrio fischery [184] (see Chapter 2, Section 5.2.1. for experimental details). This is a common acute toxicity test, already included in the International Standard Organization (ISO) standard methods list, is easy to manipulate and reproducible, and its precision is high. In the Vibrio fischery test, light emitted from the bacterium is a result of a metabolic process. This metabolic pathway is intrinsically linked to cellular respiration, so disruption of normal cellular metabolism causes a decrease in light production [185].

The last goal of toxicity assays when assessing the coupling between chemical and aerobic biological processes is to determine the potential effect of a toxic sample to activated sludge. The biological response induced in different living organisms perturbed by a chemical substance is diverse because not all microorganisms respond to all toxic substances in the same way [186]. In this way, it is generally recommended to carry out at least two toxicological tests in order to reduce the possibility of missing a particular toxic effect. Moreover, Dalzell et al. [187] suggested that although Vibrio fischery is suitable as a screening test for toxic samples, it should not be used to determine the potential effect to conventional biomass present in a WWTP. In general, Vibrio fischery is more sensitive than bacteria consortia present in the activated sludge and may give an overestimation of the acute toxicity effect. For that reason alternative methods, based directly on the effect of toxics to activated sludge, are investigated. Recent research has been focused on the particularities of different toxicity tests and their comparison [188, 189, 190].

Different methods are proposed in the literature to directly assess toxicity to activated sludge. Some examples of these methods are nitrification inhibition, respiration inhibition, ATP luminescence and, in vivo L-alanine-aminopeptidase inhibition [187]. Among the different existing tests, respirometric measurements were used in the present work to assess the potential effect of toxic samples to activated sludge because of its availability and easy use. Respirometric assays

are based on the direct relation between oxygen consumption and biomass development as explained in Section 3.1 of this introduction. The parameter used to quantify the rate of oxygen consumption by the biomass when assimilating organic matter in a determined time is named Oxygen Uptake Rate (OUR). A common respirometric technique to measure the toxicity of a certain compound consists in evaluating the slope of the dissolved oxygen profile obtained after adding a biodegradable substrate to the solution and comparing it with the slope value obtained when adding a mixture of biodegradable substrate and the possible toxic [191]. Nevertheless, this method can not distinguish toxic biodegradable compounds because the toxic consumption implies oxygen consumption as well. To overcome this difficulty, Guisasola et al. [192] suggest a new procedure based on the characterisation of the toxic consumption and the OUR profile obtained during the toxic consumption. The protocol used in this work to determine toxicity was carried out following Guisasola et al. recommendations (see Chapter 2, Section 5.2.4. for experimental details) and is compared with results obtained with Vibrio fischery tests.

Finally, it must be noted that the results of the laboratory toxicity tests do not necessarily correlate with the impact that an effluent has on a real wastewater treatment; nevertheless, such tests provide an indication of the relative hazard posed by a specific pollutant. Thus, the assessment of toxic effects to the biomass of an aerobic wastewater treatment has been investigated by measuring the Volatile Suspended Solids (VSS), which is a measure of active biomass in the activated sludge (see Chapter 2, Section 5.2.5. for more experimental details).

6.2. Ready biodegradability testing

Biodegradability can be assessed by ready biodegradability tests and inherent biodegradability tests. Ready biodegradability indicate if a compound is degradable under natural conditions without any problem whereas inherent biodegradability is related to its biodegradation in favourable conditions (i.e., pollutants-microorganisms ratio shifted in favour of the microorganisms) [193]. Moreover, since the 1980s, different predictive models have appeared to obtain qualitative and/or quantitative information concerning the biodegradability characteristics of chemicals [194]. Nevertheless, probably due to their innovation, they are not still well validated [193]. Some examples of these programs are Qualitative Substructure Model [195], Biodeg Models and Survey Models [196].

In this work inherent-biodegradability tests have been used to demonstrate the biorecalcitrant behaviour of initial compounds whereas a ready-biodegradability test has been used to assess the biodegradation of phototreated pollutants. Thus, only ready-biodegradability tests are discussed in this section.

Less discussion is necessary when using ready biodegradability tests because these methods are internationally standardized and they are mostly based on the determination of global parameters such as Biochemical Oxygen Demand (BOD), carbon dioxide evolution (CO_2), Total Organic Carbon (TOC) or Chemical Oxygen Demand (COD). Nevertheless, 28 days are necessary according to international standardized methods to perform tests [197]. In this way, simple and time-effective methods to assess biodegradability have been used and investigated in this work.

The most traditional time-effective index to measure biodegradability is the 5-days BOD/COD biodegradability index. It is commonly considered that a BOD_5/COD ratio value of 0.4 corresponds to an effluent which is totally biodegradable in a real WWTP [45]. On the other hand, ready-biodegradability assessment by means of respirometric measurement is well considered because the prompt response of activated sludge is thought to be more realistic that the sometimes misleading BOD_5/COD value [198] (see Chapter 2, Section 5.2.4. for more experimental details).

6.3. By-products identification by chromatographic methods

Much attention has been paid to the application of chemical analyses for evaluating toxicity and biodegradability of wastewater [181]. The identification of by-products generated during a chemical treatment may help us to understand the chemical nature of the effluent and predict a possible biological compatibility. Nevertheless this procedure is not always easy. Liquid chromatography-mass spectrometry (LC-MS) or gas chromatography-mass spectrometry (GC-MS) are the best methods to identify the nature of pollutants present in wastewaters.

During the degradation process of large organic pollutants by means of an AOP, more polar small compounds are normally generated. Despite the extensive use of GC-MS techniques

drawbacks like the difficulty of direct water injections or the loss of polar compounds may limit their application when analysing by-products generated along a mineralization process [199]. The characteristic GC-MS limitations can be overcome by LC-MS techniques. The adequate modality of LC-MS to analyse polar compounds is the so-called Normal Phase (NP-HPLC). Nevertheless, the organic, nonpolar eluents used in this modality, often based on hexane, produce an incompatibility with mass detectors since ionization is not easily achieved in these eluents [200]. On the other hand, the main problem associated to the use of the Reverse Phase modality (RP-HPLC) is that polar compounds can not be analysed because they are not retained in the apolar stationary phase and coelutions prevent the separation and identification of a wide range of compounds.

To enable the analysis of polar compounds while still using mass spectrometry as a comprehensive and sensitive detector, Hydrophilic Interaction Liquid Chromatography (HILIC) is one alternative. HILIC is similar to Normal Phase chromatography as a polar stationary phase, like diol, silica or amine [201, 202, 203] is used. The separation in HILIC is based on the distribution between stationary and mobile phases and differs from Normal Phase chromatography in the mobile phase which is based on an aqueous–organic mixture with water being the most abundant solvent. The retention of polar compounds is increased when the proportion of organic solvent is increased. Alpert et al. [200] suggested that the retention mechanism involves partion of the analyte between the mobile phase and a layer of mobile phase enriched with water onto the stationary phase. In this way the elution order in HPLC (HILIC) is more or less the opposite of that seen in RP-HPLC. So HILIC coupled with mass spectrometry appears to be an appropriate method for the determination of the concentration and structure of small polar compounds.

Currently, there is a need for more studies on different types of polar stationary phases in order to gain a better understanding of the HILIC separation. A window is open for further development of the by-products determination studies required in the field of coupling chemical and biological treatments for the remediation of wastewaters.

7. Life Cycle Assessment (LCA)

Nowadays, every chemical treatment must be developed taking into account its global impact on the environment. With this objective, a Life Cycle Assessment (LCA) has been used in the present work as a tool for the evaluation of the environmental impact of some of the proposed processes for the removal of herbicides from water. In this sense, the removal of herbicides from water by means of AOP and coupled AOP-biological system has been evaluated. Moreover, the possibility of using solar light as the driving force to conduct the AOP has been also considered.

LCA is a powerful management tool used to facilitate understanding and characterization of the range and scope of environmental impacts of a product, process or service. LCA investigations started in the late 1960´s [204], although until 1990 there was not a common theoretical framework to use LCA as a standardized methodology. SETAC (the Society of Environmental Toxicology and Chemistry) was the first scientific organization that provided a basis for the development of LCA [205]. After that, in 1994 the International Standard Organization (ISO) produced the first complete series of LCA standards. Traditionally there were four ISO standards specifically designed for LCA application:

-ISO 14040 (1997): Principles and Framework [206]

-ISO 14041 (1998): Goal and Scope definition and inventory analysis [207]

-ISO 14042 (2000): Life Cycle Impact assessment [208]

-ISO 14043 (2000): Interpretation [209]

Currently two new standards have been published that replace these four standards

-ISO 14040 (2006): Principles and Framework [210]

-ISO 14044 (2006): Requirements and Guidelines [211]

The new 14044 standard replaces the 14041, 14042 and 14043 but there have been no major changes in the context.

In ISO 14040, LCA is defined as:

"A technique for assessing the environmental aspects and potential impacts associated with a product by:

- compiling an inventory of relevant inputs and outputs of a product system,

- evaluating the potential environmental impacts associated with those inputs and outputs,

- interpreting the results of the inventory analysis and impact assessment phases in relation to the objectives of the study."

This technique examines all the stages implicated in a life cycle of the product, service or process submitted for analysis "from cradle to grave". The environmental impacts are calculated by evaluating the inputs (initial gathering of raw materials from the earth) and outputs (residuals returned to the earth in the form of emissions) and then, by converting them into their effects on the environment. Thus, LCA provides a picture of the interactions of an activity with the environment. By providing this complete picture, major environmental impacts and "hot-spots" may be detected and improved. Moreover, if different LCAs are conducted for alternative products, processes or services, the comparison of their overall environmental impacts is possible, thus giving the chance of selecting the best option, from an environmental point of view, among other alternatives [212].

Although useful, LCA is not a complete assessment technique. Deficiencies in address timed and localised impacts, ignorance of the non linear character of some processes and the lack of economic and social impacts make LCA part of a "tool box" [213] where other strategies such as Life Cycle Costing (LCC), Risk Assessment (RA) and Substance Flow Analysis (SFA) may overcome LCA deficiencies. Moreover, availability of data is another limitation because although databases are being developed in various countries, in practice data are frequently obsolete, incomparable, or of unknown quality [214]. Taking all this into consideration, this work has performed a LCA study as a first step of the environmental assessment of the water remediation techniques proposed.

7.1. LCA methodology

The ISO 14.040 standard establishes four basic stages for LCA studies. These stages are represented in Figure 1.8.

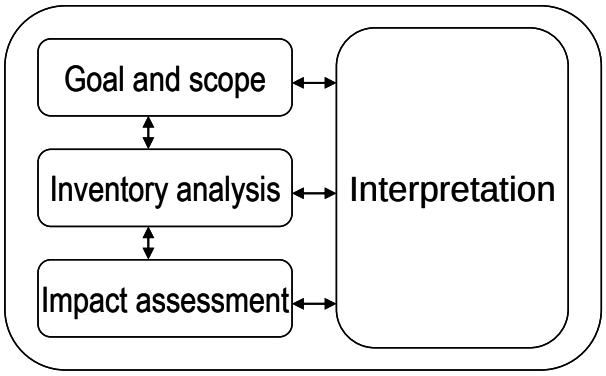

Figure 1.8. Stages in a LCA [206]

Goal and Scope definition

In this stage the purpose, scope, and main hypothesis considered in the LCA are defined. The purpose of the study is formulated in terms of the exact question, target audience and intended application [213]. The scope implies the definition of the system under study, their boundaries, the quality of the data used, the main hypothesis as well as the limitations of the study.

In this step it is also necessary to define a functional unit to enable different systems to be treated as functionally equivalent [214]. Thus, the functional unit is a quantified description of the performance of the product, process or service systems, for use as a reference unit. For example, this work has considered a specific percentage of TOC removal at the end of the water treatment as a functional unit to be able to compare different water treatments.

Inventory analysis

The inventory analysis is the process of accumulating data to quantify the inputs and the outputs of the defined system per functional unit. The inputs included (a) production of consumed electricity, including extractions of resources, transport and electricity production, (b) production of chemicals, including extraction of resources, production and transport, whereas outputs

subsume air, water and soil emissions generated through the considered scenarios as well as solid final wastes.

Impact assessment

Life Cycle Impact Assessment (LCIA) is the process that identifies and characterizes the potential effects produced in the environment by the system under study [208]. In this step, the weighted environmental interventions are classified in different impact categories or indicators based on anticipated effects on the environment.

There are several methods available for performing the characterization of environmental impacts, with the use of equivalence factors for the different impact categories being the typical methods. These equivalence factors indicate how much a substance contributes to an impact category compared to a reference substance. For example, for Global Warming the reference is carbon dioxide, thus the Global Warming contribution by other substances is then expressed in terms of the equivalent amount of carbon dioxide that would have the same effect [215].

Interpretation

This is the last step of LCA where conclusions are obtained. Interpretation involves a review of all the stages in LCA process, in order to prove the consistency of the assumptions and the quality of the selected data.

7.2. LCA application to AOP

Initially LCA was designed to analyse the environmental impacts of a product to provide a quantitative assessment of the environmental impact over their entire life cycle, with the goal of improving the manufacturing process. Nevertheless, the use of this tool to environmentally assess processes has increased in the engineering field because life-cycle studies provide a new way of analysing the benefits of pollution abatement [216]. In particular concerning wastewater treatment many studies of LCA have been reported [217, 218, 219, 220, 221, 222, 223]. Nevertheless, relating to AOP and coupled AOP-biological systems for wastewater treatment processes less information is available [224, 225, 226, 227]. Therefore, the present work

contributes to increasing the importance of this environmental tool in the assessment of wastewater process by means of this methodology.

8. Scope and aim of this thesis

The aim of this thesis is to explore new ways of remediation of water polluted with hazardous herbicides by combining chemical and biological treatments.

In the first part of the work, effective Advanced Oxidation Processes (AOPs) for the treatment of water polluted with different herbicides are investigated. The AOPs selected for the examination are photo-Fenton, TiO_2-photocatalysis, ozone/UV, photo-Fenton/ ozone and TiO_2-photocatalysis/ ozone. The reaction yield is monitored in terms of mineralization and herbicide concentration abatement. Moreover, in order to evaluate a possible coupling between chemical and biological treatments, different methods to analyze toxicity and biodegradability of phototreated effluents are employed and compared from a practical point of view.

The second part is based on the coupling between chemical and biological treatments. Although the best results concerning chemical mineralization efficiency are obtained with the photo-Fenton/ozone method, the single photo-Fenton technique is selected to perform this experimental part due to their lower operational costs comparing to those related to the ozonation process. The reactant dose of the chemical treatment is selected by means of multivariate experimental design. The biocompatibility of the phototreated solution is finally assessed by feeding a bench-scale aerobic Sequencing Batch Reactor (SBR). Furthermore, this study is improved with both, the appraisal of the effect of natural organic matter present in solution when coupling the chemical and biological treatment, and the analysis of by-products generated along the mineralization process.

Finally, the global environment impact of the treatment of water polluted with herbicides by means of the chemical/biological coupled system is assessed. This evaluation is carried out by means of Life Cycle Assessment (LCA) methodology. The environmental assessment of single photo-Fenton systems assisted with both artificial and natural sunlight is also performed and results are compared with those obtained from the chemical/biological coupled system.

REFERENCES TO CHAPTER 1

[1] Van Rensen J.J.S (1989). Herbicides interacting with photosystem II. In: Dodge A. D. (Ed). Herbicides and plant metabolism. Cambridge University. Cambridge, UK.

[2] Cobb A.H. and Kirkwood R. C. (2000). Challenges for herbicide development. In: Cobb A.H. and Kirkwood R. C. (Ed) Herbicides and their mechanisms of action. Sheffield Academic Press. England, UK.

[3] Barceló D. (2003). Emerging pollutants in water analysis. Special issue. Trends Anal. Chem. 22, xiv-xvi.

[4] European Commission (2000). The Water Framework Directive. EC directive 2000/60/EC.

[5] Chiron S., Fernández-Alba A., Rodríguez A. and García-Calvo E. (2000). Pesticide chemical oxidation: State of the art. Water Res. 34, 366-377.

[6] Pera-Titus M., García-Molia V., Baños M.A., Giménez J. and Esplugas S. (2004). Degradation of chlorophenols by means of advanced oxidation processes: a general review. Appl. Catal. B-Environ. 47, 219-256.

[7] Glaze W.H., Kang J.W. and Chapin D.H. (1987). The chemistry of water treatment processes involving ozone, hydrogen peroxide and ultraviolet radiation. Ozone Sci. Eng. 9, 335-352.

[8] Haag W.R. and Yao C.D. (1992). Rate constant for reaction of hydroxyl radicals with several drinking water contaminants. Environ. Sci. Technol. 26, 1005-1013.

[9] Buxton G.V., Greenstock C.L., Helman W.P. and Ross A.B. (1988). Critical review of rate constants for reactions of hydrated electrons, hydrogen atoms and hydroxyl radicals ($OH^{\cdot}/O^{\cdot-}$) in aqueous solutions. J. Phys. Chem. Ref. Data. 17, 513-886.

[10] Legrini O., Oliveros E. and Braun A.M. (1993). Photochemical processes for water treatment. Chem. Rev. 93, 671-698.

[11] Hoigné J. (1988). The chemistry of ozone in water. In: Stucki S. (Ed). Process technologies for water treatment. Plenum Press Corp. New York, USA.

[12] De Laat J., Truong Le G. and Legube B. (2004). A comparative study of the effects of chloride, sulphate and nitrate ions on the rates of decomposition of H_2O_2 and organic compounds by Fe^{2+}/ H_2O_2 and Fe^{2+}/ H_2O_2. Chemosphere. 55, 715-723.

[13] Schmelling D.C., Gray K.A. and Kamat P.V. (1997).The influence of solution matrix on the photocatalytic degradation of TNT in TiO_2 slurries. Water Res. 31, 1439-1447.

[14] Glaze W.H. and Kang J.W. (1989). Advanced oxidation processes. Test of a kinetic model for the oxidation of organic compounds with ozone and hydrogen peroxide in a semi batch reactor. Ind. Eng. Chem. Res. 28, 1580-1587.

[15] Andreozzi R., Caprio V., Insola A. and Marotta R. (1999). Advanced oxidtion processes (AOP) for water purification and recovery. Catal. Today. 53, 51-59.

[16] Domènech X., Jardim W.F. and Litter M. (2001). Procesos Avanzados de Oxidación para la eliminación de contaminantes. In: Blesa M.A. (Ed) Eliminación de contaminantes por Fotocatálisis Heterogénea .CYTED. La Plata, Argentina.

[17] Safarzadeh-Amiri A., Bolton J.R. and Cater S.R. (1996). The use of iron in advanced oxidation technologies. J. Adv. Oxid. Technol. 1, 18-26.

[18] Sánchez L., Domènech X., Casado J. and Peral J. (2003). Solar activated ozonation of phenol and malic acid. Chemosphere. 50, 1085-1093.

[19] Linsebigler A.L., Lu.G. and Yates J.T. (1995). Phototcatalysis on TiO_2 surfaces: Principles, mechanisms, and selected results. Chem. Rev. 95, 735-758.

[20] Bauer R., Waldner G., Fallmann H., Hager S., Klare M., Krutzler T., Malato S. and Maletzky P. (1999). The photo-Fenton reaction and the TiO_2/UV process for waste water treatment − novel developments. Catal. Today. 53, 131-144.

[21] Pignatello J., Oliveros E. and MacKay A. (2006). Advanced oxidation processes for organic contaminant destruction based on the Fenton reaction and related chemistry. Crit. Rev. Env. Sci. Tech. 36, 1-84.

[22] Fenton H.J.H. (1894). Oxidation of tartaric acid in presence of iron. J. Chem. Soc. 65, 899-910.

[23] Haber F. and Weiss J. (1934). The catalytic decomposition of hydrogen peroxide by iron salts. Proc. Roy. Soc. A. 134, 332-351.

[24] Rigg T., Taylor W. and Weiss J. (1954). The rate constant of the reaction between hydrogen peroxide and ferrous ions. J. Chem Phys. 22, 575-577.

[25] Gallard H., De Laat J. and Legube B. (1998). Influence du pH sur la vitesse d´oxydation de composés organiques par FeII/H_2O_2: Mécanismes réactionnels et modélisation. N.J. Chem. 22, 263-268.

[26] Barb W.G., Baxendale J.H., George P. and Hargrave K.R. (1951). Reactions of ferrous and ferric ions with hydrogen peroxide. Part I. The ferrous ion reaction. Trans. Faraday Soc. 47, 462-500.

[27] Barb W.G., Baxendale J.H., George P. and Hargrave K.R. (1951). Reactions of ferrous and ferric ions with hydrogen peroxide. Part II. The ferric ion reaction. Trans. Faraday Soc. 47, 591-616.

[28] Kremer M.L. and Stein G. (1959). Catalytic decomposition of hydrogen peroxide by ferric perchlorate. Trans. Faraday Soc. 55, 959-73.

[29] Kremer M.L. (1962). Nature of intermediates in the catalytic decomposition of hydrogen peroxide by ferric ions. Trans. Faraday Soc. 58, 702-707.

[30] Walling C. (1975). Fenton's reagent revisited. Acc. Chem. Res. 8, 125-131.

[31] Bossmann S.H., Oliveros E., Göb S., Siegwart S., Dahlen E.P., Payawan L., Jr Straub M., Wörner M. and Braun A.M. (1998). New evidence against hydroxyl radicals as reactive intermediates in the thermal and photochemically enhanced Fenton reactions. J. Phys. Chem. A. 102, 5542-5550.

[32] Pignatello J.J., Liu D. and Huston P. (1999). Evidence for an additional oxidant in the photoassisted Fenton reaction. Environ. Sci. Technol. 33, 1832-1839.

[33] Sychev A.Y. and Isaak V.G. (1995). Iron compounds and the mechanism of the homogeneous catalysis of the activation of O_2 and H_2O_2 and of the oxidation of organic substrates. Russ. Chem. Rev. 64, 1105-1129.

[34] Hawker P.N. and Twigg M.V. (1994). Iron: inorganic & coordination chemistry. In: King P.B. (Ed.) Encyclopaedia of Inorganic Chemistry. Wiley. Chichester, UK.

[35] Pignatello J. (1992). Dark and photoassisted Fe^{3+}- catalyzed degradation of chlorphenoxy herbicides by hydrogen peroxide. Environ. Sci. Technol. 26, 944-951.

[36] Chen R. and Pignatello J.J. (1997). Role of quinone intermediates as electron shuttles in Fenton and photoassisted Fenton oxidations of aromatic compounds. Environ. Sci. Technol. 31, 2399-2406.

[37] Sylva R.N. (1972). The hydrolysis of iron (III). Rev. Pure Appl. Chem. 22, 115-130.

[38] Balzani V. and Carassiti V. (1970). Photochemistry of coordination compounds. Academic Press, New York, USA. 777-782.

[39] Sima J. and Makanova J. (1997). Photochemistry of iron (III) complexes. Coord. Chem. Rev. 160, 161-189.

[40] Faust B.C. and Hoigné J. (1990). Photolysis of iron (III)- hydroxyl complexes as sources of hydroxyl radicals in clouds, fog and rain. Atmos. Environ. 24, 78-89.

[41] Hatchard C.G. and Parker C.A. (1956). A new sensitive chemical actinometer II. Potassium ferrioxalate as a standard chemical actinometer. Proc. Roy. Soc. A. 235, 518-536.

[42] Hislop K.A. and Bolton J.R. (1999). The photochemical generation of hydroxyl radicals in the UV-vis/ferrioxalate/H_2O_2 System. Environ. Sci. Technol. 33, 3119-3126.

[43] Safarzadeh-Amiri A., Bolton J.R. and Cater S.R. (1996). Ferrioxalate-mediated solar degradation of organic contaminants in water. Sol. Enrgy. 56, 439-443.

[44] Kiwi J., López A. and Nadtochenko V.(2000). Mechanism and kinetics of the OH radical intervention during Fenton oxidation in the presence of a significant amount of radical scavenger (Cl^-). Environ. Sci. Technol. 34, 2162-2168.

[45] Chamarro E., Marco A. and Esplugas S. (2001). Use of Fenton Reagent to improve organic chemical biodegradability. Water Res. 35, 1047-1051.

[46] Chan K.H. and Chu W. (2002). The dose and ratio effects of Fe^{2+} and H_2O_2 in Fenton's process on the removal of atrazine. Environ. Technol. 24, 703-710.

[47] Rogríguez. M., Sarria V., Esplugas S. and Pulgarín C. (2002). Photo-Fenton treatment of a biorecalcitrant wastewater generated in textile activities: biodegradability of the phototreated solution. J. Photoch. Photobio. A. 151, 129-135.

[48] Eisenhauer H.R. (1964). Oxidation of phenolic wastes. J. Water Pollut. Contr. Fed. 36, 1116-1128.

[49] Torrades F., García-Montaño J., García-Hortal J.A., Núñez L., Domènech X. and Peral J. (2004). Decolorization and mineralization of homo-and hetero-bireactive dyes under Fenton and photo-Fenton conditions. Color. Technol. 120, 188-194.

[50] Pérez M., Torrades F., García-Hortal J.A., Domènech X. and Peral J. (2002). Removal of organic contaminants in paper pulp treatment effluents under Fenton and photo-Fenton conditions. Appl. Catal. B-Environ. 36, 63-74.

[51] Amat A.M., Arques, A., López, F. and Miranda, M.A. (2005). Solar photo-catalysis to remove paper mill wastewater pollutants. Sol. Energy. 79, 393-401.

[52] Lapertot M., Pulgarín C., Fernández-Ibáñez P., Maldonado M.I., Pérez-Estrada L., Oller I., Gernjak W. and Malato S. (2006). Enhancing biodegradability of priority substances (pesticides) by solar photo - Fenton. Water Res. 40, 1086-1094.

[53] Maldonado M.I., Passarinho P.C., Oller I., Gernjak W., Fernández P., Blanco J. and Malato S. (2007). Photocatalytic degradation of EU priority substances: A comparison between TiO_2 and Fenton plus photo-Fenton in a solar pilot plant. J. Photoch. Photobio. A. 185, 354-363.

[54] Fallmann H., Krutzler T., Bauer R., Malato S. and Blanco J. (1999). Applicability of the photo-Fenton method for treating water containing pesticides. Catal. Today. 54, 309-319.

[55] Ormad M.P., Mosteo R., Ibarz C. and Ovelleiro J.L. (2006). Multivariate approach to the photo-Fenton process applied to the degradation of winery wastewaters. Appl. Catal. B-Environ. 66, 58-63.

[56] Gernjak W., Maldonado M.I., Malato S., Cáceres J., Krutzler T., Glaser A. and Bauer R. (2004). Pilot-plant treatment of olive mill wastewater (OMW) by solar TiO_2 photocatalysis and solar photo-Fenton. Sol. Energy. 77, 567-572.

[57] Lopes de Morais J. and Zamora P.P. (2005). Use of advanced oxidation processes to improve the biodegradability of mature landfill leachates. J. Hazard. Mater. 123, 181-186.

[58] Amat A.M., Arques A., Miranda M.A. and Segui, S. (2004). Photo-Fenton reaction for the abatement of commercial surfactants in a solar pilot plant. Sol. Energy. 77, 559-566.

[59] Lunar L., Sicilia D., Rubio S., Pérez-Bendito D. and Nickel, U. (2000). Degradation of photographic developers by Fenton's reagent: condition optimization and kinetics for metol oxidation. Water Res. 34, 1791-1802.

[60] Blanco J., Malato S., Maldonado M.I., Vicent M., Vicent J.P., Sánchez M. and Myro E. (2004). The Albaida Plant: first commercial step in solar detoxification. Global Symposium on Recycling, Waste Treatment and Clean Technology. REWAS´04, Madrid, Spain.

[61] Martínez F., Calleja G., Melero J.A. and Molina R. (2007). Iron species incorporated over different silica supports for the heterogeneous photo - Fenton oxidation of phenol. Appl. Catal. B-Environ. 70, 452-460.

[62] Maletzky P., Bauer R., Lahnsteiner J. and Pouresmael B. (1999). Immobilization of iron ions on Nafion and its applicability to the photo-Fenton method. Chemosphere. 38, 2315-2325.

[63] Yuranova T., Enea O., Mielczarski E., Mielczarski J., Albers P. and Kiwi J. (2004). Fenton immobilized photo-assisted catalysis through a Fe/C structured fabric. Appl. Catal. B-Environ. 49, 39-50.

[64] Fahmi A., Minot C., Silvi B. and Causa M. (1993). Theoretical analysis of the structures of titanium dioxide crystals. Phys. Rev. B. 47, 11717–11724.

[65] Diebold U. (2003). The Surface science of titanium dioxide. Surf. Sci. Reports. 48, 53-229.

[66] Hoffmann M.R. Martin S.T. Choi W. Bahnemman D.W. (1995). Environmental applications of semiconductor photocatalysis. Chem. Rev. 95, 69-96.

[67] Agrios A.G., Gray K.A. and Weitz E. (2003). Photocatalytic transformation of 2,4-Trichlorophenol on TiO_2 under Sub-Band-Gap illumination. Langmuir. 19, 1402-1409.

[68] Mills A. Le Hunte S. (1997). An overview of semiconductor photocatalysis. J. Photoch. Photobio. A. 108, 1-35.

[69] Mills A. and Lee S-K. (2002). A web-based overview of semiconductor photochemistry-based current commercial applications. J. Photoch. Photobio. A. 152, 233-247.

[70] Fujishima A. and Honda K. (1972). Electrochemical photolysis of water at a semiconductor electrode. Nature. 238, 37-38.

[71] Carey J.H, Lawrence J. and Tosine H.M. (1976). Photodechlorination of PCB's in the presence of titanium dioxide in aqueous suspensions. Bull. Environ. Contam. Toxicol. 16, 697-701.

[72] Bahnemann D. (2004). Photocatalytic water treatment: solar energy applications. Sol. Energy. 77, 445-459.

[73] Herrmann J.M. (2005). Heterogeneous photocatalysis: state of the art and present applications. Top. Catal. 34, 49-65.

[74] Litter M. (1999). Heterogeneous photocatalysis: Transition metal ions in photocatalytic systems. Appl. Catal. B-Environ. 23, 89-114.

[75] Ilisz I. and Dombi A. (1999). Investigation of the photodecomposition of phenol in near-UV-irradiated aqueous TiO_2 suspensions. II. Effect of charge-trapping species on product distribution. Appl. Catal. A-Gen. 180, 35-45.

[76] Augustynski J. (1988). Aspects of photoelectrochemical and surface behaviour of titanium(IV) oxide. J. Struct. Bonding. 69, 1-61.

[77] Fox M.A. and Dulay M.T. (1993). Heterogeneous photocatalysis. Chem. Rev. 93, 341-357.

[78] Abdullah M., Low G.K.C. and Matthews R.W. (1990). Effects of common inorganic anions on rates of photocatalytic oxidation of organic carbon over illuminated TiO_2. J. Phys. Chem. 94, 6820-6825.

[79] Hoigné J. and Bader H. (1976). The role of hydroxyl radical reactions in ozonation processes in aqueous solutions. Water Res. 10, 377-386.

[80] Staehelin J. and Hoigné J. (1982). Decomposition of ozone in water: Rate of initiation by hydroxide ions and hydrogen peroxide. Environ. Sci. Techol. 16, 676-681.

[81] Sehested K., Holeman J. Bjergbakke E. and Hart E.J. (1984). Formation of ozone in the reaction of hydroxyl with O_3^- and the decay of the ozonide ion radical at pH 10-13. J. Phys. Chem. 88, 269-273.

[82] Von Gunten U. (2003). Ozonation of drinking water: Part I. Oxidation kinetics and product formation. Water Res. 37, 1443-1467.

[83] Roche P., Volk C., Carbonnier F. and Paillard H. (1994). Water oxidation by ozone or ozone/hydrogen peroxide using the OZOTEST or PEROXOTEST methods. Ozone Sci. Eng. 16, 135-155.

[84] Yao C.C.D. and Haag W.R. (1991). Rate constants for direct reactions of ozone with several drinking waters contaminants. Water Res. 25, 761-773.

[85] Meijers R.T., Oderwald-Muller E.J., Nuhn P.A.N.M. and Kruithof J.C. (1995). Degradation of pesticides by ozonation and advanced oxidation. Ozone Sci. Eng. 17, 673-686.

[86] Peyton G.R. (1990). Oxidative treatment methods for removal of organic compounds from drinking water supplies. In: Ram N.M., Christman R.F. and Canto K.P. (Eds). Significance and treatment of volatile organic compounds in water supplies. Lewis Publisher. Boston, USA.

[87] Peyton G.R. and Glaze W.H. (1988). Destruction of pollutants in water with ozone in combination with ultraviolet light . Part 3. Photolysis of aqueous solutions. Environ. Sci. Technol. 22, 761-767.

[88] Huang C.P., Dong Ch. and Tang Z. (1993). Advanced chemical oxidation: Its present role and potential future in hazardous waste treatment. Waste Manage. 13, 361-377.

[89] Calvert J.G. and Pitts J.N. (1966). Experimental methods in photochemistry. In: Calvert J.G. and Pitts J.N. (Eds). Photochemistry. John Wiley and Sons. New York, USA.

[90] Hewes G.C. and Davinson R.R. (1972). Renovation of waste water by ozonation. Water AIChE Symposium Series. 69, 71.

[91] Hart E.J., Sehested K. and Holoman J. (1983). Molar absorptivities of ultraviolet and visible band of ozone in aqueous solutions. Anal. Chem. 55, 46-49.

[92] Nowell L.H. and Hoigné J. (1997) Interaction of iron (III) and other transition metals with aqueous ozone. In: Proceedings of 8th World Congress International Ozone Association. Naef H.R. (Ed). International Ozone Association, Zurich, Switzerland.

[93] Loegager T., Holcman J., Sehested K. and Pedersen T. (1992). Oxidation of ferrous ions by ozone in acidic solutions. Inorg. Chem. 31, 3523-3529.

[94] Agustina T.E., Ang H.M. and Vareek V.K. (2005). A review of synergistic effect of photocatalysis and ozonation on wastewater treatment. J. Photoch. Photobio. C. 6, 264-273.

[95] Sánchez L., Peral J. and Domènech X. (1998). Aniline degradation by combined photocatalysis and ozonation. Appl. Catal. B-Environ. 19, 59-65.

[96] Kopf P., Gilbert E. and Eberle S.H. (2000). TiO_2 photocatalytic oxidation of monochloroacetic acid and pyridine: influence of ozone. J. Photoch. Photobio. A. 136, 163-168.

[97] Bouzaida I., Ferronato C., Chovelon J.M., Rammah M.E. and Herrmann J.M. (2004). Heterogeneous photocatalytic degradation of the anthraquinonic dye, Acid Blue 25 (AB25): a kinetic approach. J. Photoch. Photobio. A. 168, 23-30.

[98] Peng R.Y. and Fan H.J. (2005). Ozonation kinetic order of dye decoloration in aqueous solutions. Dyes Pigments. 67, 153-159.

[99] Vogna D., Marotta R., Napolitano A., Andreozzi R. and Ischia M. (2004). Advanced oxidation of the pharmaceutical drug diclofenac with UV/H_2O_2 and ozone. Water Res. 38, 414-422.

[100] Karageorgos P., Coz A., Charalabaki M., Kalogerakis N., Xekoukoulotakis, N. P. and Mantzavinos D. (2006). Ozonation of weathered olive mill wastewaters. J. Chem. Technol. Biot. 81, 1570-1576

[101] Sevimli M.F. (2005). Post-treatment of pulp and paper industry wastewater by advanced oxidation processes. Ozone Sci. Eng. 27, 37-43.

[102] Bekbölet M. (1997). Photocatalytic bactericidal activity of TiO_2 in aqueous suspensions of E. Coli. Water Sci. Technol. 35, 95-100.

[103] Rengifo-Herrera J. A., Sanabria J., Machuca F., Dierolf C.F., Pulgarín C. and Orellana G. (2007). A Comparison of Solar Photocatalytic Inactivation of Waterborne E. coli Using Tris (2,2'-bipyridine)ruthenium(II), Rose Bengal, and TiO2. J. Sol. Energy. Eng. 129, 135-140.

[104] Pérez M., Torrades F., Domènech X. and Peral J. (2002). Removal of organic contaminants in paper pulp effluents by AOPs: an economic study. J. Chem. Technol. Biot. 77, 525-532.

[105] Moraes S.G., Freire R.S. and Duran N. (2000). Degradation and toxicity reduction of textile effluent by combined photocatalytic and ozonation processes. Chemosphere. 40, 369-373.

[106] Domínguez J.R., Beltrán J. and Rodríguez O. (2005). Vis and UV photocatalytic detoxification methods (using TiO_2, TiO_2/H_2O_2, TiO_2/O_3, $TiO_2/S_2O_8^{2-}$, O_3, H_2O_2, $S_2O_8^{2-}$, Fe^{3+}/H_2O_2 and $Fe^{3+}/H_2O_2/C_2O_4^{2-}$) for dyes treatment. Catal. Today. 101, 389-395.

[107] Ilisz I., Bokros A. and Dombi A. (2004). TiO_2-based heterogeneous photocatalytic water treatment combined with ozonation. Ozone Sci. Eng. 26, 585-594.

[108] Stephenson R.L. and Blackburn J.B. (1998). Biological treatment processes. In: Stephenson R.L. and Blackburn J.B. (Eds). The industrial wastewater systems. Handbook.(Ed) Lewis Publishers. New York, USA.

[109] Riser-Roberts E. (1998). Biological processes. In: Riser-Roberts E. (Ed). Remediation of petroleum contaminated soils. biological, physical, and chemical processes. Lewis Publishers. London, UK. 30-77.

[110] Metcalf and Eddy, Inc. (1985). Procesos biologicos unitarions. In: Metcalf-Eddy (Ed). Ingenieria Sanitaria: tratamiento, evacuación y reutilización de agues residuals. Labor, 2 Ed. Barcelona, Spain.

[111] Tchobanoglous G., Theisen H. and Vigil S. (1993). Integrated solid waste management: Engineering principles and management issues. Macgraw Hill. New York, USA.

[112] Jiménez-Gonzalez C., Overcash M.R. and Curzons A. (2001). Waste treatment modules – a partial life cycle inventory- J. Chem. Technol. Biot. 76, 707-716.

[113] Henze M., Gujer W., Mino T. and Van Loosdrecht M. (2000). Activated Sludge models ASM1, ASM2, ASM2d and ASM3. Scientific and technical report nº9. IWA. London, UK. 1-38.

[114] Guisasola A., Baeza J.A., Carrera J. and Lafuente F.J. (2002). Descripción e implementación de las técnicas respirométricas en el tratamiento de las aguas residuales. Tecnología del Agua. 224, 32-39.

[115] Franta J., Wilderer P.A., Miksch K. and Sykora V. (1994). Effects of operation conditions on advanced COD removal in activated sludge systems. Water Sci. Techol. 29, 189–192.

[116] Beardsley M. L. and Coffey J. M. (1985). Bioaugmentation: optimizing biological wastewater treatment. Pollut. Engng. 17, 30–33.

[117] Metcalf and Eddy, Inc. (1991) Wastewater Engineering: Treatment, Disposal and Reuse. Metcalf-Eddy (Ed) McGraw-Hill Inc. (3 ed). New York, USA.

[118] González S., Müller J., Petrovic M., Barceló D. and Knepper T.P. (2006). Biodegradation studies of selected priority acidic pesticides and diclofenac in different bioreactors. Environ. Pollut. 144, 926-932.

[119] Eckenfelder W. and Musterman J. (1995). Activated Sludge Treatment of Industrial Wastewater. Technomic Pub Co. Lancaster, Basel.

[120] Suh Y.J. and Rosseaux P. (2002). An LCA of alternative wastewater sludge treatment scenarios. Resour. Conserv. Recy. 35, 191-200.

[121] Lewandowski G.A. and DeFilippi L.J. (1998). Introduction to microbiological degradation of aqueous waste and its application using a fixed-film reactor. In: Lewandowski G.A. and DeFilippi L.J. (Ed). Biological treatment of hazardous wastes. John Wiley & Sons, Inc. New York, USA.

[122] Mace S. and Mata-Alvarez J. (2002). Utilization of SBR technology for wastewater treatment: an overview. Ind. Eng. Chem. Res. 41, 5539-5553.

[123] Arden E. and Lockett W.T. (1914). Experiments on the oxidation of sewage without the aid of filters. J. Soc. Chem. Ind. 33, 523-539.

[124] Wilderer P.A., Irvine R. L., Goronszy M. C. (2001). Sequencing Batch Reactor Technology. IWA Scientific and Technical Report Series. London, UK. 1-10

[125] EPA. (1999). Wastewater Technology Fact Sheet. Sequencing Batch reactors. EPA 832-F-99-073. Washington, USA.

[126] Singleton I. (1994). Microbial metabolism of xenobiotics: fundamental and applied research. J. Chem. Technol. Biotechnol. 59, 9–23.

[127] Buitron G., Gonzalez A. and Lopez-Marin L.M. (1998). Biodegradation of phenolic compounds by an acclimated activated sludge and isolated bacteria. Water Sci. Technol. 37, 371–378.

[128] Mangat S.S. and Elefsiniotis P. (1999). Biodegradation of the herbicide 2,4-dichlorophenoxyacetic acid (2,4-D) in sequencing batch reactors. Water Res. 33, 861–867.

[129] Wiggings B.A., Jones S.H. and Alexander M. (1987). Explanation for the acclimation period preceding the mineralization of organic chemicals in aquatic environments. Appl. Environ. Microbiol. 53, 791–796.

[130] Hu H.Y., Nozawa M., Fujie K., Makabe T. and Urano K. (1998). Analysis of microbial acclimation to refractory chemicals in wastewater using respiratory quinine profiles. Water Sci. Technol. 37, 407–411.

[131] Nyuk-Min C. and Tze-Yung L. (2007). Measurement of the degradation capacity of activated sludge for a xenobiotic organic. Bioresource Technol. 98, 1124-1127.

[132] Scott J.P. and Ollis D.F. (1995). Integration of chemical and biological oxidation processes for waste treatment: review and recommendations. Environ. Prog. 14, 88-103.

[133] Sarria V., Parra S., Adler N., Péringer P., Benítez N. and Pulgarín C. (2002). Recent developments in the coupling of photoassisted and aerobic biological processes for the treatment of biorecalcitrant compounds. Catal. Today. 76, 301-315.

[134] Reyes J., Dezotti M., Esposito E., Villaseñor J., Mansilla H. and Duran N. (1998). Biomass photochemistry-XXII. Combined photochemical and biological process for treatment of Kraft El effluent. Appl. Catal. B-Environ. 15, 211-219.

[135] Benítez F. J., Acero J. L., González T. and García J. (2001). Ozonation and biodegradation processes in batch reactors treating black table olive washing wastewaters. Ind. Eng. Chem. Res. 40, 3144-3151.

[136] Jones B.M., Sakaji R.H. and Daughton C.G. (1985). Effects of ozonation and ultraviolet irradiation on biodegradability of oil shale wastewater organic solutes. Water Res. 19, 1421-1428.

[137] Caberry J.B. and Benzing T.M. (1991). Peroxide pre-oxidation of recalcitrant toxic waste to enhance biodegradation. Water Sci. Technol. 23, 367-376.

[138] Manilal. V.B., Haridas A., Alexander R. and Surender G.D. (1992). Photocatalyitic treatment of toxic in wastewaters: Toxicity of photodegradation products. Water Res. 26, 1035-1038.

[139] Sarria V., Kenfack S., Guillod O. and Pulgarín C. (2003). An Inovative coupled solar-biological system at field pilot scale for the treatment of biorecalcitrant pollutants. J. Photoch. Photobio. A. 159, 89-99.

[140] Oller I., Gernjak W., Ramos Siles C., Muñoz J.A., Maldonado M.I., Pérez-Estrada L.A. and Malato S. (2006). Industrial Scale Coupling of oxidative pre-treatment (solar photo-Fenton or ozone) and immobilised biomass activated sludge biotreatment. SPEA 4. Solar Chemistry and Photocatalysis: Environmental Applications. Las Palmas de Gran Canarias, Spain.

[141] Lapertot M., Ebrahimi S., Dazio S., Rubinelli A. and Pulgarín C. (2007). Photo-Fenton and biological integrated process for degradation of a mixture of pesticides. J. Photoch. Photobio. A. 186, 34-40.

[142] Essam T., Amin M. A., El Tayeb O., Mattiasson B. and Guieysse B. (2007). Sequential photochemical-biological degradation of chlorophenols. Chemosphere. 66, 2201-2209.

[143] Suárez-Ojeda M.E., Guisasola A., Baeza J.A., Fabregat A., Stüber F., Fortuny A., Font J. and Carrera J. (2007). Integrated catalytic wet air oxidation and aerobic biological treatment in municipal WWTP of a high-strength o-cresol wastewater. Chemosphere. 66, 2096-2105.

[144] Al Momani F., Sans C., Contreras S. and Esplugas S. (2006). Degradation of 2,4-dichlorophenol by combining photo-assisted Fenton reaction and biological treatment. Water Environ. Res. 78, 590-597.

[145] Garcia A., Amat A.M., Arques A., Sanchis R., Gernjak W., Maldonado M.I., Oller I. and Malato S. (2006). Detoxification of aqueous solutions of the pesticide "Sevnol" by solar photocatalysis. Environ. Chem. Lett. 3, 169-172.

[146] Azadeh A. and Mehrab M. (2006). Degradation of aqueous methyl tert-butyl ether by photochemical, biological, and their combined processes. Int. J. Photoenergy. 19790, 1-7.

[147] Kajitvichyanukul P. and Suntronvipart N. (2006). Evaluation of biodegradability and oxidation degree of hospital wastewater using photo-Fenton process as the pretreatment method. J. Hazard. Mat. 138, 384-391.

[148] Lafi W. K. and Al-Qodah Z. (2006). Combined advanced oxidation and biological treatment processes for the removal of pesticides from aqueous solutions. J. Hazard. Mat. 137, 489-497.

[149] Tantak N. P. and Chaudhari S. (2006). Degradation of azo dyes by sequential Fenton's oxidation and aerobic biological treatment. J. Hazard. Mat. 136, 698-705.

[150] Wiszniowski J., Robert D., Surmacz-Gorska J. Miksch K. and Weber J.-V. (2006). Leachate detoxification by combination of biological and TiO2-photocatalytic processes. Water Sci. Technol. 53, 181-190.

[151] Maldonado M.I., Malato S., Pérez-Estrada L.A., Gernjak W., Oller I., Domènech P., Peral J. (2006). Partial degradation of five pesticides and industrial pollutant by ozonation in a pilot-plant scale reactor. J. Hazard. Mat. 138, 363-369.

[152] García-Montaño J., Torrades F., García-Hortal J.A., Domènech X. and Peral J. (2006). Combining photo-Fenton process with aerobic sequencing batch reactor for commercial hetero-bireactive dye removal. Appl. Catal. B-Environ. 67, 86-92.

[153] García-Montaño J., Torrades F., García-Hortal J.A., Domènech X. and Peral J. (2006). Degradation of Procion Red H-E7B reactive dye by coupling a photo-Fenton system with a sequencing batch reactor. J. Hazard. Mat. 134, 220-229.

[154] Sudarjanto G., Keller-Lehmann B., Keller J. (2006). Optimization of integrated chemical-biological degradation of a reactive azo dye using response surface methodology. J. Hazard. Mat. 138, 160-168.

[155] Gökçen F. and Özbelge T.A. (2006). Pre-Ozonation of aqueous azo dye (acid Red-151) followed by activated sludge process. Chem. Eng. J. 123, 109-115.

[156] Mohanty S., Rao N.N., Khare P. and Kaul S.N. (2005). A coupled photocatalytic-biological process for degradation of 1-amino-8-naphthol-3, 6-disulfonic acid (H-acid). Water Res. 39, 5064-5070.

[157] Contreras S., Piatkowska J., Rodriguez M., Sans C. and Esplugas S. (2005). Biodegradability improvement of aqueous 2,4-dichlorophenol and nitrobenzene solutions by means of single ozonation. Ozone Sci Eng. 27, 381-387.

[158] Al Momani F., González O., Sans C. and Esplugas S. (2004). Combining photo-Fenton process with biological sequencing batch reactor for 2,4-dichlorophenol degradation. Water Sci. Technol. 49, 293-298.

[159] di Laconi C., Bonemazzi F., Lopez A. and Ramadori R. (2004). Integration of chemical and biological oxidation in a SBBR for tannery wastewater treatment. Water Sci. Technol. 50, 107-114.

[160] Alaton I.A., Dogruel S., Baykal E. and Gerone G. (2004). Combined chemical and biological oxidation of penicillin formulation effluent. J. Environ. Manage. 73, 155-163.

[161] Fongsatitkul P., Elefsiniotis P., Yamasmit A. and Yamasmit, N. (2004). Use of sequencing batch reactors and Fenton's reagent to treat a wastewater from a textile industry. Biochem. Eng. J. 21, 213-220.

[162] In-Ock K., Xiaoling C.H., Klaus H. and Wolfram T. (2004). Leachate treatment by the combination of photochemical oxidation with biological process. J. Photoch. Photobio. A. 162, 261-271.

[163] Contreras S., Rodriguez M., Momani F. Al., Sans C. and Esplugas S. (2003). Contribution of the ozonation pre-treatment to the biodegradation of aqueous solutions of 2,4-dichlorophenol. Water Res. 37, 3164-3171.

[164] Thurman E.M. and Morgan. R.L. (1981). Preparative isolation of aquatic humic substances. Environ. Sci. Technol. 15, 463-466.

[165] Geldreich E.E. (1996). Biofilms in water distribution systems. In: Geldreich E.E. (Ed). Microbial quality of water supply in distribution system. Lewis Publishers. Florida, USA. 159-214.

[166] AWWA (1999). Coagulation and flocculation. In: Letterman R.D. (Ed) Water Quality and Treatment. American Water Works Association. New York, USA.

[167] Davies G. and Ghabbour E.A. (1998). Humic Substances- Structures, Properties and Uses. Royal Society of Chemistry, Cambridge, UK.

[168] Fukushima M. and Tatsumi K. (2006). Effects of humic substances on the oxidation of pentachlorophenol by peroxosulfate catalyzed by iron(III)-phthalocyanine-tetrasulfonic acid. Bioresource Technol. 97, 1605-1611

[169] Aguer J.P., Richard C. and Andreux F. (1999). Effect of light on humic substances: production of reactive species. Analusis. 27, 387-390.

[170] Beschkov V., Bardarska G., Gulyas H. and Sekoulov I. (1997). Degradation of triethylene glycol dimethyl ether by ozonation combined with UV irradiation or hydrogen peroxide addition. Water Sci. Technol. 36, 131-138.

[171] Konstantinou I.K., Zarkadis A.K., Albanis T.A. and Triantafyllos A. (2001). Photodegradation of selected herbicides in various natural waters and soils under environmental conditions. J. Environ. Qual. 30, 121-130.

[172] Staehelin J. and Hoigné J. (1985). Decomposition of ozone in water in the presence of organic solutes acting as promoters and inhibitors of radical chain reactions. Environ. Sci. Technol. 19, 1206-1213.

[173] Torrents A., Anderson B.G., Bilboulian S., Johnson W.E. and Hapeman C.J. (1997). Atrazine photolysis: mechanistic investigations of direct and nitrate-mediated hydroxyl radical processes and the influence of the dissolved organic carbon from the Chesapeake Bay. Environ. Sci. Technol. 31, 1476-1482.

[174] Hawari J., Demeter A. and Samson R. (1992). Sensitized photolysis of polychlorobiphenyls in alkaline 2-propanol: dechlorination of Aroclor 1254 in soil samples by solar radiation. Environ. Sci. Techol. 26, 2022-2027.

[175] Zepp R.G., Wolfe N.L., Gordon J.A. and Baughman G.L. (1975). Dynamics of 2,4-D esters in surface waters. Hydrolysis, photolysis, and vaporization. Environ. Sci. Technol. 9, 1144-1150.

[176] Hesketh N., Jones M.N. and Tipping E. (1996). The interaction of some pesticides and herbicides with humic substances. Anal. Chim. Acta. 327, 191-201.

[177] Wang G.S., Liao C.H. and Wu F.J. (2001). Photodegradation of humic acids in the presence of hydrogen peroxide. Chemosphere. 42, 379-387.

[178] Fukushima M., Tatsumi K. and Nagao S. (2001) Degradation characteristics of humic acid during photo-Fenton process. Environ. Sci. Technol. 35, 3683-3690.

[179] Esperanza-Soto M. and Westerhoff P. (2003). Biosorption of humic and fluvic acids to live activated sludge biomass. Water Res. 37, 2301-2310.

[180] Weber W.J. (1972). Physicochemical processes for water quality control. Wiley-Interscience. New York, USA.

[181] Farré M. and Barceló D. (2003). Toxicity testing of wastewater and sewage sludge by biosensors, bioassays and chemical analysis. Trends Anal. Chem. 22, 299-310.

[182] ISO, Water quality. (1996). Determination of the inhibition of the mobility of Daphnia magna Straus (Cladocera, Crustacea). ISO 6341. International Standardization Organization. Geneva, Switzerland.

[183] Purohit H.J. (2003). Biosensors as molecular tools for use in bioremediation. J. Clean. Prod. 11, 293-301.

[184] ISO, Water quality. (1998).Determination of the inhibitory effect of water samples on the light emission of Vibrio fischery (Luminescent bacteria test). ISO 11348-1, 2 and 3. International Standardization Organism. Geneva, Switzerland

[185] Malato S., Blanco J., Vidal A., Alarcón D., Maldonado M.I., Cáceres J. and Gernjak W. (2003). Applied studies in solar photocatalytic detoxification: and overview. Sol. Energy. 75, 329-336.

[186] Larson R.J. (1991). Biodegradation in regulating the environment exposure of detergent chemicals. Chem. Times Trends. 14, 47-55.

[187] Dazell D.J.B., Alte S., Aspichueta E., de la Sota A., Etxebarria J., Gutiérrez M., Hoffmann C.C., Sales D., Obst U. and Christofi N. (2002). A comparison of five rapid direct toxicity assessment methods to determine toxicity of pollutants to activated sludge. Chemosphere. 47, 535-545.

[188] Freitas L., Defrenne L. and Kerbs-Brown A. (2002).Comparison of three microbial assay procedures for measuring toxicity of chemical compounds: ToxAlert®10, Cell Sense and Biolog MT2 microplates. Anal. Chim. Acta. 456,41-54.

[189] Gutiérrez M., Etxebarria J. and de las Fuentes L. (2002). Evaluation of wastewater toxicity: comparative study between Microtox® and activated sludge oxygen uptake inhibition. Water Res. 36, 919-924.

[190] Ricco G., Tomei C., Ramadori R. and Laera G. (2004). Toxicity assessment of common xenobiotic compounds on municipal activated sludge: comparison between respirometry and Microtox®. Water Res. 38, 2103-2110.

[191] Volskay V.T and Grady C.P.L. (1990). Respiration inhibition kinetic analysis. Water Res. 24, 863-874.

[192] Guisasola A., Baeza J. A., Carrera J., Casas J. and Lafuente J. (2003). An off-line respirometric procedure to determine inhibition and toxicity of biodegradable compounds in biomass from an industrial WWTP. Water Sci. Technol. 48, 267-275.

[193] Lapertot M.E. and Pulgarín C. (2006). Biodegradability assessment of several priority hazardous substances: Choice, application and relevant regarding toxicity and bacterial activity. Chemosphere. 65, 682-690.

[194] Howard P.H. (2000). Biodegradation. In: Mackay D. (Ed). Handbook of property estimation methods for chemicals, environmental and health sciences. Lewis, Boca Raton. Florida, USA.

[195] Niemi G.J., Veith R.R., Regal R.R. and Vaishnav D.D. (1987). Structural features associated with degradable and persistent chemicals. Environ. Toxicol. Chem. 6, 515-527.

[196] Boethling R.S. Lynch D.G. and Thom G.C. (2003). Predicting ready biodegradability of premanufacture notice chemicals. Environ. Toxicol. Chem. 22, 873-844.

[197] European Commission (1992). EC directive 92/96/EEC.

[198] Arslan-Alaton I. (2003). The effect of pre-ozonation on the biocompatibility of reactive dye hydrolysates. Chemosphere. 51, 825-833.

[199] Hemström P. and Irgum K. (2006). Hydophilic interaction chromatography. J. Sep. Sci. 29, 1784-1821.

[200] Alpert A.J. (1990). Hydrophilic-interaction chromatography for the separation of peptides, nucleic acids and other polar compounds. J. Chromatogr. 499, 177-196.

[201] Garbis S.D., Melse-Boonstra A., West C.E. and van Breemen R.B. (2001). Determination of folates in human plasma using hydrophilic interaction chromatography-tandem mass spectrometry. Anal. Chem. 73, 5358-5364

[202] Strege M.A. (1998). Hydrophilic interaction chromatography-electrospray mass spectrometry analysis of polar compounds for natural product drug discovery. Anal. Chem. 70, 2439-2445.

[203] Guo Y. and Gaki S. (2005). Retention behaviour of small polar compounds on polar stationary phases in hydrophilic interaction chromatography. J. Chromatog. 1074, 71-80.

[204] Miettinen P. and Hamalainen R.P. (1997). How to benefit from decision analysis in environmental life cycle assessment (LCA). Eur. J. Oper. Res. 102, 279-294.

[205] Consoli F., Allen D., Boustead I., de Oude N., Fava J., Franklin W., Quay B., Parrish R., Perriman R., Postlethwaite D., Seguin J. and Vigon B. (1993). Guidelines for Life-Cycle Assessment: A Code of Practice. Society of Environmental Toxicology and Chemistry. Brussels, Belgium

[206] ISO. (1997). Environmental Management –Life Cycle Assessment- Principles and dramework. ISO 14040, International Standardization Organism. Geneva, Switzerland.

[207] ISO. (1998). Environmental Management –Life Cycle Assessment- Goal and scope definition and inventory analysis. ISO 14041, International Standardization Organism. Geneva, Switzerland.

[208] ISO. (2000). Environmental Management –Life Cycle Assessment- Life cycle impact assessment. ISO 14042, International Standardization Organism. Geneva, Switzerland.

[209] ISO. (2000). Environmental Management –Life Cycle Assessment- Life cycle impact interpretation. ISO 14043, International Standardization Organism. Geneva, Switzerland.

[210] ISO. (2006). Environmental Management –Life Cycle Assessment- Principles and framework. ISO 14040, International Standardization Organism. Geneva, Switzerland.

[211] ISO. (2006). Environmental Management –Life Cycle Assessment- Requirements and guidelines. ISO 14044, International Standardization Organism. Geneva, Switzerland.

[212] Azapagic A. (2002). Life-cycle Assessment: a tool for identification of more sustainable products and processes. In: Clark J., Macquarrie D.(Eds). Handbook of green chemistry and technology. Blackwell Science. Oxford, UK.

[213] Guinée J.B., Gorree M., Heijungs R., Huppes G., Kleijn R., Udo de Haes H.A., Van der Voet E. and Wrisberg M.N. (2002). Life Cycle Assessment. An operational guide to ISO standards. Vol 1, 2, 3. The Netherlands.

[214] Muñoz I., Rieradevall J., Domènech X. (2005) Definición de la unidad funional en el ACV. In: Clemente G, Sanjuán N. and Vivancos J.L. (Eds.). Análisis de Ciclo de Vida: aspectos metodológicos y casos prácticos. Universidad Politecnica de Valencia. Valencia, Spain.

[215] Burgués A.A. and Brennan D.J. (2001). Application of life cycle assessment to chemical processes. Chem. Eng. Sci. 56, 2589-2604.

[216] Berkhout F. and Howes R. (1997). The adoption of life-cycle approaches by industry: patterns and impacts. Resour. Conserv. Recy. 20, 71-94.

[217] Dennison F.J., Azapagic A., Clift R. Colbourne J.S. (1998). Assessing management options for wastewater treatment works in the context of Life Cycle Assessment. Water Sci. Technol. 38, 23-30.

[218] Roeleveld P.J., Klapwijk A., Eggels P.G. Rulkens W.H. and van Starkenburg W. (1997). Sustainability of municipal wastewater treatment. Water Sci. Technol. 35, 221-228.

[219] Tillman A.M., Svingby M. and Lundstöm H. (1998). Life Cycle Assessment of municipal waste water systems. Int. J. Life Cycle Ass. 3, 145-157.

[220] Hospido A., Moreira M.T., Fernández-Couto M. and Feijoo G. (2004). Environmental performance of a municipal wastewater treatment plant. Int. J. Life Cycle Ass. 10, 336-345.

[221] Vidal N., Poch M., Martí E. and Rogríguez-Roda I. (2002). Evaluation of the environmental implications to include structural changes in wastewater treatment plant. J. Chem. Technol. Biot. 77, 1206-1211.

[222] Jorgensen K.R., Villanueva A. and Wenzel H. (2004). Use of life cycle assessment as decision-support tool for water reuse and handling of residues at a Danish industrial laundry. Waste Manag. Res. 22, 334-345.

[223] Pillary S.D., Friedrich E. and Buckley C.A. (2002). Life cycle assessment of an industrial water recycling plant. Water Sci. Technol. 46, 55-62.

[224] Muñoz I., Rieradevall J., Torrades F., Peral J. and Domènech X. (2005). Environmental assessment of different solar driven advanced oxidation processes. Sol. Energy. 79, 369-375.

[225] Muñoz I., Rieradevall J., Torrades F., Peral J. and Doménech X. (2006). Environmental assessment of different advanced oxidation processes applied to bleaching kraft mill effluents. Chemosphere. 62, 9-16.

[226] Muñoz I., Peral J., Ayllon J.A., Malato S., Passarinho P. Doménech X. (2006). Life-cycle assessment of a coupled solar photocatalytic-biological process for wastewater treatment. Water Res. 40, 3533-3540.

[227] García-Montaño J., Ruiz N., Muñoz I., Domènech X., García-Hortal J.A. Torrades F. and Peral J. (2006). Environmental assessment of different photo-Fenton approaches for commercial reactive dye removal. J. Hazard. Mat. 138, 218-225.

CHAPTER 2
MATERIALS AND METHODS

1. Reagents

1.1. Preparation of synthetic effluents

The toxic and non biodegradable herbicides used in this work were Alachlor (95%, Aragonesas Agro S.A, technical grade), Atrazine (95%, Ciba-Greigy, technical grade), Chlorfenvinphos (93.2%, Aragonesas Agro S.A, technical grade), Isoproturon (98%, Aragonesas Agro S.A, technical grade), Diuron (98.5%, Aragonesas Agro S.A, technical grade), Linuron (92.6%, Makhteshim Agan España S.A, technical grade) and Pentachlorophenol (98%, Aldrich). Table 2.1 summarizes some physical-chemical data of the 7 herbicides used. Figure 2.1 shows their chemical structure

Table 2.1 Physical-chemical data of model herbicides

herbicides	CAS	Molecular weight $g \cdot mol^{-1}$	Melting point[a] ^oC	Solubility[b] $mg \cdot L^{-1}$	Log K_{ow}
Alachlor	15972-60-8	269.8	40	240	3.52
Atrazine	1912-24-9	215.7	173	35	2.61
Chlorfenvinphos	470-90-6	359.8	167(*)	124	3.81
Diuron	330-54-1	233.1	158	42	2.68
Isoproturon	34123-59-6	206.3	158	65	2.87
Linuron	330-55-2	249.1	180	75	3.20
Pentachlorophenol	87-86-5	266.4	174	14(**)	5.12

a) Melting points, (*boiling point) data refers to standard atmospheric pressure (1bar) and
b) Solubility data refers to 25 ^oC and pH=7, pH(**)= 5

All the aqueous solutions were prepared with water purified in a Millipore Milli-Q system (conductivity < $6 \cdot 10^{-8}$ Ω^{-1} cm^{-1} and TOC < 0.1 $mg \cdot L^{-1}$). In order to simulate real herbicides concentration, solutions of 50 $mg \cdot L^{-1}$ were prepared. When the solubility value was below 50 $mg \cdot L^{-1}$, a saturated solution of the herbicide was used as initial solution. A mixed initial saturated solution of Diuron and Linuron was prepared for the experiments of combined degradation of both herbicides. Before the degradation process started, all solutions were filtered through a 45 µm Nylon filter (Millipore).

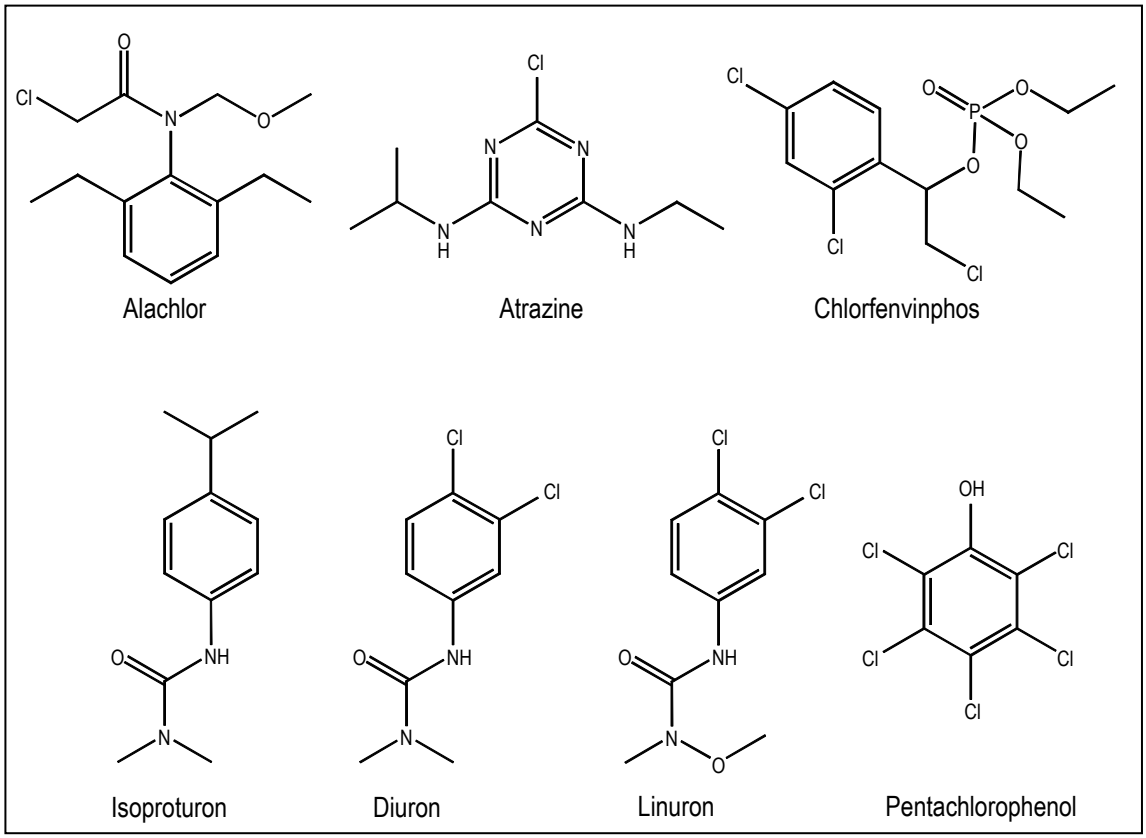

Figure 2.1 Chemical structures of model herbicides

The stoichiometry of the complete mineralization of the herbicides is expressed with the following global equations (2.1 to 2.7). When compounds contain nitrogen, the reactions have been written taking into account that nitrogen ends up in the most oxidized state. In these cases, ammonia can be formed before being oxidized to nitrate at long reaction times.

Alachlor; $C_{14}H_{20}ClNO_2 + 19\ O_2 \rightarrow 14\ CO_2 + HCl + HNO_3 + 9\ H_2O$ *(2.1)*

Atrazine; $C_8H_{14}ClN_5 + 17.5\ O_2 \rightarrow 8\ CO_2 + HCl + 5\ HNO_3 + 4\ H_2O$ *(2.2)*

Chlorfenvinphos; $C_{12}H_{14}Cl_3O_4P + 14\ O_2 \rightarrow 12\ CO_2 + 3\ HCl + H_3PO_4 + 4\ H_2O$ *(2.3)*

Diruon; $C_9H_{10}Cl_2N_2O + 13\ O_2 \rightarrow 9\ CO_2 + 2\ HNO_3 + 2\ HCl + 3\ H_2O$ *(2.4)*

Isoproturon; $C_{12}H_{18}N_2O + 18.5\ O_2 \rightarrow 12\ CO_2 + 2\ HNO_3 + 8\ H_2O$ *(2.5)*

Linuron; $C_9H_{10}Cl_2N_2O_2 + 12.5\ O_2 \rightarrow 9\ CO_2 + 2\ HNO_3 + 2\ HCl + 3\ H_2O$ *(2.6)*

Pentachlorophenol; $C_6HCl_5O + 4.5\ O_2 + 2\ H_2O \rightarrow 6\ CO_2 + 5\ HCl$ *(2.7)*

1.2. Other reagents used

$FeSO_4 \cdot 7H_2O$ (99.5%, Merck) and H_2O_2 (33% w/v, Panreac) were use as photo-Fenton reagents. TiO_2 P-25 (80% anatase and 20% rutile, Degussa) was used in heterogeneous photocatalysis experiments. Ozone was produced from Oxygen C-45 (99.995%, Carburos Metalicos). KI (99%, Aldrich), KIO_3 (Probus), $K_2H_2PO_4$ (99%, Aldrich) and $Na_2S_2O_3 \cdot 5H_2O$ (99.5%, Aldrich) were used in the measurement of O_3. In TOC measurements synthetic high purity air (79% N_2, 21% O_2, Abelló-Linde) was used as carrier gas. Potassium hydrogen phthalate ($KC_8H_5O_4$ 99%, Acros), $NaHCO_3$ (99.7%, Aldrich) and Na_2HCO_3 (99.95%, Aldrich) were used to calibrate TOC apparatus. HCl (37%, Panreac) and H_2SO_4 (96%, Panreac) were used to regenerate catalyst and to perform IC measurements. NaOH (97%, Aldrich) and H_2SO_4 (96%, Panreac) were used in pH adjustements. In order to quantify COD values, Aqualitic® vials ($HgSO_4$, $AgSO_4$, H_2SO_4, $K_2Cr_2O_7$) range 0-150 and 0-1500 $mg \cdot L^{-1}$ were used. Potassium hydrogen phthalate ($KC_8H_5O_4$ 99%, Acros) was used as standard in these analyses. KI (99%, Panreac), $(NH_4)_6Mo_7O_{24} \cdot 4H_2O$ (99%, Panreac), potato starch (Fluka), $Na_2S_2O_3 \cdot 5H_2O$ (99.5%, Aldrich) and H_2SO_4 (96%, Panreac) were used in iodometric determination of H_2O_2. The excess of H_2O_2 was eliminated with Na_2SO_3 (Merk). NH_4^+ measured with Nessler method required KI (99%, Panreac), $HgCl_2$ (Probus), NaOH (97%, Aldrich) and NH_4Cl (99.5%, Sigma). For Zahn-Wellen test NH_4Cl (99.5%, Sigma), NH_2PO_4 (99%, Panreac), KH_2PO_4 (99%, Panreac) and K_2HPO_4 (99%, Panreac) were used. Toxicity was measured with Vibrio Fischery bacterium (NRRL B-11177) provided by Lab-System. NaCl (99%, Aldrich) and catalase (Sigma) were also required in those analyses. For BOD_5 measurements, glucose ($C_6H_{12}O_6$ 99%, Fluka) and glutamic acid ($C_5H_9NO_4$ 99%, Fluka) were used as standard. Nitrification inhibitor (N-Allylthiourea, WTW), Na_2HPO_4 (99%, Aldrich), KH_2PO_4 (99%, Panreac), $MgSO_4 \cdot 7H_2O$ (98%, Panreac), $CaCl_2$ (Probus), $FeCl_3$ (Probus) and NH_4Cl (99.5%, Sigma) were also used in BOD_5 analysis. Acetic acid (CH_3COOH 99.7%,

Panreac) was used as totally biodegradable standard in respirometric measurements. $FeCl_3$ (Probus), $MgSO_4$ (98%, Panreac), $CaCl_2$ (Probus) NH_4Cl (99.5%, Sigma) and NaH_2PO_4 (99%, Aldrich) were used as nutrients for the SBR. Humic acid employed in this work was purchased from Aldrich. All the solvents used in chromatography were HPLC grade. Finally, all the standards used to identify by-products were at least of p.a grade.

2. Experimental set-up

2.1. AOP reactor

All the degradation experiments were conducted in a cylindrical Pyrex thermostatic cell of 250 cm^3 capacity (58 mm × 125 mm) provided with a magnetic stirrer. A thermostatic bath kept the temperature constant at 25.0±0.2 ^oC (Selecta S473.100). Figure 2.2 represents the scheme of the experimental set-up.

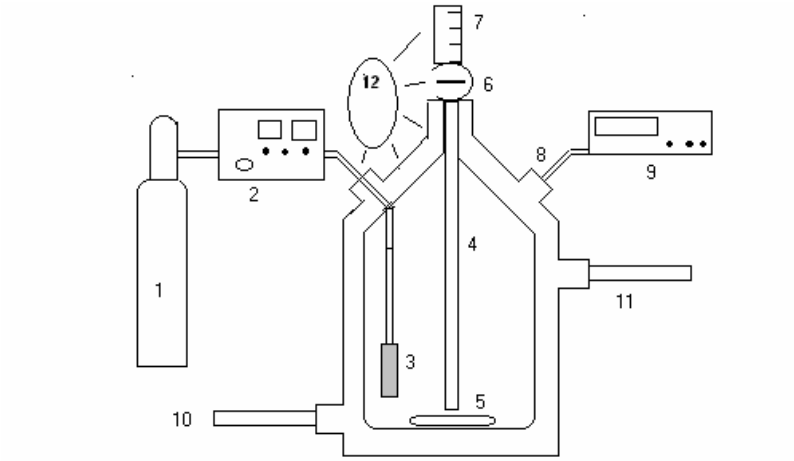

Figure 2.2 Experimental set-up.

1-oxygen cylinder, 2-ozonator, 3-diffuser, 4-sampling tube, 5-Teflon magnetic bar, 6-regulator key, 7- syringe, 8-ozone exit, 9-ozone detector, 10-cooling water inlet, 11-cooling water outlet, 12-black light

As seen in Figure 2.2, the reactor had three port lids that could be sealed. One port was used for introducing, when necessary, ozone into the reactor. The second port was used as ozone exit, and the third one was opened only to take samples from the reactor. In the photo-Fenton and heterogeneous photocatalysis experiments, the gas diffuser was removed from the experimental set-up and both, the first and second ports were sealed.

The selection of the photon source was a key point since the main objective of this experimental work was the development of environmentally-friendly and economical technologies for the treatment of wastewater. A 6 W black light with a measured intensity of 0.21 $mW \cdot cm^{-2}$

determined by means of a luminometer (Luton UVA-365, band pass 320-390 nm) was chosen to perform all the experiments. As seen in Figure 2.3, the emission range of UVA light permits carrying out photo-Fenton, heterogeneous photocatalysis and ozonation experiments (see Chapter 1, Section 2 for more details about required wavelengths).

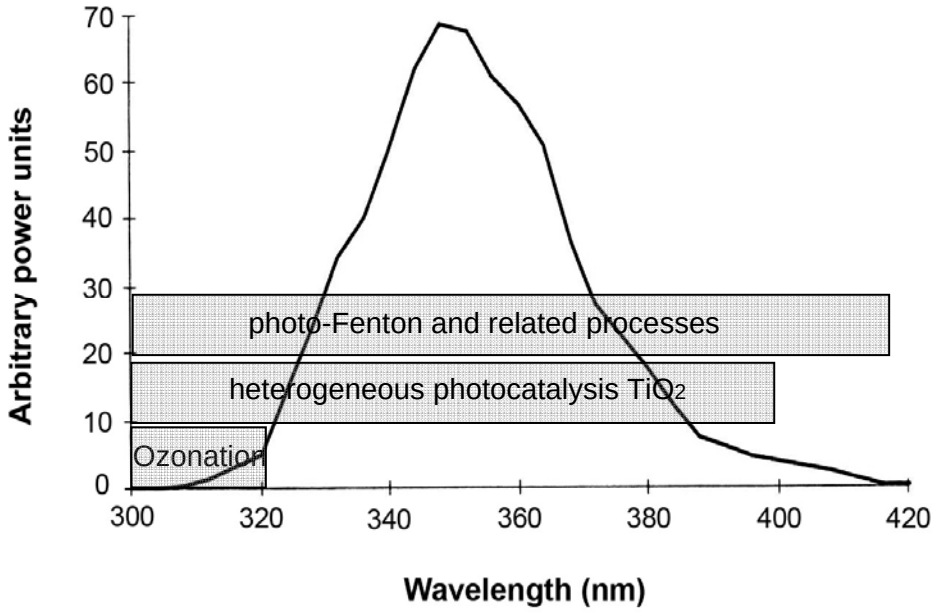

Figure 2.3 Black light emission spectra and wavelengths required in AOPs

Furthermore, an ideal AOP should use solar radiation as the driving force. Hence, the AOP efficiency by using solar radiation is guaranteed if the process is efficient under UVA radiation, due to the higher intensity and wider spectra of sun light [1, 2]. Finally, the UVA black light is more appropriate than other lamps used in similar experiments (e.g., Xenon lamp or high pressure mercury lamp) due to its lower electrical demand.

The black light was placed vertically and close to the reactor in order to achieve a constant irradiation flow during all the experiment. All the experimental set-up was protected from any external light with a dark cover.

2.1.1. Photo-Fenton experimental procedure

The experimental procedure in photo-Fenton assays was the following: in each experiment the photoreactor was charged with parent solution. The pH of the solutions was previously adjusted to 2.8. After that, $FeSO_4 \cdot 7H_2O$ was added and mixed to assure perfect dissolution. Finally, the hydrogen peroxide was added and the UVA light was switched on. The solution was continuously stirred at 500 rpm during all the degradation process. When necessary, samples were taken with a PVC syringe.

In publications 1 and 2, the amount of photo-Fenton reagent was selected according to previous research [3]. The amount of photo-Fenton reactants used in the rest of the work was selected according to an experimental design (see Chapter 2, Section 3 for details).

2.1.2. TiO_2-photocatalysis experimental procedure

Well dispersed suspensions of TiO_2 catalyst were required in heterogeneous photocatalysis experiments. Consequently, aqueous solutions were magnetically stirred during the catalyst loading process. pH was adjusted once the catalyst was loaded. The TiO_2 suspension was introduced in the reactor and kept in the dark until adsorption equilibrium was reached (i.e., 30 min). After that, the UVA light was switched on. The experiments were carried out under a continuous stirring of 500 rpm. When necessary, samples were taken with a PVC syringe.

The catalyst concentration used in these experiments was optimized in a previous work where TiO_2 levels tested ranged from 100 to 1000 $mg \cdot L^{-1}$ [4]. In that work, an increase in the kinetic constant value with the amount of TiO_2 up to 250 $mg \cdot L^{-1}$ was observed. For higher catalyst concentration, the efficiency of the process was always similar. Based on these observations, 250 $mg \cdot L^{-1}$ of TiO_2 was the concentration chosen for the experiments.

2.1.3. Ozonation experimental procedure

Ozone, generated by an Erwin Sander 301.7 equipment fed with pure oxygen flowing at 1 bar, was bubbled through the bottom of the reactor solution using a gas diffuser. The ozone input in the treated solution was 1.6 $g \cdot h^{-1}$ as determined by iodometric titration. The unreacted ozone in the flow gas was measured by means of an Erwing Sander Quantozone-1 ozone-meter. After measuring, the excess of ozone was destroyed in a KI aqueous trap. The reactor was filled with parent solution once the ozone concentration reading in the ozone-meter was stable. After that the UVA light was switched on. The solution was continuously stirred at 500 rpm during all the degradation process. When necessary, samples were taken with a PVC syringe.

2.1.4. Photocatalytic ozonation experimental procedure

As explained above, the reactor was filled with the herbicide solution once the ozone input in the reactor was constant. In the photo-Fenton/ozone and TiO_2-photocatalysis/ozone systems, the Fenton reagents or TiO_2 particles were also added to the reactor prior to start the experiment as explained in Section 2.1.1 and 2.1.2. Finally, the UVA light was switched on. The solution was continuously stirred at 500 rpm during all the degradation process. When necessary, samples were taken with a PVC syringe.

2.2. Sequencing Batch Reactor (SBR)

The aerobic bench-scale Sequencing Batch Reactor (SBR) was used to completely remove organic matter from solution after the utilization of an AOP. Experiments were conducted in a cylindrical Pyrex cell with a working liquid volume of 1.5 L. The reactor was magnetically stirred and maintained at laboratory temperature (20 ^{o}C). Air was fed through the bottom of the SBR by means of a glass diffuser.

One of the parameters to be fixed in a SBR was the Hydraulic Retention Time (HRT). This parameter measures the average time that the effluent remains in the bioreactor. Once the HRT was fixed, the corresponding volume to be replaced daily could be calculated as

$$V_{replaced} = V_{SBR}/HRT \quad (2.8)$$

As required by the SBR configuration, the experiments were performed in discontinuous mode and the volume extracted daily from the reactor was replaced by the same volume of new wastewater.

Another parameter usually controlled in a SBR is the Sludge Retention Time (SRT). This parameter measures the average time that the sludge remains in the bioreactor. Depending on this value, sludge purging is required. Due to the small scale properties of the SBR and the low Total Organic carbon (TOC) concentration used in this work, the low amount of sludge produced as consequence of organic matter assimilation was eliminated when withdrawing the supernatant. Consequently sludge purging was not required.

2.2.1. SBR experimental procedure

The activated sludge used as inoculum of the SBR was directly obtained from the aerobic stage of a full-scale urban Wastewater Treatment Plant (WWTP) located in Manresa (Spain). Initial Total Suspended Solids (TSS) value was between 3300 and 5000 $mg \cdot L^{-1}$.

The suitable amount of biomass was added to the SBR to obtain a TSS value of 600-1000 $mg \cdot L^{-1}$ in the final 1.5 L reactor. After that, the corresponding amount of different macronutrients were added in solution to obtain the following concentration; $MgSO_4$ (202.0 $mg \cdot L^{-1}$), $CaCl_2$ (73.40 $mg \cdot L^{-1}$), NH_4Cl (76.40 $mg \cdot L^{-1}$) and NaH_2PO_4 (1242 $mg \cdot L^{-1}$) [5]. Finally the SBR was filled with wastewater to 1.5 L (municipal wastewater or phototreated effluent).

The removal of hydrogen peroxide was required before feeding the SBR when this compound was used in the oxidation process. Sodium sulphite was used to eliminate hydrogen peroxide. Then, aeration was required to convert the remaining sulphite into sulphate [6]. When direct feed was not possible (several 250 ml chemical reaction batches were needed to fill the 1.5 L biological reactor) storage at around -8 ^oC was required.

Once the HRT was determined, the fill-and-draw procedure performed every day was as follows; after the aeration-reaction period (22.5 h), agitation and air flow were stopped to allow the

biomass to settle down (1h). In order to avoid false TOC measurements due to water evaporation, the liquid level in the SBR was maintained constant by adding water in the required amount. After 1 hour, the suitable volume (calculated with Equation 2.8) was withdrawn from the sample supernatant and replaced by the corresponding wastewater volume previously neutralized at pH=7. Finally, nutrients were also added to maintain the constant initial concentration. Agitation was turned on and samples were taken to perform TSS, VSS and pH analyses (readjusted to 7 if necessary). Finally the air flow was also restarted. The dissolved oxygen concentration (higher than 3 $mg \cdot L^{-1}$) was measured daily by means of a dissolved oxygen meter (model 407510 from Extech).

Prior to feed the SBR with the phototreated effluents, a start-up process was carried out in order to determine residual TOC produced by the bacteria metabolism. This start-up process was performed by feeding the SBR with municipal wastewater for 2 weeks and using a 10 days as HRT.

When the reactor was fed with phototreated solutions, the SBR experiments were continuously working for 12 or 16 cycles (depending on the experiment) to allow repetitive results (i.e., TOC variation coefficient lower than 4%) and if possible, stabilization of biomass (i.e., constant VSS value). One cycle was achieved when the total SBR initial volume had been replaced with new solution. New fresh biomass was used for each experiment.

3. Experimental design for the optimization of reagent doses

Experimental design is an interesting tool for the evaluation of a determined phenomenon by performing a minimal number of experiments. This methodology allows obtaining a surface response that depends on the different variables selected for study. By analysing the surface response, the importance of studied variables and the interaction effects between them can be found. In this way, photo-Fenton reagent concentrations to remove TOC from solution were selected by means of a multivariate experimental design. MODDE 5.0 software was used to work out the polynomial expressions and response surface.

A two factor and three levels central composite design (3^2) was adopted to investigate the effect of hydrogen peroxide and Fe^{2+} concentrations in the mineralization percentage. Volume, temperature and pH were kept constant for the experimental design. Concentration of hydrogen peroxide between 10 and 250 mg·L^{-1} and iron (II) concentration between 2 and 250 mg·L^{-1} were codified in three values within the range -1 to +1 at 95% confidence level. Eleven experiments were carried out. Three of them corresponded to the central point value that was repeated three times to check the statistical significance. Table 2.2 describes the experimental design. Additional data, corresponding to experimental design, is shown in Annexe 2.

Table 2.2 Two factor central composite design of photo-Fenton reagent optimization

Experiment	Run Order	$[Fe^{2+}]$ mg·L^{-1}	$[H_2O_2]$ mg·L^{-1}	Volume mL	Temperature °C	pH
1	11	2.0	10	250	25	2.8
2	2	20.0	10	250	25	2.8
3	10	2.0	250	250	25	2.8
4	3	20.0	250	250	25	2.8
5	1	2.0	130	250	25	2.8
6	6	20.0	130	250	25	2.8
7	8	11.0	10	250	25	2.8
8	4	11.0	250	250	25	2.8
9	5	11.0	130	250	25	2.8
10	7	11.0	130	250	25	2.8
11	9	11.0	130	250	25	2.8

4. Humic acids adsorption experiments

In publication 4, the characterization of the adsorption process of humic acid onto the biomass was required. With this aim, adsorption studies were carried out.

4.1. Adsorption kinetic study

The activated sludge used to evaluate adsorption kinetics was directly obtained from the aerobic stage of a full-scale urban WWTP in Manresa (Spain). A dilution was carried out to attain a TSS value of 1000 mg·L^{-1} in the final 1L solution. The adsorption of HA by the living activated sludge was studied as function of contact time. The adsorption kinetics were calculated by adding 200 mg of HA to the 1L biological reactor (1000 mg·L^{-1} TSS concentration). The reactor was agitated at constant temperature (20 ^{o}C). At selected time intervals, samples were collected from the reactor and the sludge was removed by centrifugation. In order to obtain the adsorption kinetic constant, TOC in solution was measured for 400 minutes.

TOC measurements were also carried out in a blank run without HA (the same amount of biomass) in order to correct the desorbed organic matter from the final TOC concentration. The final dissolved HA concentration (TOC, mg·L^{-1}) was calculated by subtracting the TOC corresponding to the blank from the TOC related to the HA

$$C_{solution} = C_{sample} - C_{desorbed} \qquad (2.9)$$

The amount of HA adsorbed was estimated as follows, where C_o is the initial TOC content of HA in solution without biomass

$$C_{adsorbed} = C_o - C_{solution} \qquad (2.10)$$

Several models can be used to analyze the kinetics of a sorption process although pseudo-first and pseudo-second-rate equations have been widely studied [7, 8]. The pseudo-first-order rate equation is

$$\frac{dq}{dt} = k_1(q_e - q_t) \qquad (2.11)$$

Where q_e and q_t are the grams of solute adsorbed per gram of adsorbent at equilibrium and at any time respectively. Integrating Eq 2.11 for the boundary conditions t=0 to t=t and q=0 to q=q gives

$$log(q_e - q_t) = logq_e - \frac{k_1 t}{2.303} \qquad (2.12)$$

Where k_1 is the rate constant of the pseudo-first-order sorption and is expressed in min^{-1}.

To fit the kinetic models it was necessary to determine q_t and q_e. These parameters were calculated as follows

$$q_t = \frac{mg\ TOC_{ad}(t)}{g\ TSS} \qquad q_e = \frac{mg\ TOC_{ad}(eq)}{g\ TSS} \qquad (2.13,\ 2.14)$$

The rate law of pseudo-second-order model is expressed as

$$\frac{dq}{dt} = k_2(q_e - q_t)^2 \qquad (2.15)$$

Integrating Equation 2.15 for the boundary conditions t=0 to t=t and q=0 to q=q gives

$$\frac{1}{(q_e - q_t)} = \frac{1}{q_e} + k_2 \cdot t \qquad (2.16)$$

Equation 2.16 can be rearranged to obtain a linear form

$$\frac{t}{q_t} = \frac{1}{k_2 q_e^{\ 2}} + \frac{1}{q_e} t \qquad (2.17)$$

Where k_2 is the pseudo-second-order rate constant of sorption expressed in $g \cdot mg^{-1} \cdot min^{-1}$ when q_e, is expressed in grams of solute adsorbed per gram of adsorbent. In order to find out the kinetic model involved in the process of biosorption of HA onto activated sludge, both the pseudo-first and pseudo-second-order kinetic models were used to fit the experimental data.

4.2. Isotherm adsorption experiments

Isotherm adsorption experiments were conducted using 250 mL vessels containing 10 mL of activated sludge (3300 mg·L^{-1} TSS). 90 mL of solutions of HA at different concentration (from 100 to 1000 mg·L^{-1}) were added, the vessels were stirred for a contact time of 24 hours at room temperature (20 ^{o}C), TOC was measured, and pH was adjusted to 7. After centrifugation TOC concentration of each sample was measured again. One vessel with biomass, but containing no HA, was added as a control experiment to correct the TOC concentration in each sample for desorbed organic matter. The HA concentration in solution (TOC) at equilibrium was calculated by subtracting the blank sample TOC measurement from the HA samples TOC measurements

$$C_e = C_{sample} - C_{desorbed} \qquad (2.18)$$

The equilibrium of biosorption of HA was modelled using Freundlich and Langmuir isotherms. The Langmuir isotherm is valid for a monolayer adsorption onto the surface with a finite number of identical adsorption sites. In this expression q_e was calculated according to Equation 2.14. Then, the Langmuir equation is expressed as follows

$$q_e = \frac{Q^0 b C_e}{1 + bC_e} \qquad (2.19)$$

The linearized form of Langmuir equation is

$$\frac{C_e}{q_e} = \left(\frac{1}{bQ^0}\right) + \left(\frac{C_e}{Q^0}\right) \qquad (2.20)$$

Where Q^0 is expressed in mg·g^{-1} and $1/b$ is expressed in mg·L^{-1}.

The Freundlich equation, that attempts to incorporate the role of substrate-substrate interactions on the surface, is given as

$$q_e = K_F C_e^{1/n} \qquad (2.21)$$

Where q_e was calculated according to Equation 2.14. This expression can be linearized as

$$\log q_e = \log K_F + \left(1/n\right) \cdot \log C_e \qquad (2.22)$$

Where K_F is expressed in mg·g^{-1}. In order to find out the isotherm model involved in the process of biosorption of HA onto activated sludge, both Langmiur and Freundlich models were used to fit the experimental data.

5. Analytical methods

5.1. Chemical analysis

5.1.1. Total Organic Carbon (TOC)

The Total Organic Carbon (TOC) is defined as the amount of CO_2 liberated when an organic sample is totally oxidized. The TOC methodology is based on the transfer of all the carbon present in solution to CO_2 to quantify the Total Carbon (TC) and the Inorganic Carbon (IC). Then, the TOC ($mg \cdot L^{-1}$) is calculated by subtracting IC to TC. Two analysers: model Shimadzu 5000 and a Shimadzu TOC-V_{CSH} were used. The test was carried out according to Standard Methods [9].

The TC measurements were based on the catalytic oxidation of the sample in a combustion tube to transform all carbon in CO_2. A platinum catalyst was supported on aluminium oxide spheres that filled the combustion tube where temperature was 680 ^oC. After the combustion, the carrier gas that consisted of CO_2 free air and flowed at 150 $mL \cdot min^{-1}$, was dehumidified and driven to a cell set containing a non-dispersive infrared gas analyzer (NDIR) where CO_2 was detected. The TC concentration was calculated by the equipment data processor. The IC was measured by previously acidifying the sample with 25% w/v phosphoric acid. Therefore, carbonate and bicarbonate were decomposed to CO_2. The IC concentration was determined by the same procedure as TC but without the catalytic oxidation (i.e., the sample does not go through the combustion tube). Finally TOC was measured as the difference between TC and IC. To determine the amount of TC, IC and TOC present in solution standard calibrations are required. Potassium hydrogen phthalate was used to calibrate the TC measurements whereas sodium carbonate and sodium hydrogen carbonate were used in IC calibration curves. All the standard solutions were prepared with water purified in a Millipore Milli-Q system and filtered through 0.45 μm pore size Nylon filter (Millipore) before analysis.

The measurement of TOC was mainly required in order to evaluate the mineralization process of the herbicides during the oxidation process. For sample measurement, 0.45 μm pore size Nylon syringe filters (Albet) were also used. When reactants could not be separated from solution (e.g., experiments containing ozone, iron and hydrogen peroxide) the TOC

measurements had to be performed directly after sampling. Each sample was injected at least twice to obtain a coefficient of variance of less than 2% for TOC measurement.

5.1.2. Chemical Oxygen Demand (COD)

The Chemical Oxygen Demand (COD) estimates the amount of organic matter present in an aqueous solution that is subject to oxidation by a strong chemical oxidizer. The measured COD is expressed in $mg \cdot L^{-1}$ (the O_2 needed to produce the stoichiometrical oxidation). The test was carried out in accordance with Standard Methods following the closed reflux method [10] commercially available from Hach Co. This analysis carried out the digestion of the sample at 150 ^oC for two hours. The digestion solution (also available from Hach Co.) consisted of an excess of potassium dichromate in presence of sulphuric acid and silver sulphate as catalyst. Mercury sulphate was also included to avoid the interference of oxidized chloride. Equation 2.23 shows the reduction of dichromate ion to oxidise organic matter.

$$Cr_2O_7^{2-} + 14\,H^+ + 6\,e^- \rightarrow 2\,Cr^{3+} + 7\,H_2O \qquad (2.23)$$

0-150 $mg \cdot L^{-1}$ and 0-1500 $mg \cdot L^{-1}$ range Aqualytic® vials were used in this study. During the digestion process, the organic matter was oxidized and the yellow dichromate was reduced to the green chromic ion. After this process, the vials were cooled to room temperature. Parallel to the determination of the COD content of a determined sample a blank was carried out with purified water. The amount of COD was colorimetrically determined at 420 nm by measuring the amount of chromic ion produced using a spectrophotometer (HACH DR/2000). The HACH spectrophotometer was calibrated to directly provide the COD value. The accuracy of the measurements was checked by preparing a potassium hydrogen phthalate standard. The tolerance of the method was estimated by Hach Co. as ± 3.5%.

COD interference due to H_2O_2 oxidation was subtracted for final result (see Section 5.1.4 for H_2O_2 quantification). On the other hand iron interference was discarded since Fe^{2+} concentration used was very low in all the processes. Even considering all the iron in its reduced form, the COD contribution of a 15.9 $mg \cdot L^{-1}$ Fe^{2+} initial dosage (the higher one employed) would not be higher than 2.3 $mg \cdot L^{-1}$.

5.1.3. O_3 measurements in gas phase

A spectrophotometric determination was performed to quantify the amount of ozone in gas phase. This measurement was conducted in the UV range by means of a gas Erwing Sander Quantozone-1 ozone meter able to detect 0-200 mg·m^{-3} of O_3. The maximum of the absorption coefficient of ozone is located at 253.7 nm and the relation between the absorption coefficient and ozone concentration was calculated according to the Lambert-Beer law.

$$A = \varepsilon \times b \times c \qquad (2.24)$$

Where A is the absorbance, ε is the molar absorbtivity with units of L·mol^{-1}·cm^{-1}, b is the path length of the cuvette in which the sample is contained, expressed in cm and finally, c is the concentration of the compound in solution, expressed in mol·L^{-1}.

As an alternative to this method, iodometric measurements were also carried out [11]. In this analysis, the gas was bubbled for 2 minutes through 100 mL of KI (0.120 mol·L^{-1}) buffered with Na_2HPO_4 (0.041 mol·L^{-1}) and $NaH_2PO_4 \cdot 2H_2O$ (0.026 mol·L^{-1}). Potassium iodide reacted with ozone generating iodine following Equation 2.25. After acidification with 5 mL of H_2SO_4, the iodine formed in the KI solution was titrated with a standardized tiosulphate solution (Equation 2.26)

$$O_3 + 2\,I^- + 2H^+ \longrightarrow I_2 + O_2 + H_2O \qquad (2.25)$$

$$I_2 + 2\,S_2O_3^{2-} \longrightarrow 2\,I^- + S_4O_6^{2-} \qquad (2.26)$$

The ozone flow was measured using Equation 2.27 and was expressed in mg·min^{-1}

$$O_3 = \frac{V_{S_2O_3^{2-}} \times C_{S_2O_3^{2-}} \times MW_{O_3}}{2 \times t_c} \qquad (2.27)$$

Where the $V_{S_2O_3^{2-}}$ is expressed in mL, the $C_{S_2O_3^{2-}}$ in eq·L^{-1}, MW_{O_3} in g·mol^{-1} and the contact time (t_c) is expressed in minutes.

5.1.4. H_2O_2 measurement by iodometric titration

The H_2O_2 quantification was performed by means of iodomety [12]. In this case, iodine was generated from the reaction between KI and H_2O_2 in an acidic media and under the presence of ammonium molybdate as catalyst. The test was carried out as follows; 10 mL of the hydrogen peroxide solution was transferred to 100 ml of purified water. After that 10 mL of 2 M sulphuric acid, 10 mL of potassium iodide 1 M solution, and 2 ml of 50 g·L^{-1} ammonium molybdate solution were sequentially added (reaction 2.28). After 5 minutes keeping the sample in the dark, the liberated iodine was titrated with standard 0.05 M sodium thiosulphate (reaction 2.26). To determine the end of the titration process, starch solution at 1% was used.

$$H_2O_2 + 2\,I^- + 2\,H^+ \rightarrow I_2 + 2\,H_2O \qquad (2.28)$$

$$I_2 + 2\,S_2O_3^{2-} \rightarrow 2\,I^- + S_4O_6^{2-} \qquad (2.26)$$

The amount of H_2O_2 was calculated with the following equation and expressed in mg·L^{-1}

$$H_2O_2 = \left(\frac{V_{S_2O_3^{2-}} \times C_{S_2O_3^{2-}}}{10}\right) \times \left(\frac{MW_{H_2O_2}}{2}\right) \times 1000 \qquad (2.29)$$

Where the $V_{S_2O_3^{2-}}$ is expressed in mL and the $C_{S_2O_3^{2-}}$ in mol·L^{-1} and $MW_{H_2O_2}$ in g·mol^{-1}.

The H_2O_2 quantification was required not only to determine the state of the mineralization process but also to perform some analytical tests. For instance, H_2O_2 was an important interference when COD was evaluated. Moreover, this toxic compound had to be eliminated prior to perform any biological analysis. H_2O_2 was eliminated by adding two times the stoichiometric demand of sodium sulphite to reduce all the H_2O_2 present in solution as explained in Section 2.2.1.

5.1.5. NH_4^+ measurement

To measure the amount of ammonia generated along the mineralization process, the Nessler method and an ammonium electrode were used.

5.1.5.1. Nessler method

The Nessler method is based on the reaction between ammonium and potassium tetraiodomercuriate (II), the later (Nessler reagent), being formed on site from mercury (II) chloride in alkaline potassium iodide media [13]. Then, the Nessler reagent complexes with ammonium ions as follows

$$NH_4^+ + 2\,[HgI]^{2-} + 4\,OH^- \rightarrow HgOHg(NH_2)I + 7\,I^- + 3\,H_2O \qquad (2.30)$$

Ammonium was measured by adding 2 mL of Nessler reagent to 5 mL of sample. After 10 minutes the absorbance was measured at 425 nm using a light path of 1 cm (Heliosγ from Thermo Electron Corporation). The relation between the absorption coefficient and ammonium concentration was calculated with the Lambert-Beer equation (Equation 2.24).

To prepare the Nessler reagent, the following procedure was followed. First, 2.2 g $HgCl_2$ and 5 g KI were dissolved in a small quantity of water. Then this mixture was added, slowly and stirring, to a cool solution of 4 g NaOH dissolved in less than 50 mL of water. The final solution was diluted to 100 mL and stored out of sunlight to maintain reagent stability. Sample pretreatment with zinc sulphate and alkali was needed to precipitate the iron when treating with Nessler reagent. A calibration curve was prepared with a NH_4Cl standard solution.

5.1.5.2. NH_4^+ electrode

An Orion 95-12 Ammonia Electrode and Crison pH/mV meter readable to 0.1 mV were used to measure the amount of ammonia generated along the mineralization process. Ammonium ion was measured after conversion to ammonia. The sensor consisted of a

hydrophobic gas-sensing membrane in order to separate the sample from the internal solution of ammonium chloride. The ammonia generated by increasing the pH of the sample entered the internal solution. The pH of ammonium chloride changed and this change was detected by means of a pH electrode. Ag/AgCl electrode was used as reference. A calibration curve was prepared with a NH_4Cl standard solution. During both, calibration and measurement stirring had to be low and constant. The log [NH_3] was plotted versus measured potential and the concentration of ammonium in the samples was calculated by interpolating the calibration curve.

5.1.6. Chromatographic methods

5.1.6.1. Reverse Phase HPLC-UV

Reverse Phase High Performance Liquid Chromatography (HPLC) coupled to UV detector was used to follow the degradation of the model compounds studied. The UV identification was possible because initial pesticides absorbed light of wavelength larger than 200 nm as shown in Table 2.3.

Table 2.3 HPLC-UV elution and detection conditions of target compounds

Herbicide	Wavelength (nm)	Mobile phase
Alachlor	225	acetonitrile/water (60/40)
Atrazine	240	acetonitrile/water (50/50)
Chlorfenvinphos	240	acetonitrile/water (60/40)
Diuron	254	acetonitrile/water (50/50)
Isoproturon	236	acetonitrile/water (50/50)
Linuron	254	acetonitrile/water (50/50)
pentachlorofenol	220	methanol/water pH 3 (80/20)

The chromatographic system employed consisted of a LC-10 AT VP pump (Shimatzu) and a UV-Visible diodearray detector (Agilent 1100 Series). The stationary phase was a C_{18}

Hypersil ODS Teknokroma column (4.6 × 250 mm × µm). The whole system control and the data evaluation were managed via a PC interface with Agilent ChemStation® software.

The mobile phase, that flowed at 1 mL·min^{-1}, was selected for the different herbicides depending on their intrinsic properties. Table 2.3 shows the conditions used for the seven herbicides studied. The mobile phase was degassed by sonication and filtered (0.45 µm Nylon filter, Millipore) before using. Prior to injection, samples were filtered through 0.20 µm Nylon syringe filters (Albet).

5.1.6.2. Reverse Phase UPLC-MS

Reverse Phase Ultra Performance Liquid Chromatography (UPLC) was used in publication a1.1 to identify by-products generated along the mineralization of Diuron and Linuron. The main differences between HPLC and UPLC are based on the length of the column employed as well as the pressure required to carry out the separation. Separation of first oxidation by-products along the herbicides mineralization was performed with an Acquity™ UPLC from Waters. The system was equipped with a UPLC™ BEH C_{18} capillary column (2.1 × 100 mm × 1.7 µm). The injection volume was 4 µL and temperature was not controlled. Two mobile phases were used; A) acetonitrile and B) acetonitrile (10%), water and formic acid (0.1%). The composition of the mobile phase changed according to the following gradient: 20% of A was maintained for 4 minutes. From 4 to 5 minutes, B was steadily increased to attain the 95%. Finally, the mobile phase returned to the initial composition until the end of the run (6 minutes). Prior to injection, samples were filtered through 0.20 µm PVDF syringe filters (Whatman).

The identification of by-products was performed with a mass spectrometer Quattro Premier -Micromass- also from Waters. Mass spectra were obtained by electro-spray ionization (ESI) in negative mode. Cone voltage of 25 V in full scan mode (40-380 m/z) and 23 V in the Multi Residual Monitoring mode (MRM) were used under the following conditions: source temperature: 120 ^{o}C, cone gas flow: 20.5 mL·min^{-1}. When sample concentration was required, OASIS HLB 6cc cartridges were used for solid phase extraction and ethanol was used as eluent. Mass spectra obtained from those experiments are presented in the Annexe 2.

5.1.6.3. Hydrophilic Interaction HPLC (HILIC-MS)

Small polar compounds were supposed to be generated at the end of the mineralization of most organic compounds. As explained in Chapter 1, Section 6.3. Hydrophilic Interaction Liquid Chromatography (HILIC) coupled to a mass spectrometer is a suitable method to analyze this type of compounds. HILIC was used to identify final by-products in the degradation of Diuron and Linuron.

The experimental setup was formed by a liquid chromatograph (Agilent 1100) equipped with a diol column (Nucleosil 4 × 150 mm × 7µm). The injection volume was 5.00 µL and temperature was not controlled. The mobile phase consisted of A) acetonitrile and B) 20 mM aqueous ammonium formate, the pH of which was adjusted to 3.3 with formic acid (B). The composition of the mobile phase changed following the next gradient: 95% of A was maintained for 3 minutes, and then it changed from 95% to 50 % in three more minutes. After that, A steadily decreased to 20 % up to minute 10. From 10 to 14 minutes the composition was kept stable at 20% A. Finally from 14 to 30 minutes the mobile phase returned to initial conditions. Prior to injection, samples were filtered through 0.20 µm Nylon syringe filters (Albet). An Esquire 3000 (Bruker) detector with electro-spray ionization (ESI) in positive mode was used in scan mode (50-200 m/z) under the following conditions: nebuliser pressure: 60. psi, drying gas flow: 10 $mL \cdot min^{-1}$, drying gas temperature: 360 ^{o}C, capillary voltage: 5000V. Mass spectra obtained from those experiments are presented in the Annexe 2.

5.1.6.4. Gas chromatography (GC-MS)

To identify other by-products generated during the mineralization process of Diuron and Linuron herbicides, Gas Chromatography coupled to mass spectrometry detector (GC-MS) was used. A previous solid phase extraction (Maxi-Clean C18 600 mg, Alltech) was carried out. A mixture of dichlormethane and ethyl acetate (1/1, v/v) was used to elute the products retained in the solid phase. This solution was concentrated under nitrogen flow for the by-products analysis. The GC-MS was performed using a HP 6890 series GC equipped with a MS detector (HP 5973). The system was equipped with a HP-5MS capillary column (30 m × 0.25 mm × 0.25 µm), splitless injection, and helium was used as carrier gas flowing at 1 $mL \cdot min^{-1}$. The GC oven temperature

was programmed to initially hold at 50º C for 3 min, then to increase from 50º C to 275 ºC at a rate of 5 ºC·min^{-1} and to hold at 275 ºC for 15 min. The injector and interface temperature were kept at 250 ºC. Mass spectra were obtained by the electron-impact mode (EI) at 70eV, using scan mode (30-800 m/z) under the following conditions: pressure: 7.63 psi, purge flow: 26.5 mL·min^{-1}, purge time: 1 min. Mass spectra obtained from those experiments are presented in the Annexe 2.

5.1.6.5. Ion Chromatography (IC)

Cl^- and NO_3^- ions generated along the mineralization process of Diuron and Linuron were analyzed with a Dionex DX120 Ion Chromatograph (IC) equipped with a conductivity detector using an IonPac® AS19 anion-exchange column (4 × 250 mm) as stationary phase. A gradient of KOH in water (10 mM from 0 to 10 min and then increasing to 45 mM from 10 to 25 min) was used as mobile phase. The flow rate was 1 mL·min^{-1} and the injection volume was 500 µL.

For the determination of short chain acids (oxalic, acetic and formic acids) the same system was used but the gradient was changed (10 mM from 0 to 10 min and then increasing to 58 mM from 10 to 40 min). Before measurement the sample was filtered through 0.45 µm cellulose acetate filters (Sartorius, Ministar).

5.2. Biological analysis

5.2.1. Toxicity evaluation by BioTox™ (EC_{50})

The commercial BioTox™ test is based on the inhibition of the light emission of luminescent bacteria Vibrio fischery due to the toxic properties of a sample. In concrete, the method used measures the concentration that causes the death of 50% of the bacteria population after a specific time of bacteria-toxic contact (effective concentration giving 50% inhibition of light output EC_{50}, expressed in $mg \cdot L^{-1}$). The toxicity evaluation was quantified according to ISO 11348-3 [14].

The procedure to obtain EC_{50} was as follows. For sample preparation iron, TiO_2, O_3 or H_2O_2 were previously removed before carrying out the experiment. To eliminate iron from solution pH was increased until 11 and, after iron precipitation, the sample was filtered through a 0.20µm Nylon syringe filter. On the other hand, TiO_2 was directly removed from solution by filtering the sample through a 0.20µm Nylon syringe filter. H_2O_2 was eliminated by adding catalase to the solution and O_3 was removed by bubbling air to the phototreated solution. Once the sample did not contain any impurities, the pH was adjusted to 7.0±0.2. During pH adjustment, the volume of the sample should not increase more than 5% in volume. After that, the salinity of the sample was adjusted with NaCl to 2% (w/v). Samples were kept at 15 ^oC until the beginning of the experiment (Biocold, Selecta).

To reconstitute Vibrio fischery, the reagent diluent, also included in the BioTox™ kit and previously cooled at 4 ^oC, was added to the microorganisms. This reconstituted reagent was equilibrated at 4 ^oC for 30 minutes and then at 15 ^oC for 15 more minutes. After that time, 0.5 mL of the final bacteria suspension was pipetted in the polystyrene cuvettes required to run the test and was stabilized at 15 ^oC for at least 15 more minutes.

The EC_{50} value was determined by combining different dilutions of the potential toxic sample with the bacteria. First, the luminescence intensity (IT_0) of initial bacteria was measured and immediately 0.5 mL of sample was added to the bacteria solution. After the selected contact time (i.e., 15 minutes), the luminescence intensity (IT_{15}) was measured again. The inhibitory effect of dilution was compared to a control free of toxic sample (IC_0 and IC_{15}). In this way, the percentage of inhibition (%INH) was calculated as follows

$$KF = \frac{IC_{15}}{IC_o} \qquad \%INH = 100 - \left(\frac{IT_{15}}{KF \times IT_0} \right) \times 100 \qquad (2.31, 2.32)$$

%INH value was plotted against the dilution factor and the curve obtained was used to calculate the EC_{50} value of the sample. The EC_{50} was directly provided by the BioTox™ software. The software determined the value by using standard linear regression analysis. If the value was out of the linearized range, the EC_{50} was graphically determined by using a double logarithmic co-ordinate system.

5.2.2. Biochemical Oxygen Demand (BOD)

The Biochemical Oxygen Demand (BOD) estimates the amount of biologically degradable organic matter present in a given volume of water at defined temperature over a specified time period and is expressed in $mg \cdot L^{-1}$. This parameter usually reflects the amount of oxygen consumed by aerobic bacteria in five days (BOD_5) of organic matter degradation at 20 ^oC.

The BOD_5 test was performed by means of an Hg free WWW 2000 OxiTop® system by measuring differences in pressure via electronic sensors as a result of oxygen consumption. The procedure to obtain BOD_5 was as follows. Before starting, a buffered solution and additional nutrients were prepared. The buffered solution consisted of 6.8 $g \cdot L^{-1}$ Na_2HPO_4 and 2.8 $g \cdot L^{-1}$ KH_2PO_4. The different nutrient solutions were prepared separately; 22.5 $g \cdot L^{-1}$ $MgSO_4 \cdot 7\ H_2O$, 27.5 $g \cdot L^{-1}$ $CaCl_2$, 0.15 $g \cdot L^{-1}$ $FeCl_3$ and 2.0 $g \cdot L^{-1}$ NH_4Cl [15].

To seed the wastewater with microorganisms, 100 g of garden ground was dissolved in 1L water to obtain the bacteria solution. After 10 minutes, 10 ml were withdrawn from the supernatant and diluted to 1L with Cu free water. A solution of glutamic acid (150 $mg \cdot L^{-1}$) and glucose (150 $mg \cdot L^{-1}$) neutralized at pH=7 by adding KOH was used as control (BOD_5=220 $mg \cdot L^{-1}$).

Depending on the range of BOD estimated in the experiment, the total volume of the BOD bottle was different. Table 2.4 summarizes this relation between BOD and volume. The BOD reading should be multiplied by the selected factor depending on this relation.

Table 2.4 Relation between BOD value and sample volume

Sample volume (mL)	Measuring range ($mg \cdot L^{-1}$)	Factor
432	0-40	1
365	0-80	2
250	0-200	5
164	0-400	10
97	0-800	20
43.5	0-2000	50

Expected values of BOD_5 of herbicides were lower than 40 $mg \cdot L^{-1}$, therefore the volume selected to carry out experiments was 432 mL. On the other hand 164 mL were required to run the control experiment (glucose/glutamic acid).

Prior to samples seeding, O_3 or H_2O_2 were removed when present in solution. To eliminate H_2O_2 sodium sulphite was added as explained in Section 2.2.1. O_3 was removed by bubbling air to the phototreated solution. Then, the pH was adjusted to 7.0±0.2. After that, 4 mL of buffered solution, 800 µL of each nutrient solution and 50 mL of microorganism solution were added to a well aerated sample obtaining a final volume of 432 mL. When control sample was prepared, 1.25 mL of buffer solution, 250 µL of each nutrient solution and 20 mL of microorganism solution were added to the well aerated glucose/glutamic acid solution obtaining 164 mL as final volume. The aeration was required to assure sufficient dissolved oxygen in the sample during microorganism incubation. A blank run was also carried out in all the experiments to determine the residual BOD_5 produced by the microorganism. To run the blank, 4 mL of buffered solution and 762 µL of each nutrient solution were added to 432 mL of microorganism solution. Nitrification was inhibited in all the experiments by adding 10 $mg \cdot L^{-1}$ of N-Allylthiourea. All the solutions were prepared and analyzed at least twice. When the bottles were filled, 2 NaOH tablets were added in a rubber quiver to remove carbon dioxide, thereby eliminating some of the potential for algae growth that could render erroneous data. Finally the bottles were sealed with the OxyTop® membrane. Zero was reset and bottles were kept in the incubator thermostatically controlled at 20 ^oC with constant agitation for 5 days. Results were directly obtained from the OxyTop® system. The result was corrected by subtracting the reading obtained from the blank and also by recalculating the initial sample volume.

5.2.3. Zahn-Wellens inherent-biodegradability test

The purpose of the Zahn-Wellens static test is the evaluation of the potential inherent biodegradability of water-soluble non-volatile organic matter when exposed to relative high concentrations of microorganisms. The biodegradability was investigated under aerobic conditions according to OECD Guideline [16].

The microorganisms used in this test were obtained from the aerobic stage of a full-scale urban WWTP in Manresa (Spain). A nutrient solution was prepared by dissolving 3.85 g NH_4Cl, 3.34 g $NaHPO_4 \cdot 2H_2O$, 0.84 g KH_2PO_4 and 2.175 g K_2HPO_4 in 100 mL of deionised water.

Three vessels were set. The first one contained 2 L of wastewater (i.e., initial polluted effluent) whose pH was previously adjusted to 7.0±0.2. 2.5 mL·L^{-1} of nutrient solution and 0.6 g·L^{-1} dry matter activated sludge were added to the final mixture. A blank was run in the second vessel. This vessel contained 2 L of Cu free water, 2.5 mL·L^{-1} of nutrient solution, and 0.6 g·L^{-1} dry matter activated sludge. Finally the third vessel, containing a pulse of ethylenglycol solution, nutrients and microorganisms, was run as control to assess the activity of the biomass.

The test vessels, working at room temperature, were agitated with magnetic stirrers and covered from any external light. Air was flowed into the reactor by means of a non controlled glass air diffuser for 28 days. TOC was measured daily by centrifuging a sample withdrawn from the vessel. Water losses from evaporation, which could be a source of experimental errors, were made up just before each sampling by adding deionised water in the required amount. Moreover, pH was controlled daily and, if necessary, readjusted to pH 7.0±0.2.

Physico-chemical adsorption onto the microorganisms was evaluated by taking samples after 3 hours of test time. The Biodegradability in the Zahn-Wellens test was calculated as follows

$$D_t = \left[1 - \left(\frac{C_T - C_B}{C_A - C_{AB}}\right)\right] \times 100 \qquad (2.33)$$

Where D_t is the percentage of biodegradation, C_A the TOC value in the test mixture three hours after the beginning of the test, C_T the TOC value in the test mixture at time of sampling, C_B the TOC value of the blank at time of sampling and, finally, C_{AB} is the TOC value of the blank

measured three hours after the beginning of the test. The percentage of biodegradability was plotted against the time to give the biodegradability curve.

5.2.4. Respirometry

The respirometric assay was used to investigate the Oxygen Uptake Rate (OUR). The OUR gives an idea of the rate of oxygen consumption by the biomass when assimilating organic matter. This measure is defined as the amount of oxygen consumed per time unit. Furthermore it is a rapid and straightforward method for the evaluation of the biodegradability and toxicity of a particular wastewater.

The measurements were carried out by controlling the oxygen input and output in a biological reactor (i.e., respirometer) at 25.0±0.2 ^{o}C by following Standard Methods [17]. A liquid-static-static (LSS) respirometer was used in this work. In this type of reactor, the oxygen measure was performed in the liquid phase by keeping under static conditions the liquid and gas phase. Figure 2.4 shows the LSS respirometer.

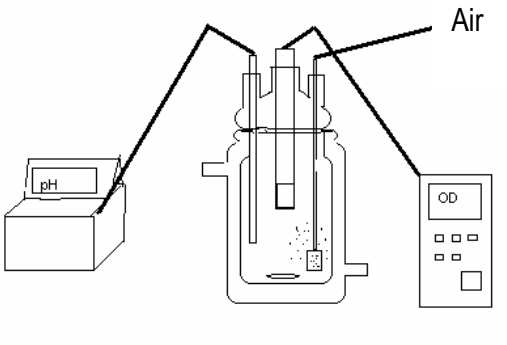

Figure 2.4 Experimental LSS respirometer

The variation of dissolved oxygen (DO) was plotted versus time and the OUR was determined as follows

$$d(V_L \times S_o) \big/ dt = -OUR \times V_L \qquad (2.34)$$

Where V_L is the volume of liquid phase expressed in m^3 and S_o is the concentration of dissolved oxygen expressed in kg DO $\cdot$ m^{-3}. Finally, *OUR* is expressed in kg $\cdot$DO $\cdot m^{-3} \cdot s^{-1}$.

The activated sludge used as inoculum of the respirometer was directly obtained from the aerobic stage of a full-scale urban WWTP in Manresa (Spain). Initial TSS value was between 3000 and 4000 mg·L^{-1}. 250 mL of activated slugged suspension were placed in the reactor and air flowed until dissolved oxygen reached 7 mg·L^{-1}. After that, the air diffuser was removed from solution and the reactor was closed. The OUR of the microorganisms in absence of any nutrient (OUR endogenous) was measured by plotting the DO vs time. The measurement of OUR endogenous was required prior to any measurement, then the exogenous consumption of the organic matter of the sample was determined as

$$OUR_{exogeneous} = OUR_{sample} - OUR_{endogenous} \quad (2.35)$$

From now on, the OUR of a sample is referred to its $OUR_{exogenous}$.

Quantification of OUR corresponding to a completely biodegradable standard (acetic acid) was carried out and used as a reference (OUR_{st}) to compare with the OUR of an herbicide sample of the same COD content. In this way, biodegradability was assessed. A pulse of acetic acid was firstly added and OUR_{st} was calculated until this product was completely assimilated by the biomass. After that, the biomass was settled down and 125 mL of supernatant were replaced by the herbicide solution. Concentration of herbicide was reduced to half with this process. When feeding the respirometer with phototreated solutions, the elimination of H_2O_2 and O_3 was required. To eliminate H_2O_2 sodium sulphite was added as explained in Section 2.2.1. O_3 was removed by bubbling air to the phototreated solution. Then, the pH was adjusted to 7.0±0.2. Finally OUR of the herbicide was measured and biodegradability was calculated as follows

$$\%biodegradability = \left(1 - \left(\frac{1^{st}OUR_{st} - OUR_{herbicide}}{1^{st}OUR_{st}}\right)\right) \times 100 \quad (2.36)$$

Toxicity was also evaluated by means of respirometry [18]. To assess toxicity, the OUR of a new acetic acid solution (2^{nd} OUR_{st}) once the biomass had been in contact with the potential toxic solution was measured. If the solution did not have a toxic effect on the biomass, the OUR of the same biomass exposed for a second time to acetic acid (2^{nd} OUR_{st}) would be the same as

the OUR of the same reference solution in contact with the fresh biomass (1^{st} OUR_{st}). Thus, toxicity was calculated as follows

$$\%toxicity = \left(\frac{1^{st} OUR_{st} - 2^{nd} OUR_{st}}{1^{st} OUR_{st}} \right) \times 100 \qquad (2.37)$$

5.2.5. Total and Volatile Suspended Solids (TSS, VSS)

Total and Volatile Suspended Solid (TSS and VSS) were required in order to characterize the biomass. These measurements were carried out according to Standard Methods [29, 20].

TSS corresponds to suspended matter with a diameter higher than 20 µm. To perform this analysis a homogenized sample was filtered through a weighted glass-fibre filter (Albet FV-C) and the residue retained in the filter was dried at 103-105 ºC for 1 hour. After cooling to room temperature in a dissector, the filter weight increase corresponds to the TSS value.

$$TSS = \left(\frac{W_A - W_B}{V} \right) \times 1000 \qquad (2.38)$$

Where W_A is the weight of dried residue and dried filter and W_B is the weight of dried filter both expressed in mg. V is the volume of the sample expressed in mL.

To estimate the amount of VSS the weighed filter with the residue was ignited at 500 ºC. The remaining solid represents the Fixed Total Solids while the weight lost on ignition was the VSS. This determination offered a rough approximation of the amount of activated sludge in solution and was calculated as follows

$$VSS = \left(\frac{W_A - W_C}{V} \right) \times 1000 \qquad (2.39)$$

Where W_A is the weight of residue before ignition and W_c the weight of residue after ignition both expressed in mg. V is the volume of the sample expressed in mL.

6. Life Cycle Assessment (LCA)

The Life Cycle Assessment (LCA) was used in this study to compare, from an environmental point of view, different small-scale wastewater treatments. For the application of the LCA tool, the ISO 14040 Standard was used [21]. As already mentioned in the introduction (Chapter 1, Section 7), the ISO 14040 Standard determines four basic stages for LCA studies that are; goal and scope, inventory analysis, impact assessment and the interpretation. For the application of the LCA methodology SimaPro 7.0 s using mainly the Ecoinvent database version 1.2 was used [22].

The scope of the LCA performed in this study is to compare different wastewater treatment-based AOPs. The functional unit enabled different systems to be treated as functionally equivalent and allowed reference flows to be determined for each of them [24]. Thus, in order to compare different scenarios, a functional unit was selected. The information about the scope of the study is widely described in the second work accepted for publication presented in Annexe 1 of this thesis.

The inventoried data, which corresponded to the inputs and outputs of the system, was classified considering the potential environmental impacts categories included in the CML 2 baseline 2000 method [23]. The impact categories contemplated in this work were the following:

- Abiotic Resource Depletion (ARD), which are natural resources (including energy resources) which are regarded as non renewable in a short term,
- Global Warming Potential (GWP), which refers to the impact of human emissions on the radiative forcing of the atmosphere,
- Ozone Depletion Potential (ODP), which refers to the thinning of the stratospheric ozone layer as a result of anthropogenic emissions,
- Human Toxicity Potential (HTP), which covers the impacts on human health of toxic substances present in the environment,
- Freshwater Aquatic Toxicity Potential (FATP), which refers to the impacts of toxic substances on freshwater aquatic ecosystems,
- Marine Aquatic Ecotoxicity Potential (MAEP), which refers to the impacts of toxic substances on marine aquatic ecosystems,

- Terrestrial Ecotoxicity Potential (TEP), which refers to the impacts of toxic substances on terrestrial ecosystems,
- Photochemical Oxidation Potential (POP), which refers to the formation of photooxidants such as ozone by the action of sunlight on certain primary air pollutants,
- Acidification Potential (AP), which contains a wide variety of impacts on soil, groundwater, surface waters, biological organisms, ecosystems and materials due to acidifying pollutants such as SO_2, NO_x and NH_x,
- Aquatic Eutrophication Potential (AEP), which covers all potential impacts of excessively high levels of macronutrients, the most important of which are nitrogen and phosphorous.

REFERENCES TO CHAPTER 2

[1] Hulstrom R., Bird. and Riordan C. (1985). Spectral solar irradiance data sets for selected terrestrial conditions. Solar Cells. 15, 365-391.

[2] ASTM (1987). Standard Tables for terrestrial solar spectra irradiance and or mass 1.5. American Society for Testing and Materials E 891-87.

[3] Maldonado M.I., Gernjak W., Oller I., Carrión A., Berruelo R. and Malato S. (2003). Photo-Fenton degradation of target compounds. CADOX-T110-CIEMAT-01 in CADOX project. www.psa.es.

[4] Passarinho P. (2003).Titanium dioxide photodegradation of target compounds. CADOX-T110-INETI-01 in CADOX project. www.psa.es.

[5] Contreras S. (2003). Degradation and biodegradability enhancement of nitrobenzene and 2,4-dichlorophenol by means of Advanced Oxidation Processes based on ozone. PhD thesis. U. B. Barcelona.

[6] Adams C.D., Scanlan P.A., Secrist N.D. (1994). Oxidation and biodegradability enhancement of 1,4-dioxane using hydrogen peroxide and ozone. Environ. Sci. Technol. 26, 1812-1818.

[7] Ho Y.S. and McKay G. (1999). Pseudo-second order model for sorption processes. Process Biochem. 34, 451-465.

[8] Ho Y.S., Ng J.C.Y., and McKay G. (2000). Kinetics of pollutant sorption by biosorbents: Review. Sep. Purif. Methods. 29, 189-232.

[9] APHA-AWWA-WEF (1992). Standard Methods for the examination of water and wastewater nº 5310B. (18th ed). American Public Health Association. Washington, USA.

[10] APHA-AWWA-WEF (1992). Standard Methods for the examination of water and wastewater nº 5220D. (18th ed). American Public Health Association. Washington,USA.

[11] Beyer M and Walter E. (1987). Manual de química orgánica. Reverté S.A. Barcelona, Spain.

[12] Jeffery G.H., Basset J., Mendham J. and Denny R.C. (1989). Vogel´s Textbook of Quantitative Chemical Analysis. Longman. (5th ed). New York, USA.

[13] Nichols M.L. and Willits C.O. (1934). Reactions of Nessler´s solution. J. Am. Chem. Soc. 56, 769-774.

[14] ISO, Water quality. (1998).Determination of the inhibitory effect of water samples on the light emission of Vibrio fishery (Luminescent bacteria test). ISO 11348-1. International Standardization Organism. Geneva, Switzerland

[15] PNE 77-003. (1978). Métodos de análisis de agua. Determinación de la demanda bioquímica de oxígeno. Método de dilución y siembra. Madrid, Spain.

[16] OECD. (1992). Inherent biodegradability modified Zahn Wellens test. Test Guideline 302B. Paris, France.

[17] APHA-AWWA-WEF (1992). Standard Methods for the examination of water and wastewater nº 2710B. (18th ed). American Public Health Association. Washington, USA

[18] Guisasola A., Baeza J. A., Carrera J., Casas J. and Lafuente J. (2003). An off-line respirometric procedure to determine inhibition and toxicity of biodegradable compounds in biomass from an industrial WWTP. Water Sci. Technol. 48, 267-275.

[19] APHA-AWWA-WEF (1992). Standard Methods for the examination of water and wastewater nº 2540D. (18th ed). American Public Health Association. Washington, USA

[20] APHA-AWWA-WEF (1992). Standard Methods for the examination of water and wastewater nº 2540E. (18th ed). American Public Health Association. Washington, USA.

[21] ISO, Water quality (1997). Environmental Management –Life Cycle Assessment- Principles and framework.. ISO 14.040. International Standardization Organism. Geneva, Switzerland.

[22] Ecoinvent www.ecoinvent.ch. (2006) Program SIMAPRO 7.0 database.

[23] Guinée JB, Gorree M, Heijungs R, Huppes G, Kleijn R, Udo de Haes HA, Van der Voet E, Wrisberg M.N. (2002) Life Cycle Assessment. An operational guide to ISO standards. Vol 1, 2, 3. Centre of Environmental Science, Leiden University (CML), The Netherlands.

CHAPTER 3
RESULTS AND DISCUSSION

1. Main results and discussion

This doctoral dissertation is presented in the form of a compendium of articles which have already been published (see later in the chapter). Consequently only the most significant results are highlighted in order to summarize the accomplished goals. Each publication is commented on individually enclosing all of them in a same general context; the coupling of AOPs with biological treatment for the remediation of water polluted with herbicides.

Publication 1

- Farré M.J. et al. (2005). Degradation of some biorecalcitrant pesticides by homogeneous and heterogeneous photocatalytic ozonation. *Chemosphere.* 58, 1127-1133.

The starting point for this experimental work was the selection of an effective Advanced Oxidation Process (AOP) for the removal of different herbicides from water. The herbicides investigated were Alachlor (50 mg·L^{-1}), Atrazine (35 mg·L^{-1}), Chlorfenvinphos (50 mg·L^{-1}), Diuron (42 mg·L^{-1}), Pentachlorophenol (50 mg·L^{-1}), and Isoproturon (50 mg·L^{-1}). All considered Priority Hazardous Substances by the Water Framework Directive of the European Commission [1]. The tested AOPs were photo-Fenton, TiO_2-photocatalysis, Ozone/UV, photo-Fenton/ozone and TiO_2-photocatalysis/ozone all performed under similar experimental conditions previously imposed to attain the goals of a wider project where this work was enclosed (EC CADOX, EVK1-CT-2002-00122) (i.e., T=25 ^oC and pH=3 except for Pentachlorophenol for which the initial pH was 7 to increase the solubility of this herbicide in water). The photo-Fenton reagent concentrations were $[Fe^{2+}]$=2 mg·L^{-1} and $[H_2O_2]$=200% stoichiometric amount necessary for the complete mineralization of parent herbicide. On the other hand, $[TiO_2]$=250 mg·L^{-1} was used in heterogeneous photocatalysis tests. Finally, the ozone flux was adjusted to 1.6 g·h^{-1} when necessary. A UVA black light, with a measured intensity of 0.21 mW·cm^{-2}, was employed as photon source.

Results obtained from mineralization of herbicides solutions are shown in Table 3.1. The presented values correspond to the percentage of Total Organic Carbon (TOC) removal after 75 minutes of photo-treatment time.

Table 3.1. % of TOC removal after 75 minutes of AOPs application to solutions of Alachlor (50 mg·L^{-1}), Atrazine (35 mg·L^{-1}), Chlorfenvinphos (50 mg·L^{-1}), Diuron (42 mg·L^{-1}), Pentachlorophenol (50 mg·L^{-1}) and Isoproturon (50 mg·L^{-1}) T=25 ^{o}C, pH=3 except for Pentachlorophenol pH=7. [Fe^{2+}]=2 mg·L^{-1} and [H_2O_2]=200% stoichiometric demand. [TiO_2]=250 mg·L^{-1}. [O_3]=1.6 g·h^{-1}. I=0.21 mW·cm^{-2}.

	photo-Fenton	TiO_2-photocatalysis	ozone/UV	photo-Fenton/ozone	TiO_2-photocatalysis/ozone
Alachlor	2±1	-(*)	20±3	50±3	40±4
Atrazine	5±1	-(*)	-(*)	25±3	8±3
Chlorfenvinphos	20±2	25±2	50±2	78±4	42±3
Diuron	-(*)	-(*)	30±3	69±3	45±3
Isoproturon	-(*)	-(*)	20±2	60±3	45±4
Pentachlorophenol	15±5	-(*)	60±5	90±5	50±3

n=3, α=95. (*) Negligible mineralization

The low percentages observed on TOC removal when herbicides were treated with photo-Fenton and TiO_2-photocatalysis were probably obtained due to the low Fenton reagents concentration utilized (i.e., [Fe^{2+}]=2 mg·L^{-1}) and the low intensity of the photon source employed (i.e., 0.21 mW·cm^{-2}). Nevertheless, higher mineralization yields were obtained when adding ozone to both techniques (see Table 3.1). Furthermore, initial biorecalcitrant herbicides disappeared after a few minutes of the photo-Fenton/ozone and TiO_2-photocatalyisis/ozone process as shown in Figure 3.1.

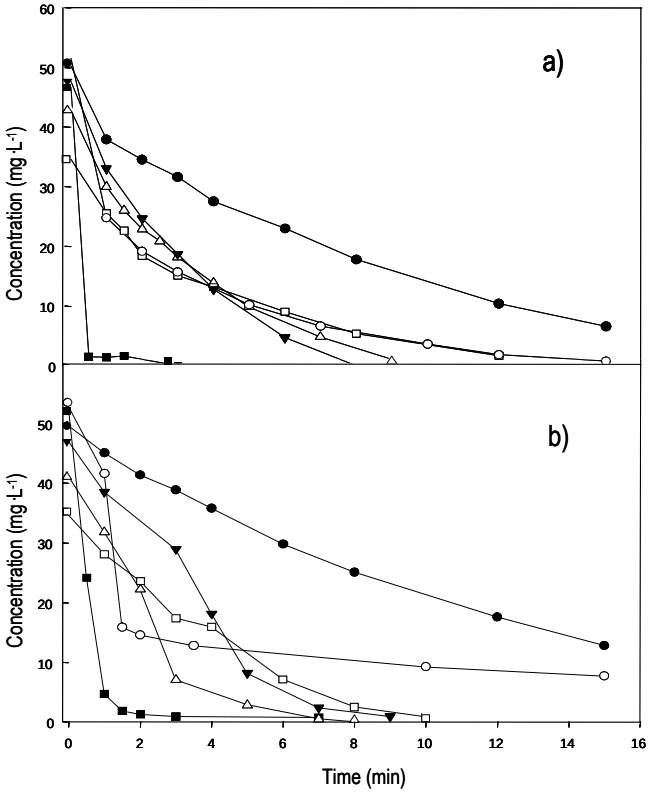

Figure 3.1. Time course of the concentration of different herbicides in aqueous solutions during the application of a) photo-Fenton/ozone and b) TiO_2-photocatalysis/ozone: (●) Alachlor, (■) Pentachlorophenol, (Δ) Diuron, (□) Atrazine, (▼) Isoproturon and (o) Chlorphenvinphos. T=25 ^{o}C, pH=3 except pH=7 for Pentachlorophenol. [Fe^{2+}]=2 mg·L^{-1}, [H_2O_2]=200% stoichiometric amount necessary for the complete mineralization, [TiO_2]= 250 mg·L^{-1} and ozone flux= 1.6 g·h^{-1}

Initial degradation rates of the aqueous herbicide solutions followed first-order reaction kinetics for photo-Fenton/ozone system, whereas when using TiO_2-photocatalysis/ozone, zero-order kinetics could be used to describe the initial degradation process [2, 3]. It was assumed a direct hydroxyl radical attack during the herbicides degradation mechanism, thus a first-order kinetic is consistent with a constant concentration of these radicals as a result of the photo-Fenton process, the ozonation system, and the synergy of both methods. Hence, degradation rates were only pollutant concentration dependant. On the other hand, the zero-order kinetics obtained when TiO_2-photocatalysis/ozone was used as degradation system were probably related to the slow radical production at the semiconductor surface (see Chapter 1, Section 2.1.2.1.1).

Of these two degradation techniques, the photo-Fenton/ozone system gave optimal results concerning herbicide degradation (see Figure 3.1). Thus, this process was considered the most effective for a rapid removal of toxic and non biodegradable chemicals with relation to the other alternatives tested. As explained in the introduction, when coupling photo-Fenton and ozone systems HO· radicals production is increased due to the synergy between both methods (see Chapter 1, Section 2.1.2.2.2). Apart from radicals produced by the photo-Fenton and UV/ozone processes, when mixing both Fenton´s reagents and ozone, the HO· concentration increases as a consequence of Fe^{2+} oxidation by ozone as follows [4].

$$Fe^{2+} + O_3 \rightarrow [FeO]^{2+} + O_2 \qquad (3.1)$$

$$[FeO]^{2+} + H_2O \rightarrow Fe^{3+} + HO\cdot + HO^- \qquad (3.2)$$

As mentioned previously, although herbicides disappeared promptly from solution, large amounts of TOC remained dissolved after photocatalytic degradation. Depending on the biorecalcitrant character of the remaining TOC, a subsequent biological treatment could be used to completely eliminate organic matter from solution. In this way, the assessment of acute toxicity of phototreated effluents was performed as a first attempt to envisage a possible coupling between chemical and biological systems for the removal of herbicides from water. Acute toxicity was investigated by means of BioTox™ system which is based on the response of Vibrio fischery

microorganism. Preliminary results showed an acute toxicity increase during the first minutes of the mineralization process of all the selected herbicides, even so detoxification could be achieved before 100 minutes of photo-Fenton/ozone treatment for Diuron, Isoproturon and Chlorfenvinphos. On the other hand, the chemical treatment was not able to detoxify Atrazine and Alachlor solutions, at least at treatment times lower than 2 and 3 hours respectively. In the case of Pentachloropheol, non toxic solution was achieved after 30 minutes of chemical treatment. Nevertheless, it must be noted that after this time, the TOC reduction of Pentachlorophenol solution was 80%, thus making the quantitative determination of such parameter difficult.

In order to investigate a possible coupling between chemical and conventional biological processes more information concerning toxicity and biodegradability of phototreated effluents was required. In fact, some authors [5, 6, 7, 8] suggest that although Vibrio fischery is suitable as a screening test for toxic samples, it should not be used to determine the potential effect to the biomass present in a conventional biological treatment. In general, Vibrio fischery is more sensitive than the bacteria consortium present in an activated sludge and may give an overestimation of the acute toxicity effect (see Chapter 1, Section 6.1). Hence, publication 2 was focused on the evaluation of different methods to assess the required parameters, based on the direct response of activated sludge, to envisage a possible coupling between chemical and biological treatments.

Publication 2

-Farré et al. (2007). Biodegradability of treated aqueous solutions of biorecalcitrant pesticides by means of photocatalytic ozonation. *Desalination.* 211, 22-33.

The herbicides selected were Alachlor (50 mg·L^{-1}), Atrazine (35 mg·L^{-1}), Diuron (42 mg·L^{-1}), Pentachlorophenol (50 mg·L^{-1}), and Isoproturon (50 mg·L^{-1}). In agreement with results obtained from publication 1, the photo-Fenton/ozone system was the most effective method to degrade aqueous solutions of selected herbicides. Nevertheless, after the degradation of the initially toxic and non biodegradable parent compound, large amounts of TOC remained in solution.

As emphasized before, depending on the biocompatibility of the remaining dissolved TOC, an economical biological treatment could be used to completely eliminate organic matter from solution, mimising in that way operational cost mainly related to the chemical process. Hence, ready biodegradability and acute toxicity of phototreated effluents was investigated by means of conventional analytical tests based on the evaluation of well-known parameters such as 5-days Biochemical Oxygen Demand (BOD_5) and toxic effective concentration (EC_{50}). Moreover, the estimation of real Wastewater Treatment Plant (WWTP) bacterial response to photodegraded effluents was accomplished by means of respirometric measurements of activated sludge.

A preliminary step was performed by measuring acute toxicity of the different initial and phototreated solutions by means of BioTox™ system. Results showed that after the disappearance of parent herbicides, toxicity decreased only for the Diuron polluted effluent while Isoproturon and Pentachlorophenol solutions showed a discrete improvement that could be within the experimental margin of error. Nevertheless, the toxicity of Isoproturon and Pentachlorophenol phototreated solutions was completely removed with longer pretreatment times. On the other hand, the toxicity of Alachlor and Atrazine phototreated solutions increased after parent compound removal and, even after 3 h of pretreatment both solutions remained toxic for Vibrio fischery.

Ready biodegradability of phototreated effluents was quantified by means of BOD_5/COD, which is the most extensive index to quantify such parameter. A ratio higher than 0.4 is commonly accepted for completely biodegradable wastewater while a value between 0.2-0.4 corresponds to partially biodegradable samples [9]. Results obtained after the disappearance of parent compounds showed that, with the exception of Pentachlorophenol, the BOD_5/COD ratio increased reaching values close or above 0.4. Thus, it seemed that more biodegradable by-products were generated along the mineralization process except for Pentachlorophenol solution.

As emphasized before, in order to evaluate the possible coupling between chemical and biological processes, real activated sludge from a WWTP was required. In this way, respirometric analyses were performed to initially polluted effluents and results were compared with those obtained with the Vibrio fischery test. The BioTox™ data indicated the following order of toxicity: Pentachlorophenol > Diuron > Isoproturon > Atrazine > Alachlor, while respirometric data gave

the order Pentachlorophenol > Alachlor > Atrazine > Isoproturon = Diuron. These differences were explained based on the different nature of the biological material used. BioTox™ utilized the seawater Vibrio fischery whereas respirometry used the bacterial consortium present in activated sludge. It is well known that the biological response induced in different living organisms challenged by a chemical substance is diverse because not all microorganisms respond to all toxic substances released in the same way [10]. On the other hand, the same low biodegradability was obtained with both respirometric and BOD_5/COD tests.

When phototreated solutions were analysed by means of respirometry of activated sludge, Isoproturon and Diuron solutions remained non toxic, while Atrazine, Alachlor and Pentachlorophenol did. Thus, concerning toxicity, there was a reasonable agreement between the respirometric and the BioTox™ acute toxicity results. Comparing biodegradability of phototreated solutions by both, BOD_5/COD and respirometric assays the same conclusions were obtained. Biomass was able to assimilate Diuron, Isoproturon, Atrazine and Alachlor but not Pentachlorophenol phototreated solutions. Nevertheless different values comparing biodegradability percentages were obtained with respirometric assays and the BOD_5/COD ratio. The differences between those values could be explained because respirometric assays measure biodegradability in a short period of time (minutes), whereas the BOD_5/COD ratio measures biodegradability in a five day scenario.

Finally, a possible coupling between chemical and biological treatments could be inferred for phenylureas Diuron and Isoproturon polluted effluents. For Pentachlorophenol, the remained TOC fraction in solution was non biodegradable, thus giving no chance to a possible coupled treatment without a stronger previous oxidation. Finally, with relation to Alachlor and Atrazine, toxic solutions were clearly obtained after parent degradation of initial polluted effluents. For these compounds, the AOP should also be extended in time to achieve detoxification.

Publication 3

- Farré M.J. et al. (2006). Assessment of photo-Fenton and biological treatment coupling for Diuron and Linuron removal from water. *Water Research.* 40, 2533-2540.

In agreement with preceding results, the photo-Fenton/ozone system was the most effective AOP, among all the alternative processes tested, to remove the selected herbicides from water. Nevertheless, due to the high operational costs related to the ozone production (see Chapter 1, Section 2.1.2.2), and the numerous advantages concerning the photo-Fenton system (see Chapter 1, Section 2.1.1), the coupling between single photo-Fenton and biological treatment for the removal of herbicides from water was preferred. Diuron (42 $mg \cdot L^{-1}$) was selected as target compound to ascertain such a possible coupling. However, due to the low solubility of Diuron (i.e., TOC_o=20 $mg \cdot L^{-1}$), Linuron herbicide (75 $mg \cdot L^{-1}$), with similar chemical structure, was added to the solution in order to increase the initial TOC concentration (i.e., TOC_o=50 $mg \cdot L^{-1}$). In this way the target polluted effluent was a mixture of Diuron and Linuron, both phenylurea compounds.

There are two important factors affecting the rate of photo-Fenton reaction once the photon source is fixed: hydrogen peroxide and iron concentrations. The hydrogen peroxide is important in order to obtain quantitative degradation, while the iron concentration is important for the reaction kinetics [13]. However, the increase of the concentration of hydroxyl radical scavengers when an excess of reactants is added to the solution can be detrimental. Thus, the concentration of photo-Fenton reagents was optimized by means of multivariate experimental design.

Since the scope of the present study was the coupling between chemical and biological treatment, minimization of the former was required. In keeping with this, one hour of photo-treatment time was fixed to perform all the degradation experiments and results were compared based on the percentage of TOC removal. Other parameters such as pH and temperature were also maintained constant (i.e., pH=2.8, T=25 ^oC). Figure 3.2 shows the surface response obtained from the photo-Fenton reagent optimization by means of multivariate experimental design at 95% of confidence level. The single polynomial expression obtained from the experimental design was shown through Equation 3.3.

$$Y=-6.24 + 2.61\,[Fe^{2+}] - 0.00818\,[H_2O_2] - 0.118\,[Fe^{2+}]^2 + 0.00981\,[Fe^{2+}][H_2O_2] \qquad (3.3)$$

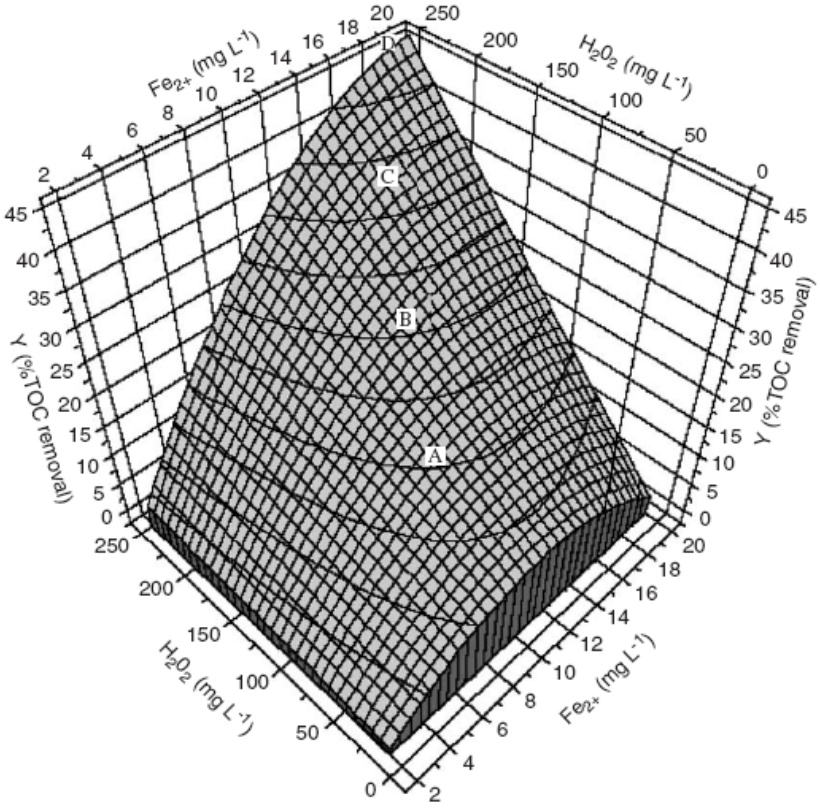

Figure 3.2. The mineralization percentage (Y) surface of Linuron and Diuron solutions as function of the reactant dose after 1h of photo-Fenton pre-treatment. T=25 ºC, pH=2.8. 95% confidence level. A: $[Fe^{2+}]$=9.25 mg·L^{-1}, $[H_2O_2]$=97.1 mg·L^{-1} (16% TOC removal); B: $[Fe^{2+}]$=13.3 mg·L^{-1}, $[H_2O_2]$=143 mg·L^{-1} (25% TOC removal); C: $[Fe^{2+}]$=15.9 mg·L^{-1}, $[H_2O_2]$=202 mg·L^{-1} (36% TOC removal); and D: $[Fe^{2+}]$=20.0 mg·L^{-1}, $[H_2O_2]$=250 mg·L^{-1}, (46% TOC removal)

As seen in Equation 3.3, the percentage of TOC removal was mainly influenced by Fe^{2+} concentration. Nevertheless, a negative effect was observed when using a reagent overload, due to HO· scavenger side reactions that reduced the concentration of those radicals in solution (see Chapter 1, Section 2.1.1.1) [11]. From this experimental design, four different reactant dose combinations were considered (i.e., A, B, C and D), each one corresponding to the minimum quantities of Fe^{2+} and H_2O_2 needed to achieve a desired mineralization percentage. The selected doses were A: $[Fe^{2+}]$=9.25 mg·L^{-1}, $[H_2O_2]$=97.1 mg·L^{-1} (16% TOC removal); B: $[Fe^{2+}]$=13.3 mg·L^{-1}, $[H_2O_2]$=143 mg·L^{-1} (25% TOC removal); C: $[Fe^{2+}]$=15.9 mg·L^{-1}, $[H_2O_2]$=202 mg·L^{-1} (36% TOC removal); and D: $[Fe^{2+}]$=20.0 mg·L^{-1}, $[H_2O_2]$=250 mg·L^{-1} (46% TOC removal)

TOC, Average Oxidation State (AOS), acute toxicity and ready biodegradability evolution were assessed in order to predict a possible AOP-biological coupling. Satisfactory results were obtained with C and D phototreated effluents, whereas further oxidation prior to biological treatment was envisaged for solutions treated with reagent doses A and B. Nevertheless, conclusive results were obtained after feeding a Sequencing Batch Reactor (SBR) with the phototreated effluents. In this step, phototreated effluent D was eliminated from the investigation because similar results to phototreated effluent C were obtained concerning TOC, AOS and acute toxicity, thus similar by-products generation after phototreatment of both solutions was assumed. TOC removal after coupling the photo-Fenton and biological system was analysed and results are shown in Figure 3.3. The remaining 13.6% obtained when coupling phototreated effluent C with biological treatment matched the concentration of residual TOC due to the biomass metabolism previously determined in a SBR start-up process. Therefore, 1 hour of photo-treatment time with photo-Fenton reagent dose C was considered adequate to produce biocompatible by-products that could be completely removed in a subsequent biological treatment.

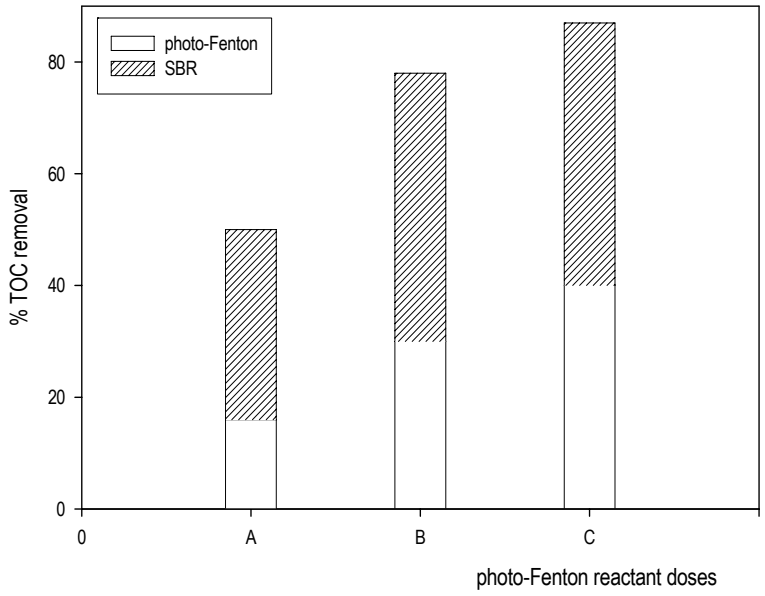

Figure 3.3. Total TOC removal of polluted effluents using optimized photo-Fenton reagent doses in the chemical and biological coupled system by using a SBR. T=20 ^{o}C, HRT=2 days, VSS_{SBR}=0.60±0.1 g·L^{-1} (A: [Fe^{2+}]=9.25 mg·L^{-1}, [H_2O_2]=97.1 mg·L^{-1}; B: [Fe^{2+}]=13.3 mg·L^{-1} , [H_2O_2]=143 mg·L^{-1}; C:[Fe^{2+}]=15.9 mg·L^{-1} , [H_2O_2]=202 mg·L^{-1}).

Publication 4

- Farré M.J. et al. (2007). Combined photo-Fenton and biological treatment for Diuron and Linuron removal from water containing humic acid. *Journal of Hazardous Materials. In press.*

A common source of highly polluted effluents with herbicides are lixiviates coming from agricultural fields which may contain dissolved organic matter (DOM), mainly humic substances. Thus, the elimination of Diuron and Linuron herbicides in the presence of DOM by means of coupling chemical and biological treatment was assessed.

From the previous publication, the treatment of water polluted with Diuron (42 $mg \cdot L^{-1}$) and Linuron (75 $mg \cdot L^{-1}$) herbicides by means of photo-Fenton process generated biocompatible by-products that were successfully removed in a subsequent SBR. Thus, photo-Fenton reagent dose C (i.e., $[Fe^{2+}]$=15.9 $mg \cdot L^{-1}$, $[H_2O_2]$=202 $mg \cdot L^{-1}$) was used to degrade Diuron and Linuron herbicides in the presence of humic acid (HA, 200 $mg \cdot L^{-1}$). Preliminary research was focused on the TOC abatement when phototreating HA solutions. It was observed that TOC corresponding to HA did not decrease after the photo-Fenton process probably due to the low intensity of the light source used (i.e., 0.21 $mW \cdot cm^{-2}$). As a result, photodegradation of HA was discarded under the experimental conditions used in the present work (see Chapter 1, Section 5 for details about HA degradation). On the other hand, when different amounts of HA were added to the solution, it was observed that the more HA was present, the slower the degradation of pesticides until reaching a limiting value at approximately 200 $mg \cdot L^{-1}$ of HA. The decrease of herbicide degradation rates was probably explained by HA hydroxyl radical scavenging as well as a light screening effect.

The formation of biocompatible by-products, which could be successfully degraded in a subsequent biological treatment, was estimated after testing toxicity and biodegradability of the phototreated solution containing Diuron, Linuron and HA. Therefore, a SBR was used to carry out such estimation. Nevertheless, HA adsorption onto the biomass was observed and the characterization of this process was performed. A pseudo-second-order model was used to describe the kinetics of the biosorption process, whereas the Freundlich model was used to determine the isotherm constants.

Finally, whilst feeding SBR with phototreated solution containing Diuron, Linuron and HA, complete removal of TOC related to by-products generated along the herbicides degradation was achieved. Figure 3.4 shows the results obtained from the SBR feeding. Residual TOC observed in Figure 3.4 corresponds to HA that was not biodegradable. Therefore, it can be inferred that the coupling between the photo-Fenton and biological treatment was able to eliminate Diuron and Linuron herbicides from solution also in the presence of HA.

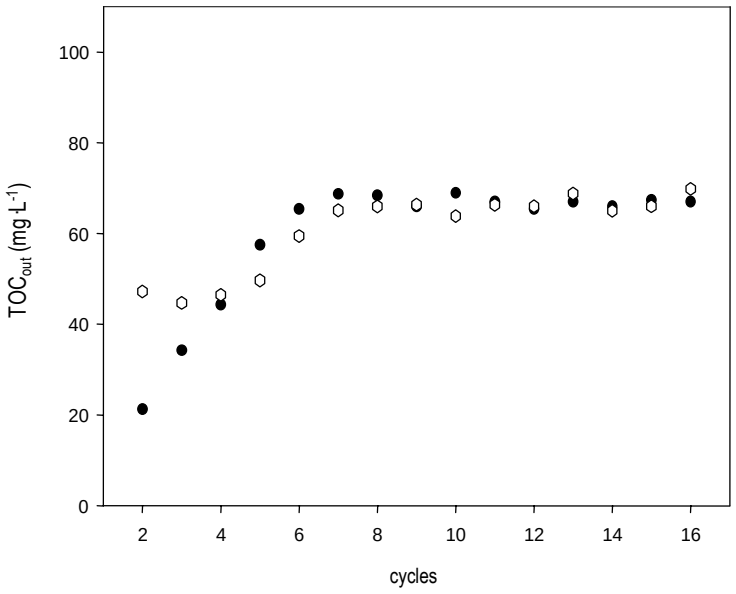

Figure 3.4. TOC concentration at the end of the biological treatment for phototreated solutions containing (o) Diuron, Linuron and HA (200 mg·L^{-1}), (●) HA (200 mg·L^{-1}). T=20 ^{o}C, HRT=2 days. Stabilized VSS_{SBR}=0.56±0.03 g·L^{-1}

Unpublished results presented in Annexe a1.1

- Farré M.J. et al. (2007). Evaluation of the intermediates generated during the degradation of Diuron and Linuron herbicides by the photo-Fenton reaction. *Accepted for publication in Journal of Photochemistry and Photobiology A: Chemistry.*

The aim of this work was to enhance the knowledge about the chemical composition of the effluents treated with different photo-Fenton reagent doses (i.e., A, B and C from publication 3), with the goal of understanding the diverse biodegradable properties of each solution as well as to determine a possible reaction pathway of Diuron and Linuron herbicides with hydroxyl radical.

Several analytical methods such as Reverse Phase Ultra Pressure Chromatography (RP-UPLC /MS), Ion Chromatography (IC), and Gas Chromatography (GS/MS) were used to elucidate the degradation mechanism. Beyond conventional analytical methods, Hydrophilic Interaction Liquid Chromatography coupled with mass spectrometry (HILIC/MS) was used to identify small polar compounds produced along the mineralization process (see Chapter 1, Section 6.3 for more details about HILIC).

Based on the results obtained concerning heteroatoms and short-chain acids as well as first and end by-products evolution, and in conjunction with results obtained by other researchers [12, 13, 14], improved pathways for Diuron and Linuron degradation by means of photo-Fenton reaction were proposed and are represented in schemes 3.1 and 3.2. It was found that along the oxidation process, the hydroxyl radical firstly attacked the aromatic ring and methyl group leading to the formation of more oxidized compounds with different biorecalcitrant nature. 1,1-dimethylurea, methylurea, oxalic, acetic and formic acids as well as 3,4-dichloroaniline, 3,4-dichlorophenyl isocyanate among other minority compounds were detected during the mineralisation process.

Moreover, differences in biodegradability of phototreated effluents A, B and C seemed to be based on the presence of urea derivates (methylurea and 1,1-dimethylurea) and unidentified chlorinated compounds.

Scheme 3.1. Proposed degradation pathway of Diuron herbicide with hydroxyl radical

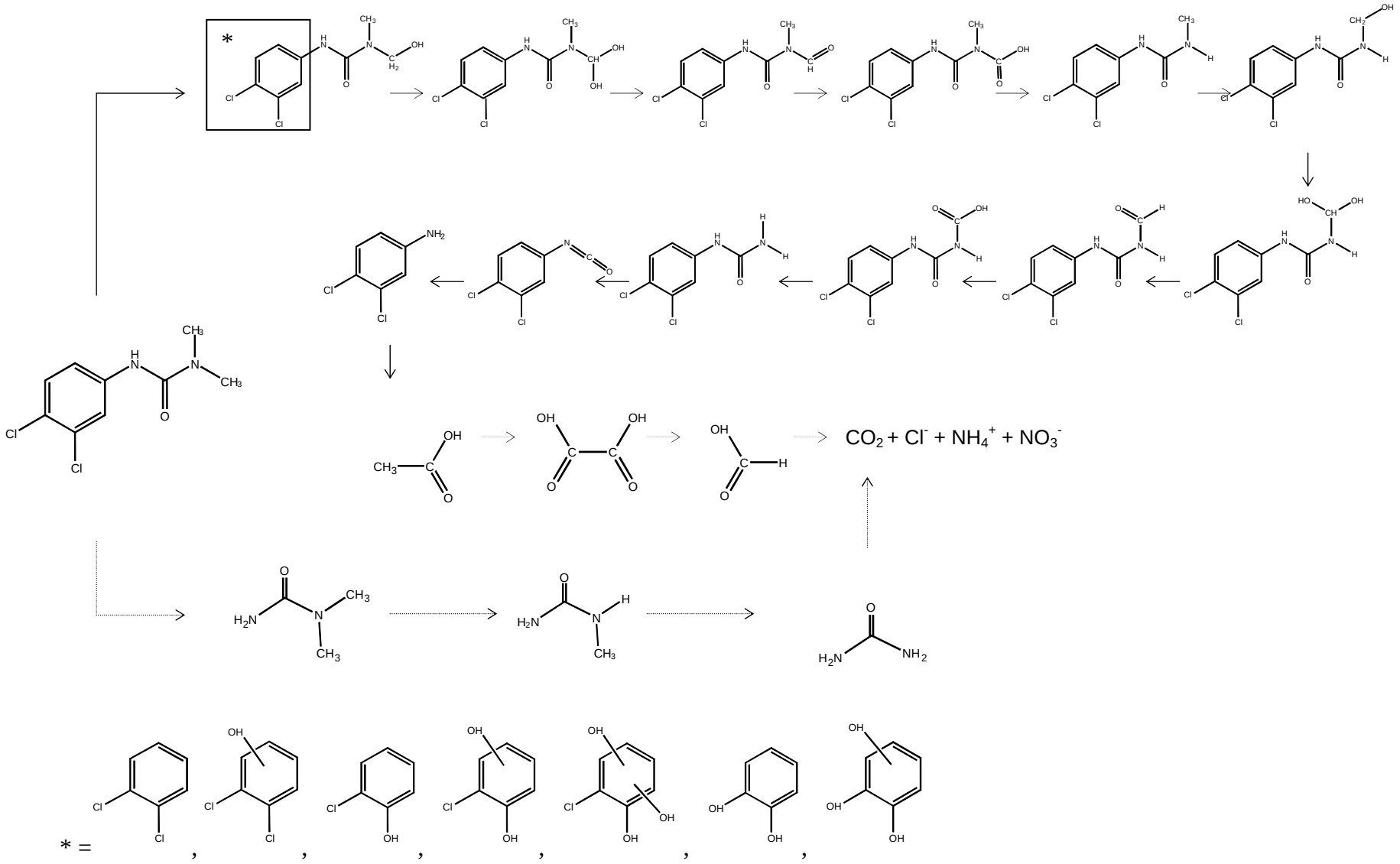

Scheme 3.2. Proposed degradation pathway of Linuron herbicide with hydroxyl radical

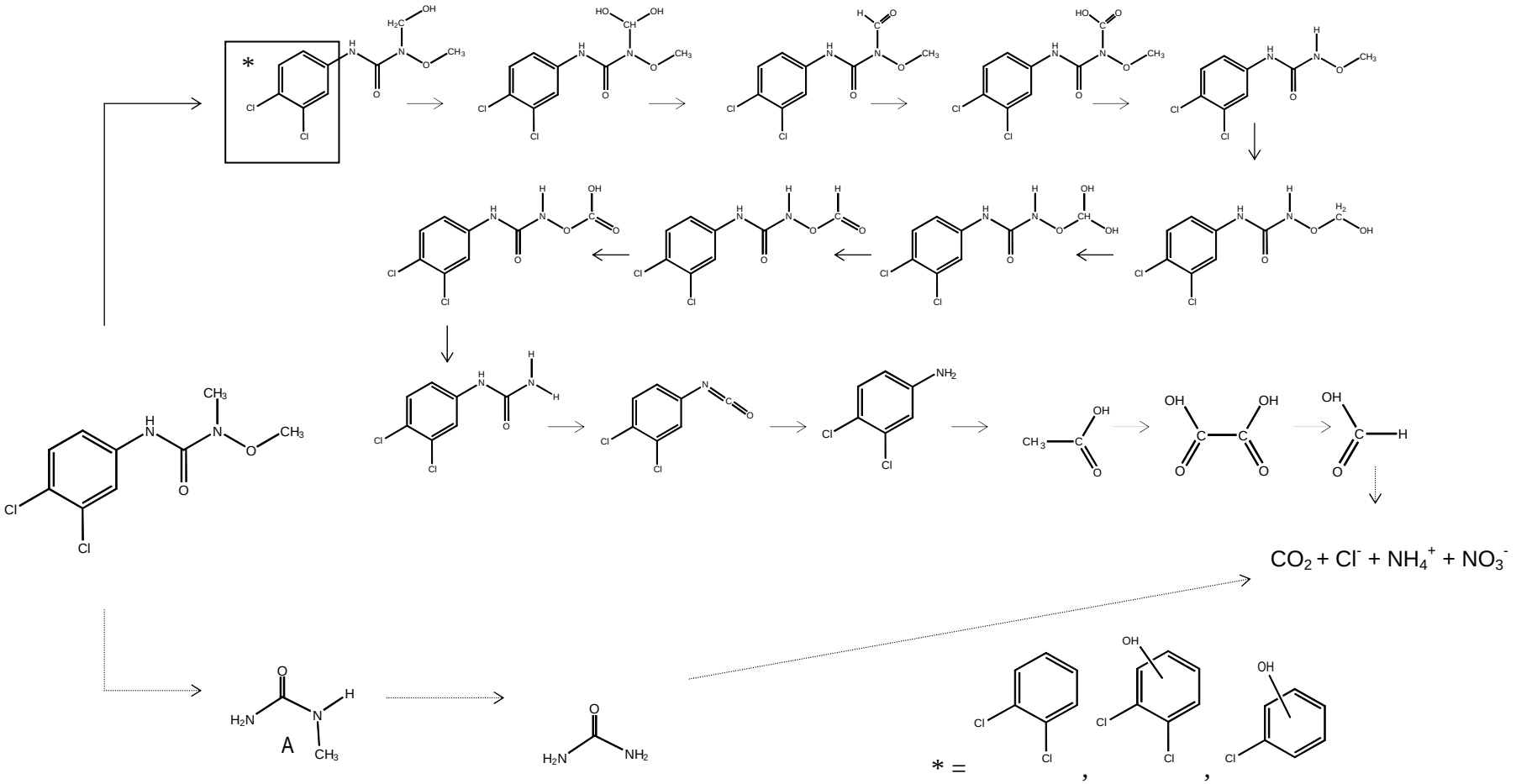

Unpublished results presented in Annexe a1.2

- Farré M.J. et al. (2007). Life cycle assessment for the removal of Diuron and Linuron herbicides from water using three environmental friendly technologies. *Accepted for publication in Environmental Technology.*

Finally, the global environmental impacts of the proposed chemical/biological coupled system for the removal of Diuron and Linuron herbicides from water was performed by means of Life Cycle Assessment (LCA). Moreover, artificial light assisted single photo-Fenton process as well as simulated solar assisted single photo-Fenton process were also evaluated as techniques for treating wastewater. Finally, the three alternative processes were compared in terms of environmental impact.

The inventory analysis necessary to perform LCA included the following information: (i) production of consumed electricity, including extractions of resources, transport, and electricity production, (ii) production of chemicals, including extractions of resources, production, and transport, and (iii) air and water emissions generated through the considered scenarios. The construction and end-of-life of the infrastructure required in each case was not considered. Among the most important hypothesis considered to perform the analysis, which are detailed in publication a1.2, the excess of sludge production when coupling photo-Fenton and biological treatment must be noted. Thus, a sludge treatment system composed of thickening, dewatering, stabilization, and final landfill disposal unit processes was considered. Moreover the main environmental emissions from the landfill were calculated according to ORWARE model [15].

The impact assessment of inventoried data for the removal of Diuron and Linuron herbicides from water was classified considering the potential environmental impact categories included in the CML 2 baseline 2000 (see Chapter 2, Section 6). Figure 3.5 shows the environmental profile, that is, the characterization scores obtained for each treatment considered. In this figure, the highest environmental impact (that always corresponds to artificial light assisted photo-Fenton) was set to 100% for each category and the impacts associated to the solar assisted photo-Fenton as well as the photo-Fenton coupled to biological treatment were calculated according to this percentage. As can be seen from the environmental impact data graphically represented in Figure 3.5, the coupling of photo-Fenton and biological treatment was the most environmentally friendly process for the treatment of water polluted with both herbicides.

Specifically, the impacts associated to the coupled treatment are less than half of those related to artificial light assisted photo-Fenton process, except for aquatic eutrophication potential.

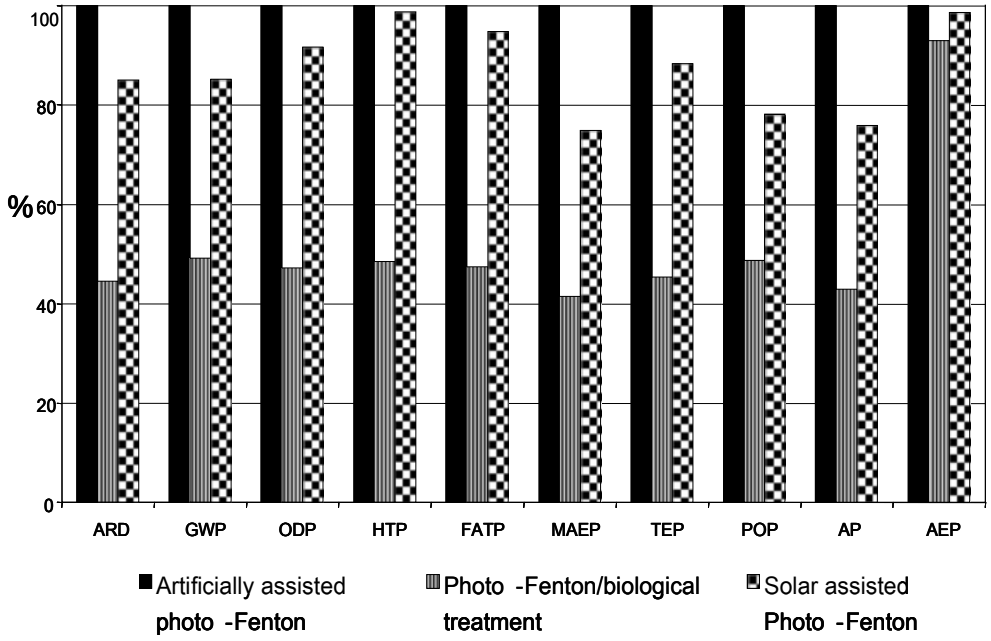

Figure 3.5. General environmental impact data for the three water Treatments considered environmentally friendly. ARD: Abiotic Resource Depletion, GWP: Global Warming Potential, ODP: Ozone Depletion Potential, HTP: Human Toxicity Potential, FATP: Freshwater Aquatic Toxicity Potential, MAEP: Marine Aquatic Ecotoxicity Potential, TEP: Terrestrial Ecotoxicity Potential, POP: Photochemical Oxidation Potential, AP: Acidification Potential, AEP: Aquatic Eutrophication Potential.

In order to identify the critical sub-systems associated to each treatment, an individual analysis for each alternative process and impact category was performed. Sub-systems were defined by grouping those processes inventoried by means of the same source of information. In that way iron, hydrogen peroxide, transport, electricity emissions, and other materials used in sludge treatment were individually considered. Figure 3.6 shows the results obtained for the individual assessment of the coupling between the photo-Fenton and biological system for the remediation of water polluted with Diruon and Linuron herbicides. In this analysis, every impact indicator is expressed as 100%, the contribution of a sub-system being a fraction of the figure.

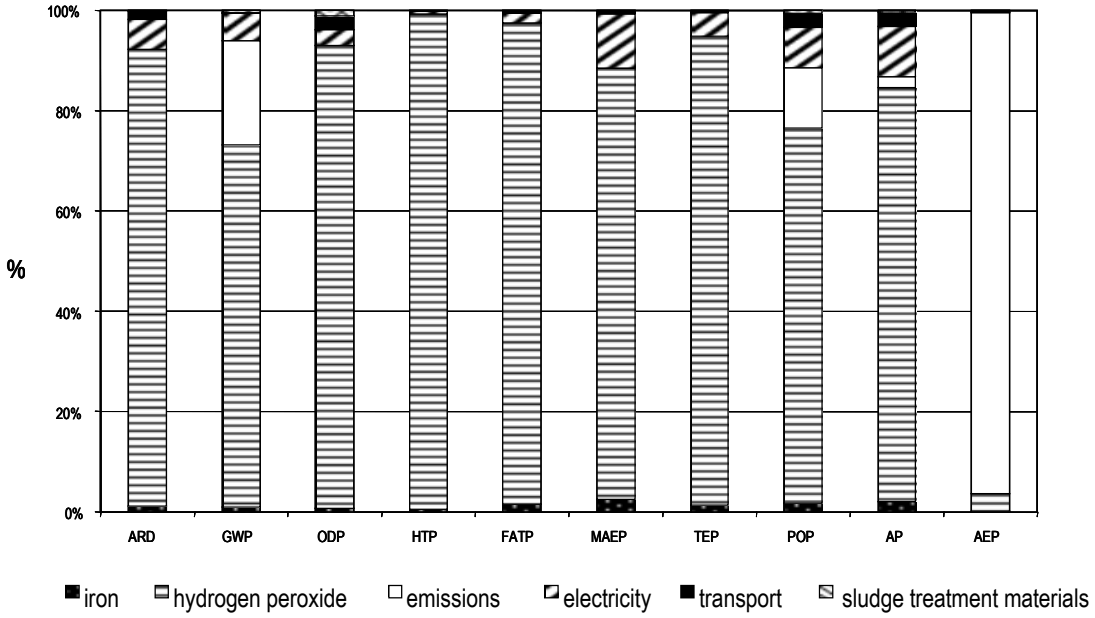

Figure 3.6. Individual analysis of environmental impact data for photo-Fenton coupled to biological treatment. ARD: Abiotic Resource Depletion, GWP: Global Warming Potential, ODP: Ozone Depletion Potential, HTP: Human Toxicity Potential, FATP: Freshwater Aquatic Toxicity Potential, MAEP: Marine Aquatic Ecotoxicity Potential, TEP: Terrestrial Ecotoxicity Potential, POP: Photochemical Oxidation Potential, AP: Acidification Potential, AEP: Aquatic Eutrophication Potential.

As seen in Figure 3.7, the main environmental impact for the coupling of photo-Fenton with biological treatment for the removal of Diuron and Linuron from water was mainly associated to hydrogen peroxide followed by electricity production. Consequently, an evident environmental improvement could be expected if solar assisted photo-Fenton coupled to a biological treatment was applied to remove Diuron and Linuron herbicides from water. Individual analysis of other scenarios is described in detail in Annexe 2.

REFERENCES TO CHAPTER 3

[1] European Parliament. Decision No. 2455/2001/EC of the European Parliament and f the Council of 20 November 2001. Official Journal of the European Communities. 15.12.2001, L331/1-L331/5.

[2] Beltran F., Rivas F. and Montero-de-Espinosa R. (2002). Catalytic ozonation of oxalic acid in aqueous TiO_2 slurry reactor. Appl. Catal. B-Environ. 39, 221-231.

[3] Hernández-Alonso M., Coronado J., Maira A., Soria J., Loddo V. and Augugliario V. (2002). Ozone enhanced activity of aqueous titanium dioxide suspensions for photocatalytic oxidation of free cyanide ions. Appl. Catal. B-Environ. 39, 257-267.

[4] Loegager T., Holcman J., Sehested K. and Pedersen T. (1992). Oxidation of ferrous ions by ozone in acidic solutions. Inorg. Chem. 31, 3523-3529.

[5] Dazell D.J.B., Alte S., Aspichueta E., de la Sota A., Etxebarria J., Gutiérrez M., Hoffmann C.C., Sales D., Obst U. and Christofi N. (2002). A comparision of five rapid direct toxicity assessment methods to determine toxicity of pollutants to activated sludge. Chemosphere. 47, 535-545.

[6] Freitas L., Defrenne L. and Kerbs-Brown A. (2002).Comparison of three microbial assay procedures for measuring toxicity of chemical compounds: ToxAlert®10, CellSense and Biolog MT2 microplates. Anal. Chim. Acta. 456,41-54.

[7] Gutiérrez M., Etxebarria J. and de las Fuentes L. (2002). Evaluation of wastewater toxicity: comparative study between Microtox® and activated sludge oxygen uptake inhibition. Water Res. 36, 919-924.

[8] Ricco G., Tomei C., Ramadori R. and Laera G. (2004). Toxicity assessment of common xenobiotic compounds on municipal activated sludge: comparison between respirometry and Microtox®. Water Res. 38, 2103-2110.

[9] Sarria V., Parra S., Nevenka A., Péringer P., Benítez N. and Pulgarín C. (2002). Recent developements in the coupling of photoassisted and aerobic biological processes for the treatment of biorecalcitrant compounds. Catal. Today. 76, 301-315.

[10] Larson R.J. (1991). Biodegradation in regulating the environment exposure of detergent chemicals. Chem. Times Trends. 14, 47-55.

[11] Chamarro E., Marco A. and Esplugas S. (2000). The use of Fenton reagent to improve organic chemical biodegradablity. Water Res. 35, 1047-1051.

[12] Malato S., Cáceres J., Fernández-Alba A.R., Piedra L., Hernando M.D., Agüera A. and Vidal J. (2003). Photocatalytic treatment of Diuron by solar photocatalysis: Evaluation of main intermediates and toxicity. Environ. Sci. Technol. 37, 2516-2524.

[13] Katsumata H., Kaneco S., Suzuki T., Ohta K. and Yobik Y. (2005). Degradation of Linuron in aqueous solution by the photo-Fenton reaction. Chem. Eng. J. 108, 269-276.

[14] Tahmasseb L.A., Nélieu S., Kerhoas L. and Einhorn J. (2002). Ozonation of Chlorophenylurea in water: reaction monitoring and degradation pathways. Sci. Total Environ. 29, 33-44.

[15] Mingarini K. (1996). Systems Analysis of Organic waste with Emphasis on Modelling of the Incineration and the Landfilling Process. Licentiate Thesis. Dept. of Environmental Technology and Work Science, Stockholm.

[16] Dalemo M. (1997). The ORWARE simulation model. Anaerobic digestion and sewage plant sub-models. Licenthiate thesis. Swedish Institute of Agricultural Engineering, Swedish University of Agricultural Sciences. Uppsala, Sweden.

2. Publications

Next section includes the following published articles:

2.1. Degradation of some biorecalcitrant pesticides by homogeneous and heterogeneous photocatalytic ozonation.

Chemosphere 58 (2005) 1127-1133.

Maria José Farré, Maria Isabel Franch, Sixto Malato, José Antonio Ayllón, José Peral and Xavier Domènech.

2.2. Biodegradability of treated aqueous solutions of biorecalcitrant pesticides by means of photocatalytic ozonation.

Desalination 211 (2007) 22-33.

Maria José Farré, Maria Isabel Franch, José Antonio Ayllón, José Peral and Xavier Domènech.

2.3. Assessment of photo-Fenton and biological treatment coupling for Diuron and Linuron removal from water.

Water Research 40 (2006) 2533-2540.

Maria José Farré, Xavier Domènech and José Peral.

2.4. Combined photo-Fenton and biological treatment for Diuron and Linuron removal from water containing humic acid.

Journal of Hazardous Materials *in press.*

Maria José Farré, Xavier Domènech and José Peral.

ELSEVIER

Chemosphere 58 (2005) 1127–1133

CHEMOSPHERE

www.elsevier.com/locate/chemosphere

Degradation of some biorecalcitrant pesticides by homogeneous and heterogeneous photocatalytic ozonation

Maria José Farré [a], Maria Isabel Franch [a], Sixto Malato [b], José Antonio Ayllón [a], José Peral [a], Xavier Doménech [a,*]

[a] *Departament de Química, Universitat Autónoma de Barcelona, 08193 Bellaterra, Spain*
[b] *Química Solar, Plataforma Solar de Almería (CIEMAT), Crta de Senes, 04200 Tabernas (Almería), Spain*

Received 2 February 2004; received in revised form 8 September 2004; accepted 13 September 2004

Abstract

Photo-Fenton/ozone (PhFO) and TiO_2-photocatalysis/ozone (PhCO) coupled systems are used as advanced oxidation processes for the degradation of the following biorecalcitrant pesticides: alachlor, atrazine, chlorfenvinfos, diuron, isoproturon and pentachlorophenol. These organic compounds are considered Priority Hazardous Substances by the Water Framework Directive of the European Commission. The degradation process of the different pesticides, that occurs through oxidation of the organic molecules by means of their reaction with generated OH radical, follows a first and zero-order kinetics, when PhFO and PhCO are applied, respectively. These two Advanced Oxidation Processes, together with the traditional ozone + UV, have been used to investigate TOC reduction of the different pesticide aqueous solutions. The best results of pesticide mineralization are obtained when PhFO is applied; with the use of this advanced oxidation process the aqueous pesticide solutions become detoxyfied except in the case of atrazine and alachlor aqueous solutions for which no detoxification is achieved at the experimental conditions used in the work, at least after 2 and 3 h of treatment, respectively.

Keywords: Photo-Fenton; TiO_2-photocatalysis; Ozone coupling; Pesticide degradation

1. Introduction

The presence of highly biorecalcitrant organic contaminants in the hydrosphere due to industrial and intensive agricultural activities is of particular concern for the freshwater (surface and groundwater), coastal and marine environments. In view of this, it is advisable to develop technologies that promote the easy degradation of these biorecalcitrant organic compounds. A promising way to perform the mineralization of these type of substances is the application of advanced oxidation processes (AOP), that are characterized by the "in situ" production of OH radicals under mild experimental conditions (e.g. Peyton, 1990). Among the different technologies proposed as AOP, are those based on the use of dissolved ozone (e.g. Glaze, 1987; Peyton, 1990). More recently, catalytic ozone based systems have been developed in order to enhance the OH radical production. In this way, it has been proposed the use of

* Corresponding author.
E-mail address: xavier.domenech@uab.es (X. Doménech).

0045-6535/$ - see front matter © 2004 Published by Elsevier Ltd.
doi:10.1016/j.chemosphere.2004.09.064

some metals in homogeneous solution (Fe(II), Mn(II), Ni(II) or Co(II)) to induce an increase of total organic carbon (TOC) removal compared to ozonation alone (e.g. Legube and Karpel, 1999), or the use of metal oxides for the enhancement of the ozonation in heterogeneous processes (e.g. Legube and Karpel, 1999). Another alternative to increase the OH radical production is the photocatalytic ozonation (both homogeneous and heterogeneous) by using Photo-Fenton (e.g. Logager et al., 1992; Piera et al., 2000) or TiO_2-photocatalysis (e.g. Sánchez et al., 1998; Piera et al., 2000; Beltrán et al., 2002).

In the present paper, both homogeneous and heterogeneous photocatalytic ozonation are applied to assess the suitability of these AOP to promote mineralization of organic biorecalcitrant compounds. Concretely, water soluble pesticides included in Decision No. 2455/2001/EC of the European Parliament and of the Council of 20 November 2001, in which a list of priority substances in the field of water policy is established, i.e. alachlor, atrazine, chorofenvinfos, diuron, isoproturon and pentachorophenol (PCP) have been chosen as target compounds. These organic pesticides, which exhibit a high degree of biotoxicity, have a moderate solubility in water (between $15\,mg\,dm^{-3}$ for pentachlorophenol to $240\,mg\,dm^{-3}$ for alachlor at 25° C) and low to moderate octanol–water constants, with $\log K_{OW}$ around 2.7–2.9, except for pentachlorophenol ($\log K_{OW} = 5.1$) and chlorofenvinfos ($\log K_{OW} = 3.8$).

2. Experimental

2.1. Reagents

Alachlor (95%, Aragonesas Agro SA technical grade), Atrazine (95%, Ciba-Geigy technical grade), Chlorfenvinphos (93.2%, Aragonesas Agro SA technical grade), Diuron (98.5%, Aragonesas Agro SA technical grade) and Isoproturon (98%, Aragonesas Agro SA technical grade) were used as target compounds in the experiments. PCP (98%) was purchased from Aldrich. All the aqueous solutions were prepared with water purified in a Millipore Milli-Q system. $FeSO_4 \cdot 7H_2O$ (Merck, 99.5%) and H_2O_2 (Panreac, 33% p/v) were used in the Photo-Fenton experiments. TiO_2P-25 (80% anatase–20% rutile, $59.1\,m^2\,g^{-1}$, non-porous) was supplied by Degussa. KI (Panreac, analytical grade), KIO_3 (Probus, analytical grade), $K_2H_2PO_4$ (Aldrich, analytical grade) and $Na_2S_2O_3 \cdot 5H_2O$ (Aldrich, analytical grade) were used for the iodometric titrations. Acetonitrile (Probus, HPLC grade) was used to prepare the mobile phases in the HPLC system. All the other chemicals mentioned hereafter were at least of reagent grade and used as received.

2.2. Apparatus and analytical methods

The pesticide degradation experiments were carried out in a Pyrex glass cell provided of a thermostatic jacket (25.0 ± 0.1 °C) and under magnetic stirring. Ozone, generated by an Erwin Sander 301.7 equipment fed with pure oxygen (99.995% C-45, Carburos Metálicos flow at P = 1 bar), was bubbled into the bottom of the reactor by means of a diffuser. The ozone input in the treated solution was $1.6\,g\,h^{-1}$ as determined by iodometric titration (Method 001/95 International Ozone Association-EAG). The unreacted ozone in the flow gas was measured by means of an Erwin Sander Quantozone-1 ozone-meter. A 6 W black light (Philips) lamp was used as UVA source in the irradiation experiments.

The concentration of the pesticides was measured by HPLC technique. The HPLC system was constituted by a LC-10 AT VP pump (Shimadzu) and a UV–Visible diode array detector (Agilent 1100 Series). The stationary phase was a Hypersil ODS Teknokroma column (250×4.6 mm). An acetonitrile/water mixture (50/50 but 60/40 for alachlor) was employed as the mobile phase, except for PCP analysis for which a methanol/water mixture (80/20) as the mobile phase was used. The mobile phase was degassed by sonication and filtered (0.45 μm) before using. TOC determination was carried out with a TOC-5000 Shimadzu Total Carbon Analyser. The toxicity tests were performed by means of a BioTox equipment (Lab-system) using the Vibrio fischery luminescence inhibition to assess the EC_{50} values. Before TOC and HPLC analysis, all the samples were filtered trough 0.45 μm pore size nylon filters in order to remove any particulates. It must be noted that no pesticide adsorption occurs on these type of filters.

2.3. Pesticide degradation experiments

The experiments were performed with 200 ml of an approximately $50\,mg\,l^{-1}$ aqueous solution of the studied pesticide except for Atrazine and Diuron. For the latter products saturated solutions were prepared and filtrated before being used. All experiments were performed at an initial pH of 3.0, except for PCP for which the initial pH was 7.0. HCl and NaOH diluted aqueous solutions were used to adjust the initial pH values. Although Cl^- ions in the aqueous medium can react with ·OH radicals in a process with a relatively high rate constant ($4.3 \cdot 10^9\,mol^{-1}\,l\,s^{-1}$) (Buston et al., 1988), recently it has been observed that the ·OH scavenging properties of Cl^- ion are only relevant at high concentrations (higher than 0.1 M (Kiwi et al., 2000). The reactor was filled with the pesticide solution once the ozone dosage input in the reactor was constant. In the Photo-Fenton/ozone and TiO_2-photocatalysis/ozone systems, the Fenton reagent (5.0 ml of a $FeSO_4 \cdot 7H_2O$ ($80.0\,mg\,l^{-1}$) aqueous solution and the suitable volume of H_2O_2) or

TiO_2 powders (0.0500 g) were also added to the reactor cell. The quantity of H_2O_2 employed was twice the stoichiometric amount necessary for the complete mineralization of the studied pesticide. Concretely, the concentrations of H_2O_2 used in the Photo-Fenton and Photo-Fenton/ozone systems were the following: $0.48\,g\,l^{-1}$, $0.38\,g\,l^{-1}$, $0.26\,g\,l^{-1}$, $0.32\,g\,l^{-1}$, $0.61\,g\,l^{-1}$ and $0.11\,g\,l^{-1}$ for alachlor, atrazine, chlorfenvinfos, diuron, isoproturon and PCP, respectively. The excess of H_2O_2 used in this work is not enough to affect the efficiency of pesticide degradation due to OH radical consumption by H_2O_2. This only occurs when a very high H_2O_2 concentration is used (Pérez et al., 2002).

Samples were periodically taken along time from the reactor to measure the pesticide concentration, TOC, and toxicity values. For the Photo-Fenton and TiO_2-photocatalysis experiments the same procedure as PhFO and PhCO was followed but without ozone supply. In the experimental conditions of the degradation assays, the pesticides adsorption over the TiO_2 powders in the dark does not significantly contribute to their elimination from the aqueous solution.

3. Results and discussion

The coupling between ozone and Photo-Fenton (Fe(II), H_2O_2 and UV) and heterogeneous (TiO_2 and UV) photocatalysis, was applied to the elimination of the following pesticides in aqueous solutions: alachlor, atrazine, chlorfenvinfos, diuron, isoproturon and PCP. All experiments were performed at initial pH of 3.0, except for PCP degradation for which the initial pH was 7.0 to increase the solubility of this pesticide in water. Along the photodegradation process the pH of the different pesticides solutions remains almost constant, except in the case of PCP solutions in which a decrease of pH is observed during the first minutes of irradiation attaining a limiting value of about 3, due to the acidity generated from the mineralization process.

Fig. 1 shows the time course of the concentrations of the different pesticides investigated when Photo-Fenton/ozone (PhFO) and TiO_2-photocatalysis/ozone (PhCO) systems are applied to the aqueous pesticide solutions. From data depicted in Fig. 1, the kinetics of degradation of the different studied pesticides has been deduced and the corresponding kinetic rate constants obtained are summarized in Table 1.

With relation to PhFO system, a first-order kinetics for the degradation of all pesticides is deduced. For PCP, the decrease of pesticide concentration is very strong, resulting in a 98% elimination after only 30 s, that precludes to perform a suitable kinetic analysis. In fact, in this case the experiments were performed at neutral pH at which O_3 is able, in comparison to pH 3, to increase OH radical concentration trough a series of

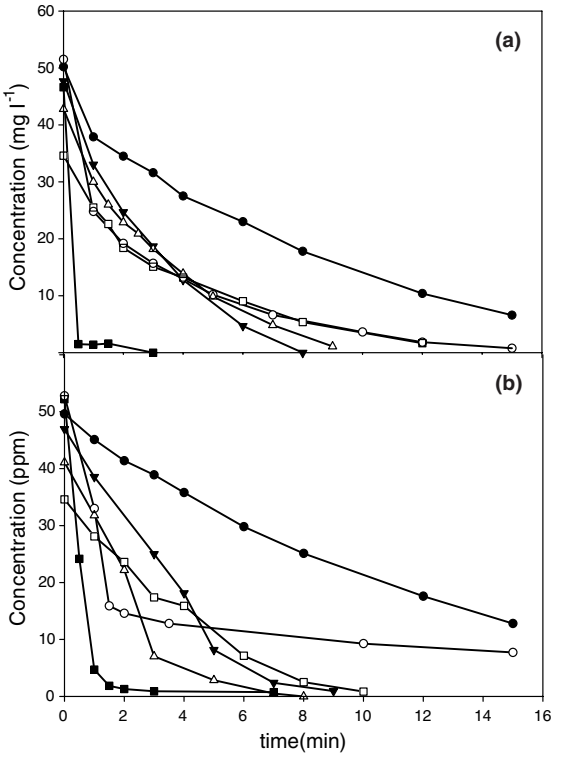

Fig. 1. Time course of the concentration of different pesticides in aqueous solution during the application of the (a) PhFO system and (b) PhCO system: (●) alachlor, (■) PCP, (△) diuron, (□) atrazine, (▼) isoproturon and (○) chlorfenvinfos. See Section 2 for experimental details.

Table 1
First and zero order rate constants, k_{PhFO} and k_{PhCO}, respectively, of photocatalytic ozonation (PhFO and PhCO), of the different investigated pesticide in aqueous solutions at initial pH = 3.0 and at 25 °C

Pesticide	$k_{PhFO} \cdot 10^3/s^{-1}$	$k_{PhCO} \times 10^7/mol\,l^{-1}\,s^{-1}$
Alachlor	2.2	1.5
Atrazine	4.0	3.3
Chlorfenvinfos	4.2	11
Diuron	6.2	7.8
Isoproturon	6.2	6.0
PCP[a]	–	29

See Section 2 for experimental details.
[a] Initial pH = 7.0.

chemical and photochemical processes (see latter in the text). It can be assumed that the degradation of the pesticides occurs by direct OH attack to the organic molecule. The OH radical is produced by the Fenton reaction that occurs at acid pH (process (1)) (e.g. Faust and Hoigné, 1990):

$$Fe^{2+} + H_2O_2 \rightarrow Fe(OH)^{2+} + \cdot OH \quad (1)$$

Under irradiation of $\lambda < 400$ nm Fe(III) can be reduced to Fe(II) closing a loop mechanism where Fe species act as catalyst, giving rise to additional ·OH (e.g. Faust and Hoigné, 1990):

$$Fe(OH)^{2+} + h\nu \rightarrow Fe^{2+} + {\cdot}OH \quad (2)$$

A further increment in the OH radicals production occurs when ozone is added to the solution; in this case, dissolved O_3 reacts with Fe^{2+} giving rise to FeO^{2+} that further undergoes hydrolysis to give Fe^{3+} producing more ·OH (e.g. Logager et al., 1992):

$$Fe^{2+} + O_3 \rightarrow FeO^{2+} + O_2 \quad (3)$$

$$FeO^{2+} + H_2O \rightarrow Fe^{3+} + {\cdot}OH + OH^- \quad (4)$$

Due to the catalytic role of Fe, the constant supply of ozone and photons to the reactive system and the excess of H_2O_2, the concentration of ·OH produced remains constant and consequently the rate of pesticide degradation depends only on its concentration according to a first order kinetics.

With respect to the PhCO system, the reaction also proceed by radical attack to the organic molecule. The OH radical is produced by (i) reaction of adsorbed H_2O molecules with photogenerated holes at the illuminated TiO_2 particle (process (6)) and (ii) by reaction of adsorbed O_3 and photogenerated electrons at the TiO_2 particle (processes (7) and (8)) (e.g. Sánchez et al., 1998):

$$TiO_2 + h\nu \rightarrow e^- + h^+ \quad (5)$$

$$H_2O + h^+ \rightarrow {\cdot}OH + H^+ \quad (6)$$

$$O_3 + e^- \rightarrow O_3^{-\bullet} \quad (7)$$

$$O_3^{-\bullet} + H^+ \rightarrow OH^{\bullet} + O_2 \quad (8)$$

The presence of dissolved ozone in the irradiated TiO_2 aqueous suspension increases the OH radical production and decreases the electron–hole recombination, increasing the efficiency of the photocatalytic process. The observed zero-order kinetics, that has also been observed for other PhCO degradation processes (e.g. Beltrán et al., 2002; Hernández-Alonso et al., 2002), can be an indication that the rate determining step is the production of radical OH at the semiconductor surface.

As can be seen, a similar rate constant of degradation of the studied pesticides by PhFO is obtained, except for alachlor that has the lowest rate constant; for PCP a high initial rate of elimination is estimated ($1.5\,mg\,l^{-1}\,s^{-1}$). With relation to PhCO system, alachlor and PCP are also the pesticides that show lower and higher rate constants of degradation respect to the other pesticides.

The mineralization process of the studied pesticides by means of the application of different treatment procedures has been investigated. These treatment procedures are: heterogeneous TiO_2-photocatalysis, Photo-Fenton, ozone + UV, PhCO and PhFO. At the experimental conditions used in this work and after at least 120 min of treatment, no TOC reduction has been observed when TiO_2-photocatalysis and Photo-Fenton are applied at atrazine, diuron, isoproturon and PCP aqueous solutions and also when ozone + UV and Photo-Fenton are used for treating atrazine and alachlor solutions, respectively. TiO_2-photocatalysis shows a low activity respect to TOC reduction for alachlor and chlorfenvinfos aqueous systems, attaining in both cases a limiting TOC reduction of 24% and 25% at 180 and 60 min of treatment, respectively. On the other hand, chlorofenvinfos is rather stable when Photo-Fenton process is applied at the studied experimental conditions, achieving a limiting TOC reduction of only 20% after 75 min of treatment.

In Figs. 2–4, the variation of the ratio TOC/TOC_0 as a function of irradiation time for the different pesticide aqueous systems treated by means of PhFO, PhCO and ozone + UV processes is represented. As can be seen, atrazine is the studied pesticide more resistant to mineralization by these three treatment systems, i.e., after 90 min of treatment only 30% and 10% of the initial TOC is reduced, when PhFO and PhCO systems are used, respectively, while no noticeable degradation occurs when ozone + UV is applied. The best results concerning to TOC reduction are obtained by the application of PhFO system for all pesticides solutions investigated. PhCO gives better results than ozone + UV for the degradation of all pesticides except for PCP. It has to be remembered that for PCP all the experiments have been performed at an initial neutral pH. This is particularly relevant when using ozone + UV system, for which besides the direct attack of ozone to the

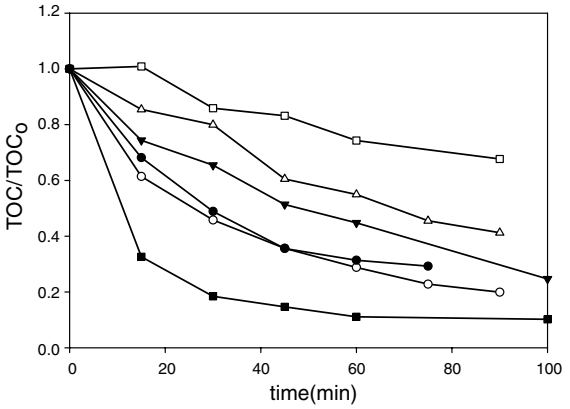

Fig. 2. Time course of the ratio TOC/TOC_0 of different pesticides in aqueous solution during the application of the PhFO system: (●) alachlor, (■) PCP, (△) diuron, (□) atrazine, (▼) isoproturon and (○) chlorfenvinfos. See Section 2 for experimental details.

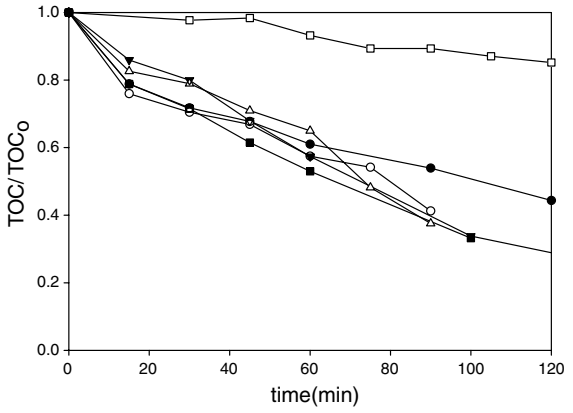

Fig. 3. Time course of the ratio TOC/TOC_0 of different pesticides in aqueous solution during the application of the PhCO system: (●) alachlor, (■) PCP, (△) diuron, (□) atrazine, (▼) isoproturon and (○) chlorfenvinfos. See Section 2 for experimental details.

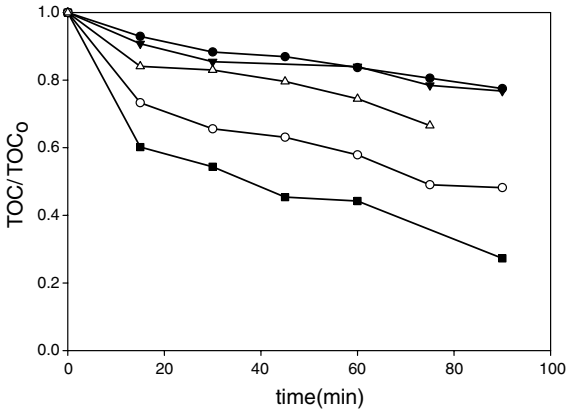

Fig. 4. Time course of the ratio TOC/TOC_0 of different pesticides in aqueous solution during the application of the ozone + UV system: (●) alachlor, (■) PCP, (△) diuron, (▼) isoproturon and (○) chlorfenvinfos. See Section 2 for experimental details.

organic molecule, at neutral to alkaline environments the indirect process of degradation trough OH radical reaction becomes relevant. At this pH, the OH radicals are generated by means of reaction between O_3 and OH^- ions (e.g., Staehelin and Hoigné, 1982):

$$O_3 + OH^- \rightarrow O_2^{-\bullet} + HO_2^{\bullet} \quad (9)$$

$$O_2^{-\bullet} + O_3 \rightarrow O_2 + O_3^{-\bullet} \quad (10)$$

$$O_3^{-\bullet} + H^+ \rightarrow HO_3^{\bullet} \rightarrow {}^{\bullet}OH + O_2 \quad (11)$$

The production of OH radical is increased under UV illumination through the formation of H_2O_2 (process (12)), which after acid–base dissociation and reaction with O_3 give rise to the formation of $O_3^{-\bullet}$ (processes (13) and (14)) (e.g. Peyton, 1990):

$$O_3 + H_2O + h\nu \rightarrow H_2O_2 + O_2 \quad (12)$$

$$H_2O_2 \leftrightharpoons HO_2^- + H^+ \quad (13)$$

$$O_3 + HO_2^- \rightarrow O_3^{-\bullet} + HO_2^{\bullet} \quad (14)$$

The $O_3^{-\bullet}$ radicals generated in the last step produce OH radicals through reaction (11).

The initial rates of pesticide mineralization through the application of PhFO, PhCO and ozone + UV systems obtained from the slopes of the TOC/TOC_0 vs. t curves up to the first 15 min (Figs. 2–4) are summarized in Table 2. From that data the order of degradability of the different pesticides through the application of PhFO and ozone + UV systems is:

PCP > chlorfenvinfos > diuron > isoproturon > alachlor > atrazine

On the other hand, when the PhCO system is applied, the initial rate of mineralization of all pesticides investigated varies in a very narrow range (between 7 and 12 $g\,l^{-1}\,s^{-1}$), except for atrazine for which an initial rate value of an order of magnitude lower is observed (see Table 2). Further, it is interesting to note that after, approximately, the first 15 min of irradiation, the rate of mineralization of all pesticides are very similar (about 0.5% TOC reduction per min), except for atrazine which TOC reduction rate is much lower (about 0.1% TOC per min).

As it has been said previously, atrazine is the most recalcitrant pesticide studied in this work, i.e., very low TOC reduction values are achieved when PhFO and PhCO systems are applied (i.e., 34% and 15% TOC reduction after 100 min of irradiation, respectively),

Table 2
Initial rate of pesticide mineralization in $mg\,l^{-1}\,s^{-1}$ through the application of PhFO (r_{PhFO}), PhCO (r_{PhCO}) and ozone + UV (r_{ozone}) AOPs at initial pH = 3.0 and at 25 °C

Pesticide	$r_{PhFO} \cdot 10^3$	$r_{PhCO} \cdot 10^3$	$r_{ozone} \cdot 10^3$
Alachlor	8.3	12	3.8
Atrazine	2.2	0.8	0.4
Chlorfenvinfos	22	14	16
Diuron	15	7.8	7.2
Isoproturon	14	7.3	4.7
PCP[a]	35	12	23

See Section 2 for experimental details.
[a] Initial pH = 7.0.

while no TOC reduction is observed when ozone + UV is used. In fact, it is well known the formation of cyanuric acid during degradation of atrazine, a compound that is very stable to OH radical attack (e.g., Pelizzetti et al., 1992; Huston and Pignatello, 1999). Also, in the case of diuron and PCP, although they are strongly degraded by means of PhFO application, a limiting value of TOC reduction of 70% and 90% at 60 min of irradiation, respectively, is attained indicating the formation of recalcitrant intermediates at the last steps of degradation (Malato et al., 2003).

The toxicity of the pesticide solutions treated by means of PhFO system, which is the AOP that gives the best results concerning pesticide degradation, has been assessed. The EC_{50}-values obtained for the different pesticide initial aqueous solutions were: 70.8, 55.2, 153.9, 49.2, 28.0 and 0.25 for alachlor ($TOC_0 = 31.1\,mg\,l^{-1}$), diuron ($TOC_0 = 17.3\,mg\,l^{-1}$), atrazine ($TOC_0 = 15.8\,mg\,l^{-1}$), chlorofenvinfos ($TOC_0 = 21.2\,mg\,l^{-1}$), and isoproturon ($TOC_0 = 32.7\,mg\,l^{-1}$) and PCP ($TOC_0 = 12.9\,mg\,l^{-1}$), respectively. In Fig. 5, the $1/EC_{50}$ TOC values for pesticides solutions, except for PCP, are represented as a function of treatment time. It is observed that in all cases, except for alachlor, an increase of toxicity occurs achieving a maximum value at a treatment time that depends on the pesticide nature. An increase of toxicity has also been reported in the photocatalytic degradation of isoproturon and diuron, a fact that has been ascribed to the formation of more toxic intermediates than the parent compound (Parra et al., 2002; Malato et al., 2003). For diuron, isoproturon and chlorfenvinfos, their solutions become detoxified after passing the maximum toxicity and at treatment times no longer than 100 min at the reported experimental conditions. It must be signaled that for these three pesticides, detoxification is attained when the TOC remaining in solution becomes lower than $10\,mg\,l^{-1}$.

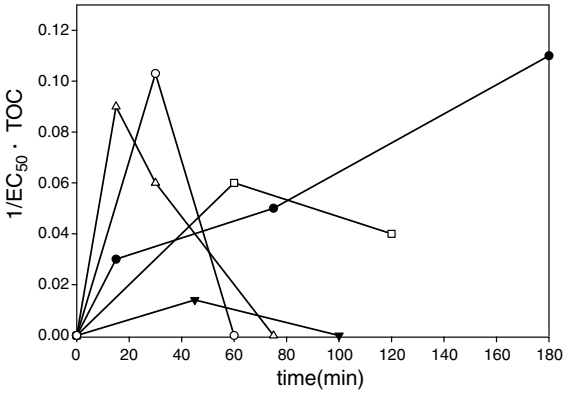

Fig. 5. Time course of the biotoxicity ($1/E_{50}$. TOC, where E_{50} and TOC are expressed in $mg\,l^{-1}$) of the different pesticide aqueous solutions at initial pH = 3, treated with PhFO system. (●) alachlor, (□) atrazine, (△) diuron, (▼) isoproturon and (○) chlorfenvinfos. Temperature: 25 °C.

On the other hand, PhFO system is not able to detoxify atrazine and alachlor solutions at least at treatment times lower than 2 and 3 h, respectively. For alachlor the toxicity of their aqueous solutions increases with increasing treatment time, at least after 3 h of irradiation (see Fig. 5). Other authors have reported the formation of 2,6-diethylaniline as degradation product of alachlor, being responsible of the observed increased toxicity of treated alachlor aqueous solutions (Osano et al., 2002). In the case of PCP aqueous solution, for which the initial $1/E_{EC} \cdot TOC$ value is 0.31, 30 min of treatment is enough to produce a detoxified solution, particularly due to the strong TOC reduction that occurs when PhCO is applied (see Fig. 2).

4. Conclusions

The PhFO and PhCO advanced oxidation processes lead to a rapid decrease of the concentration of the biorecalcitrant pesticides, alachlor, atrazine, chlorfenvinfos, diuron and PCP in aqueous solutions. The degradation processes, that occur through oxidation of the organic molecules by means of their reaction with generated OH radical, follow a first and zero-order kinetics, when PhFO and PhCO are applied respectively. The application of PhFO, PhCO and ozone + UV systems to the pesticide aqueous solutions leads to a strong TOC reduction, except for atrazine for which no TOC reduction is observed with the ozone + UV treament and very low values of TOC decrease are observed when PhFO and PhCO systems are used. The best results of pesticide degradation are obtained when PhFO is applied. The pesticide solutions, after being treated by means of PhFO system, become detoxyfied except for atrazine and alachlor aqueous solutions for which no detoxification is achieved at least after 2 and 3 h of treatment, respectively. In the case of alachlor the toxicity of the treated solutions increases with increasing irradiation time, at least after 3 h of irradiation.

Acknowledgement

This work has been carried out in the frame of CADOX project by the grant No. EVK1-CT-2002-00122, from the European Commission.

References

Beltran, F., Rivas, F., Montero, R., 2002. Catalytic ozonation of oxalic acid in an aqueous TiO_2 slurry reactor. Appl. Catal. B 39, 221–231.

Buston, G.V., Greenstock, C.L., Helman, W.P., Rose, A.B., 1988. Critical review of data constants for reaction of hydrated electrons, hydrogen atoms and hydroxil radicals in aqueous solutions. J. Phys. Chem. Ref. Data 17, 513–886.

Faust, B.C., Hoigné, J., 1990. Photolysis of iron(III)-hydroxy complexes as sources of hydroxyl radicals in clouds, fog and rain. Atmos. Environ. 24, 79–89.

Glaze, W.H., 1987. Drinking water treatment with ozone. Environ. Sci. Technol. 21, 224–230.

Hernández-Alonso, M., Coronado, J., Maira, A., Soria, J., Loddo, V., Augugliaro, V., 2002. Ozone enhanced activity of aqueous titanium dioxide suspensions for photocatalytic oxidation of free cyanide ions. Appl. Catal. B 39, 257–267.

Huston, P.L., Pignatello, J.J., 1999. Degradation of selected pesticide active ingredients and commercial formulations in water by the photo-assisted Fenton reaction. Wat. Res. 33, 1238–1246.

Kiwi, J., López, A., Nadtochenko, V., 2000. Mechanism and kinetics of the OH-radical intervention during Fenton oxidation in the presence of a significant amount of radical scavenger (Cl^-). Environ. Sci. Technol. 34, 2162–2168.

Legube, B., Karpel, N., 1999. Catalytic ozonation: a promising advanced oxidation technology for water treatment. Catal. Today 53, 61–72.

Logager, T., Holcman, J., Sehested, K., Pedersen, T., 1992. Oxidation of ferrous ions by ozone in acidic solutions. Inorg. Chem. 31, 3523–3529.

Malato, S., Cáceres, J., Fernández-Alba, A.R., Piedra, L., Hernando, M.D., Agüera, A., Vial, J., 2003. Photocatalytic treatment of Diuron by solar photocatalysis: evaluation of main intermediates and toxicity. Environ. Sci. Technol. 37, 2516–2524.

Osano, O., Admiraal, W., Klamer, H.J.C., Pastor, D., Bleeker, E.A.J., 2002. Comparative toxic and genotoxic effects of chloroacetanilides, formamides and their degradation products on *Vibrio fischeri* and *Chironomus riparius*. Environ. Pollut. 119, 195–202.

Parra, S., Malato, S., Pulgarin, C., 2002. New integrated photocatalytic-biological flow system using supported TiO_2 and fixed bacteria for the mineralization of isoproturon. Appl. Catal. B 36, 131–144.

Pelizzetti, E., Carlin, V., Minero, C., Pramauro, E., Vincenti, M., 1992. Degradation pathways of atrazine under solar light and in the presence of titanium oxide colloidal particles. Sci. Total Environ. 123–124, 161–169.

Pérez, M., Torrades, F., García-Hortal, J.A., Doménech, X., Peral, J., 2002. Removal of organic contaminants in paper pulp treatment effluents by Fenton and Photo-Fenton reactions. Appl. Catal. B 36, 63–74.

Peyton, G.R., 1990. Significance and treatment of volatile organic compounds in water supplies. In: Ram, N.M., Christman, R.F., Canto, K.P. (Eds.), Oxidative Treatment Methods for Removal of Organic Compounds from Drinking Water Supplies. Lewis Publisher, Boston, USA, pp. 313–362.

Piera, E., Calpe, J., Brillas, E., Doménech, X., Peral, J., 2000. 2,4-Dichlorophenoxyacetic acid degradation by catalyzed ozonation: TiO_2/UVA/O_3 and Fe(II)/UVA/O_3 systems. Appl. Catal. B 27, 169–177.

Sánchez, L., Peral, J., Doménech, X., 1998. Aniline degradation by combined photocatalysis and ozonation. Appl. Catal. B 19, 59–65.

Staehelin, J., Hoigné, J., 1982. Decomposition of ozone in water: rate of initiation by hydroxide ions and hydrogen peroxide. Environ. Sci. Technol. 16, 676–681.

ELSEVIER

Desalination 211 (2007) 22–33

DESALINATION

www.elsevier.com/locate/desal

Biodegradability of treated aqueous solutions of biorecalcitrant pesticides by means of photocatalytic ozonation

Maria José Farré, Maria Isabel Franch, José Antonio Ayllón, José Peral, Xavier Domènech*

Departament de Química, Universitat Autónoma de Barcelona, 08193 Bellaterra, Spain
Tel. +34 (93) 5811702; Fax +34 (93) 5812920; email: Xavier.Domenech@uab.es

Received 25 October 2005; revised 19 January 2006; accepted 16 February 2006

Abstract

A preliminary chemical treatment of pentachlorophenol, isoproturon, diuron, alachlor and atrazine pesticide aqueous solutions (all them belonging to the list of priority pollutants of the European Union) based on a combination of ozone and photo-Fenton reagents has been used to generate intermediates of partial degradation that could be more conveniently degraded with a secondary biological treatment. Quantification of the biodegradability and the toxicity of the treated solutions have been carried out in order to ascertain the suitability of the coupling between the chemical and the biological step. Biotox®, BOD_5/COD and respirometric measurements have been performed. The data obtained with the three techniques point towards a potential coupling for the treatment of isoproturon, diuron, alachlor and atrazine, but not for pentachlorophenol, for which non biodegadable and toxic solutions are obtained after chemical treatment.

Keywords: Photocatalytic ozonation; Biodegradability; Pesticides

1. Introduction

The presence of highly biorecalcitrant organic contaminants in the environment due to industrial and intensive agricultural activities is of particular concern for the preservation of aquatic ecosystems. Since biorecalcitrant compounds are, by definition, non treatable in conventional wastewater treatment plants based on the activity of a microbiological consortium, the development of new technologies that pursue the easy degrada-

*Corresponding author.

Presented at the 9th Environmental Science and Technology Symposium, September 1–3, 2005, Rhodes, Greece. Organized by the Global NEST organization and prepared with the editorial help of the University of Aegean, Mytilene, Greece and the University of Salerno, Fisciano (SA), Italy.

0011-9164/07/$– See front matter

tion of such substances is of practical interest. Advanced oxidation processes (AOP), a group of chemical reactions characterized by the "in situ" production of OH radicals under mild experimental conditions [1], have shown to rapidly degrade many different biorecalcitrant compounds. Different AOP are TiO_2-assisted photocatalysis [2], Fenton and photo-Fenton processes [3], ozonation [4], and the combination of them (i.e. TiO_2/O_3 [5–7] and Fenton/O_3 and photo-Fenton/O_3 [6,8]). Due to the fact that those technologies involve chemical oxidation, the consumption of chemical reagents and/or energy is required, thus making their extensive application difficult. A good solution to this drawback is to reduce the use of AOP to strictly produce a non-toxic and biodegradable intermediate solution that could be treated in a biological secondary step. In this way, complete mineralization of the contaminants may be achieved with a partial use of AOP and a complementary biological treatment [9–11].

In a previous paper performed in the frame of EC CADOX project (EVK1-CT-2002-00122), we have studied the degradation of some biorecalcitrant pesticides (alachlor, atrazine, chlorfenvinfos, diuron, isoproturon and pentachlorophenol) by homogeneous and heterogeneous photocatalytic ozonation, in order to select the most efficient AOP for a rapid removal of such toxic and non-biodegradable chemicals from solution along with a partial mineralization of the original solution [12]. In this previous study, it has been concluded that photo-Fenton coupled with ozone is the most efficient technique [12]. This is a practical case where a coupling of an AOP with a biological treatment can be a suitable alternative for complete mineralization of the original contaminants. Consequently, it is important to show, by using different experimental techniques, that at some point, the toxicity and the biodegradability of the intermediate mixtures obtained after the AOP meet the requirements needed to feed a biological reactor in the secondary treatment. In the present paper the evolution of toxicity, biodegradability, and respirometric behavior of different pesticide solutions that are treated with a combination of ozone and photo-Fenton techniques is studied. The objective is to ascertain whether chemically pretreated solutions of typical diluted wastewater polluted with pesticides are suitable for a secondary biological treatment.

2. Materials and methods

2.1. Reagents

Alachlor (95%, Aragonesas Agro S.A. technical grade), Atrazine (95%, Ciba-Geigy technical grade), Diuron (98.5%, Aragonesas Agro S.A. technical grade) and Isoproturon (98%, Aragonesas Agro S.A. technical grade) were used as target compounds in the experiments. Pentachlorophenol (PCP, 98%) was purchased from Aldrich. All aqueous solutions were prepared with water purified in a Millipore Milli-Q system. $FeSO_4 \cdot 7H_2O$ (Merck, 99.5%) and H_2O_2 (Panreac, 30% w/w) were used in the photo-Fenton experiments. Acetonitrile (Probus, HPLC grade) was used to prepare the mobile phases in the HPLC system. All the other chemicals mentioned hereafter were at least of reagent grade and used as received.

2.2. Apparatus and analytical methods

The pesticide degradation experiments were carried out in a Pyrex glass cell provided of a thermostatic jacket (25.0±0.1°C) and under magnetic stirring. Ozone, generated by an Erwin Sander 301.7 model equipment fed with oxygen of 99.995% purity, was bubbled into the bottom of the reactor by means of a metallic diffuser. The ozone input in the treated solution was 1.75 $g \cdot h^{-1}$ as determined by iodometric titration. A relatively high ozone input value is used to ensure the chemical step effectiveness. The unreacted ozone in the flow gas was first measured by means of an Erwin Sander Quantozone-1 ozone-meter, and then destroyed with a KI trap. A 6 W black light (Philips)

lamp with a measured intensity inside the photoreactor of 0.21 mW·cm^{-2} was used as UVA source in the irradiation experiments. Fig. 1 shows a schematic diagram of the photochemical system.

The concentration of the pesticides was measured by HPLC technique. The HPLC system was constituted by a LC-10 AT VP pump (Shimadzu) and a UV-visible diode array detector (Agilent 1100 Series). Under this conditions the detection limit of the pesticides is 0.01 mg·L^{-1}. The stationary phase was a Hypersil ODS Teknokroma column (250 × 4.6 mm). An acetonitrile/water mixture (50/50 but 60/40 for alachlor) was employed as mobile phase, except for PCP analysis for which a methanol/water mixture (80/20) was used. The mobile phase was degassed by sonication and filtered (0.45 μm) before using. TOC determination was carried out with a TOC-5000 Shimadzu Total Carbon Analyser. The concentration of H_2O_2 was analyzed by the iodometric method [13].

The toxicity tests were performed by means of a BioTox® equipment (Lab-system) using the *Vibrio fischeri* luminescence inhibition to assess the EC_{50} values. 0–150 mg·L^{-1} range Aqualytic® vials were used for chemical oxygen demand test (COD) determination based on a close reflux determination method [14]. This analysis was done in a COD reactor from HACH Co, using a HACH DR/2000 spectrophotometer for colorimetric measurements. The accuracy measurement was checked preparing a potassium acid phthalate standard solution, being the estimated detection limit for this technique 1.1 mg·L^{-1}. Correction for the hydrogen peroxide interference on standard COD test was carried out [15]. Biological oxygen demand (BOD_5) was performed by means of Hg free WTW 2000 Oxytop unit thermostated at 20ºC. In these analyses the accuracy measurement was checked by means of BOD measurements on a mixture of 150 mg·L^{-1} glucose and 150 mg·L^{-1} glutamic acid. The detection limit for this technique was 5 mg·L^{-1}. In all biological analysis hydrogen peroxide was eliminated by adding an excess of sodium sulphite. Aeration was then used to convert the remaining sulphite into sulphate [11]. When direct analysis was not possible storage over –8ºC was necessary.

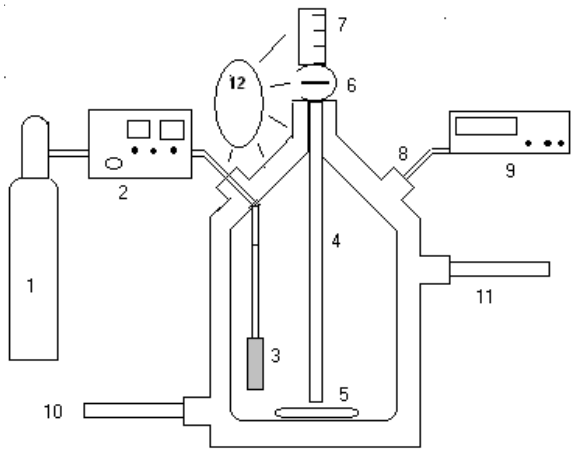

Fig. 1. Experimental set-up. 1 oxygen cylinder, 2 ozonizator, 3 diffusor, 4 sampler, 5 stirrer, 6 sampler key, 7 syringe, 8 gas output, 9 ozone-meter, 10 and 11 input and output thermostatic bath, 12 6W UVA light.

Respirometric analyses were carried out with a LSS respirometer. Since the oxygen uptake rate (OUR) of a microbiological consortium depends on the substrate concentration, quantification of OURs corresponding to different concentrations of a completely biodegradable standard (acetic acid) were carried out (1st OUR_{st}) and used as a reference to compare with the OURs of the pesticide samples of same COD content. In this way a biodegradability index can be defined from the expression:

$$\%\ \text{biodegradability} = \left(1 - \frac{1\text{st OUR}_{st} - \text{OUR}}{1\text{st OUR}_{st}}\right) \times 100 \quad (1)$$

Toxicity can also be evaluated with respirometric procedures [16]: once the biomass has been in contact with the pesticide sample, it is recovered and used again for the assessment of the OUR

of a new acetic acid solution (2nd OUR_{st}). If the pesticide sample has a toxic effect on the biomass, the OUR of the same biomass exposed to acetic acid solutions would be lower than the OUR of the same reference solution in contact with the fresh biomass. In this sense, toxicity can be quantified through the expression:

$$\%\ \text{toxicity} = \left(\frac{1\text{st OUR}_{st} - 2\text{nd OUR}_{st}}{1\text{st OUR}_{st}}\right)\times 100 \quad (2)$$

A sludge sample taken from the aerobic stage of a full-scale urban wastewater treatment plant in Manresa (Spain) was used as inoculum to prepare respirometric suspensions of 3000–4000 mg·L^{-1} of volatile suspended solids (VSS). VSS concentrations were determined according to Standard Methods [14]. All analytical determinations were repeated at least three times. Before the analysis, all the samples were filtered trough 0.45 μm pore size nylon filters in order to remove any particulates. No pesticide adsorption was detected on the filters.

2.3. Pesticide degradation experiments

The experiments were performed with 200 mL of an approximately 50 mg·L^{-1} aqueous solution, of the studied pesticide, which is a typical concentration in polluted effluents, except for atrazine and diuron, for which 38 mg·L^{-1} and 42 mg·L^{-1}, were used due to their low aqueous solubility; for the latter products saturated solutions were prepared and filtrated before being used. All experiments were performed at an initial pH of 3.0, that is the optimum pH for photo-Fenton reaction, except for PCP for which the initial pH was 7.0, due to its very low solubility at pH = 3. HCl and NaOH diluted aqueous solutions were used to adjust the initial pH values. Once the ozone dosage input in the reactor was constant, this latter was filled with the pesticide solution to start degradation experiments. The Fenton reagent (2.0 mg·L^{-1} Fe(II)) aqueous solution and the suitable volume of H_2O_2) was also added to the reactor cell. The quantity of H_2O_2 employed was twice the stoichiometric amount necessary for the complete mineralization of the studied pesticide (H_2O_2 equivalent): 0.48 g·L^{-1}, 0.38 g·L^{-1}, 0.26 g·L^{-1}, 0.32 g·L^{-1}, 0.61 g·L^{-1} and 0.11 g·L^{-1} for alachlor, atrazine, chlorfenvinfos, diuron, isoproturon and PCP, respectively. Residual H_2O_2 remaining after chemical reaction was eliminated with Na_2SO_3 [11] to avoid unexpected effects in the toxicity and respirometric analysis.

3. Results and discussion

The pesticides investigated were alachlor, atrazine, diuron, isoproturon, and PCP, all of them water soluble pesticides listed as priority pollutants by the European Union [17]. These organic pesticides, which exhibit a high degree of biotoxicity, have a moderate solubility in water (between 50 mg·L^{-1} for PCP to 240 mg·L^{-1} for alachlor at 25ºC at neutral pH) and low to moderate octanol–water partition coefficients constants, with log K_{OW} around 2.7–2.9, except for pentachlorophenol (log K_{OW} = 5.1, at 25ºC). Their chemical structures are shown in Fig. 2. The initial analytical parameters of the pesticides aqueous solutions used through the experiments are shown in Table 1.

The first chemical technique used for biodegradability enhancement in the pesticides solutions has been homogeneous photocatalytic ozonation that consists of the combined treatment of ozone and photo-Fenton reagents (H_2O_2 + Fe(II) + UVA light). As it has been stated in the introduction, a previous work showed that this was the most efficient AOP, among several others for the detoxification of the pesticides solutions [12]. In this photocatalytic ozonation process, besides the production of OH radicals by means of the photo-Fenton process [3]:

$$Fe^{2+} + H_2O_2 \rightarrow Fe(OH)^{2+} + \cdot OH \quad (3)$$

Table 1
Initial concentration, total organic carbon, chemical and biological oxigen demands (COD and BOD_5) and effective concentrations (EC_{50}) of the different aqueous pesticide solutions

Pesticide	C_0 (mg·L^{-1})	TOC (mg·L^{-1})	COD (mg·L^{-1})	BOD_5 (mg·L^{-1})	EC_{50} (mg·L^{-1})
Alachlor	50±1	31±3	104±2	6±0.5	35±3
Isoproturon	50±1	35±2	108±7	7±0.5	19±1
Diuron	42±1	20±1	42±1	6±0.5	22±2
Atrazine	38±1	16±1	38±4	7±0.5	27±3
Pentachlorophenol	50±1	13±1	30±1	< 5	0.25±1

$n = 3$, $\alpha = 0.95$

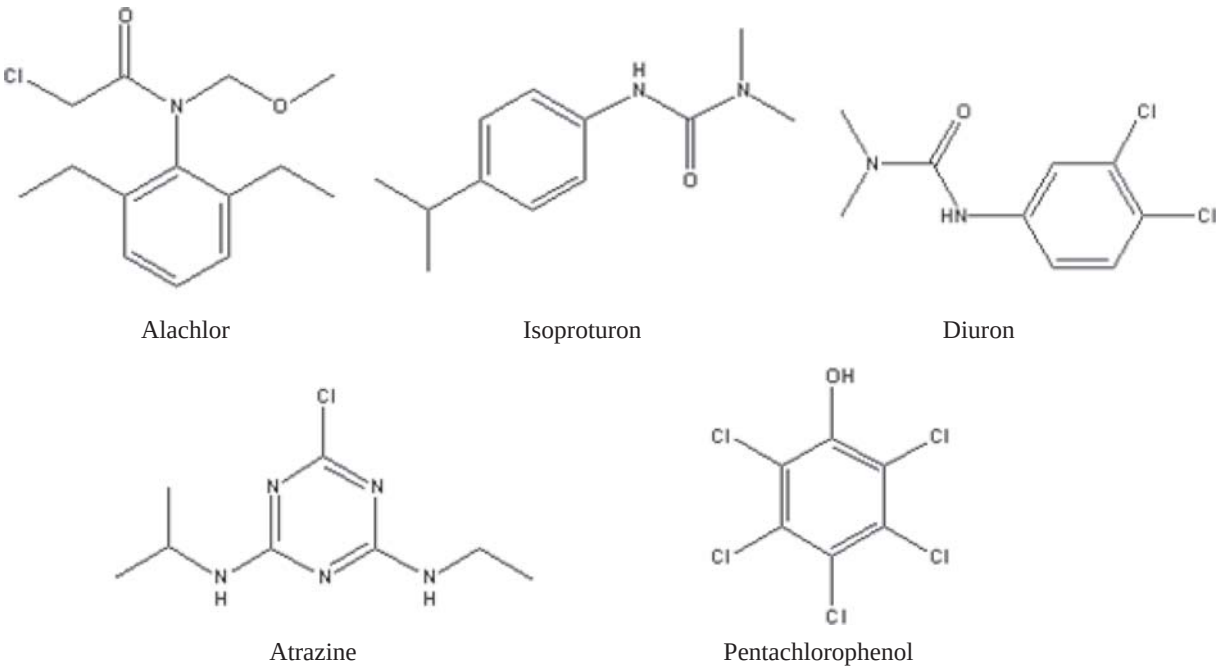

Fig. 2. Chemical structures of the pesticides used in this work.

$$Fe(OH)^{2+} + h\nu \rightarrow Fe^{2+} + \cdot OH \quad (4)$$

On the other hand, ozone reacts with Fe(II) simultaneously leading to the formation of FeO^{2+} species that are readily hydrolyzed giving in more OH radicals [6]:

$$Fe^{2+} + O_3 \rightarrow FeO^{2+} + O_2 \quad (5)$$

$$FeO^{2+} + H_2O \rightarrow Fe^{3+} + \cdot OH + OH^- \quad (6)$$

Fig. 3 shows the time course of the concentration of the original pesticides (Fig. 3a) and normalized TOC (Fig. 3b) of the treated solutions. As can be seen the disappearance of the original pesticide is fast under the tested conditions; four of the five pesticides are completely removed in

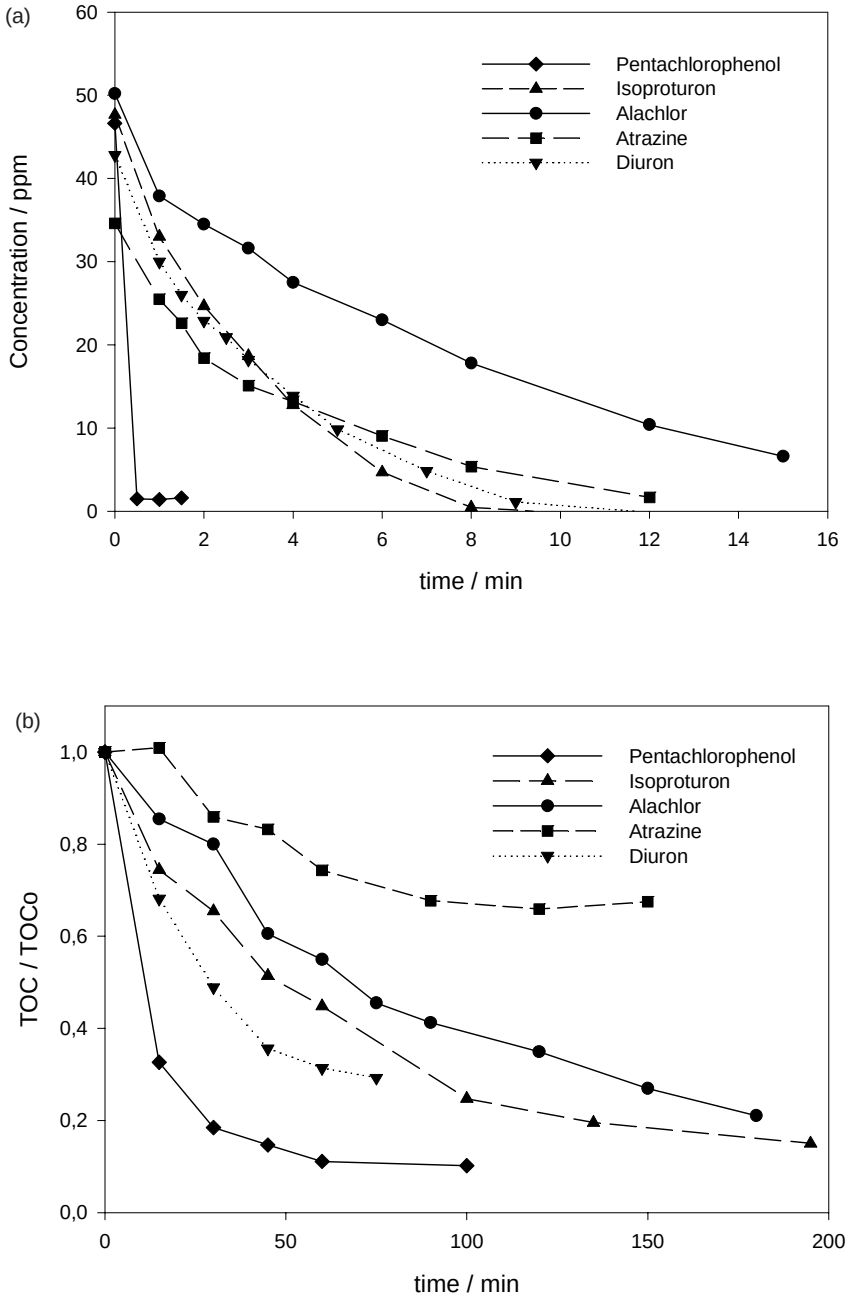

Fig. 3. Time course of: a) the pesticide concentration and b) the normalized TOC of the different pesticide solutions treated by means of photocatalytic ozonation at pH = 3 (pentachlorophenol pH = 7), T = 25ºC, [Fe(II)] = 2 mg L^{-1}, [H_2O_2] = 200% of the stoichiometric requirement for total mineralization of the original pesticide, O_3 flow = 1.75 g h^{-1}, 6 W UVA light irradiation.

less than 15 min, while the concentration of the fifth one, i.e. alachlor, becomes less than 10 mg·L^{-1} during the same treatment time. The mineralization of the solutions proceeds more slowly; while PCP solutions can be almost completely mineralized after 100 min of reaction, only 30% of the original TOC is removed in atrazine solutions after 150 min. Thus, after pesticide disappearance within few minutes of reaction, large quantities of TOC remain in solution. Depending on the toxic character of those reaction solutions after photocatalytic degradation a biological treatment step could be used for further oxidation. The assessment of the acute toxicity of the intermediates remaining in solution is essential to envisage such a possibility. Table 2 summarizes the TOC and EC_{50} values of the initial solutions and after parent pesticides were totally removed from the solution by chemical treatment. The data indicates a clear decrease of toxicity (increase of the EC_{50} value) for diuron, while isoproturon and PCP solution experiences a discrete improvement that could be within the experimental margin of error. Nevertheless, toxicity of the isoproturon and PCP solutions could be completely removed after 45 and 30 min of chemical treatment, respectively, which may be due to the strong decrease on the total organic carbon. On the other hand, the toxicity of alachlor and atrazine solutions increases after pesticide removal; even after 3 h of pretreatment atrazine and alachlor solutions remain toxic. Consequently, acute toxicity assays by means of Biotox® system show that pretreatment is only beneficial for diuron.

Being biological process the scope of the work, biodegradability of such pretreated effluents must be assessed. Since the Biotox® system has a large intrinsic experimental error and is too sensitive (many chemicals that give positive toxicity with Biotox® are found non-toxic with other analytical techniques), it seems reasonable to test alternative methods for the quantification of the biodegradability of the intermediates generated during the pesticides degradation. The most extended way to quantify biodegradability is the assessment of the BOD_5/COD ratio [18]. It is commonly accepted that a wastewater is completely biodegradable when that ratio is above 0.4, while a value between 0.3–0.4 corresponds to partial biodegradability [18]. Thus, BOD_5 and COD analysis were also carried out. Table 3 summarizes BOD_5 and COD data and their ratio with the respective initial values corresponding to the same pesticide degradation experiments and times of chemical reaction that appear in Table 2. As can be seen BOD_5 values increase for all the treated pesticide solutions except in the case of PCP, for which it remains lower than 5 mg·L^{-1}. As expected, the COD values decrease for all the solutions after the chemical oxidation. It is important to notice

Table 2
TOC and EC_{50} values for treated pesticide solutions and EC_{50} values of the initial pesticide solutions. The treatment time refers to the time required to remove the parent compound from solution

Pesticide	Treatment time (min)	TOC after treatment (mg·L^{-1})	EC_{50} treated solution (mg·L^{-1} of TOC)	EC_{50} initial solution (mg·L^{-1} of TOC)
Alachlor	30	16±1	11±1	35±3
Isoproturon	10	31±2	21±2	19±1
Diuron	15	15±1	— (*)	10±2
Atrazine	15	16±1	14±2	27±3
Pentachlorophenol	5	6±1	0.50±2	0.25±1

(*) The EC_{50} value is out of the scope of the analyzer (large decrease of toxicity)
$n = 3$, $\alpha = 0.95$

Table 3
BOD_5 and COD values of treated pesticide solutions (initial values shown in Table 1), together with the BOD_5/COD ratios of the initial and treated pesticide solutions

Pesticide	Treatment time (min)	BOD_5 after treatment (mg L^{-1})	COD after treatment (mg L^{-1})	BOD_5/COD after treatment	Initial BOD_5/COD
Alachlor	30	31±1	86±1	0.36	0.06
Isoproturon	10	31±1	79±2	0.39	0.07
Diuron	15	13±1	33±1	0.39	0.15
Atrazine	15	12±1	22±2	0.58	0.17
Pentachlorophenol	5	<5	20±1	<0.25	<0.25

$n = 3$, $\alpha = 0.95$

that again, with the exception of PCP, the BOD_5/COD ratios increase for all the solutions reaching values close or above 0.4, thus, indicating the existence of a biodegradable character [18]. Both isoproturon and diuron solutions clearly change their properties after chemical treatment, becoming suitable candidates for a secondary biological treatment. However, for alachlor and atrazine the BOD_5/COD ratios seem to be in disagreement with the toxicity analysis, since their solutions were found to increase toxicity after treatment.

In order to clarify such an apparent discrepancy between acute toxicity and BOD_5/COD ratios, respirometric analysis were also carried out. As an example of the measurements carried out, Fig. 4 shows the evolution of the dissolved oxygen (DO in $mg \cdot L^{-1}$) recorded during the respirometric studies of the original PCP solutions. The OUR values of samples and standards are obtained from the slope of the DO vs. time curves, subtracting the OUR associated to endogenous respiration that is also represented in Fig. 4. The presence of acetic acid clearly increases the OUR of the biomass. In the presence of PCP the OUR has the same value that the one associated to endogenous respiration, meaning that the biomass can not degrade PCP. Furthermore, when the same biomass is mixed with a new acetic acid solution, an OUR decrease is observed (going even below the endogenous value), indicating that the biomass has been partially damaged in the previous contact with the pesticide solution due to its toxic character. Since that value is lower than the endogenous OUR, it can be concluded that the biomass has completely lost its ability to consume acetic acid and the toxicity is considered to be 100% (see Table 4).

Respirometric data for all the original pesticide solutions are shown in Table 4. As can be seen, even the qualitative behavior of toxicity is not the same if the assessment is carried out with different analytical techniques. The Biotox® data indicates the following order of toxicity: PCP > diuron > isoproturon > atrazine > alachlor (see EC_{50} values in Table 1), while respirometric data gives the order: PCP > alachlor > atrazine > isoproturon = diuron. Thus, the two techniques have the only coincidence of the prediction of the high toxicity of PCP. These differences could be explained considering the different nature of the biological material used: Biotox® utilizes the seawater *Vibrio fischeri*, whereas respirometry uses the bacterial consortium in activated sludge [19]. Low biodegradability of the initial pesticides is predicted by both techniques: biodegradability values not higher than 6% from respirometric assays (see Table 4), and values not higher than 0.17 for BOD_5/COD ratios (see Table 3).

In Table 5 respirometric data for all the chemically treated pesticide solutions are summarized. As can be seen by comparing with Table 4, except in the case of PCP all pesticide solutions in-

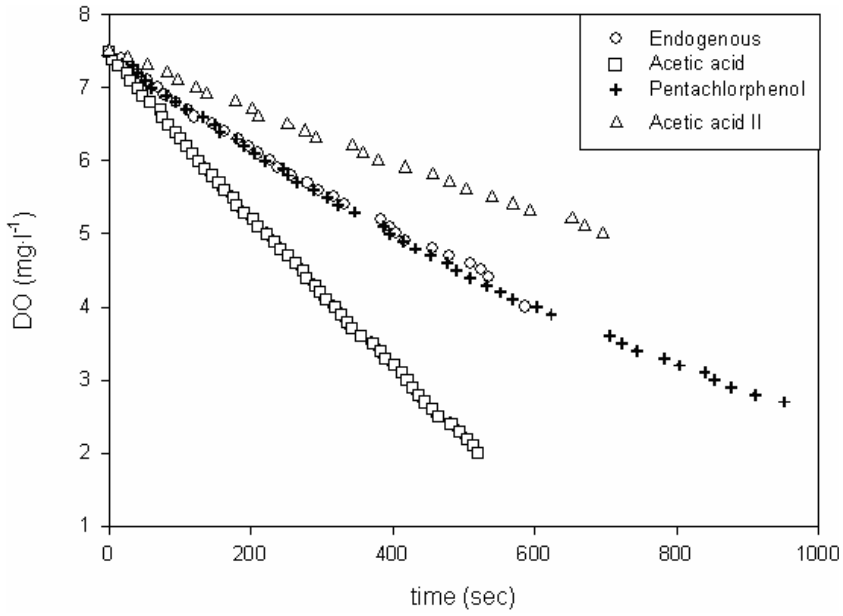

Fig. 4. Respirometric measurements (dissolved oxygen vs. time) of a 50 mg L^{-1} (13 mg L^{-1} of C) PCP solution (curve +). Also depicted is the endogenous respiration of the 3.5 g l^{-1} VSS biomass (o), and respiration of a 31 mg L^{-1} (13 mg L^{-1} of C) acetic acid solution before (o) and after (Δ) PCP treatment. VSS = volatile suspended solids.

Table 4
Respirometric data of the five original pesticide solutions (see Matherials and methods for calculation details). Concentration of the respirometric solutions: 3000–4000 mg·L^{-1} VSS, temperature 25ºC

Herbicide	1st OUR_{st} (mg L^{-1} h^{-1} VSS^{-1})	OUR sample (mg L^{-1} h^{-1} VSS^{-1})	% biodegradability	2nd OUR_{st} (mg L^{-1} h^{-1} VSS^{-1})	% toxicity
Alachlor	8.64	4.79	6	7.80	10
Isoproturon	7.92	0.00	0	0.792	0
Diuron	4.73	1.93	4	4.73	0
Atrazine	5.76	0.514	1	5.66	2
Pentachlorophenol	4.08	0.206	5	0.00	>100

n =3, α = 0.95

crease their biodegradability, as expected after partial chemical treatment. On the other hand, isoproturon and diuron solutions experience no increase of toxic character, while alachlor and atrazine solution do. PCP treated solution shows lower toxicity than the original solution. According to the Biotox® measurements (see Table 2) alachlor and atrazine solutions increase their toxicity (the EC_{50} value decreases), isoproturon solution experience no important change, while the toxicity of diuron solution clearly decreases. The PCP solution toxicity also decreases. Thus, concerning toxicity there is a reasonable agreement between the repirometric and the Biotox® toxicity

Table 5
Respirometric data of the five chemically treated pesticide solutions (see Materials and methods for calculation details). Concentration of the respirometric solutions: 3000–4000 mg·L^{-1} VSS; temperature 25ºC.

Herbicide	Treatment time (min)	1st OUR_{st} (mg L^{-1} h^{-1} VSS^{-1})	OUR sample (mg L^{-1} h^{-1} VSS^{-1})	% bio-degradability	2nd OUR_{st} (mg L^{-1} h^{-1} VSS^{-1})	% toxicity
Alachlor	30	3.67	3.13	85	0.29	92
Isoproturon	10	4.63	3.08	67	5.04	0
Diuron	15	5.89	1.52	26	5.88	0
Atrazine	15	2.97	0.78	26	0.87	71
Pentachlorophenol	5	2.91	0.00	0	1.15	61

n =3, α = 0.95

measurements; with differences that can be ascribed to the inherent error associated to these biology-based analytical techniques. This is remarkable since the Biotox® technique is appropriated for inter-laboratory comparisons because it is a well standardized procedure, while respirometry can be considered an intra-laboratory technique due to the variability of the cultures used for the analyses. In any case, concerning the interest of the present research, the robust respirometric measurements seem to rule out the possibility of too sensitive analysis with Biotox® measurements. Comparing biodegradability of the pretreated effluents analyzed by both BOD_5/COD and respirometric assays, the same conclusions can be obtained since biomass is able to assimilate diuron, isoproturon, atrazine, alachlor but not PCP. The difference between biodegradability percentage obtained from respirometry and BOD_5/COD ratio corresponds to the fact that respirometric assays measure biodegradability in a short periode of time (about 30 min), while BOD_5/COD ratio measures the biodegradability in a five days scenario.

From the obtained results, the application of a chemical step prior to biological treatment to decrease acute toxicity of pesticide aqueous solutions, without decreasing to much the organic carbon of the effluent, seems to work for diuron and isoproturon solutions. These pesticides, after the AOP has been applied to remove the respective parent compound, are biodegradable and become detoxified, remaining 75% and 89% of the initial TOC in solution for diuron and isoproturon, respectively. For the PCP solutions, after complete removal of the parent pesticide compound by means of AOP treatment only 46% of the initial TOC remains in solution and the obtained solution is not biodegradable.

With relation to alachlor and atrazine aqueous solutions, the TOC remaining in the effluents once an AOP has been applied to remove the parent pesticides, are 52% and 100% for alachlor and atrazine, respectively, and the toxicity of the resulting solutions clearly increased. For these effluents, the AOP treatment must be extended in time to achieve detoxification. In this way, recently published results related with Photo-Fenton treatment of different chlorinated pesticides, indicate that detoxification occurs when full dechlorination of parent and intermediated compounds is attained [20]. This is the case for diuron, for which dechlorination occurs in conjunction with parent compound elimination and detoxification takes place at this point, while for atrazine and alachlor solutions, dechlorination occurs after disappearance of the pesticide [20].

Particularly interesting is the case of atrazine solutions, for which the elimination of the parent compound does not imply a decrease of TOC. In

fact, it is known that the more prominent degradation routes give rise to the formation of the imine and amide derivatives of atrazine, ATRA-imine (2-chloro-4-ethylimino-6-isopropylamino-s-triazine) and CDIT (4-acetamido-2-chloro-6-ethylamino-s-triazine) [21]:

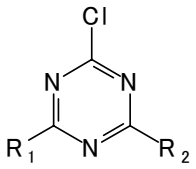

ATRA-imine	CDIT
R_1: N=CHCH$_3$	R_1: NHCOCH$_3$
R_2: NHCH(CH$_3$)$_2$	R_2: NHCH(CH$_3$)$_2$

which must be the responsible of the increased toxicity observed for treated solutions with respect to the initial atrazine aqueous solutions. Dechlorination occurs when only 3/8 of the initial TOC remain in solution, probably by formation of cyanuric acid (2,4,6-trihydroxy-s-triazine)[22]:

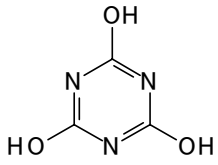

that keeps three of the eight carbon atoms of the initial atrazine molecule.

4. Conclusions

PCP, isoproturon, diuron, alachlor and atrazine pesticide solutions have been partially degraded by using a chemical pretreatment method based on a combination of ozone and photo-Fenton reagents. The removal of the parent pesticide takes place in a few minutes, but the complete mineralization of all the organic content takes longer times. The possibility of coupling the chemical treatment with biological treatment has been studied by the assessment of biodegradability and acute toxicity of the intermediate solutions. The toxicity has been quantified with both the Biotox technique and carrying out respirometric measurements, while biodegradability assessment has been done on the basis of BOD_5/COD ratio and respirometric measurements.

Data obtained with the different techniques, although they show differences that could be explained due to the different bacteria employed in toxicity analysis and different experimental time for biodegradation assessment, they seems to indicate that biodegradability increases in the case of isoproturon, diuron, alachlor and atrazine pesticide solutions, but not in the case of pentachlorophenol solution. In the case of alachlor and atrazine the increase of biodegradability takes place with a simultaneous increase of toxicity. In any case, the suitability of the coupling of chemical and biological treatments will depend on the particular chemical nature of the pollutant.

Acknowlegments

The authors wish to thank to CICYT (project: PPQ2002-04060-C02-01) and EC (CADOX project, EVK1-CT-2002-00122) for financial support.

References

[1] G.R. Peyton, In: N.M. Ram, R.F. Christman and K.P. Canto, eds., Oxidative Treatment Methods for Removal of Organic Compounds from Drinking Water Supplies. Lewis Pub., Boston, USA, 1990, pp. 313–362.
[2] A. Mills and S. Le Hunte, An overview of semiconductor photocatalysis. J. Photochem. Photobiol., 108 (1997) 1–35.
[3] G. Ruppert, R. Bauer and G. Heisler, The photo-Fenton reaction — an effective photochemical wastewater treatment process. J. Photochem. Photobiol., A: Chem., 73 (1993) 75–78.
[4] W.H. Glaze, Drinking water treatment with ozone. Environ. Sci. Technol., 21 (1987) 224–230.

[5] L. Sánchez, J. Peral and X. Doménech, Aniline degradation by combined photocatalysis and ozonation. Appl.Catal. B: Environ., 19 (1998) 59–65.
[6] E. Piera, J. Calpe, E. Brillas, X. Domènech and J. Peral, 2,4-dichlorophenoxyacetic acid degradation by catalyzed ozonation: TiO_2/UVA/O_3 and Fe(II)/UVA/O_3 systems. Appl.Catal. B: Environ., 27 (2000) 169–177.
[7] F. Beltran, F. Rivas and R. Montero, Catalytic ozonation of oxalic acid in an aqueous TiO_2 slurry reactor. Appl. Catal. B: Environ., 39 (2002) 221–231.
[8] T. Logager, J. Holcman, K. Sehested and T. Pedersen, Oxidation of ferrous ions by ozone in acidic solutions. Inorg. Chem., 31 (19992) 3523–3529.
[9] S. Parra, S. Malato and C. Pulgarín, New integrated photocatalytic-biological flow system using supported TiO_2 and fixed bacteria for the mineralization of isoproturon. Appl. Catal. B: Environ., 36 (2002) 131–144.
[10] W. Nishijima, Fahmi, T. Mukaidani and M. Okada, DOC removal by multi-stage ozonation-biological treatment. Water Res., 37 (2003) 150–154.
[11] C.D. Adams, P.A. Scanian and N.D. Secrist, Oxidation and biodegradability enhancement of 1,4-dioxane using hydrogen peroxide and ozone. Environ. Sci. Technol., 28 (1994) 1812–1818.
[12] M.J. Farré, M.I. Franch, S. Malato, J.A. Ayllón, J. Peral and X. Doménech, Degradation of some biorecalcitrant pesticides by homogeneous and heterogeneous photocatalytic ozonation. Chemosphere, 58 (2005)1127–1133.
[13] G.J. Jeffery, J. Basset, J. Mendham and R.C. Denny. Vogel's Textbook of Quantitative Chemical Analysis. 5th ed., Longman, New York, 1989, pp. 368–395.
[14] APHA-AWWA-WPCF, Standard Methods for the Examination of Water and Wastewater, ASTM D1252-00, 17th ed., Washington, DC, 1989.
[15] Y.W. Kang, M.J. Cho and K.Y. Hwang, Correction of hydrogen peroxide interference on standard chemical oxygen demand test. Water Res., 33 (1998) 1247–1251.
[16] A. Guisasola, J.A. Baeza, J. Carrera, C. Casas and J. Lafuente, An off-line respirometric procedure to determine inhibition and toxicity of biodegradable compounds in biomass from an industrial WWTP, Water Sci. Technol., 11–12 (2003) 267–275.
[17] European Parliament, Decision No. 2455/2001/EC of the European Parliament and of the Council of 20 November 2001. Official Journal of the European Communities., 15.12.2001, L331/1–L331/5.
[18] V. Sarria, S. Parra, A. Nevenka, P. Péringer, N. Benitez and C. Pulgarin, Recent developements in the coupling of photoassisted and aerobic biological processes for the treatment of biorecalcitrant compounds. Catalysis Today, 76 (2002) 301–315.
[19] M. Gutiérrez, J. Etxebarria and L. de las Fuentes, Evaluation of wastewater toxicity: comparative study between Microtox® and activated sludge oxygen uptake inhibition. Water Res., 36 (2002) 919–924.
[20] M. Hincapié, M.I. Maldonado, I. Oller, W. Gernjak, J.A. Sánchez-Pérez, M.M Ballesteros and S. Malato, Solar photocatalytic degradation and detoxyfication of EU priority substances. Catalysis Today, 101 (2005) 203–210.
[21] J.L. Acero, K. Stemmler and U.V. Gunten, Degradation kinetics of atrazine and its degradation products with ozone and OH radicals: a predictive tool for drinking water treatment. Environ. Sci. Technol., 34 (2000) 591–597.
[22] C. Minero, E. Pelizzetti, S. Malato and J. Blanco, Large solar plant photocatalytic water decontamination: Degradation of atrazine. Solar Energy, 56 (1996) 411–419.

WATER RESEARCH 40 (2006) 2533–2540

Available at www.sciencedirect.com

SCIENCE DIRECT®

journal homepage: www.elsevier.com/locate/watres

Assessment of photo-Fenton and biological treatment coupling for Diuron and Linuron removal from water

*María José Farré, Xavier Doménech, José Peral**

Departament de Química, Universitat Autónoma de Barcelona, 08193 Bellaterra, Spain

ARTICLE INFO

Article history:
Received 18 November 2005
Received in revised form
18 April 2006
Accepted 26 April 2006
Available online 14 June 2006

Keywords:
Herbicides
Photo-Fenton
SBR
Multivariate experimental design
Water treatment
Advanced oxidation processes

ABSTRACT

The coupling of photo-Fenton (chemical) and biological treatments has been used for the removal of Diuron and Linuron herbicides from water. The chemical reaction was employed as a pre-treatment step for the conversion of the toxic and non-biodegradable herbicides into biodegradable intermediates that were subsequently removed by means of a biological sequencing batch reactor (SBR). Multivariate experimental design was used to select four photo-Fenton reagent dose combinations for the coupling experiments. Concentrations of hydrogen peroxide between 10 and 250 mg L^{-1}, and iron (II) concentrations between 2 and 20 mg L^{-1} have been tested. 15.9 mg L^{-1} of Fe(II) and 202 mg L^{-1} of H_2O_2 were needed to convert initial toxic and non-biodegradable herbicides into suitable intermediates for a subsequent biological treatment. Detrimental effects due to the excess of reactants were detected. Chemical oxygen demand (COD), average oxidation state (AOS), total organic carbon (TOC) and hydrogen peroxide concentration are the parameters used to trace the experiments course. Also, toxicity (EC_{50}^{15}) and biodegradability (BOD_5/COD) tests were carried out at the end of each chemical oxidation.

Complete disappearance of the herbicides from water was observed after the chemical treatment, while 3,4-dichloroaniline and 3,4-dichlorophenyl isocyanate were identified as the main by-products of the degradation process. Complete TOC removal was achieved after biological treatment in a SBR using a hydraulic retention time (HRT) of 2 days.

1. Introduction

The presence of pesticides in natural and drinking waters is a problem of environmental and human health concern. The main sources of pesticides pollution are agricultural runoffs and wastewaters generated at pesticide manufacturing plants (Chiron et al., 2000). Groundwater contamination with these compounds is a serious problem since the lifetime of the pesticides might be of several years, posing a serious threat to the one-half of the world population that obtains drinking water from wells (Pimentel, 1996).

Since their discovery in 1950, phenylurea compounds have been widely used to prevent the growth of undesirable plants. Diuron and Linuron are two phenylurea herbicides that inhibit photosynthesis, thus impeding weed growth. Both herbicides are toxic and non-biodegradable and they are mainly used for the control of germinating grass and broad-leaved weeds in many crops (e.g., cereals) (Tixier et al., 2000).

Since herbicides, due to their biorecalcitrant and toxic properties, cannot be directly treated in conventional wastewater treatment plants based on the activity of a microbiological consortium, the development of new technologies aimed at the easy degradation of such substances is of practical interest.

Due to the combination of both environmental and economic advantages, the coupling between advanced oxidation processes (AOPs) and biological treatments can be a suitable solution for the removal of toxic compounds from

*Corresponding author. Tel.: +34 93 581 2772; fax: +34 93 581 2920.
E-mail address: jose.peral@uab.es (J. Peral).
0043-1354/$ - see front matter © 2006 Elsevier Ltd. All rights reserved.
doi:10.1016/j.watres.2006.04.034

water (Kotsou et al., 2004; Al Momani et al., 2004; Garcia-Montaño et al., 2006).

AOPs are based in the use of the highly-reactive hydroxyl radicals ($E^0 = 2.8$V versus SHE) that can efficiently oxidize organic matter to CO_2. The main idea of coupling is to apply an AOP to a toxic and/or non-biodegradable effluent during a short time, optimizing chemicals and energy consumption, and generating an intermediate sample that is fully biodegradable, thus opening the possibility of a subsequent biological treatment for the complete removal of organic matter.

Available AOPs are ozonation (Glaze, 1987), heterogeneous photocatalysis with TiO_2 (Mills and Le Hunte, 1997) and the photo-Fenton reaction. The last one offers high reaction yields with a low treatment cost, mainly because of the possibility of using solar light as photon source (Bauer and Fallmann, 1997). Although the Fenton reaction is known since the end of the XIX century, only in the last few years it has been applied for water and soil treatment. In the Fenton reaction $OH^{\bullet}$ is produced by combining Fe(II) and H_2O_2 at acid pH (Faust and Hoigné, 1990). Under irradiation of $\lambda < 400$ nm, the Fe(III) generated in Fenton reaction can be reduced to Fe(II), closing a loop mechanism where Fe species acts as catalyst, giving additional $OH^{\bullet}$ (photo-Fenton process).

If minimization of Fenton reagents (Fe(II) and hydrogen peroxide) consumption is the goal to be achieved, multivariate experimental design is a clever option. Experimental design is a modern approach to the study of the simultaneous effects of several experimental parameters on chemical reaction (Box et al., 1978). By following this methodology, optimization of reaction conditions can be achieved with a minimum number of experiments.

Sequencing batch reactor (SBR), based on the biodegradation activity of a bacteria consortium, has been gaining considerable popularity as treatment method in recent years because of its high efficiency and flexibility (USEPA, 1999) and it can be considered suitable for biological system modelling at laboratory scale because of the small volumes of effluent that can handle and because of the good control it offers. Conventional SBR operation involves four steps—filling, reaction, settling and drawing—all steps being sequentially conducted in a single reactor (Irvine and Ketchum, 1989; Wilderer et al., 1999).

The goal of this paper is to use an experimental design for the choice of minimum Fenton reactant doses able to convert Diuron and Linuron containing waters into biocompatible effluents, seeking the subsequent coupling to a biological SBR for complete organic load removal.

2. Materials and methods

2.1. Preparation of initial wastewater

Diuron (98.5% Aragonesas Agro S.A. technical grade) and *Linuron* (92.6% Makhteshim Agan España ,S.A.) were used as target compounds in the experiments (see Fig. 1 for chemical structures). Solutions of 42 mg L^{-1} of Diuron and 75 mg L^{-1} of Linuron were prepared in Milli-Q quality water. Those values correspond to the maximum solubility of both herbicides in water at 25 °C. A saturated initial solution was prepared and then filtered by means of a 20 μm nylon filter. The initial features of the filtered solution were as follow: pH = 5.7, total organic carbon (TOC) = 50 ± 2 mg L^{-1}, chemical oxygen demand (COD) = 139 ± 7 mg L^{-1}, $BOD_5 = 5 \pm 1$ mg L^{-1} and BOD_5/COD = 0.033. The initial solutions were transparent and colourless. It was also non-biodegradable, as seen by the Zahn–Wellens test (OECD 302B, 1996). Adsorption of TOC on the biomass was not observed after 28 days of the test duration.

2.2. Photo-Fenton experimental procedure

$FeSO_4 \cdot 7H_2O$ (Merck) and H_2O_2 (Panreac, 33% w/v) were used as photo-Fenton reagents. Experiments were conducted at 25 ± 0.2 °C in a cylindrical Pyrex thermostatic cell of 0.25 L capacity equipped with a magnetic stirrer. A 6 W Philips black light was used as light source, providing a light intensity of 0.21 mW cm^{-2} into the reactor. In all the experiments, pH was adjusted to 2.8.

Photo-Fenton reagent concentrations were selected by means of multivariate experimental design. A central composite design was used to investigate the effect of hydrogen peroxide and iron (II) concentrations in the mineralization percentage. Eleven experiments were carried out. Concentration of hydrogen peroxide between 10 and 250 mg L^{-1} and iron (II) concentrations between 2 and 20 mg L^{-1} were codified in three values within the range −1 to +1. The experiment with the central point values was repeated three times to check the statistical significance. The polynomial expression and response surface were worked out with the MODDE 5.0 software. From the experimental design, four combinations of reagent doses were selected (A, B, C and D).

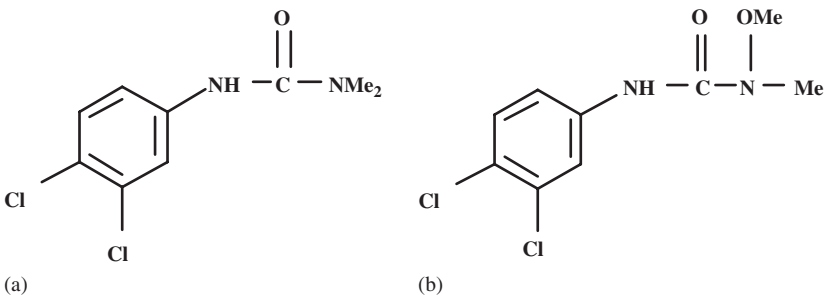

Fig. 1 – Diuron (a) and Linuron (b) chemical structure.

2.3. Aerobic SBR experimental procedure

A sludge sample taken from the aerobic stage of an urban wastewater treatment plant in Manresa (Spain) and containing an initial volatile suspended solids (VSS) value around $5\,g\,L^{-1}$ was used as inoculum of the SBR. A dilution was carried out to obtain a final VSS value of $0.6\,g\,L^{-1}$ in the 1.5 L SBR. The procedure performed in every SBR experiment was as follow: after an aeration-reaction period (22.5 h), agitation was stopped to let the biomass to settle down. After 1 h, a suitable volume was withdrawn from the sample supernatant and replaced by a phototreated solution (pH previously adjusted to 7). Before entering the SBR, hydrogen peroxide was removed from the treated solution by adding an excess of sodium sulphite. Aeration was then used to convert the remaining sulphite into sulphate (Adams et al., 1994). Nutrients were also added to reach a constant concentration in the SBR: $MgSO_4$ ($202\,mg\,L^{-1}$), $CaCl_2$ ($73.4\,mg\,L^{-1}$), NH_4Cl ($76.4\,mg\,L^{-1}$) and NaH_2PO_4 ($1242\,mg\,L^{-1}$). This cycle was repeated 12 times in each experiment in order to obtain repetitive results (i.e., variation coefficients lower than 4% in TOC measurements). A whole cycle was completed when the SBR total initial volume had been replaced with new solution. The hydraulic retention time (HRT) in the SBR experiments was 2 days. Thus, the volume of solution replaced after each batch was

$$V_{replaced} = V_{SBR}/HRT. \quad (1)$$

Sample pH—around 7—and dissolved oxygen—not lower than $3\,mg\,L^{-1}$—were controlled daily. The reactor was maintained at laboratory temperature (20 °C) and mixed by a magnetic stirrer. Air was supplied by a gas diffuser.

2.4. Analytical methods

Initial herbicide concentration (HPLC), TOC, COD and hydrogen peroxide evolution were recorded along the oxidation process. The HPLC system included a LC-10 AT VP pump (Shimadzu) and a UV–Visible diode array detector (Agilent 1100 Series). The detection limit of the pesticides was $0.001\,mg\,L^{-1}$. Acetonitrile (Pobus, HPLC grade) was used to prepare the mobile phases of the HPLC system and a 5 μm Hypersil column (250 × 0.46 mm) from Teknocroma® was used as a stationary phase. TOC was analysed with a Shimadzu 5000 apparatus. Samples of 10 ml were needed for those analyses. COD determinations based on a close reflux method (APHA-AWWA-WPCF, 1989) were carried out by using 0–$150\,mg\,L^{-1}$ range Aqualytic® vials. Samples of 2 ml were required for those analyses. A HACH COD reactor and a HACH DR/2000 spectrophotometer were used during the analysis. The accuracy of the COD measurements was checked by preparing a potassium hydrogen phthalate standard, and the estimated detection limit of the technique was $1.1\,mg\,L^{-1}$. Correction for hydrogen peroxide interference on the standard COD test was carried out (Kang et al., 1999). The concentration of H_2O_2 was analysed by the iodometric method (Jeffery et al., 1989): (a) 10 ml of the hydrogen peroxide solution was transferred to 100 ml of purified water; (b) 10 ml of 2 M sulphuric acid, 10 ml of 1 M potassium iodide solution, and 2 ml of $50\,g\,L^{-1}$ ammonium molybdate solution were sequentially added; (c) the liberated iodine was immediately titrated with 0.05 M standard sodium thiosulphate. A blank was run at the same time.

At the end of the oxidation process toxicity (EC_{50}^{15}), biodegradability (BOD_5/COD) and main intermediates were analysed. The toxicity tests were performed with a BioTox® instrument (Labsystem), using the *Vibrio fischery* bacteria to asses the effective concentration of a test sample that caused a 50% reduction in bacteria light emission during 15 min of bacteria-toxic contact (EC_{50}^{15}). Samples of 20 ml were required for those analyses. A WTW OxyTop system was used for BOD_5 determinations. Samples of 432 ml were needed. In those analyses, the measurement accuracy was checked by making BOD_5 measurements of a mixture of $150\,mg\,L^{-1}$ glucose and $150\,mg\,L^{-1}$ glutamic acid. The detection limit of this technique was $5\,mg\,L^{-1}$.

In all biological analyses, hydrogen peroxide and iron in solution were previously removed to avoid errors in the measurement. Iron in solution was eliminated by raising pH to 8 and then filtering the solution. Hydrogen peroxide was eliminated by adding sodium sulphite, as explained above.

The intermediate products of the photodegradation of both pesticides were extracted by solid phase extraction (Maxi-Clean C18 600 mg, Alltech). A mixture of dichlormethane and ethyl acetate (1/1, v/v) was used to elute the intermediate products. This solution was concentrated under nitrogen flow for the by-products analysis. The GC-MS was performed using a GC (HP 6890 series) equipped with an MSD (HP 5973). The system was equipped with an HP-5MS capillary column (30 × 0.25 i.d. × 0.25 μm), splitless injection, and used helium as carrier gas ($1\,ml\,min^{-1}$). The GC oven temperature was programmed to initially hold at 50 °C for 3 min, to increase from 50 to 275 °C at a rate of $5\,°C\,min^{-1}$ and to hold at 275 °C for 15 min. The injector and interface temperature were kept at 250 °C. Mass spectra were obtained by the electron-impact mode at 70 eV, using scan mode (30–800 *m/z*).

When SBR was used, volatile and total suspended solids (VSS and TSS) concentrations, using samples of 10 ml, and TOC were determined daily according to Standard Methods (APHA-AWWA-WPCF, 1989).

3. Results and discussion

Oxidation of a Linuron and Diuron solution by photo-Fenton reagents was carried out in a batch reactor in order to ascertain whether this reaction could be used to generate an intermediate solution that could be subsequently degraded in a biological reactor. Thus, the possibility of coupled chemical–biological treatment of water containing Diuron and Linuron herbicides has been explored. Multivariate experimental design has been used to choose the best reactant combination needed for a given mineralization degree. Evolution of primary parameters like TOC, average oxidation state (AOS) and residual H_2O_2 during photo-Fenton experiments was investigated. Other factors like toxicity (EC_{50}^{15}) and biodegradability (BOD_5/COD) of the intermediate solutions obtained with the different reactant doses were also assessed.

There are two important factors affecting the rate of photo-Fenton reaction once the photon source is fixed: hydrogen peroxide dose and iron concentration. The hydrogen peroxide

dose is important in order to obtain quantitative degradation, while the iron concentration is important for the reaction kinetics (Chamarro et al., 2000). Nevertheless, formation of different scavengers of reactive species when an excess of reactants is added to the solution can be detrimental. Thus, the most efficient reagent concentration needs to be carefully determined. Multivariate experimental design has been used to accomplish such a goal.

Eleven experiments were needed to obtain the following single polynomial expression used to fit experimental data:

$$Y = -6.24 + 2.61(Fe^{2+}) - 0.00818(H_2O_2) - 0.118(Fe^{2+})^2 + 0.00981(Fe^{2+})(H_2O_2). \quad (2)$$

This expression shows the response factor (Y) corresponding to the percentage of herbicide mineralization (i.e., TOC removal) after 1 h of treatment time in a defined range of Fe(II) and H_2O_2 concentration values (95% confidence level). The different doses used to built the multivariate experimental design were 2, 11 and 20 mg L^{-1} for Fe(II) and 10, 130 and 250 mg L^{-1} for hydrogen peroxide. Fig. 2 shows the 3D response surface obtained from Eq. (2).

The TOC removal was mainly influenced by Fe(II) concentration, as seen by the high coefficient of this factor in Eq. (2). Nevertheless, an excess of ferrous ions in the system produced a decrease in mineralization yield. The negative coefficient of the parameter $(Fe)^2$ in the polynomial expression accounts for this effect. The possible formation of futile intermediate iron (IV) species (ferryl iron FeO^{2+}) could be the cause of this negative behaviour, producing a possible side reaction that interferes with the formation of hydroxyl radicals that are critical for the oxidation of organic matter (Eqs. (3)–(5)) (Chan and Chu, 2003)

$$H_2O_2 + Fe(II) \rightarrow FeO^{2+} + H_2O, \quad (3)$$

$$FeO^{2+} + Fe(II) + H^+ \rightarrow Fe(OH)^{2+} + Fe(III), \quad (4)$$

$$Fe(OH)^{2+} + H^+ \rightarrow Fe(III) + H_2O. \quad (5)$$

The formation of such a ferryl iron intermediate in iron-peroxide systems was firstly proposed by Bay and Groin (1932).

As seen in Fig. 2 different reactant dose combinations were considered, each one corresponding to the minimum quantities of Fe(II) and hydrogen peroxide needed to achieve a desired mineralization percentage. The selected doses were A: [Fe(II)] = 9.25 mg L^{-1}, [H_2O_2] = 97.1 mg L^{-1} (16% TOC removal); B: [Fe(II)] = 13.3 mg L^{-1}, [H_2O_2] = 143 mg L^{-1} (25%TOC removal); C: [Fe(II)] = 15.9 mg L^{-1}, [H_2O_2] = 202 mg L^{-1} (36% TOC removal); and D: [Fe(II)] = 20.0 mg L^{-1}, [H_2O_2] = 250 mg L^{-1} (46% TOC removal). The percentage of TOC removal was obtained from Eq. (2).

Fig. 3 shows the TOC evolution (i.e., mineralization process) when A, B, C and D reagent combinations, obtained from the experimental design, were used. The hydrogen peroxide concentration remaining in solution and the AOS evolution are also shown in Fig. 4. AOS was estimated according to the following equation (Scott and Ollis, 1995):

$$AOS = 4(DOC - COD)/DOC, \quad (6)$$

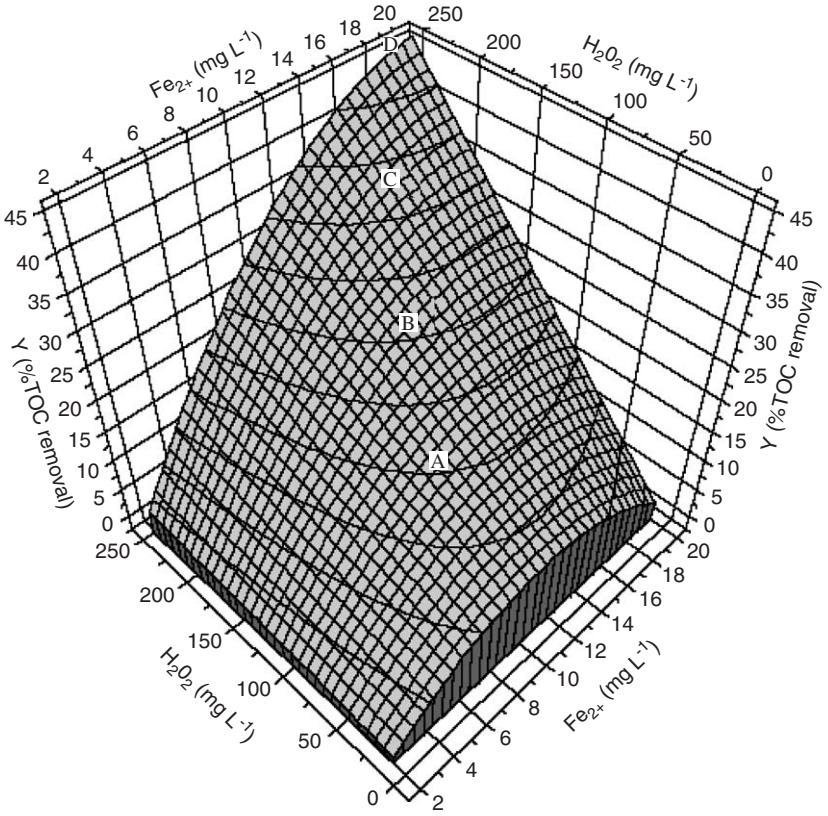

Fig. 2 – The mineralization percentage (Y) surface of a Linuron and Diuron solution (50 mg L^{-1} TOC) as a function of the reactant dose after 1 h of reaction with a 6 W black light lamp, pH = 2.8 and $T = 25\,^{\circ}C$.

where DOC and COD are expressed in moles of C L^{-1} and moles of O_2 L^{-1}, respectively. The TOC removal data were collected during 150 min experiments. The AOS and H_2O_2 evolution data were collected during 90 min experiments.

Although the reactant dose D was much higher than the reactant dose B, similar results were obtained when comparing the experimental TOC removal and the AOS data ($\cong$2) after photo-Fenton treatment (see Figs. 3 and 4). Since the hydroxyl radical, the main reactive species, gives a non-selective attack, and taking into account that when the constant TOC in solution was achieved (after 60 min. for dose C and 30 min. for dose D) there was still H_2O_2 (hydroxyl radical precursor), it seemed appropriate to assume that, in both cases, the same by-products were obtained. It is well known that in the case of aromatic contaminants, OH radical attack gives rise to the hydroxylation of the benzene ring, followed by ring opening and the formation of carboxylic acids at the final steps of the degradation process. In fact, under some experimental conditions, these carboxylic acids become responsible of the residual TOC remaining in solution at long reaction times (Franch et al., 2002).

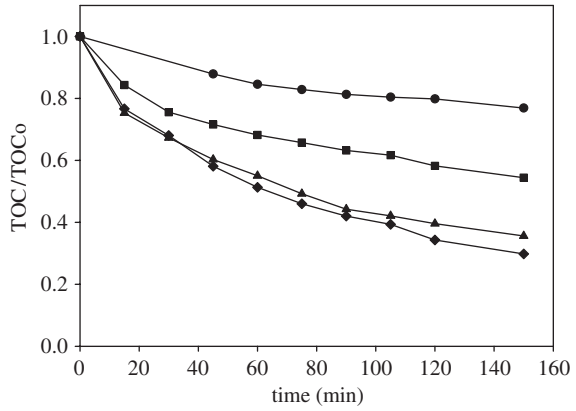

Fig. 3 – The TOC removal versus irradiation time during the photo-Fenton pre-treatment of water containing Diuron and Linuron (50 mg TOC L^{-1}) using optimized reagent doses; (A) (●): [Fe(II)] = 9.25 mg L^{-1}, [H_2O_2] = 97.1 mg L^{-1}; (B) (■): [Fe(II)] = 13.3 mg L^{-1}, [H_2O_2] = 143 mg L^{-1}; (C) (▲): [Fe(II)] = 15.9 mg L^{-1}, [H_2O_2] = 202 mg L^{-1}; (D) (♦): [Fe(II)] = 20.0 mg L^{-1}, [H_2O_2] = 250 mg L^{-1}. pH = 2.8 and T = 25 °C.

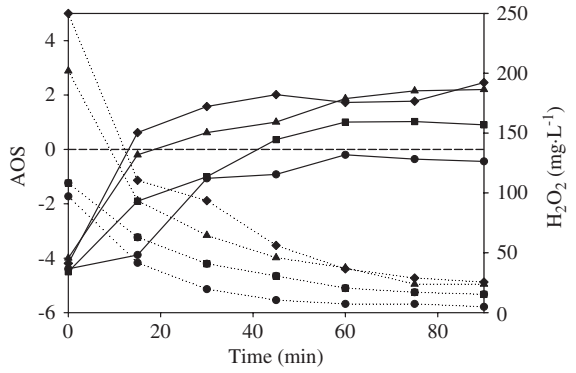

Fig. 4 – The AOS (line) evolution and hydrogen peroxide concentration remaining in solution (dotted) versus irradiation time during the photo-Fenton pre-treatment of water containing Diuron and Linuron (50 mg TOC L^{-1}) using optimized reagent doses; (A) (●): [Fe(II)] = 9.25 mg L^{-1}, [H_2O_2] = 97.1 mg L^{-1}; (B) (■): [Fe(II)] = 13.3 mg L^{-1}, [H_2O_2] = 143 mg L^{-1}; (C) (▲): [Fe(II)] = 15.9 mg L^{-1}, [H_2O_2] = 202 mg L^{-1}; (D) (♦): [Fe(II)] = 20.0 mg L^{-1}, [H_2O_2] = 250 mg L^{-1}. pH = 2.8 and T = 25 °C.

Concerning effluents treated with reactant doses A and B, important differences on the TOC removal and the AOS recorded data during pre-treatment were observed. They were also noticeably different than the values obtained for effluents treated with reactant doses C and D (see Figs. 3 and 4). It is important to remark that in experiments A and B, different AOS limiting values were achieved when low residual hydrogen peroxide was present in solution. At this point, it was reasonable to think that AOS values would increase until 2 if more hydrogen peroxide would be added to the solutions. AOS$\cong$2 was the higher value attained among the four experiments and is characteristic of rather oxidized and biocompatible aliphatic compounds like oxalic acid (Sarria et al., 2002).

The acute toxicity of the four different pre-treated effluents after 1 h of photo-Fenton reaction (the time applied to the chemical part of the chemical–biological coupled system) was estimated. The data obtained was: EC_{50}^{15}(A) = 15.1$\pm$1.1, EC_{50}^{15}(B) = 26.5$\pm$1.5 and EC_{50}^{15}(C, D) > 100%). Since the initial EC_{50}^{15} value for Diuron and Linuron solution is 5.6$\pm$1.2, a steady toxicity reduction was observed when reactant dose increased. Effluents treated with reactant doses C and D were considered non-toxic since EC_{50}^{15} values exceed TOC of the original samples (indicated as EC_{50}^{15} > 100%) (Garcia-Montaño et al., 2006).

The biodegradability of the treated effluents after 1 h of photo-Fenton reaction was also tested by incubating the pre-treated effluent over a 5-days period (see Fig. 5). BOD_5/COD ratio is the most used parameter to quantify the biodegradability of a contaminated effluent. The threshold value of such ratio for a wastewater to be considered easily biodegradable is 0.4 while a value between 0.2 and 0.4 corresponds to a partially biodegradable wastewater (Sarria et al., 2002).

Complete TOC removal of the phototreated effluents could be achieved by means of secondary biological treatment when doses C and D were used because BOD_5/COD ratios exceeded the threshold value 0.4. Phototreated effluents obtained using reactant doses A and B might need further oxidation before being biologically compatible. In an attempt to gain more knowledge about the biodegradability of the pre-treated solutions, they were fed an SBR to simulate a real biological treatment. Only pre-treated A, B and C samples were tested. Sample D was discarded assuming its similarity to sample C. The SBR start-up was done by feeding the reactor with municipal wastewater coming from a real wastewater treatment plant, lasting 2 weeks for each experiment, until constant TOC and VSS values were obtained. New and fresh biomass was used for each experiment. After the start-up process, the SBR was fed with the tested samples A, B or C

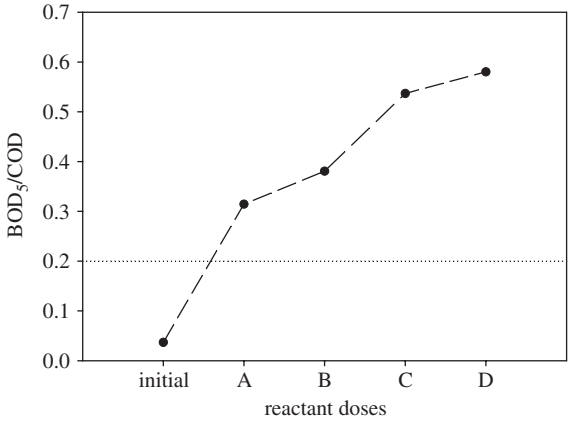

Fig. 5 – The BOD_5/COD ratio after photo-Fenton pre-treatment using the optimized reagent doses obtained from experimental design. (A): [Fe(II)] = 9.25 mg L^{-1}, [H_2O_2] = 97.1 mg L^{-1}; (B): [Fe(II)] = 13.3 mg L^{-1}, [H_2O_2] = 143 mg L^{-1}; (C): [Fe(II)] = 15.9 mg L^{-1}, [H_2O_2] = 202 mg L^{-1}; (D): [Fe(II)] = 20.0 mg L^{-1}, [H_2O_2] = 250 mg L^{-1}. Phototreatment time = 1 h, pH = 2.8 and T = 25 °C.

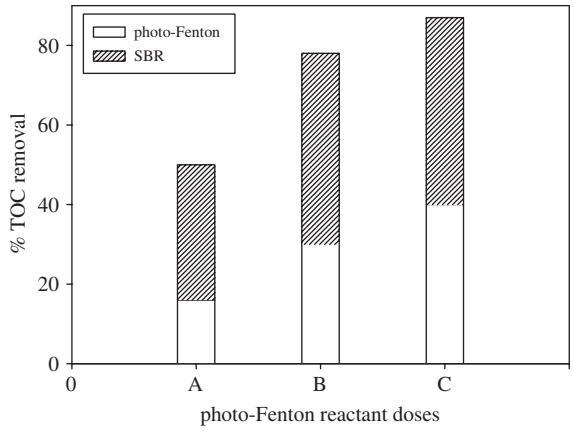

Fig. 6 – Total TOC removal of polluted effluents using optimized photo-Fenton reagent doses in the chemical and biological coupled system. (A): [Fe(II)] = 9.25 mg L^{-1}, [H_2O_2] = 97.1 mg L^{-1}; (B): [Fe(II)] = 13.3 mg L^{-1}, [H_2O_2] = 143 mg L^{-1}; (C): [Fe(II)] = 15.9 mg L^{-1}, [H_2O_2] = 202 mg L^{-1}. HRT = 2 days, T = 20 °C.

and it was continuously working during 12 cycles to allow repetitive results (i.e., a TOC variation coefficient lower than 4%) and stabilization of biomass (constant VSS value). When the SBR was fed with effluent treated with dose A, it was not possible to achieve a constant VSS value. In this case a 30% reduction of VSS was observed, possibly due to the toxic nature of the metabolites formed during photo-Fenton process (low EC_{50}^{15}).

Fig. 6 summarizes the results obtained for samples A, B and C after the complete chemical–biological treatment. Photo-Fenton pre-treatment using reactant dose A achieved a 16% of TOC removal after 1 h of reaction time. Biological treatment applied to this pre-treated effluent allowed a 50% of total TOC removal. This meant that there were still non-biodegradable species in solution after the chemical pre-treatment.

A GC–MS analysis was carried out in order to elucidate those by-products that could be formed during Diuron and Linuron phototreatment. The analysis was done for the sample treated with dose C and after 15 min of photo-Fenton process.

3,4-dichloroaniline and 3,4-dichlorophenyl isocyanate were identified by the mass of the molecular and fragment ions and also through comparison with the Wiley library data with similarities up to 86%. Katsumata et al. (2005) observed 3,4-dichlorophenyl isocyanate in the degradation pathway of Linuron. Moreover, 3,4-dichloroaniline and 3,4-dichlorophenyl isocyanate were also proposed as the main degradation intermediates by Salvestrini et al. (2002) in Diuron kinetic studies.

HPLC analyses showed that the initial herbicides had disappeared before 40 min when using reactant dose A (see Fig. 7). This guarantee that the initial herbicides had been eliminated from aqueous solution in less than 1 h (the time used for the chemical pre-treatment). Moreover, no

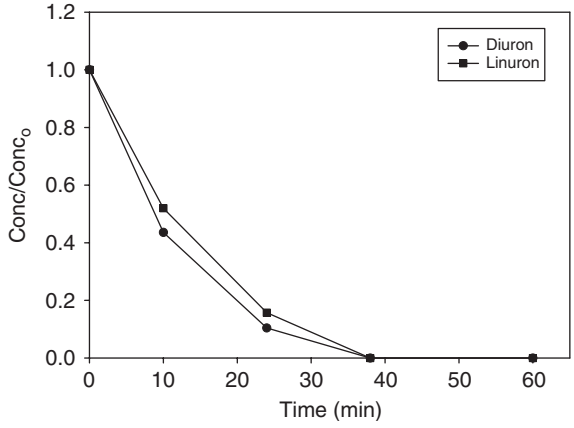

Fig. 7 – The time course of both herbicides (42 mg L^{-1} Diuron and 75 mg L^{-1} Linuron) using [Fe(II)] = 9.25 mg L^{-1} and [H_2O_2] = 97.1 mg L^{-1}, pH = 2.8 and T = 25 °C.

presence of the parent compounds was noticed in the GS–MS analysis.

A 30% of TOC reduction was obtained in the chemical step when wastewater was treated with dose B while 78% of the TOC was removed when using the coupled photo-Fenton and biological system (see Fig. 6). Concerning TOC evolution for reactant dose C, a total TOC removal was observed after the coupled chemical–biological system (i.e., 87% of TOC removal). The remaining 13.6% (6.5 mg L^{-1} TOC) matched the concentration of the residual TOC due to biomass metabolism. A 40% of TOC removal was achieved in the chemical step while biological process degraded 78% (see Fig. 6). Fig. 8 shows the constant TOC remaining in solution as well as the constant TOC removal in the biological treatment using reactant dose C when this coupled system was carried out during 12 cycles.

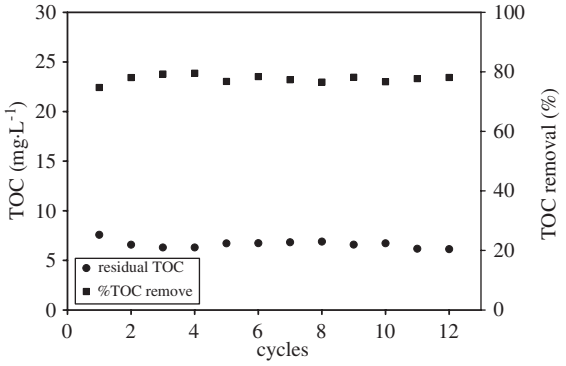

Fig. 8 – Final TOC and percentage of TOC removal after SBR treatment of pre-treated effluent with reagent dose C ($[Fe(II)] = 15.9\,mg\,L^{-1}$, $[H_2O_2] = 202\,mg\,L^{-1}$) during 12 cycles. HRT = 2 days, $T = 20\,^{\circ}C$.

4. Conclusions

A combined photo-Fenton and biological treatment has been evaluated for the treatment of water containing Diuron and Linuron herbicides. Multivariate experimental design has been applied to optimize Fenton reactant doses. The conclusions derived from this study are

- The excess in reactant doses, specially Fe(II), slow down mineralization rate during the photo-Fenton process. This fact could be due to the side reactions derived from oxidized forms of reactant species. Focusing on this fact, it has been demonstrated that there is an optimum reagent dose combination to reach a determined mineralization degree.
- With these optimized reagent doses, initial herbicides disappear from wastewater under mild conditions, and more biodegradable by-products are formed, and could be successfully degraded by means of a biological treatment. 3,4-dichloroaniline and 3,4-dichlorophenyl isocyanate have been identified as intermediates in the degradation pathway.
- The combined photo-Fenton and biological process can completely remove Diuron and Linuron herbicides from water when this is treated with $[Fe(II)] = 15.9\,mg\,L^{-1}$ and $[H_2O_2] = 202\,mg\,L^{-1}$ during 1 h of UVA irradiation. After this, complete TOC removal has been achieved in an aerobic SBR.

Acknowledgements

This work was supported by MEC (project CTQ2005-02808) and European Commission (CADOX project, EVK1-CT-2002-00122). We thank Makhteshim Agan España, S.A. for providing the Linuron herbicide.

REFERENCES

Adams, C.D., Scanlan, P.A., Secrist, N.D., 1994. Oxidation and biodegradability enhancement of 1,4-dioxane using hydrogen peroxide and ozone. Environ. Sci. Technol. 28, 1812–1818.

Al Momani, F., Gonzalez, O., Sans, C., Esplugas, S., 2004. Combining photo-Fenton process with biological sequencing batch reactor for 2,4-dichlorophenol degradation. Water Sci. Technol. 49 (4), 293–298.

APHA-AWWA-WPCF, 1989. Standard Methods for the Examination of Water and Wastewater, ASTM D1252-00, 17th ed. Washington, DC.

Bauer, R., Fallmann, H., 1997. The photo-Fenton oxidation—a cheap and efficient wastewater treatment method. Res. Chem. Intermed. 23, 341–354.

Box, G.E.P., Hunter, W.G., Hunter, J.S., 1978. Statistics for Experimenters: and Introduction to Design, Data Analysis and Model Building. Wiley, New York.

Bay, W.C., Groin, M.H., 1932. Ferryl ion, a compound of tetravalent iron. J. Am. Chem. Soc. 54, 2124.

Chamarro, E., Marco, A., Espulgas, S., 2000. Use of Fenton reagent to improve organic chemical biodegradability. Water Res. 35 (4), 1047–1051.

Chan, K.H., Chu, W., 2003. The dose and ratio effects of Fe(II) and H_2O_2 in Fenton's process on the removal of atrazine. Environ. Technol. 24, 703–710.

Chiron, S., Fernández-Alba, A., Rodríguez, A., García-Calvo, E., 2000. Pesticide chemical oxidation: state-of-the-art. Water Res. 34 (2), 366–377.

Faust, B.C., Hoigné, J., 1990. Photolysis of iron (III)-hydroxyl complexes as sources of hydroxyl radicals in clouds, fog and rain. Atmos. Environ. 24, 78–89.

Franch, M.I., Ayllón, J.A., Peral, J., Domènech, X., 2002. Fe(III) photocatalyzed degradation of low chain carboxylic acids. Appl. Catal. B: Environ. 50 (2), 89–99.

Garcia-Montaño, J., Torrades, F., García-Hortal, J.A., Doménech, X., Peral, J., 2006. Degradation of Porcion Red H-E7B reactive dye by coupling a photo-Fenton system with a Sequencing batch reactor. J. Hazard. Mater. B 134 (2006) 220–229.

Glaze, W.H., 1987. Drinking water treatment with ozone. Environ. Sci. Technol. 21, 224–230.

Irvine, R.L., Ketchum Jr., L.H., 1989. Sequencing batch reactors for biological wastewater treatment. CRC Crit. Rev. Environ. Control 18, 255–294.

Jeffery, G.H., Basset, J., Mendham, J., Denny, R.C., 1989. Vogel's Textbook of Quantitative Chemical Analysis, fifth ed. Longman, New York (pp. 368–395).

Kang, Y.W., Cho, M.J., Hwang, K.Y., 1999. Correction of hydrogen peroxide interference on standard chemical oxygen demand test. Water Res. 33 (5), 1247–1251.

Katsumata, H., Kaneco, S., Suzuky, T., Ohta, K., Yobico, Y., 2005. Degradation of Linuron in aqueous solution by the photo-Fenton reaction. Chem. Eng. J. 108, 269–276.

Kotsou, M., Kyriacou, A., Lasaridi, K., Pilidis, G., 2004. Integrated aerobic biological treatment and chemical oxidation with Fenton's reagent for the processing of green table olive wastewater. Process Biochem. 39, 1653–1660.

Mills, A., Le Hunte, S., 1997. An overview of semiconductor photocatalysis. J. Photochem. Photobiol. 108, 1–35.

OECD Guidelines for Testing of Chemicals, vol. 2. Test 302B, 1996.

Pimentel, D., 1996. Green revolution agriculture and chemical hazards. Sci. Tot. Environ. 188 (1), S86–S98.

Salvestrini, S., Di Cerbo, P., Capasso, S., 2002. Kinetics of the chemical degradation of Diuron. Chemosphere 78, 69–73.

Sarria, V., Parra, S., Nevenka, A., Péringer, P., Benitez, N., Pulgarin, C., 2002. Recent developements in the coupling of photo-assisted and aerobic biological processes for the treatment of biorecalcitrant compounds. Catal. Today 76, 301–315.

Scott, J.P., Ollis, D.F., 1995. Environmental progress integration of chemical and biological oxidation processes for wastewater treatment: review and recommendations. Environ. Progress 14 (2), 88–101.

Tixier, C., Bogaerts, P., Sancelme, M., Bonnemoy, F., Twagilimana, L., Cuer, A., Bohatier, J., Veschambre, H., 2000. Fungal biodegradation of phenylurea herbicide, Diuron: structure and toxicity of metabolites. Pest Manage. Sci. 56, 455–462.

USEPA, 1999. Wastewater technology fact sheet sequencing batch reactors. EPA/832-F-99-073.

Wilderer, P.A., Irvine, R.L., Gorzonsky, M.C. (Eds.), 1999. Sequencing Batch Reactor Technology. International Water Association, London.

Available online at www.sciencedirect.com
ScienceDirect
Journal of Hazardous Materials xxx (2007) xxx–xxx
Journal of Hazardous Materials
www.elsevier.com/locate/jhazmat

Combined photo-Fenton and biological treatment for Diuron and Linuron removal from water containing humic acid

María José Farré, Xavier Doménech, José Peral *

Departament de Química, Universitat Autónoma de Barcelona, 08193 Bellaterra, Spain

Received 18 September 2006; received in revised form 20 December 2006; accepted 22 December 2006

Abstract

A combined chemical (photo-Fenton) and biological treatment has been proposed for Diuron and Linuron degradation in water containing natural dissolved organic matter (DOM). Humic acid (HA) was used to simulate the DOM. During the photo-Fenton process ($[Fe(II)] = 15.9\,mg\,L^{-1}$, $[H_2O_2] = 202\,mg\,L^{-1}$, 60 min of UVA irradiation time), the chemical oxygen demand (COD), total organic carbon (TOC), toxicity (EC_{50}^{15}) and biodegradability (BOD_5/COD) of the generated intermediates were assessed. A reduction of photo-Fenton efficiency was observed when HA was present in solution. This effect has been explained as the result of a UVA light screening as well as a $OH^{\bullet}$ radical quenching process by the HA. After the photo-Fenton process, the initial toxic and non-biodegradable herbicides were transformed into intermediates suitable for a subsequent aerobic biological treatment that was performed in a sequencing batch reactor (SBR). Complete elimination of the intermediates in presence of HA was reached at the end of the chemical–biological coupled system. Biosorption of HA onto the aerobic biomass was characterized. The results indicate that the Freundlich model adequately describes the adsorption of HA, a phenomena that follows a pseudo second-order adsorption kinetic model.

Keywords: Biosorption; Herbicides; Humic acid; Photo-Fenton; Sequencing batch reactor

1. Introduction

Water shortage is an important environmental problem that could be ameliorated by using regenerated wastewaters [1,2]. Those are waters that after use are treated and disinfected for subsequent re-use. For example, water polluted with herbicides after agricultural practices would be a good candidate for wastewater regeneration.

Herbicides pollution is of main concern for the environment and public health due to the general toxic and non-biodegradable nature of the pollutants [3]. Among the herbicides used to prevent the growth of undesirable plants, phenylurea compounds have been widely employed since their discovery in 1950. Diuron and Linuron are two phenylurea herbicides that prevent weed growth by inhibiting the photosynthesis.

Traditional chemical methods for wastewater regeneration are, for instance, coagulation, precipitation [4] or adsorption [5]. The phase transference of pollutants, instead of their elimination, is the main disadvantage associated to those techniques. They require a post-treatment to remove the pollutant from the newly contaminated environment.

In the last decades, advanced oxidation processes (AOP) have been proposed as suitable degradation techniques for pesticide removal, since they are effective for degradation of water and soil soluble organic contaminants [6]. AOPs are based on the production of highly reactive hydroxyl radical ($OH^{\bullet}$) under mild experimental conditions. This radical oxidizes organic matter ($E_{red} = 2.8$ versus NHE) producing CO_2 as the final product.

Among all the AOP described, photo-Fenton is frequently preferred to others like ozonation [7] or heterogeneous photocatalysis with TiO_2 [8]. This AOP achieves high reaction yields with low treatment costs, mainly due to the possibility of using solar light as photon source [9]. In the Fenton process hydroxyl radical promoters are Fe(II) and hydrogen peroxide [10] (reaction (1), Fenton process):

$$Fe(II) + H_2O_2 \rightarrow Fe(III) + OH^- + OH^{\bullet} \quad (1)$$

* Corresponding author. Tel.: +34 93 581 2772; fax: +34 93 581 2920.
E-mail address: jose.peral@uab.es (J. Peral).

0304-3894/$ – see front matter © 2007 Elsevier B.V. All rights reserved.
doi:10.1016/j.jhazmat.2006.12.063

Nomenclature

AOP	advanced oxidation process
b	energy of Lagmuir sorption constant (L mg^{-1})
BOD_5	biochemical oxygen demand (mg L^{-1})
C_e	equilibrium TOC (HA) concentration (mg L^{-1})
COD	chemical oxygen demand (mg L^{-1})
DO	dissolved oxygen (mg L^{-1})
DOM	dissolved organic matter
EC_{50}^{15}	effective toxic concentration that causes a 50% bacteria reduction during 15 min contact (mg L^{-1})
HA	humic acid
HPLC	high-pressure liquid chromatography
HRT	hydraulic retention time
k_1	rate constant of first-order sorption (min^{-1})
k_2	rate constant of second-order sorption (g mg^{-1} min^{-1})
K_F	Freundlich adsorption capacity (mg g^{-1})
n	Freundlich intensity constant
q_e	equilibrium sorption capacity (mg TOC/g TSS)
Q^0	maximum adsorption capacity Lagmuir constant (mg g^{-1})
TOC	total organic carbon (mg L^{-1})
TSS	total suspended solids (mg L^{-1})
SBR	sequencing batch reactor
VSS	volatile suspended solids (mg L^{-1})

Under irradiation of $\lambda < 410$ nm, Fe(III) can be reduced to Fe(II) closing a loop mechanism where Fe species act as catalyst, producing additional OH$^\bullet$ [11] (reaction (2), photo-Fenton process):

$$\text{Fe(III)} + \text{OH}^- + h\nu \rightarrow \text{Fe(II)} + \text{OH}^\bullet \quad (2)$$

The main advantage associated with this AOP is not only the possibility of using solar light as the photon source, but also the environmental compatibility of reactants. At the end of photo-Fenton process any remaining hydrogen peroxide decomposes to H_2O. On the other hand, Fe(II) can be eliminated by raising the pH of the solution if its concentration exceeds the legal environmental disposal level.

Recently, the coupling of an AOP and a biological treatment has been proposed as a new approach to regenerate polluted effluents [12–15]. The objective of this strategy is the use of an AOP to convert initial toxic and non-biodegradable compounds into by-products that can be assimilated by the biomass. Accordingly, the economic cost and environmental impact, that are often associated with the chemical process, are substantially minimized.

A sequencing batch reactor (SBR), based on the biodegradation activity of an aerobic bacteria consortium, is used in this study after chemical treatment to completely remove organic matter. This biological treatment configuration has become popular for its efficiency and flexibility [16]. Also, it is considered suitable as a biological system "model" due to the small volumes of effluent to be treated in a laboratory study, as well as the good control it offers. The conventional SBR operation is based on the principle of four sequential steps – i.e., fill, react, settle and draw – all them being operated in a single reactor [17,18].

Many efforts have been made by different research groups to eliminate phenylureas from synthetic wastewaters [19–22]. As real effluents also contain natural dissolved organic matter (DOM), it is important to study the degradation of those herbicides in the presence of humic substances. Humic substances generally constitute 30–50% of the dissolved organic carbon (DOC) of natural DOM in surface waters [23]. Zepp et al. [24] suggest that the phenolic humic substances, which are present in most inland waters, inhibit the free radical chain reaction that takes place in all AOPs. In addition of being a radical scavenger, humic acid (HA) may also trap photons during the photolysis process [25].

Previous studies have shown the optimal properties of chemical–biological coupled systems for the removal of Diuron and Linuron from water without interferences [22].

In this work, we study the Diuron and Linuron removal from water in the presence of HA. With this aim, COD, TOC, herbicide concentration, EC_{50}^{15} and BOD_5/COD of the intermediates generated at the end of the chemical step have been measured. Moreover, a SBR has been used to evaluate the feasibility of the coupled chemical–biological treatment for water containing those herbicides in the presence of high concentrations of HA.

Since adsorption of HA onto the biomass was observed, characterization of this process has been also required.

2. Experimental

2.1. Preparation of initial wastewater

Diuron (98.5% Aragonesas Agro S.A. technical grade), Linuron (92.6% Makhteshim Agan España, S.A.) and HA (Aldrich Co.) were used as target compounds in the experiments (see Fig. 1 for herbicides chemical structures). A unique solution of 42 mg L^{-1} of Diuron and 75 mg L^{-1} of Linuron in Millipore Milli-Q purified water was prepared. These values correspond to the maximum solubility of both herbicides in water at 25 °C. A saturated initial solution was prepared and then filtrated by means of a 20 μm nylon filter (solution A). The initial features of the filtered solution A were as follows; pH 5.7, TOC = 50 ± 2 mg L^{-1}, COD = 139 ± 7 mg L^{-1}, $BOD_5 < 5$ (detection limit). The initial solution was transparent and colorless. The solution was non-biodegradable and TOC abatement,

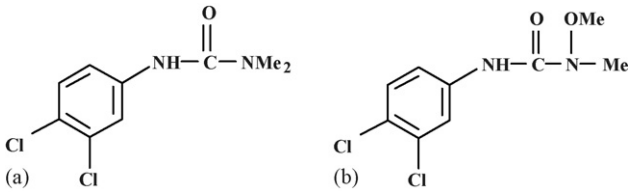

Fig. 1. Diuron (a) and Linuron (b) molecular structures.

Please cite this article in press as: M.J. Farré et al., Combined photo-Fenton and biological treatment for Diuron and Linuron removal from water containing humic acid, J. Hazard. Mater. (2007), doi:10.1016/j.jhazmat.2006.12.063

due adsorption onto the biomass, was not observed after 28 days of Zahn–Wellens test [26].

A mixed herbicide–HA solution (solution B) was prepared by continuously stirring solid HA in the solution A. The initial features of solution B were as follows: 200 mg L^{-1} of HA, pH 8.3, TOC = 123 ± 6 mg L^{-1}, COD = 342 ± 10 mg L^{-1}, BOD_5 < 5 (detection limit). This solution was brown in color.

Finally, a HA solution (200 mg L^{-1}) was prepared as control sample (solution C). The initial features of solution C were as follow: pH 8.3, TOC = 73 ± 7 mg L^{-1}, COD = 203 ± 10 mg L^{-1}, BOD_5 < 5 (detection limit). TOC abatement due to HA adsorption onto the biomass was observed and characterized.

2.2. Experimental procedure

2.2.1. Humic acid adsorption studies

The activated sludge was directly obtained from the aerobic stage of a full-scale urban wastewater treatment plant (WWTP) in Manresa (Spain). Initial total suspended solids (TSS) value was around 3300 mg L^{-1}. A dilution was carried out to obtain a TSS value of 1000 mg L^{-1} in the final 1 L solution. The adsorption of HA by the living activated sludge was studied as a function of contact time. The adsorption kinetics were calculated by adding 200 mg L^{-1} of HA to the 1 L biological reactor (1000 mg L^{-1} TSS concentration). The reactor was agitated at a constant temperature (20 °C). Samples were periodically collected from the reactor and the sludge was removed by centrifugation. In order to obtain the adsorption kinetic constant value, TOC in solution was measured during 400 min.

Isotherm adsorption experiments were conducted using 250 mL vessels that contained 10 mL of activated sludge (3300 mg L^{-1} TSS) and 90 mL of HA solutions of different concentration (from 100 to 1000 mg L^{-1}). pH was adjusted to 7. The vessels content was stirred at room temperature during 24 h (20 °C). After that, TOC was measured.

In both experiments TOC measurements were also done in a blank run without HA (the same amount of biomass) in order to correct the final TOC values of each sample for desorbed organic matter. The final dissolved HA concentration (TOC) was calculated by subtracting the blank sample TOC values from the HA samples TOC values.

2.2.2. Photo-Fenton experimental procedure

$FeSO_4 \cdot 7H_2O$ (Merck) and H_2O_2 (Panreac, 33%, w/v) were used in the photo-Fenton experiments. Experiments were conducted at 25 ± 0.2 °C in a cylindrical Pyrex thermostatic cell of 0.275 L capacity provided with a magnetic stirrer. A 6 W Philips black light was used as photon source. The intensity of the light entering the photo-reactor, measured by actinometry, was 0.21 mW cm^{-2}.The photo-Fenton reactor was protected from any external light with a dark cover. The photo-treatment time selected was 60 min. pH was adjusted to 2.8 in all solutions before starting the photo-Fenton reaction [27]. Samples were periodically taken from solution with a syringe. TOC, COD and hydrogen peroxide evolution were measured. At the end of the photo-treatment BOD_5/COD and toxicity were assessed.

2.2.3. Aerobic sequencing batch reactor experimental procedure

Three identical sequencing batch reactors of 1.5 L (SBR 1, SBR 2 and SBR 3) were used to simulate the activated sludge process. A dilution of biomass from the urban wastewater treatment plant was carried out to obtain a TSS value of 1000 mg L^{-1} in the final sequencing batch reactor.

SBR 1 was fed with Diuron–Linuron photo-treated solution (A). SBR 2 was fed with Diuron–Linuron and HA (200 mg L^{-1}) photo-treated solution (B). Finally, SBR 3 worked as a control and was fed with a HA (200 mg L^{-1}) solution (C). Prior to feed the SBR, hydrogen peroxide was removed from the photo-treated solutions by adding an excess of sodium sulphite. Aeration was then used to convert the remaining sulphite into sulphate [28]. When direct fed was not possible (several 250 mL chemical reaction batches were needed to fill the 1.5 L biological reactor) storage at around −8 °C was required.

The procedure followed every day was: after the aeration–reaction period (22.5 h), agitation was stopped to let the biomass to settle down. After 1 h, the volume to be changed according to the hydraulic retention time (HRT) was decanted from the supernatant and replaced by the corresponding photo-treated solution (pH 7 previously adjusted). The HRT of the SBR experiments, that measures the average time that the effluent remains in the bioreactor, was two days. Thus, the volume of solution replaced after each batch was:

$$V_{\text{replaced}} = \frac{V_{\text{SBR}}}{\text{HRT}} \quad (3)$$

Minerals were also daily added to reach a constant nutrient concentration in the SBR: $MgSO_4$ (202 mg L^{-1}), $CaCl_2$ (73.4 mg L^{-1}), NH_4Cl (76.4 mg L^{-1}) and NaH_2PO_4 (1242 mg L^{-1}).

TOC measurement of the replaced solution was carried out. This process was repeated 16 cycles in each run in order to obtain repetitive results (i.e., a variation coefficient of TOC measurements lower than 4%). One cycle was achieved when the total SBR initial volume had been replaced with new solution. Volatile and total suspended solids (VSS and TSS) were measured daily.

The pH around 7 and dissolved oxygen (DO) – not lower than 3 mg L^{-1} – were daily controlled. The reactor was maintained at laboratory temperature (20 °C) and mixed by a magnetic stirrer. Air was supplied by a gas diffuser.

2.3. Analytical methods

The initial herbicide concentration, TOC and COD data were recorded during the oxidation process. The HPLC system, used in the determination of herbicides concentration, was formed by a LC-10 AT VP pump (Shimadzu) and a UV–vis diode array detector (Agilent 1100 Series). Acetonitrile (Pobus, HPLC grade) was used to prepare the mobile phases in the HPLC system and a 5 μm Hypersil column (250 mm × 0.46 mm) from Teknocroma was used as stationary phase. TOC was analyzed with a Shimadzu TOC-V_{CSH} apparatus. 0–150 and 0–1500 mg L^{-1} range Aqualytic vials were used for chemical COD determination based on a close reflux

Please cite this article in press as: M.J. Farré et al., Combined photo-Fenton and biological treatment for Diuron and Linuron removal from water containing humic acid, J. Hazard. Mater. (2007), doi:10.1016/j.jhazmat.2006.12.063

determination method [29]. This analysis was done in a COD reactor from HACH Co., and a HACH DR/2000 spectrophotometer was used for colorimetric measurement. The accuracy of the COD measurements was checked by preparing a potassium hydrogen phthalate standard. Correction for hydrogen peroxide interference on the standard COD test was carried out [30]. The concentration of H_2O_2 was analyzed by the iodometric method [31].

At the end of the oxidation process, toxicity (EC_{50}^{15}) and biodegradability (BOD_5/COD) were analyzed. The toxicity tests were performed with the BioTox® equipment (Lab-system) using the *Vibrio fischery* bacteria to asses the effective concentration of a test sample that caused a 50% reduction in bacteria light emission during 15 min of bacteria-toxic contact (EC_{50}^{15}). A WTW OxyTop system was used for BOD_5 determinations. In those analyses, the data accuracy was checked by making BOD_5 measurements of a mixture of 150 mg L^{-1} of glucose and 150 mg L^{-1} of glutamic acid. In all the biological analysis hydrogen peroxide and iron were previously eliminated from solution to avoid interferences. Iron was eliminated by raising the pH to 8 and then filtering the solution. Hydrogen peroxide was eliminated by adding sodium sulphite.

When the SBR was used, VSS and TSS were determined according to Standard Methods [32]. All analytical measurements were repeated at least two times.

3. Results and discussion

3.1. Kinetic experiments of humic acid biosorption

In this paper Diuron and Linuron removal from water in the presence of HA by means of a coupled chemical and biological system is examined. Adsorption of HA onto de biomass was observed and its characterization was required.

Lagergren suggested a rate equation for the solutes adsorption onto a solid surface [33]. This pseudo-first-order rate linearized equation is

$$\log(q_e - q_t) = \log q_e - \frac{k_1 t}{2.303} \quad (4)$$

where k_1 is the rate constant of the pseudo-first-order sorption. The pseudo-first-order equation has been extensively used to describe the sorption kinetics [34,35]. Nevertheless, not complete regression adjustment was obtained when this model was used to fit biosorption of HA onto the biomass (i.e., $R^2 = 0.958$, $k_1 = 33 \times 10^{-4}$ min^{-1}).

Thus, a pseudo-second-order model was used to analyze the data. The resulting linearized rate law for this system was

$$\frac{1}{q_t} = \frac{1}{k_2 q_e^2} + \frac{1}{q_e} t \quad (5)$$

where k_2 is the rate constant of the pseudo-second-order sorption. This model has been applied to analyze sorption kinetics in liquid–solid interfaces by Ho et al. [36,37]. Comparing both pseudo-first and pseudo-second-order models, a closer to 1.0 correlation coefficient is observed for the pseudo-second-order model (i.e., $R^2 = 0.999$). Thus, this model is better to describe the biosorption kinetics of HA (see Fig. 2) and, consequently, a pseudo-second-order rate constant of HA adsorption onto the biomass has been determined (31×10^{-4} g mg^{-1} min^{-1}).

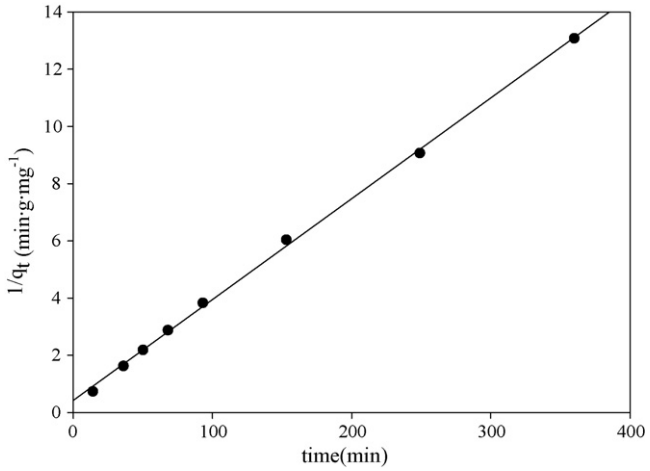

Fig. 2. Linearized pseudo-second-order kinetic model for the adsorption of humic acid onto alive aerobic biomass (initial humic acid concentration of 200 mg L^{-1}). $T = 20\,^{\circ}C$, pH 7, VSS = 1.05 g L^{-1}.

Azizian [38] concludes that the pseudo-second-order model is suitable for sorption kinetics when the initial substrate/adsorbent concentration ratio is low. On the other hand, when the initial ratio is high the pseudo-first-order model becomes more adequate. This is in agreement with the present experimental situation since a HA/biomass ratio used is 0.2 has been used, and this is considered a relatively low quantity of substrate for the available adsorption sites.

3.2. Isotherm study

The equilibrium of HA biosorption was modeled using Freundlich and Langmuir isotherms. The Langmuir isotherm is valid for a monolayer adsorption onto the surface with a finite number of identical sites. The linearized Langmuir equation is given as

$$\frac{C_e}{q_e} = \left(\frac{1}{bQ^0}\right) + \left(\frac{C_e}{Q^0}\right) \quad (6)$$

where Q^0 and b are the Langmuir constants characteristic of the system.

The linearized Freundlich equation, that attempts to incorporate the role of substrate–substrate interactions on the surface, is given as

$$\log q_e = \log K_F + \left(\frac{1}{n}\right) \log C_e \quad (7)$$

where K_F and n are the Freundlich constants characteristic of the system. These constants indicate the adsorption capacity and adsorption intensity, respectively.

Table 1 shows the parameters obtained for the Langmuir and Freundlich models. The closer to 1.0 correlation coefficient of the Freundlich suggests that this model better describes the biosorption equilibrium of HA (see Fig. 3). The Freundlich

Please cite this article in press as: M.J. Farré et al., Combined photo-Fenton and biological treatment for Diuron and Linuron removal from water containing humic acid, J. Hazard. Mater. (2007), doi:10.1016/j.jhazmat.2006.12.063

Table 1
Lagmuir and Freundlich isotherm constants of humic acid adsorption onto alive aerobic biomass

	Parameters
Langmuir	
Q^0 (mg g^{-1})	245
$1/b$ (mg L^{-1})	54.0
R^2	0.976
Freundlich	
K_F (mg g^{-1})	24.2
$1/n$	0.392
R^2	0.990

$T = 20\,^{\circ}C$; pH 7.

model describes a monolayer adsorption on a solid surface characterized by an asymmetrical energy distribution, for instance a biomass surface. Furthermore, the experimental data of the present work agrees with the results obtained in a previous work [39].

3.3. Photo-Fenton oxidation of Diuron and Linuron

Diuron and Linuron removal from water using a chemical–biological coupled system via photo-Fenton process has been previously studied in our research group [22]. Results showed that 202 mg L^{-1} of H_2O_2 and 15.9 mg L^{-1} of Fe(II) were required to convert initial toxic and non-biodegradable herbicides into by-products that could be assimilated by the biomass. The photo-treatment time was 60 min.

The mineralization of Diuron and Linuron herbicides in presence of HA has been carried out in order to evaluate the effects of DOM as interference. Thus, the Diuron–Linuron–HA solutions were treated with the same chemical reactant dose that rendered biocompatible photo-treated effluents when no HA was in the media (i.e., 202 mg L^{-1} of H_2O_2 and 15.9 mg L^{-1} of Fe(II)).

Preliminary experiments were performed in order to establish the adequate HA load. It was observed that in absence of

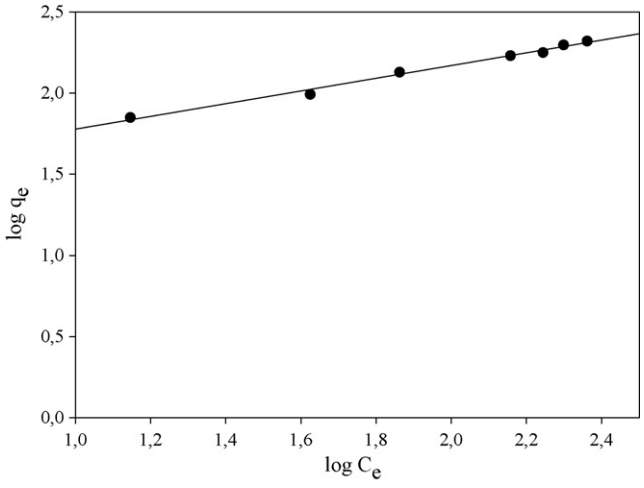

Fig. 3. Linearized Freundlich adsorption isotherm model at 20 °C. pH 7, VSS = 0.33 g L^{-1}.

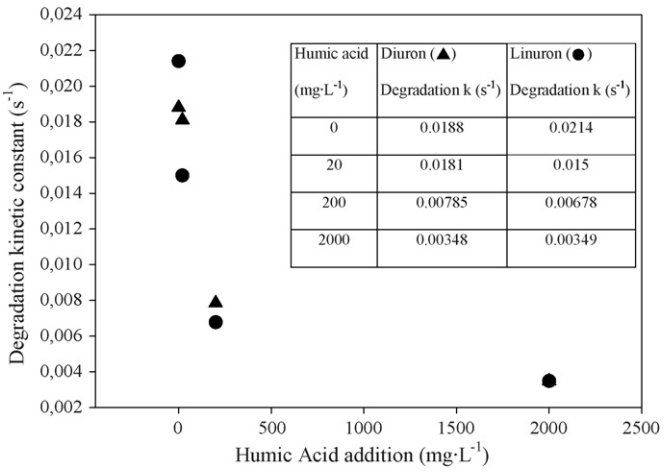

Fig. 4. Diuron and Linuron pseudo-first order degradation kinetic constants in presence of different concentrations of humic acid during photo-Fenton treatment. Fe(II)] = 15.9 mg L^{-1}, [H_2O_2] = 202 mg L^{-1}, $T = 25\,^{\circ}C$.

all photo-Fenton components (i.e., reactants and UVA light) there was no herbicides degradation. On the other hand, TOC corresponding to HA did not decreased after the photo-Fenton treatment, probably due to the low intensity of the light source used in this experimental work (i.e., 0.21 mW cm^{-2}).

As shown in Fig. 4, the Diuron and Linuron degradation kinetics by photo-Fenton are significantly affected by the presence of HA. The more HA is present in the solution, the slower the degradation of pesticides results. For HA concentration above 200 mg L^{-1} only minor differences in herbicide removal were found. This effect was also observed in a similar work when O_3/UV process was used [40].

Therefore, a concentration of 200 mg L^{-1} of HA was selected for subsequent experiments. The TOC corresponding to this HA concentration is 73 ± 7 mg L^{-1}. This high concentration ensures the applicability of the present proposed degradation strategy in a real water sample since TOC corresponding to humic substances in surface waters generally ranges from 3 to 20 mg L^{-1} [42].

Fig. 5 shows the relative TOC evolution of solution A (Diuron and Linuron), B (Diuron, Linuron and 200 mg L^{-1} of HA) and C (200 mg L^{-1} HA) during the photo-Fenton treatment. The TOC concentration of photo-treated solution B was 110 ± 5 mg L^{-1}. The subtraction of 73 ± 7 mg L^{-1} of TOC, corresponding to HA, was required at the end of photo-Fenton process of solution B in order to compare the mineralization results in the presence of HA with the results in absence of the interference (i.e., $TOC_{B-C} = 37 \pm 9$ mg L^{-1}, $TOC_A = 32 \pm 4$ mg L^{-1}). It has been reported that HA can compete with target compounds for hydroxyl radicals, thus slowing down the degradation of those compounds [41]. Moreover, a UVA light screening can be also a possible explanation of the slower degradation of Diuron and Linuron with increasing HA concentration.

3.4. Assessment of photo-treated effluent biodegradability

After photo-Fenton process, A and B solutions were proposed for a posterior biological treatment. The analysis of BOD_5

Please cite this article in press as: M.J. Farré et al., Combined photo-Fenton and biological treatment for Diuron and Linuron removal from water containing humic acid, J. Hazard. Mater. (2007), doi:10.1016/j.jhazmat.2006.12.063

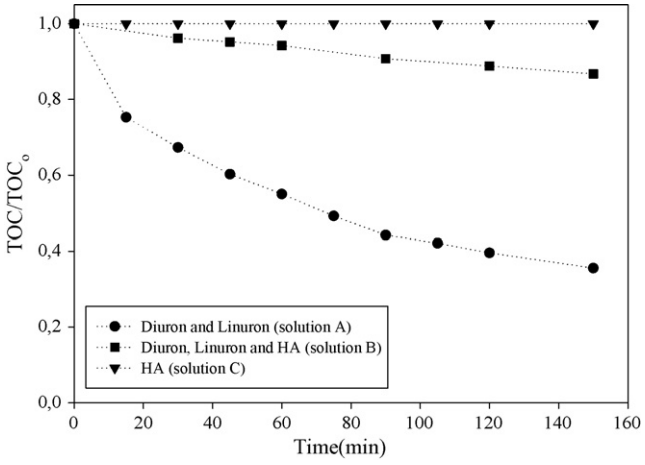

Fig. 5. Relative TOC evolution versus irradiation time of solutions A (Diuron and Linuron) and B (Diuron, Linuron and HA) and C (HA) during photo-Fenton treatment. [Fe(II)] = 15.9 mg L^{-1}, [H_2O_2] = 202 mg L^{-1}, T = 25 °C.

and toxicity were required in order to assess the compatibility with the biological system. To assess the biodegradability of the photo-treated solutions that contained Diuron, Linuron and HA, it was necessary to evaluate the biodegradability of solution C (i.e., HA alone). Results indicate that the biomass was not able to assimilate HA after the photo-Fenton treatment (i.e., $[BOD_5]_C < 5$ mg L^{-1}, $COD_C = 203 \pm 10$ mg L^{-1}, $[BOD_5/COD]_C < 0.02$). A BOD_5/COD ratio higher than 0.40 ensures the biocompatibility of photo-treated solution A ($[BOD_5/COD]_A = 0.51 \pm 0.1$) [43].

COD value of photo-treated solution B (i.e., $COD_B = 264 \pm 10$ mg L^{-1}) was corrected with COD value of solution C as HA was recalcitrant to $OH^\bullet$ attack in the chemical process. On the other hand, the BOD_5 value of solution C was used to correct the corresponding values of photo-treated solution B (i.e., $[BOD_5]_B = 28 \pm 1$ mg L^{-1}). In this way, $[BOD_5]_{B-C} = 26 \pm 3$ mg L^{-1} and $COD_{B-C} = 61 \pm 14$ mg L^{-1}.

These corrected results of photo-treated solution B were compared with the results obtained with photo-treated solution A (i.e., $[BOD_5/COD]_{B-C} = 0.41 \pm 0.1$, $[BOD_5/COD]_A = 0.51 \pm 0.1$). Both can be considered biodegradable since the BOD_5/COD threshold for a wastewater to be considered easily biodegradable is 0.4 [43]. Nevertheless, a difference in COD measurements was observed ($COD_{B-C} = 61 \pm 14$ mg L^{-1}, $COD_A = 33 \pm 4$ mg L^{-1}), thus indicating a different oxidation state in the by-products formed during the mineralization process. This different oxidation state of the generated by-products is due to the reduction of photo-Fenton efficiency as explained above.

Toxicity of photo-treated effluents was analyzed by means of BioTox equipment. EC_{50}^{15} values for all the solutions after photo-Fenton process were higher than TOC effluent concentration. This means that none of the solutions (A, B or C) were toxic [14]. According to BOD_5, COD and EC_{50}^{15} data, it can be suggested that intermediates coming from Diuron and Linuron herbicide oxidation with or without the presence of HA are good candidates for a SBR treatment.

3.5. Biological treatment of photo-treated solutions

In an attempt to gain more insight into the biodegradability of the pre-treated solutions, a SBR was used to simulate a real biological treatment. Three SBR were studied in parallel. The SBR 1 was fed with photo-treated solution A (Diuron and Linuron). SBR 2 was fed with photo-treated solution B (Diuron, Linuron and HA). Finally, SBR 3 was fed with solution C (HA). A start-up period (one 10-day hydraulic retention time (HRT) cycle for each SBR) was initially required. The influent was a completely biodegradable municipal wastewater obtained from the WWTP. The purpose of this preliminary step was to ensure the biomass viability and to establish, as a reference, the residual TOC that the SBR system is not able to handle. The steady TOC obtained, attributed to the metabolites released by the biomass, remained stable at 6.5 mg L^{-1}.The operation with the herbicides samples was performed once the blank cycle was completed.

When SBR 1 was feed with photo-treated solution A, around 80% of TOC removal was daily achieved without any required acclimation process. The residual TOC present in SBR 1 matched the TOC concentration attributed to the metabolites released by the stabilized biomass (VSS = 0.60 ± 0.03 g L^{-1}). Fig. 6 shows data obtained along this experiment for a total of 16 cycles. From the data it was concluded that Diuron and Linuron herbicides could be completely removed from water with the coupled chemical–biological process. More details about those experimental results are reported elsewhere [22].

SBR 2 and SBR 3 were used to investigate the biodegradability of Diuron and Linuron photo-treated effluents in the presence of HA. The initial TOC of the photo-treated solution B was 110 ± 10 mg L^{-1} while the initial TOC of recalcitrant solution C was 73 ± 7 mg L^{-1}. Removal of TOC in the SBR 3 was not expected since $(BOD_5/COD)_C$ ratio was 0.02. Nevertheless, due to the previous detected HA biosorption, TOC measurements at the end of the biological treatment in the SBR 3 (65 ± 3 mg L^{-1}) did not match the TOC measurements of the initial solution (73 ± 7 mg L^{-1}). Non-adsorbed HA was replaced according to the HRT, and TOC accumulation was not observed. Stabilization

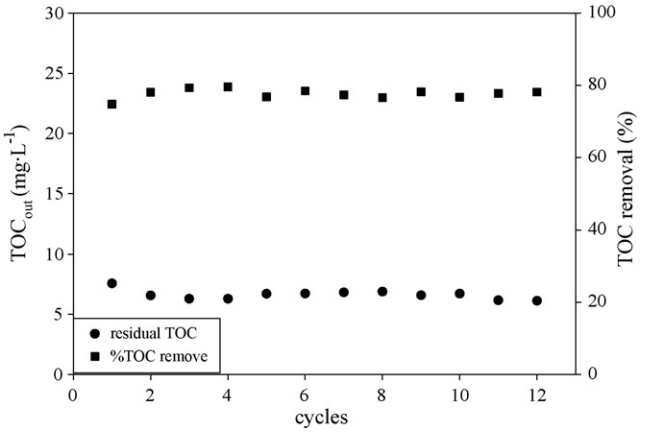

Fig. 6. Final TOC and percentage of TOC removal after aerobic biological treatment (SBR 1) of photo-treated solution A (Diuron and Linuron). ([Fe(II)] = 15.9 mg L^{-1}, [H_2O_2] = 202 mg L^{-1}) during 12 cycles. HRT = 2 days, T = 20 °C. Stabilized VSS = 0.60 ± 0.03 g L^{-1}.

Please cite this article in press as: M.J. Farré et al., Combined photo-Fenton and biological treatment for Diuron and Linuron removal from water containing humic acid, J. Hazard. Mater. (2007), doi:10.1016/j.jhazmat.2006.12.063

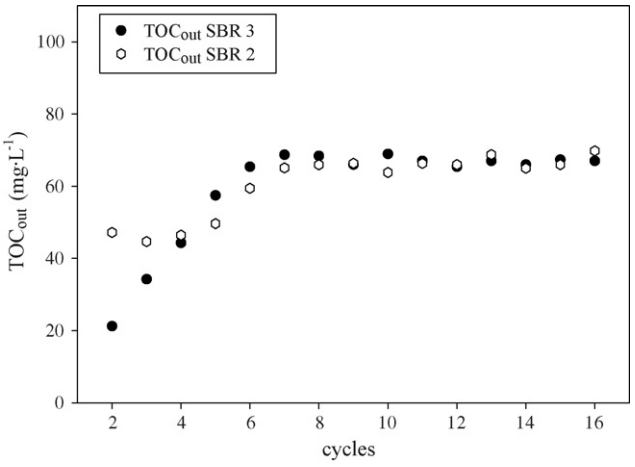

Fig. 7. TOC concentration at the end of the biological treatment for photo-treated B (SBR 2) and C (SBR 3) solutions. $T = 20\,^{\circ}C$, HRT = 2 days. Stabilized $VSS_{SBR\,2} = 0.56 \pm 0.03\ g\,L^{-1}$, $VSS_{SBR\,3}$ = not stable.

of VSS in the SBR 3 was not possible, giving more evidence of the biorecalcitrant nature of HA. On the other hand, when the SBR 2 was fed with photo-treated solution B, 42% of TOC reduction was observed. The final TOC in the SBR 2 matched the final TOC in the SBR 3. This value corresponds to the HA that could not be assimilated by the biomass (i.e., $65 \pm 3\ mg\,L^{-1}$). Fig. 7 shows the TOC evolution at the end of the biological treatment for both, SBR 2 and SBR 3 during 16 cycles. VSS stabilization was reached in SBR 2 (i.e., $VSS = 0.56 \pm 0.03\ g\,L^{-1}$).

From the data it can be concluded that by-products generated during the chemical treatment could be completely assimilated by the biomass in a secondary biological process. Therefore, the elimination of herbicides by means of a chemical and biological coupled system, in the presence of HA, was possible.

4. Conclusions

The coupled photo-Fenton (chemical) and biological treatment is an effective method for the elimination of Diuron and Linuron herbicides from water when HA is also present in solution.

Pesticides degradation via photo-Fenton process becomes slower with increasing HA concentration. A UVA light screening as well as $OH^{\bullet}$ radicals quenching process can be the explanation of this negative effect on the degradation rates.

$[Fe(II)] = 15.9\ mg\,L^{-1}$ and $[H_2O_2] = 202\ mg\,L^{-1}$ are required in the chemical step to convert initial toxic and non-biodegradable herbicides into intermediates suitable for a posterior biological treatment. The complete removal of the TOC that has been generated during the chemical herbicide oxidation is achieved in a SBR using 2 days of HRT. The residual TOC, observed at the end of the biological treatment, corresponds to the biorecalcitrant HA that cannot be assimilated by the biomass.

Adsorption of HA onto the aerobic alive biomass has been observed and characterized. The adsorption process follows a pseudo-second-order adsorption kinetic model. Moreover, biosorption equilibrium has been described by the Freundlich isotherm model.

Acknowledgements

This work was supported by the Spanish Government (MEC, project CTQ2005-02808) and the European Commission (CADOX project, EVK1-CT-2002-00122). We also want to thank Makhteshim Agan España, S.A. for providing the Linuron herbicide.

References

[1] S.T. Leong, S. Muttamara, P. Laortanakul, Reutilization of wastewater in a rubber-based processing factory: a case study in Southern Thailand, Resour. Conserv. Recycl. 37 (2003) 159–172.
[2] Z. Ou, T. Sum, P. Li, A. Yediler, G. Yang, A. Kettrup, A production-scale ecological engineering forest system for the treatment and reutilization of municipal wastewater in the Inner Mongolia, China, Ecol. Eng. 9 (1997) 71–88.
[3] D. Pimentel, Green revolution agriculture and chemical hazards, Sci. Total Environ. 188 (S1) (1996) S86–S98.
[4] S. Šostar-Turk, I. Petrinić, M. Simonič, Laundry wastewater treatment using coagulation and membrane filtration, Resour. Conserv. Recycl. 44 (2005) 185–196.
[5] G. Crini, Non-conventional low-cost adsorbents for dye removal: a review, Bioresour. Technol. 97 (2006) 1061–1085.
[6] M. Pera-Titus, V. García-Molina, M.A. Baños, J. Jiménez, S. Espulgas, Degradation of chlorphenols by means of advanced oxidation processes: a general review, Appl. Catal. B 47 (2004) 219–256.
[7] W.H. Glaze, Drinking-water treatment with ozone, Environ. Sci. Technol. 21 (1987) 224–230.
[8] A. Mills, S. Le Hunte, An overview of semiconductor photocatalysis, J. Photochem. Photobiol. A Chem. 108 (1997) 1–35.
[9] R. Bauer, H. Fallmann, The photo-Fenton oxidation -a cheap and efficient wastewater treatment method, Res. Chem. Intermed. 23 (1997) 341–354.
[10] F. Haber, J. Weiss, The catalytic decomposition of H_2O_2 by iron salts, Proc. R. Soc. Ser. A 147 (1934) 332–351.
[11] J. Pignatello, Dark and photoassisted iron(3+)-catalyzed degradation of chlorophenoxy herbicides by hydrogen peroxide, Environ. Sci. Technol. 26 (1992) 944–951.
[12] F. Al Momani, O. Gonzalez, C. Sans, S. Esplugas, Combining photo-Fenton process with biological sequencing batch reactor for 2,4-dichlorphenol degradation, Water Sci. Technol. 49 (2004) 293–298.
[13] M. Kotsou, A. Kyriacou, K. Lasaridi, G. Pilidis, Integrated aerobic biological treatment and chemical oxidation with Fenton's reagent for the processing of green table olive wastewater, Process Biochem. 39 (2004) 1653–1660.
[14] J. Garcia-Montaño, F. Torrades, J.A. García-Hortal, X. Doménech, J. Peral, Degradation of Procion Red H-E7B reactive dye by coupling a photo-Fenton system with a sequencing batch reactor, J. Hazard. Mater. 134 (2006) 220–229.
[15] E.M. Scherer, Q.-Q. Wang, A.G. Hay, A.T. Lemley, The binary treatment of aqueous metribuzin using anodic Fenton treatment and biodegradation, Arch. Environ. Contam. Toxicol. 47 (2004) 154–161.
[16] U.S. EPA, EPA/832-F-99-073 (1999).
[17] P.A. Wilderer, R.L. Irvine, M.C. Gorzonsky, Sequencing Batch Reactor Technology, International Water Association, London, 1999.
[18] R.L. Irvine, L.H. Ketchum, Sequencing batch reactors for biological wastewater treatment, Crit. Rev. Environ. Control. 18 (1989) 255–294.
[19] S. Malato, J. Caceres, A.R. Fernandez-Alba, L. Piedra, M.D. Hernando, A. Agueera, J. Vial, Photocatalytic treatment of diuron by solar photocatalysis: evaluation of main intermediates and toxicity, Environ. Sci. Technol. 37 (2003) 2516–2524.

Please cite this article in press as: M.J. Farré et al., Combined photo-Fenton and biological treatment for Diuron and Linuron removal from water containing humic acid, J. Hazard. Mater. (2007), doi:10.1016/j.jhazmat.2006.12.063

[20] H. Katsumata, S. Kaneco, T. Suzuky, K. Ohta, Y. Yobico, Degradation of Linuron in aqueous solution by the photo-Fenton reaction, Chem. Eng. J. 108 (2005) 269–276.
[21] L.A. Tahmasseb, S. Nelieu, L. Kerhoas, J. Einhorn, Ozonation of chlorophenylurea pesticides in water: reaction monitoring and degradation pathways, Sci. Total Environ. 291 (2002) 33–44.
[22] M.J. Farré, X. Doménech, J. Peral, Assessment of photo-Fenton and biological treatment coupling for Diuron and Linuron removal from water, Water Res. 40 (2006) 2533–2540.
[23] E.M. Thurman, R.L. Morgan, Preparative isolation of aquatic humic substances, Environ. Sci. Technol. 15 (1981) 463–466.
[24] R.G. Zepp, N.L. Wolfe, J.A. Gotdon, G.L. Baughman, Dynamics of 2,4-D esters in surface waters. Hydrolysis, photolysis, and vaporization, Environ. Sci. Technol. 9 (1975) 1144–1149.
[25] J. Hawari, A. Demeter, R. Samson, Sensitized photolysis of polychlorobiphenyls in alkaline 2-propanol: dechlorination of Aroclor 1254 in soil samples by solar radiation, Environ. Sci. Techol. 26 (1992) 2022–2027.
[26] OECD Guidelines for Testing of Chemicals, vol. 2, Test 302B, 1996.
[27] J. Pignatello, E. Oliveros, A. MacKAY, Advanced oxidation processes for organic contaminant destruction based on the fenton reaction and related chemistry, Crit. Rev. Environ. Sci. Technol. 36 (2006) 1–84.
[28] C.D. Adams, P.A. Scanlan, N.D. Secrist, Oxidation and biodegradability enhancement of 1,4-dioxane using hydrogen peroxide and ozone, Environ. Sci. Technol. 28 (1994) 1812–1818.
[29] APHA-AWWA-WPCF, Standard Methods for the Examination of Water and Wastewater, ASTM D5220, 18th ed., Washington, DC, 1992.
[30] Y.W. Kang, M.J. Cho, K.Y. Hwang, Correction of hydrogen peroxide interference on standard chemical oxygen demand test, Water Res. 33 (1998) 1247–1251.
[31] G.H. Jeffery, J. Basset, J. Mendham, R.C. Denny, Vogel's Textbook of Quantitative Chemical Analysis, fifth ed., Longman, New York, 1989.
[32] APHA-AWWA-WPCF, Standard Methods for the Examination of Water and Wastewater, ASTM D2540 E2540, 18th ed., Washington, DC, 1992.
[33] S. Lagergren, Zur theorie der sogenannten adsorption gelöster stoffe, Kungliga Svenska Vetenskapsakademiens, Handlingar 24 (1898) 1–39.
[34] C.W. Chenug, J.F. Porter, G. MacKay, Sorption kinetics for the removal of copper and zinc from effluents using bone char, Sep. Purif. Technol. 19 (2000) 55–64.
[35] M. Ajmal, R.A.K. Rao, R. Ahmad, J. Ahmad, Adsorption studies on *Citrus reticulata* (fruit peel of orange): removal and recovery of Ni(II) from electroplating wastewater, J. Hazard. Mater. 79 (2000) 117–131.
[36] Y.S. Ho, J.C.Y. Ng, G. McKay, Kinetics of pollutant sorption by biosorbents: review, Sep. Purif. Methods 29 (2000) 189–232.
[37] Y.S. Ho, G. McKay, Pseudo-second order model for sorption processes, Process Biochem. 34 (1999) 451–465.
[38] S. Azizian, Kinetic models of sorption. A theoretical analysis, J. Col. Interf. Sci. 276 (2004) 47–52.
[39] M. Esperanza-Soto, P. Wasterhoff, Biosorption of humic and fulvic acids to live activated sludge biomass, Water Res. 37 (2003) 2301–2310.
[40] A. Latifoglu, M. Gurol, The effect of humic acids on nitrobenzene oxidation by ozonation and O_3/UV processes, Water Res. 37 (2003) 1879–1889.
[41] Q. Wang, A.T. Lemley, Kinetic effect of humic acid on alachlor degradation by anodic fenton treatment, J. Environ. Qual. 33 (2004) 2343–2352.
[42] E.E. Geldreich, Microbial quality of Water Supply in distribution System, CRC: Lewis Publishers, Boca Raton, Florida, 1996.
[43] V. Sarria, S. Parra, A. Nevenka, P. Péringer, N. Benitez, C. Pulgarin, Recent developments in the coupling of photoassisted and aerobic biological processes for the treatment of biorecalcitrant compounds, Catal. Today 76 (2002) 301–315.

Please cite this article in press as: M.J. Farré et al., Combined photo-Fenton and biological treatment for Diuron and Linuron removal from water containing humic acid, J. Hazard. Mater. (2007), doi:10.1016/j.jhazmat.2006.12.063

CHAPTER 4
CONCLUDING REMARKS

1. Concluding remarks

The necessity for sustainable treatment of wastewater polluted with biorecalcitrant compounds was the grounds for the evaluation of coupling AOPs with biological treatment to remove herbicides from water. In the first part of this thesis, an effective AOP for the removal of different herbicides from water was selected. The AOPs tested were photo-Fenton, TiO_2-photocatalysis, ozone/UV, photo-Fenton/ozone and TiO_2-photocatalysis/ozone. The subsequent complete TOC abatement by means of a biological treatment was then undertaken. From such evaluation the following conclusions were drawn:

- Among the AOPs selected and tested under similar experimental conditions, the photo-Fenton/ozone coupled system is the most effective method to degrade aqueous solutions of Alachlor, Atrazine, Chlorphenvinfos, Diuron, Isoproturon and Pentachlorophenol herbicides.

- The initial herbicide degradation process, that occurs through oxidation of organic molecules by means of their reaction with the generated hydroxyl radical, follows a first and zero-order kinetics when photo-Fenton/ozone and TiO_2-photocatalysis/ozone are applied respectively.

- After degradation of parent herbicide by means of the photo-Fenton/ozone process, biodegradability increases for Isoproturon, Diuron, Alachlor and Atrazine herbicides solutions, but not for Pentachlorophenol. In the case of Alachlor and Atrazine solutions the biodegradability increase takes place with a simultaneous increase in toxicity.

The second part of the thesis was based on the combination of photo-Fenton with biological treatment for the remediation of water polluted with Diuron and Linuron phenylurea herbicides. From that assessment the following conclusions were inferred:

- An optimized photo-Fenton process can be effectively used to completely degrade and significantly mineralize a mixed solution of Diuron and Linuron herbicides.

- An excess of reactants, especially Fe^{2+}, slows down the mineralization rate due to the side reactions derived from oxidized forms of reactant species. Thus, there is an optimum reagent dose combination to reach a determined mineralization degree.

- Along the oxidation process, the hydroxyl radical firstly attacks the aromatic ring and methyl group leading to the formation of more oxidized compounds with different biorecalcitrant nature. 1,1-dimethylurea, methylurea, oxalic, acetic and formic acids as well as 3,4-dichloroaniline, and 3,4-dichlorophenyl isocyanate among other minority compounds are generated during the mineralisation process.

- An optimized photo-Fenton/biological coupled treatment can be used to completely mineralize Diuron and Linuron herbicide solutions. Optimised photo-Fenton reagent concentrations are $[Fe^{2+}]$=15.9 $mg \cdot L^{-1}$ and $[H_2O_2]$=202 $mg \cdot L^{-1}$. After one hour of UVA irradiation time, the remaining TOC is completely eliminated in an SBR.

- The coupled photo-Fenton/biological treatment is an effective method to remove Diuron and Linuron herbicides from water also in the presence of humic acid. Nevertheless, the presence of this interference slows down the herbicide degradation rates due to a UVA light screening as well as a hydroxyl radical quenching process.

- Adsorption of humic acid onto the biomass follows a pseudo-second-order kinetics model and biosorption equilibrium is correctly described by the Freundlich isotherm model.

- In terms of environmental impact, the coupling between photo-Fenton and biological treatment is the best option to remove Diuron and Linuron herbicides from water when comparing with single artificial light assisted photo-Fenton and single solar assisted photo-Fenton. The environmental impacts associated to the production of hydrogen peroxide, followed by electricity required to run the UVA light are significant. Consequently, a noticeable environmental improvement could be expected if solar assisted photo-Fenton coupled to a biological treatment was applied to remove Diuron and Linuron herbicides from water.

ANNEXE 1

UNPUBLISHED RESULTS

a1.1. Evaluation of the intermediates generated during the degradation of Diuron and Linuron herbicides by the photo-Fenton reaction. *Accepted for publication in Journal of Photochemistry and Photobiology A: Chemistry*

María José Farré[a], Stephan Brosillon[b], Xavier Domènech[a] and José Peral[a].

[a]Departament de Química. Universitat Autónoma de Barcelona, 08193 Bellaterra, Spain. [b]Laboratoire Rennais de Chimie et Ingénierie des Procédés, Ecole Nationale Supérieure de Chimie de Rennes, Avenue du Général Leclerc, 3700 Rennes, France.

Abstract

Freshwater polluted with herbicides is a problem of general concern since these compounds are commonly toxic and non biodegradable. An innovative technology for the elimination of such compounds is the coupling between an AOP (Advanced Oxidation Process) and a biological treatment. The success of this coupled methodology depends on the biodegradable nature of the by-products originated at the end of the chemical stage. The present paper is based on the analysis of the intermediates generated during the chemical oxidation of Diuron and Linuron herbicides using three different doses of photo-Fenton reactants. Among the three effluents obtained after the chemical pre-treatment, only the most oxidised is completely biodegradable. Several analytical methods: reverse phase ultra pressure liquid chromatography UPLC(RP)/MS, ionic chromatography IC and gas chromatography/MS have been used to elucidate the degradation mechanism. Beyond conventional separation methods, hydrophilic interaction chromatography HILIC coupled with mass spectrometry has been necessary to identify small polar compounds at the end of oxidation process. The first steps of the degradation mechanism have been ascertained. Furthermore, different by-products have been found at the end of the chemical process when different reactant doses were used. These differences have been based on the presence of urea derivates (methylurea, 1,1-dimethylurea) and unidentified chlorinated compounds.

Keyword: biodegradability, herbicides, by-products, biological treatment, photo-Fenton.

1. Introduction

Nowadays herbicides are indispensable for agricultural practices. Nevertheless herbicides also represent a water quality risk factor because these substances are generally toxic and non biodegradable. A part from lixiviates coming from agricultural fields, washing of herbicide containers and unused treatment solutions also contribute to this problem producing highly polluted effluents that should be treated before their disposal to the environment.

Conventional technologies for the removal of pollutants include biological, physical and chemical treatments. The drawbacks of biological wastewater treatment plants (WWTP) are based on the requirement of a long residence time to degrade the pollutants because microorganisms are affected by the toxicity of the herbicides [1]. Physical treatments require a post-treatment to remove the pollutant from the newly contaminated environment. Finally, chemical treatments require a large amount of reactant and generally are expensive. In this situation, the development of new technologies aimed at the straight forward degradation of such substances is of practical interest.

In recent years the coupling between an Advanced Oxidation Process (AOPs) and biological systems for the treatment of different polluted effluents has been proposed [2-7]. In this way the AOP is performed as a first step to enhance the biodegradability and generate a new effluent able to be treated in a biological plant. AOPs are based on the production of the highly reactive hydroxyl radical (OH·) under mild experimental conditions. This radical can react with organic matter (redox standard potential 2.8 V *vs* NHE) producing CO_2 as final product. Due to the reactivity of free hydroxyl radicals, their attack is non-selective, which is useful for the treatment of wastewater containing many different pollutants.

Photo-Fenton is preferred among the other AOPs because it achieves high reaction yields with low treatment costs, mainly due to the possibility of a more effective use of solar light as a photon source [8]. In this process the hydroxyl radical promoters are Fe(II) and hydrogen peroxide [9] (reaction a1.1.1, Fenton process).

$$Fe^{2+} + H_2O_2 \longrightarrow Fe^{3+} + OH^- + OH\cdot \qquad (a1.1.1)$$

Under irradiation of λ<410 nm, Fe(III) can be reduced to Fe(II) closing a loop mechanism where Fe species act as catalyst, giving rise to additional OH· [10] (reaction a1.1.2, photo-Fenton process).

$$Fe(OH)^{2+} + h\nu \longrightarrow Fe^{2+} + OH\cdot \qquad (a1.1.2)$$

The best optimization of a chemical-biological coupled system can be achieved by using a low amount of reactants in the chemical step. However, these reactant doses should assure the biocompatibility of the by-products generated. With this objective, the monitoring of the intermediates produced in the chemical treatment is indispensable to understand the biological compatibility of the phototreated effluent. This monitoring is not always easy since by-products generated in such oxidation processes can be small polar compounds with different chemical structure and low concentration. In this situation, reversed phase liquid chromatography HPLC (RP) is not the best separation method because polar compounds are not retained on non polar stationary phases. On the other hand, normal phase HPLC eluents (often based on hexane) produce an incompatibility with mass detectors since ionization is not easily achieved in totally organic, nonpolar eluents. When hydrophilic interaction chromatography (HILIC) [11] is performed aqueous mobile phases, usually containing more than 50% of organic solvent, and a polar stationary phase like diol, silica or amine are used. The retention of polar compounds is increased when the proportion of organic solvent is increased. Alpert et al [11] suggested that the retention mechanism involves portioning of the analyte between the mobile phase and a layer of mobile phase enriched with water on the stationary phase. In this way the elution order in HPLC(HILIC) is more or less the opposite of that seen in HPLC (RP). So HPLC (HILIC) coupled with mass spectrometer appears to be an appropriate method for the determination of the concentration and structure of small polar compounds.

Phenylurea compounds are herbicides which have been widely used since their discovery in 1950. Linuron, 3-[3,4-(dichlorophenyl)-1-methoxy-1-methylurea] and Diuron 3-[3,4-(dichlorophenyl)-1,1-dimethylurea] were selected as target compounds.

The degradation of Diuron and Linuron herbicides by means of the coupling of photo-Fenton and biological treatment was performed and published in a previous work [5]. In that study, three different photo-Fenton reagent doses were used in the chemical treatment (i.e., A:

[Fe(II)]=9.25 mg·L^{-1}, [H_2O_2]=97.1 mg·L^{-1}; B: [Fe(II)]=13.3 mg·L^{-1}, [H_2O_2]=143 mg·L^{-1} ; C: [Fe(II)]=15.9 mg·L^{-1}, [H_2O_2]=202 mg·L^{-1}.). The photo-Fenton reaction was run for 60 minutes. The disappearance of initial herbicides during the photo-Fenton process was determined by HPLC/UV analyses for all the doses used. The percentages of TOC removal after the chemical step when dose A, B and C were used were 16, 25 and 36% respectively. After that, a biological system was used in order to completely remove organic matter from solution. Among the three photo-Fenton doses selected, only dose C successfully converted the initial toxic and non biodegradable effluent into a new form which was able to be assimilated by the biomass. Figure a1.1.1 shows the percentage of TOC removal after the chemical-biological coupled system for the treatment of Diuron and Linuron.

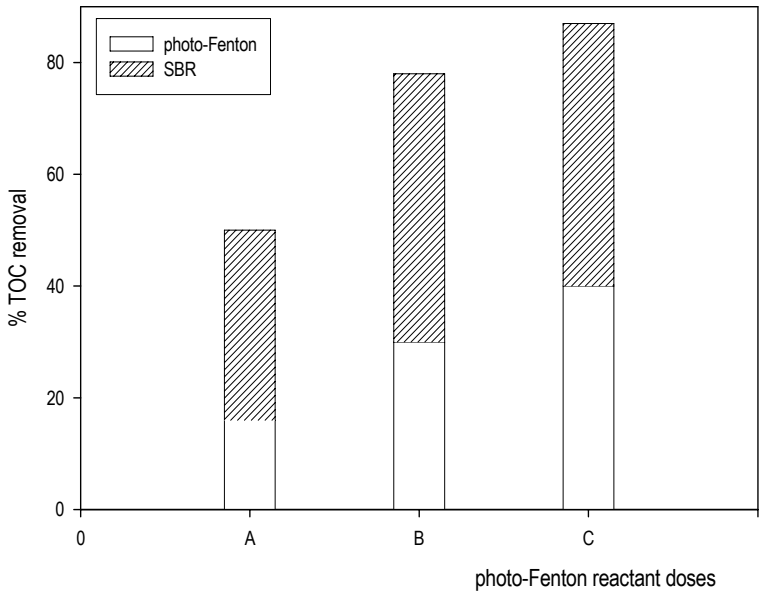

Figure a1.1.1. % TOC removal in photo-Fenton pre-treatment and biological Sequencing Batch Reactor (SBR) coupling system as function of photo-Fenton dose. A: 9.25 mg·L^{-1} Fe(II), 97.1 mg·L^{-1} H_2O_2; B: 13.3 mg·L^{-1} Fe(II), 143 mg·L^{-1} H_2O_2 and C: 15.9 mg·L^{-1} Fe(II), 202 mg·L^{-1} H_2O_2.

The aim of the present paper is to enhance the knowledge on the chemical composition of the three effluents after photo-Fenton in view to understand the difference of biodegradability of each effluent as well as to determine a possible reaction mechanism of the oxidation of both

herbicides. Heteroatoms, short acids as well as oxidized by-products evolution were analyzed in order to obtain such information.

2. Materials and methods

2.1. Preparation of initial wastewater

Diuron (98.5% Aragonesas Agro S.A. technical grade) and *Linuron* (92.6% Makhteshim Agan España ,S.A.) were used as target compounds in the experiments. A initial saturated solution was prepared in water purified in a Millipore Milli-Q system and then filtrated by means of a 20 μm nylon filter. The concentration of the initial solution was 42 $mg \cdot L^{-1}$ and 75 $mg \cdot L^{-1}$ of Diuron and Linuron respectively. These values correspond to the maximum solubility of both herbicides in water at 25 ^{o}C. The initial solution was transparent and colourless.

2.2. Photo-Fenton experimental procedure

$FeSO_4 \cdot 7H_2O$ (Merck) and H_2O_2 (Panreac, 33% w/v) were used in the photo-Fenton experiments. Experiments were conducted at 25±0.2 ^{o}C in a cylindrical Pyrex thermostatic cell of 250 cm^3 capacity provided with a magnetic stirrer. A 6W Philips black light with a measured intensity of 0.21 mW/cm^2 was used as a photon source. In all the experiments pH was adjusted to 2.8 with H_2SO_4. Three different combinations of photo-Fenton reagents were used (i.e., A: $[Fe(II)]=9.25\ mg \cdot L^{-1}$, $[H_2O_2]=97.1\ mg \cdot L^{-1}$; B: $[Fe(II)]=13.3\ mg \cdot L^{-1}$, $[H_2O_2]=143\ mg \cdot L^{-1}$; C: $[Fe(II)]=15.9\ mg \cdot L^{-1}$, $[H_2O_2]=202\ mg \cdot L^{-1}$.)

The experimental procedure was as follows: in each experiment the photo-reactor was charged with 0.250 L of solution to be photo-treated. The pH of these solutions was always adjusted to 2.8 and after that $FeSO_4 \cdot 7H_2O$ was added. Finally, the hydrogen peroxide was added to the solution and UV light was switched on. The total photo-treatment time selected was 60 minutes.

2.3. Analytical Methods

TOC was analyzed with a Shimadzu TOC-V_{CSH} apparatus. Cl^- and NO_3^- ions were analyzed by Dionex DX120 ion chromatography equipped with a conductivity detector using an IonPac® AS19 anion-exchange column (4×250 mm) as the stationary phase. A gradient of KOH in water: 10 mM from 0 to 10 min and then increasing to 45 mM from 10 to 25 min was used as mobile phase. The flow rate was 1 mL·min^{-1} and the injection volume was 500 µL. The mobile phase was electrolitically generated by means of a EGC II KOH. For the determination of short acids (oxalic, acetic and formic acids) the same system was used but the gradient was changed: 10 mM from 0 to 10 min and then increasing to 58 mM from 10 to 40 min. Ammonium was analyzed using an Orion 95-12 Ammonia Electrode and a Crison pH/mV meter with readability to 0.1 mV. Separation and identification of first oxidation by-products were performed with an Acquity™ ultra performance LC (Waters), equipped with a mass spectrometer Quattro Premier -Micromass- (Waters). The mobile phase was a mixture of (A) acetonitrile and (B) acetonitrile (10%), water and formic acid (0.1%). The composition of the phase changed according to the following gradient: 20% of A was kept during 4 minutes. From 4 to 5 minutes, B was steadily increased to attain the 95%. Finally the phase turned to the initial composition until the end of the run. The system was equipped with a UPLC™ BEH C_{18} capillary column (2.1 × 100 mm × 1.7 µm). Mass spectra were obtained by electro-spray ionization (ESI) in negative mode. Cone voltage of 25 V in full scan mode and 23 V in the MRM mode were used. When samples concentration was required, OASIS HLB 6cc cartridges were used for solid phase extraction and ethanol was used as eluent. 3,4-dichloroaniline and 3,4-dichlorophenyl isocyanate were identified during photodegradation of both pesticides by means of GS-MS. These products were extracted from the treated solution by solid phase extraction (Maxi-Clean C18 600mg, Alltech). A mixture of dichloromethane and ethyl acetate (1/1, v/v) was used to elute the intermediate products. This solution was concentrated under nitrogen flow for the analysis of the by-products. The GC-MS was performed using a HP 6890 series GC equipped with a MS (HP 5973). The system was fitted with a HP-5MS capillary column (30 × 0.25 i.d. × 0.25 µm), splitless injection, and helium was used as carrier gas (1 mL · min^{-1}). The GC oven temperature was programmed to initially hold at 50 ^{o}C for 3 min, to increase from 50 ^{o}C to 275 ^{o}C at a rate of 5 ^{o}C·min^{-1} and to hold at 275 ^{o}C for 15 min. The injector and interface temperature were kept at 250 ^{o}C. Mass spectra were obtained by electron-impact (EI) in negative mode at 70eV, using scan mode (30-800 m/z). Small polar compounds were analysed with a HPLC (HILIC) coupled with an Esquire 3000 (Bruker) mass

spectrometer, using a Agilent 1100 liquid chromatograph equipped with a Nulcleosil diol column (7µm×15×0.4 cm). The injection volume was 5.00 µL and temperature was not controlled. The mobile phase consisted of (A) acetonitrile and (B) 20 mM aqueous ammonium formate, the pH of which was adjusted to 3.3 with formic acid. The composition of the phase changed following a gradient: 95% of A was kept during 3 minutes, then it changed from 95% to 50% of A in three more minutes, steady decrease to 20% of A up to minute 10. From 10 to 14 minutes the composition was kept stable at 20% A. Finally from 14 to 30 minutes the mobile phase was returned to initial conditions. Electro-spray (ESI) in positive mode was used for detection. The capillary voltage was optimized to 5000V using full scan mode (50-200 m/z).

3. Results and Discussion

3.1. Heteroatoms evolution

Mineralization of Diuron and Linuron herbicides, using A, B and C photo-Fenton reactant dose, was followed by means of TOC measurements over 150 minutes (see Figure a1.1.2 for relative TOC abatement). The mineralization rate did not follow simple first or zero-order kinetics models and overall reaction rate constants could not be estimated. The complexity of the data is due to the fact that TOC is a parameter which is often the consequence of the parallel degradation of several compounds.

The stoichiometry of the complete mineralization of Diuron and Linuron can be expressed with the following global equations:

$$C_9H_{10}Cl_2N_2O + 13O_2 \rightarrow 2HNO_3 + 2HCl + 9CO_2 + 3H_2O \qquad (a1.1.3)$$

$$C_9H_{10}Cl_2N_2O_2 + 12.5O_2 \rightarrow 2HNO_3 + 2HCl + 9CO_2 + 3H_2O \qquad (a1.1.4)$$

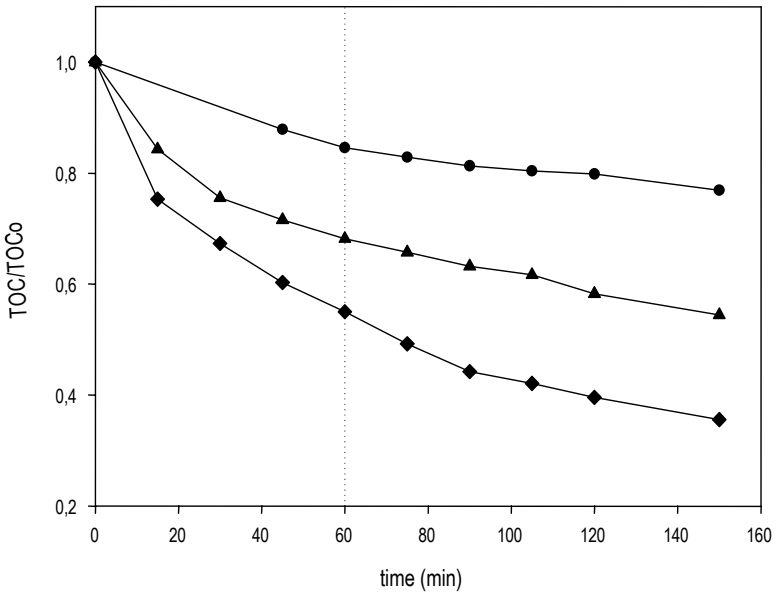

Figure a1.1.2. Relative TOC evolution *vs*. irradiation time with A (●), B (▲) and C (♦) reagent doses for Diuron and Linuron herbicides. A: 9.25 mg·L^{-1} Fe(II), 97.1 mg·L^{-1} H_2O_2; B: 13.3 mg·L^{-1} Fe(II), 143 mg·L^{-1} H_2O_2 and C: 15.9 mg·L^{-1} Fe(II), 202 mg·L^{-1} H_2O_2. pH=2.8, T=25 ^{o}C.

It is well known that chlorinated compounds are generally not biodegradable [13], consequently it is important to access the ratio of mineralization of chlorine during irradiation. For that reason, the formation of chloride ion was investigated. Figure a1.1.3 shows chloride evolution when the three selected doses were used. Chloride evolves very quickly suggesting an early degradation/dechlorination stage, as described before [12]. From Figure a1.1.3 it is seen that chlorine was completely removed from the aromatic ring before 60 minutes in the effluents treated with dose B and C. In both experiments the total amount of Cl^- produced at the end of the reaction was approximately 32.3 mg·L^{-1} (100% of the Diuron and Linuron chlorine content). On the other hand, 7.8% of chlorine remained linked to the aromatic ring after 60 minutes when dose A was used to treat the polluted effluent. This means that a chlorinated intermediate is present in the residual TOC at the end of the chemical treatment with reagent dose A.

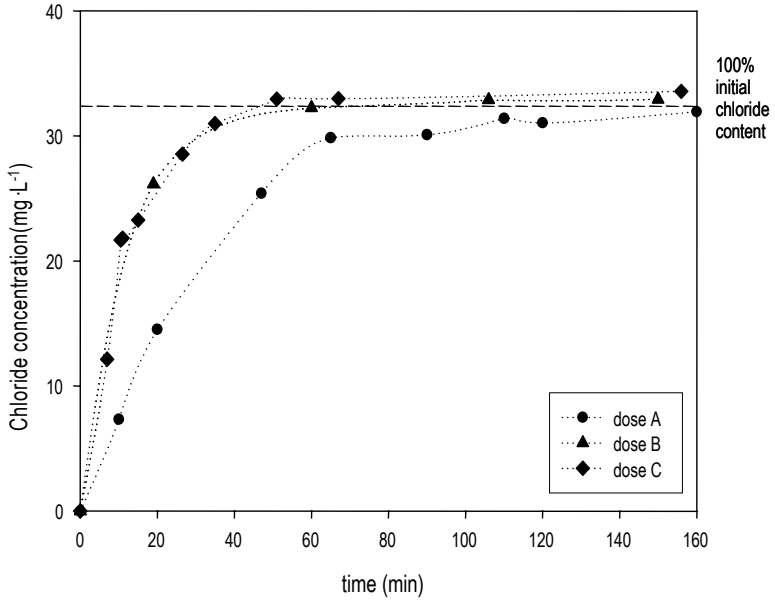

Figure a1.1.3. Chloride concentration *vs*. irradiation time with A, B and C reagent doses for diuron and Linuron herbicides. A: 9.25 mg·L^{-1} Fe(II), 97.1 mg·L^{-1} H_2O_2; B: 13.3 mg·L^{-1} Fe(II), 143 mg·L^{-1} H_2O_2 and C: 15.9 mg·L^{-1} Fe(II), 202 mg·L^{-1} H_2O_2. pH=2.8, T=25 ^{o}C

Nitrogen release was monitored by the combination of free ammonia and nitrate. Although the reactions shown above have been written taking into account the most oxidized state, ammonia could be formed and then oxidized to nitrate at long irradiation times. Both, ammonia and nitrate have been detected at different relative concentrations depending on the dose used in the pre-treatment. By observing Figure a1.1.4, it can be concluded that the amount of nitrate and ammonia formed in the oxidation process is directly proportional to the concentration of oxidant used.

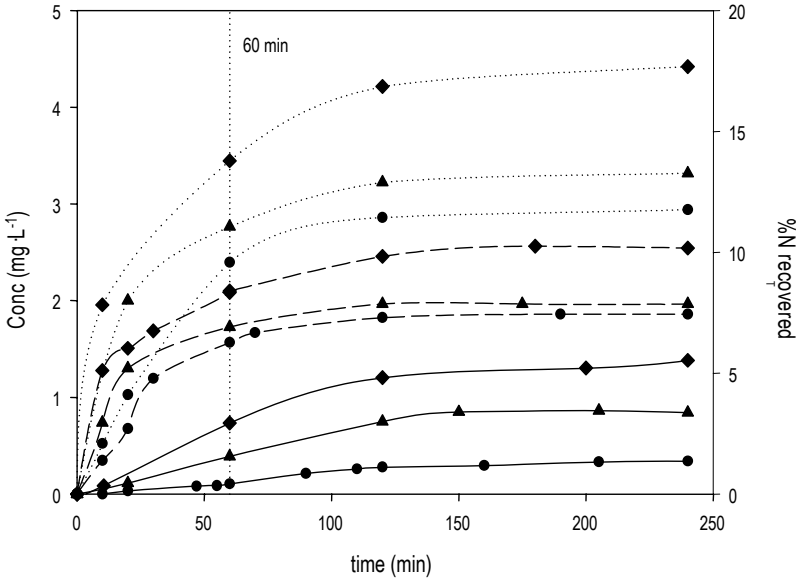

Figure a1.1.4. Nitrate (—), ammonium (--) and total nitrogen recovered (···) evolution *vs*. irradiation time during the photo-degradation of Diuron and Linuron with A (●), B (▲) and C (♦) reagent doses. A: 9.25 mg·L^{-1} Fe(II), 97.1 mg·L^{-1} H_2O_2; B: 13.3 mg·L^{-1} Fe(II), 143 mg·L^{-1} H_2O_2 and C: 15.9 mg·L^{-1} Fe(II), 202 mg·L^{-1} H_2O_2. pH=2.8, T=25 ^{o}C.

When dose C was selected (the highest oxidant concentration used in the present study), only 18% of total nitrogen present in the initial molecules was recovered. Incomplete nitrogen mass balance indicates that other nitrogen containing compounds must be present in the solution during the process. At this point it was necessary to find an analytical technique able to determine this type of compounds dissolved in complex matrixes

3.2. Short organic acids evolution

The evolution of acetic, formic and oxalic acids concentration along 350 minutes of photo-Fenton oxidation reaction was investigated. As seen in Figure a1.1.5, the concentration of acetic acid increases to reach a maximum after approximately 50 minutes when dose A was used to oxidized Diuron and Linuron. After 60 minutes of irradiation, the time used to perform biological coupling, acetic acid concentration was 4.88 mg·L^{-1}. On the other hand, when doses B and C

were applied in the photo-Fenton process, less than 1.2 mg·L^{-1} were found before the biological coupling.

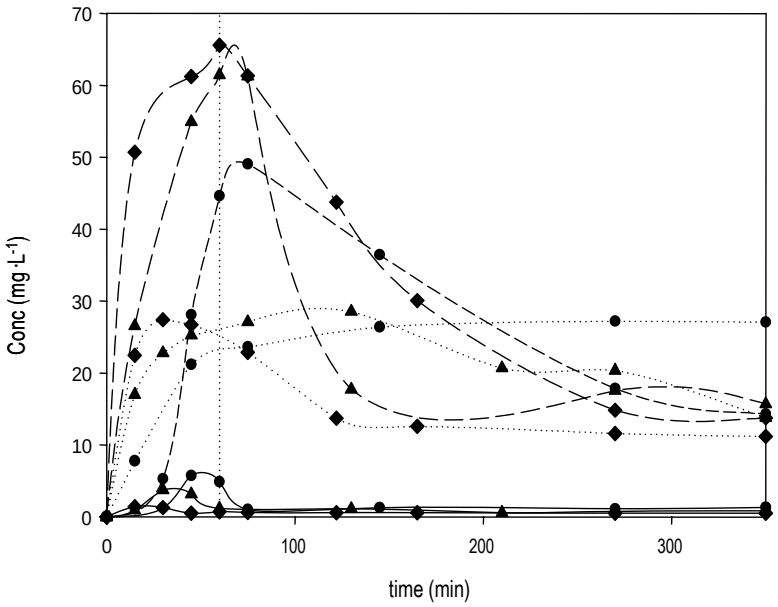

Figure a1.1.5. Acetic acid (—), Oxalic acid (--) and formic acid (···) evolution *vs*. irradiation time during the photo-degradation of Diuron and Linuron with A (●), B (▲) and C (♦) reagent doses. A: 9.25 mg·L^{-1} Fe(II), 97.1 mg·L^{-1} H_2O_2; B: 13.3 mg·L^{-1} Fe(II), 143 mg·L^{-1} H_2O_2 and C: 15.9 mg·L^{-1} Fe(II), 202 mg·L^{-1} H_2O_2. pH=2.8, T=25 ^{o}C.

The monitoring of oxalic acid evolution over 350 minutes showed that its production was higher for doses B and C (61.5 and 65.5 mg·L^{-1}, respectively) than for dose A (44.6 mg·L^{-1}). Maxima in the evolution curves were achieved at the moment selected for the coupling with the biological system. Both, acetic and oxalic acid were produced after ring opening, as described before [14]. Soft oxidant conditions favour the production of acetic acid, while an increase in OH· concentration produces a higher concentration of oxalic acid, which is the product of the oxidation of acetic acid.

Formic acid can be generated from the direct oxidation of methyl groups or from oxalic or acetic acid oxidation [15]. At 60 minutes, the formic acid concentration of effluents treated with doses B and C was approximately 25 mg·L^{-1}, while the concentration for effluent treated with dose A was 22.5 mg·L^{-1}. High concentration of formic acid remained in solution after 350 minutes

when the polluted effluent was treated with photo-Fenton dose A (i.e., 27 mg·L^{-1}), thus suggesting that formic acid is more resistant to degradation than acetic or oxalic acid. On the other hand, when the effluent was treated with doses B or C, due to the higher OH· concentration used, formic acid concentration decrease to 13.8 and 11.2 mg·L^{-1}, respectively.

Short acids percentages at the end of photo-Fenton process are represented in Figure a1.1.6. The 100% value corresponds to the residual TOC present in solution after 60 min of photo treatment and the value of carbon content in the form of short acids is calculated according to this percentage. The figure also shows the existence of non identified organic matter (NIOM) for the three treated effluents. In order to understand differences between biodegradability at the end of the chemical process UPLC/MS (RP), GS/MS and HPLC(HILIC)/MS were used in an attempt to characterize the NIOM.

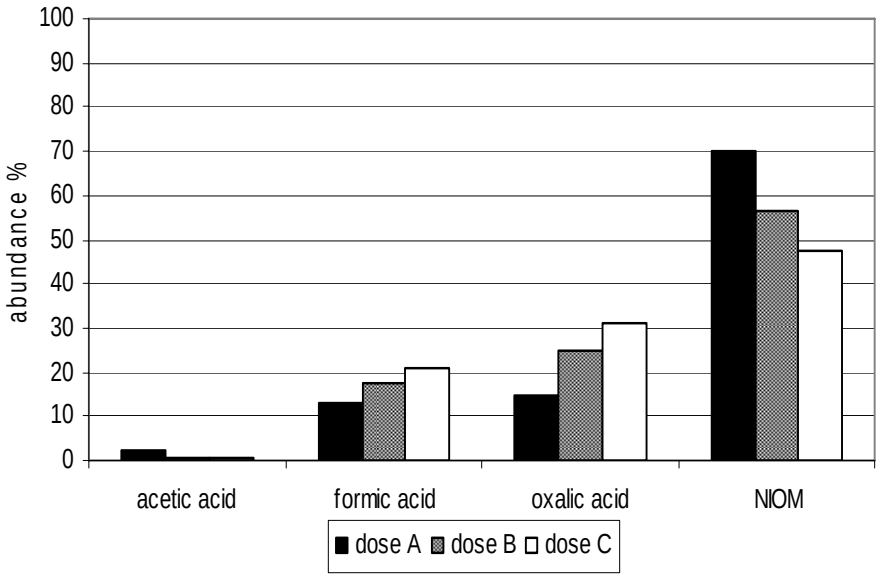

Figure a1.1.6. Relative abundance of different acids and non identified organic matter (NIOM) after 60 minutes of irradiation of Diuron and Linuron with A, B and C reagent doses. A: 9.25 mg·L^{-1} Fe(II), 97.1 mg·L^{-1} H_2O_2; B: 13.3 mg·L^{-1} Fe(II), 143 mg·L^{-1} H_2O_2 and C: 15.9 mg·L^{-1} Fe(II), 202 mg·L^{-1} H_2O_2. pH=2.8, T=25 ^{o}C.

According to the results on the chloride, nitrogen, and short acid release, it could be infer that a part of the identified organic compounds present after 60 min contain chlorine in the case A and nitrogen for the three cases A, B and C.

3.3. Identification of first by-products formed and degradation mechanism

The photoproducts formed in the first steps of the oxidation process of Diuron and Linuron herbicides when A, B and C photo-Fenton reagent doses were used were investigated by means of UPLC(RP)-MS (See Figure a1.1.7 for UPLC chromatogram).

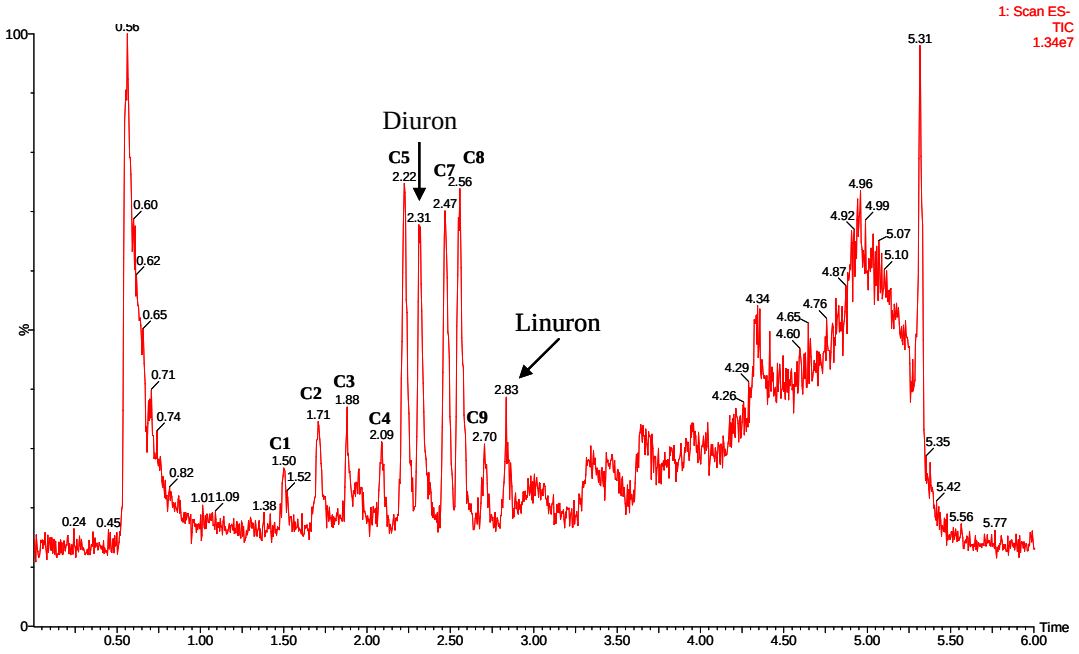

Figure a1.1.7. UPLC chromatogram in scan mode obtained at 25 V and corresponding to 15 minutes of an experiment of photo-Fenton with reactant dose A (9.25 mg·L^{-1} Fe(II), 97.1 mg·L^{-1} H_2O_2).

The short column employed in the UPLC technique enabled the identification of unstable products. Ten products were identified by the molecular ions and mass fragment ions detected at the MS. The structures of the by-products as well as the main fragmentations are summarized in Table a1.1.1. In addition, initial compounds (Linuron, Diuron) were also found in the chromatogram (i.e., compound 6 and 10).

Due to the characteristic isotopic distribution of the presence of chloride atoms in a molecule (Cl^{35} and Cl^{37}), it can be confirmed the presence of two chloride atoms in all the structures determined (i.e., three peaks with isotopic abundance 100%, 66% and 10.6%). Moreover, no recombination between by-products formed has been observed.

Table a1.1.1. Main fragments arising from MS analysis of Diuron and Linuron degradation samples

Compound	Retention time(min)	Molecular weight (m/z)	Molecular ion and fragmentations	Photoproduct
1	1.50	220	219 (100), 176(22)	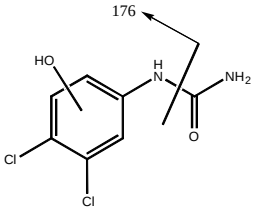
2	1.71	250	249(5), 203(100), 160(5)	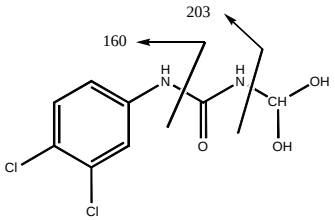
3	1.88	248	247(7), 217(100), 160(68)	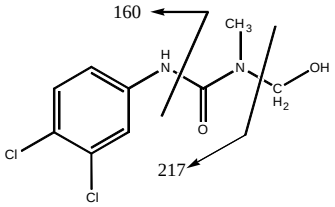
4	2.09	264	263(8),217(100), 160(23)	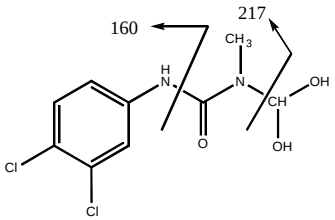
5	2.22	248	247(25), 202(100)	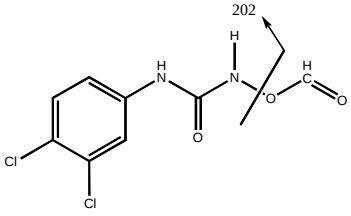

6 (Diuron)	2.31	232	231	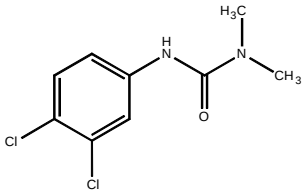
7, 8	2.47, 2.55	264	263(20),202(100)	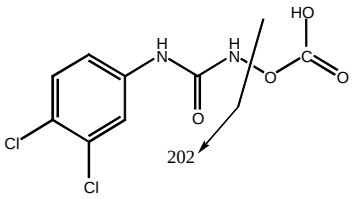
9	2.70	246	245(100),217(30), 188(52),160(28)	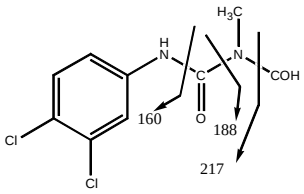
10 (Linuron)	2.83	248	247	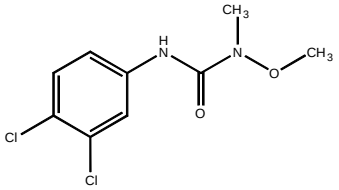

By interpreting the mass spectra, compound 3: N'-(3,4-dichlorophenyl)-N-(hydroxymethyl)-N-methyl-urea, and compound 4: N'-(3,4-dichlorophenyl)-N-(dihydroxymethyl)-N-methyl-urea, were identified as the products formed by the first and second attack of OH· to the methyl group of Diuron, respectively. Compound 2: N-(3,4-dichlorophenyl)-N'-(dihydroxymethyl)-urea was identified as the product formed by the attack of OH· to the second methyl group of Diuron once the first methyl group had been eliminated. This demethylation process has been proposed previously and occurs through the formation of hydroxylated or carboxylated compounds as follows [14]:

$$R\text{-}CH_3 \rightarrow R\text{-}CH_2OH \text{ and/or } R\text{-}CHO \text{ and/or } R\text{-}COOH \rightarrow R\text{-}H \qquad (a1.1.5)$$

Compound 9: N'-(3,4-dichlorophenyl)-N-formyl-N-methyl- urea was identified as the oxidation product of compound 4. Compound 5: N'-(3,4-dichlorophenyl)-N-formoxy-urea, was the result of oxidation of Linuron with the elimination of a methyl group.

Compound 7 and 8, that show the same spectra, were identified as the products of the oxidation of compound 5 (see Figure a1.1.8 for mass spectrum of compounds 5, 7 and 8). No explanation has been found to explain the difference in retention time. The fragment at m/z =202 obtained in MS spectra of compounds 5, 7 and 8 can be explained assuming the formation of a radical anion during the fragmentation process in the electro-spray. In compounds 5, 7 and 8 NH-O-COOH and NH-O-CHO bond were present at the end of the molecule. It can be supposed that in the fragmentation process, the hydrogen atom bonded to the nitrogen atom can be transferred producing the lost of H_2O and CO_2 on the one hand, and H_2O and CO on the other. In those cases Katsumata et al. [16] and Tahmasseb et al. [20] suggest the first attack of OH· radical in the methoxy group of Linuron. Then, OH· attacks the methyl group after eliminate the methoxy group of parent compound. This assumption is contrary to our results.

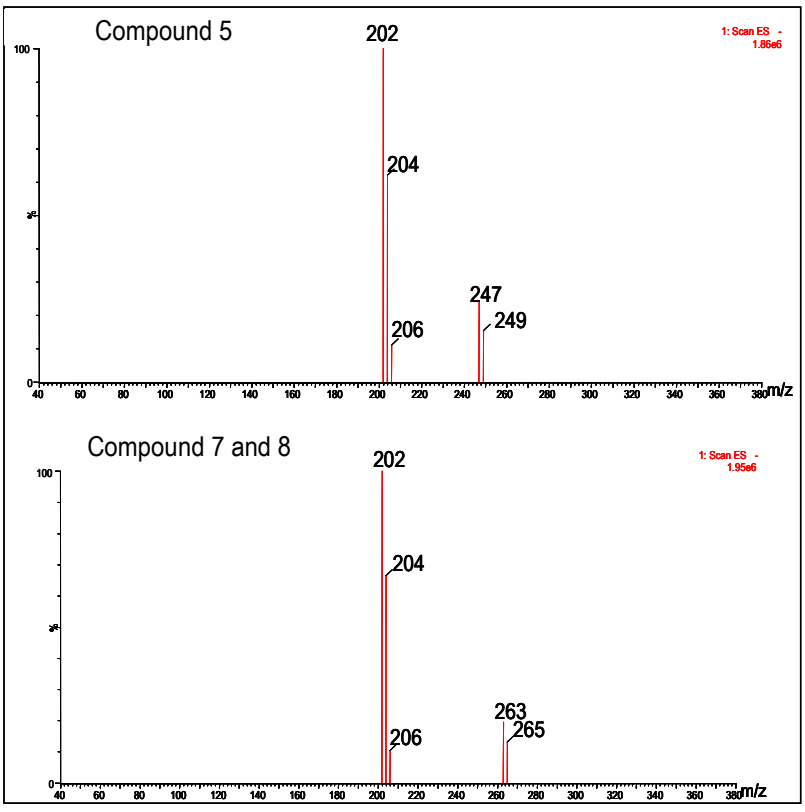

Figure a1.1.8. LC-ESI-MS spectrum of compounds 5, 7 and 8 (Table a1.1.1).

Finally, compound 1 appears to be the product of hydroxyl addition to the benzene ring of the target compounds, once the methyl or hydroxymethyl groups had been eliminated.

All the results, except those for compound 5, 7 and 8, are consistent with previous publications where the presence of two main sites of initial attack by OH· radical in these kinds of compounds was suggested: the aromatic ring and the methyl group [12, 14, 16].

Two different compounds were found in short reaction time experiment. A GC-MS analysis was carried out after 15 minutes of photo-Fenton process using reagent dose A. 3,4-dichloroaniline and 3,4-dichlorophenyl isocyanate were identified by the mass of the molecule and fragment ions and also, through comparison with Wiley library data with similarities up to 86%. Katsumata et al [16] observed 3,4-dichlorophenyl isocyanate in the degradation pathway of Linuron. Moreover, 3,4-dichloroaniline and 3,4-dichlorophenyl isocyanate were also proposed as the main degradation intermediates by Salvestrini et al. [17] in Diuron kinetic studies. These two compounds were no longer detected after 60 minutes of irradiation time for dose A.

Multi residual monitoring (MRM) without concentrating the samples was used to detect the evolution of the first by-products formed during photo-Fenton reaction. Figure a1.1.9 shows the relative evolution of by-products when dose A was used in the oxidation process.

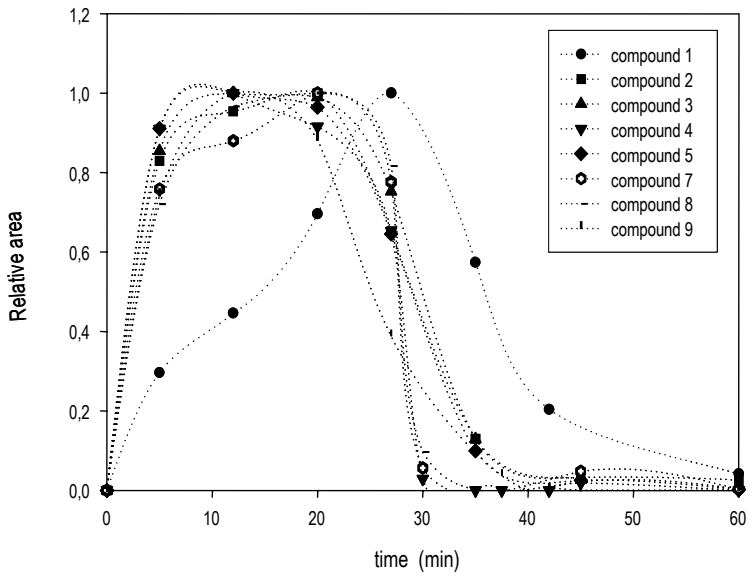

Figure a1.1.9. Relative first by-products evolution during photo-Fenton degradation of Diuron and Linuron herbicides with dose A(9.25 mg·L^{-1} Fe(II), 97.1 mg·L^{-1} H_2O_2). pH=2.8, T=25 ºC.

The kinetic behaviour of the detected by-products clearly confirms that these aromatic compounds undergo further transformation since the concentration at 60 minutes was negligible. Moreover, from Figure a1.1.9 it appears that the oxidation and decarboxilation processes that eliminate alkyl groups seem more favoured than the attack to the aromatic ring by OH· radicals. Samples at 60 minutes of irradiation time were concentrated by means of solid phase extraction on C_{18} cartridges and some traces of compounds 1 to 10 were found. Traces of the intermediates resist the OH· attack as expected at the end of a mineralization process. Similar results were obtained when effluent treated with doses B and C were investigated. In addition to these thirteen compounds, other degradation products could exist in the photo-Fenton system. Nevertheless, they were not detected because of the high polarity of the eluent employed and the low concentrations used.

3.4. Relation between the end by-products formed and biodegradability

The differences between the organic matter present at the end of the three photo-treated effluents were investigated. Smaller and increasingly polar compounds are supposed to be generated along the oxidation process. As described in the introduction, HPLC(HILIC)/MS is the analytical technique that can correctly analyze those small polar compounds.

Differences were found when solutions treated with doses A, B and C were analyzed by means of HPLC(HILIC)/MS. Higher concentrations of methylurea, and 1,1-dimethylurea were identified in the solution treated with dose A. The isotopic distribution of methylurea peak as well as molecular mass and retention time coincided with that of an authentic standard. On the other hand, a N,N´-dimethylurea standard was used to determined the second product detected. Isotopic distribution as well as molecular mass coincided with the standard but retention time was different. Therefore we can consider that the methylurea formed in the degradation of parent compounds was the 1,1-dimethylurea. This assumption is in accordance with the logical order in the degradation pathway.

The percentages of these two final products generated in the oxidation process were analyzed. 100% was arbitrary assigned to the product found in photo-treated solution A, then, based on this the relative amounts in samples B and C were calculated. Methylurea present in

solution B and C reach 43% and 21% respectively. On the other hand 1,1-dimethylurea was not present in phototreated solution C, while only 5% was founded in solution B. Although urea should be present at the end of the oxidation process [18] the comparison of both, the photo-treated solutions with an standard solution of urea indicates its absence.

Biodegradability between 27.3-53.1% has been determined for dimethylurea after 14 days of aerobic domestic sludge treatment [19]. This means that when this product is generated in the chemical step, a higher hydraulic retention time (HRT) in the sequencing batch reactor would be needed to completely eliminate organic matter from solution. In such a case, economic considerations should be necessary in order to give priority to stronger chemical pre-treatment or a longer secondary biological process.

It should be mentioned that the presence of other by-products as methylaniline or short chlorinated compounds can not be rejected but their presence is difficult to determine with the analytical methods used in this work. In fact no total chloride was recovered in photo-treatment of Diuron and Linuron solution with dose A as explain above. Further experiments are required in order to completely close nitrogen and carbon balances in this oxidation process. Based on the intermediate products found in this work and the results obtained by other researchers [12, 16, 20], an improved possible degradation pathway for Diuron and Linuron is proposed in Schemes a1.1.1 and a1.1.2, respectively.

Scheme a1.1.1. Degradation pathways of Diuron by OH·. (A) by-products identified in this work,(B) by-products identified by Malato et al [12] and (C) by-products identified by Tahmasseb et al [20].

* radical attack to benzene ring.

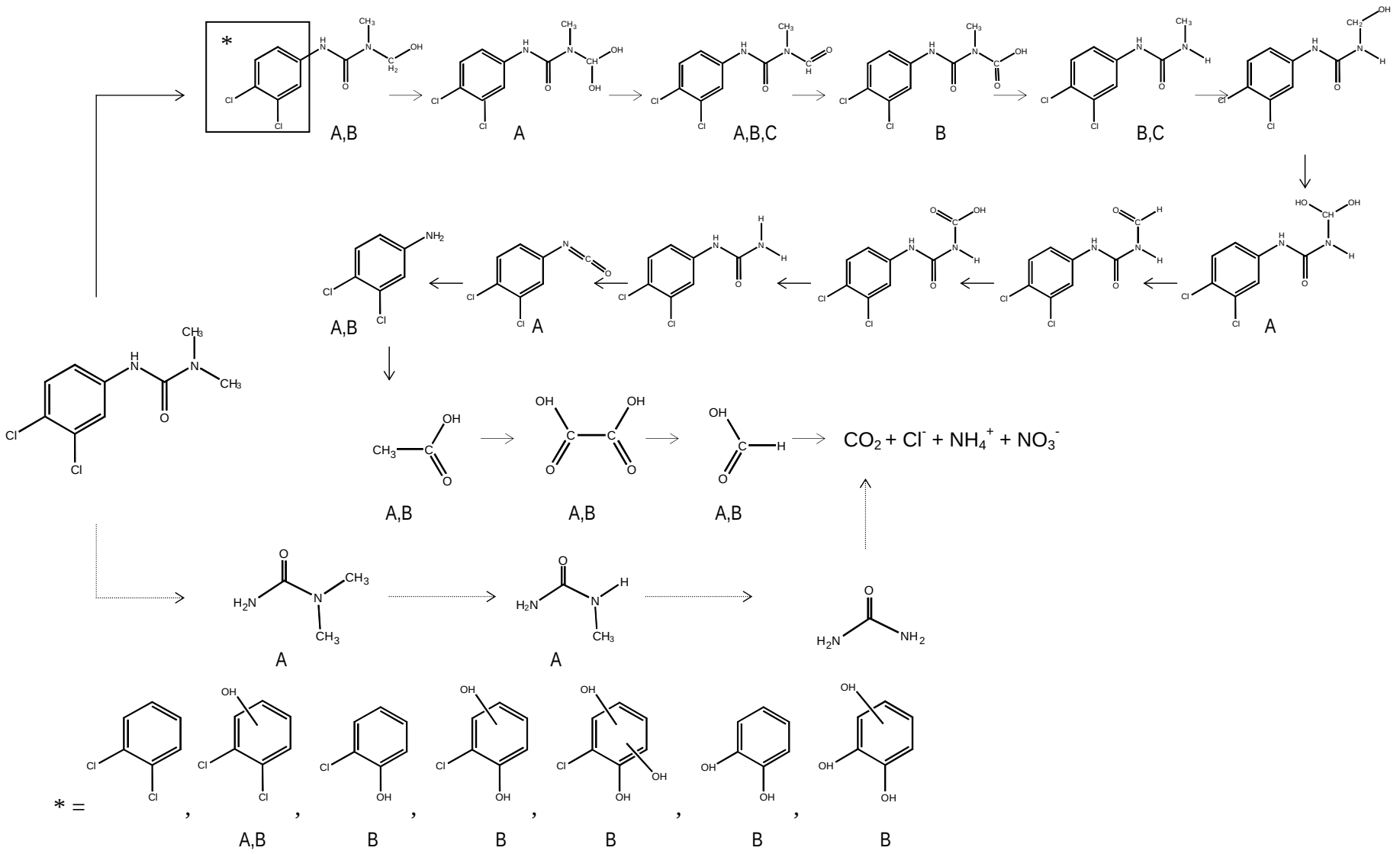

Scheme a1.1.2. Degradation pathways of Linuron by OH·.(A) by-products identified in this work, (C) by-products identified by Tahmasseb et al [20] and (D) by-products identified by Katsumata et al [16].

* radical attack to benzene ring.

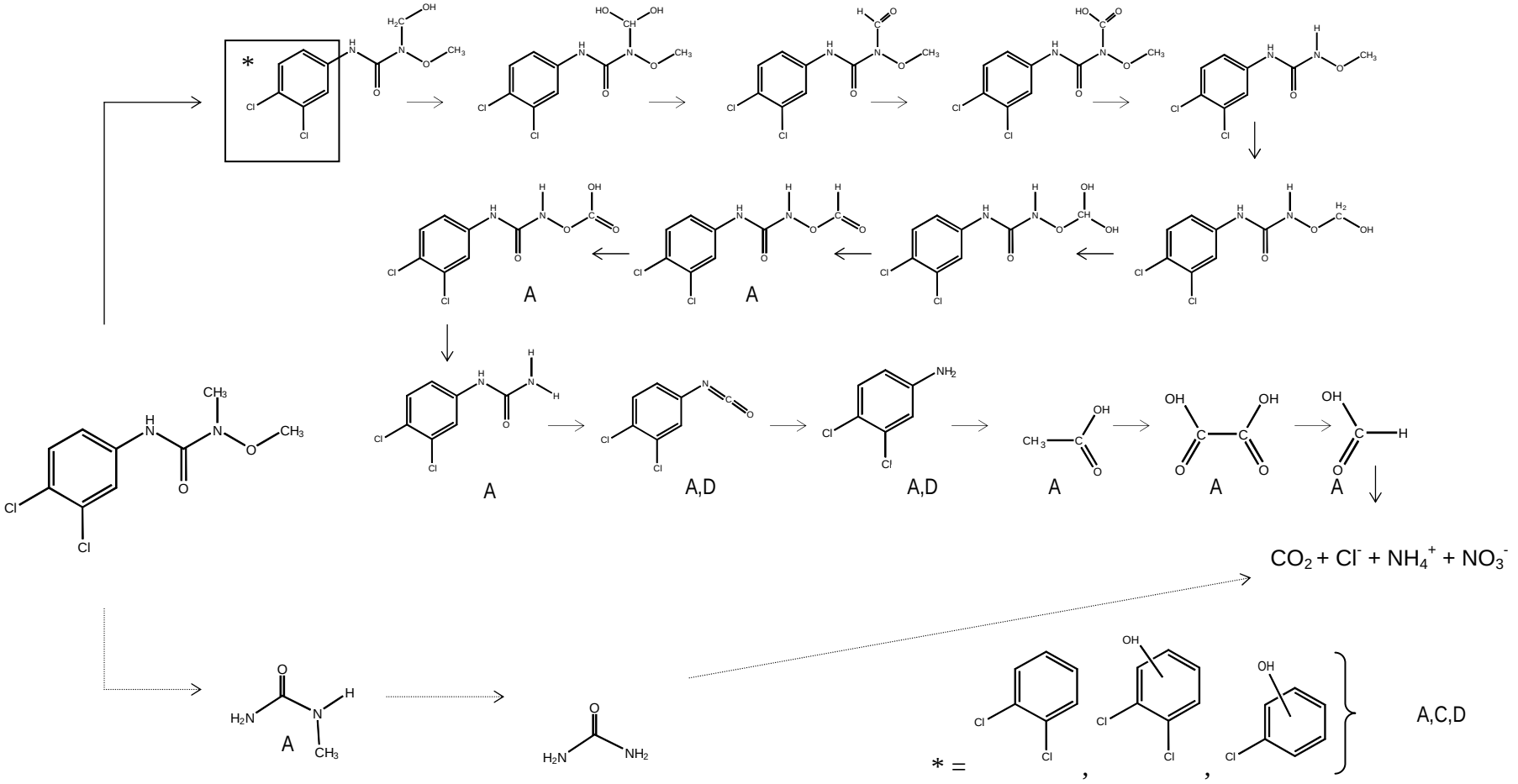

4. Conclusions

The degradation of Diuron and Linuron herbicides has been carried out by means of a chemical (photo-Fenton) and a biological coupled system. Three combinations of reactant dose have been used in the chemical step. Different degrees of elimination of total organic matter have been achieved in the secondary biological treatment depending on the by-products generated in the chemical stage. Formic, oxalic and acetic acids appear at different concentration during the photo-Fenton experiments. The presence of acetic acid has been found to be higher under soft oxidant conditions while an increase in OH· concentration produces a higher concentration of oxalic acid. 3,4-dichloroaniline and 3,4-dichlorophenyl isocyanate have been found as intermediates in the oxidation processes among other hydroxilated by-products.

The presence of methylurea and 1,1-dimethylurea as well as some non identified chlorinated compound seem to be the cause of the different biodegradability of the photo-treated effluents.

Acknowledgements

This work was supported by the Spanish Goverment (MEC, project CTQ2005-02808) and the European Commission (CADOX project, EVK1-CT-2002-00122). We also want to thank Makhteshim Agan España ,S.A. for providing the Linuron herbicide.

REFERENCES TO ANNEXE 1.1.

[1] Pera-Titus M., García-Molia V., Baños M.A., Giménez J. and Esplugas S. (2004). Degradation of chlorophenols by means of advanced oxidation processes: a general review. Appl. Catal. B-Environ. 47, 219-256.

[2] Sarria V., Kenfack S., Guillod O. and Pulgarín C. (2003). An Inovative coupled solar-biological system at field pilot scale for the treatment of biorecalcitrant pollutants. J. Photoch. Photobio. A. 159, 89-99.

[3] Parra S., Malato S. and Pulgarín C. (2002). New integrated photocatalytic-biological flow system using supported TiO_2 and fixed bacteria for the mineralization of isoproturon Appl. Catal. B-Environ. 36, 131-144.

[4] García-Montaño J., Torrades F., García-Hortal J.A., Domènech X. and Peral J. (2006). Combining photo-Fenton process with aerobic sequencing batch reactor for commercial hetero-bireactive dye removal. Appl. Catal. B-Environ. 67, 86-92

[5] Farré M.J., Domènech X. and Peral J. (2006). Assessment of photo-Fenton and biological treatment coupling for Diuron and Linuron removal from water. Water Res. 40, 2533-2540.

[6] Kotsou M., Kyriacou A., Lasaridi K. and Pilidis G. (2004). Integrated aerobic biological treatment and chemical oxidation with Fenton's reagent for the processing of green table olive wastewater. Process Biochem. 39, 1653-1660.

[7] Al Momani F., González O., Sans C. and Esplugas S. (2004). Combining photo-Fenton process with biological sequencing batch reactor for 2,4-dichlorophenol degradation. Water Sci. Technol. 49, 293-298.

[8] Bauer R. and Fallmann H. (1979). The photo-Fenton oxidation a cheap and efficient wastewater treatment method. Res. Chem. Intermed. 23, 341-354.

[9] Haber F. and Weiss J. (1934). The catalytic decomposition of hydrogen peroxide by iron salts. Proc. Roy. Soc. A. 134, 332-351

[10] Pignatello J. (1992). Dark and photoassisted Fe^{3+}- catalyzed degradation of chlorphenoxy herbicides by hydrogen peroxide. Environ. Sci. Technol. 26, 944-951.

[11] Alpert A.J. (1990). Hydrophilic-interaction chromatography for the separation of peptides, nucleic acids and other polar compounds. J. Chromatogr. 499, 177-196.

[12] Malato S., Cáceres J., Fernández-Alba A.R., Piedra L., Hernando M.D., Agüera A. and Vidal J. (2003). Photocatalytic treatment of Diuron by Solar photocatalysis: Evaluation of main intermediates and toxicity. Environ. Sci. Technol. 37, 2516-2524.

[13] Keith L.H. and Telliard W.A. (1979). ES&T Special Report: Priority pollutants: I-a perspective view. Environ. Sci. Technol. 13, 416-423.

[14] Lhomme L., Brosillon S., Wolbert D. and Dussaud J. (2005). Photocatalytic degradation of a phenylurea, chlortoluron, in water using an industrial titanium dioxide coated media. Appl. Catal. B-Environ. 61, 227-235.

[15] Franch M.I., Ayllon J.A., Peral J. and Domènech X. (2002). Photocatalytic degradation of short-chain organic diacids. Catal. Today, 76, 221-233.

[16] Katsumata H., Kaneco S., Suzuki T., Ohta K and Yobiko Y. (2005). Degradation of Linuron in aqueous solution by the photo-Fenton reaction. Chem. Eng. J. 108, 269-276.

[17] Salvestrini S., Di Cerbo P. and Capasso S. (2002). Kinetics of the chemical degradation of Diuron. Chemosphere. 48, 69-73.

[18] Hincapié M., Peñuela G., Maldonado M.I., Malato O., Fernández-Ibáñez P., Oller I., Gernjak W. and Malato S. (2006). Degradation of pesticides in water using solar advanced oxidation processes**.** Appl. Catal. B-Environ. 64, 272-281.

[19] OECD HPV Chemical Programme, SID Dossiers (SIAM 17, 2003)

[20] Tahmasseb L.A., Nélieu S. and Kerhoas L. and Einhorn J. (2002). Ozonation of chorophenylurea pesticides in water: reaction monitoring and degradation pathways. Sci. Total Environ. 291, 33-44.

a1.2. Life Cycle Assessment of the removal of Diuron and Linuron herbicides from water using three environmentally friendly technologies.

Accepted for publication in Environmental Technology.

MªJosé Farré, Julia García-Montaño, Nilbia Ruiz, Ivan Muñoz, Xavier Domènech and José Peral*.

Departament de Química. Universitat Autónoma de Barcelona. 08193 Bellaterra. Spain

Abstract

Nowadays, every chemical treatment must be developed taking into account its global impact on the environment. With this objective a life cycle assessment (LCA) has been used as a tool for the evaluation of the environmental impact of three environmentally friendly processes for the removal of Diuron and Linuron herbicides from water: artificial light assisted photo-Fenton, photo-Fenton coupled to biological treatment and solar assisted photo-Fenton. The inventoried data has been classified considering the potential environmental impacts categories included in the CML 2 baseline 2000 method. Among the three scenarios considered, photo-Fenton coupled to biological treatment proved to have the lowest environmental impact in all the studied categories due to the lower hydrogen peroxide and electricity consumptions. The environmental impacts associated to hydrogen peroxide and electricity production imply more than 72% in all the impact categories of the three scenarios, except for aquatic eutrophication potential category, in which main impacts are related to nitrogen emissions.

Keywords: Advanced oxidation process, photo-Fenton, biological treatment, coupling, environmental impact.

1. Introduction

Nowadays, wastewaters polluted with pesticides are an important problem for human health. A part from lixiviates coming from agricultural fields, washing of herbicide containers and unused treatment solutions also contribute to this problem producing highly polluted effluents that should be treated before their disposal in the environment [1]. The World Health Organization estimates that around 20.000 deaths are produced by agrochemical poisons every year and the 99% of them take place in developing countries. In those situations, wastewater treatment is indispensable.

Due to their biorecalcitrant and toxic properties wastewaters polluted with pesticides can not be directly treated in a conventional wastewater treatment plant based on the activity of a microbiological consortium. Thus, the development of new technologies that pursue the easy degradation of such substances is of practical interest.

Advanced oxidation processes (AOPs) are new technologies based on the *in situ* production of the highly reactive hydroxyl radical (HO·) (E^o= 2.8 vs SHE) that oxidizes organic matter to CO_2 under mild experimental conditions. Among the most studied AOPs like ozonation [2] or heterogeneous photocatalysis with TiO_2 [3], photo-Fenton is frequently preferred because it achieves high reaction yields with low treatment costs, mainly due to the possibility of a more efficient use of solar light as photon source [4]. In the Fenton process hydroxyl radicals promoters are Fe(II) salts and hydrogen peroxide [5].

$$Fe(II) + H_2O_2 \rightarrow Fe(III) + OH^- + HO\cdot \qquad (a1.2.1)$$

Under irradiation of λ<410 nm, Fe(III) can be reduced to Fe(II) closing a loop mechanism where Fe species act as catalyst, giving rise to additional HO· [6](photo-Fenton process).

$$Fe(III) + H_2O + h\nu \rightarrow Fe(II) + HO\cdot + H^+ \qquad (a1.2.2)$$

Advanced oxidation processes (AOPs) coupled to a biological treatment by means of a Sequencing Batch Reactor (SBR) is of emerging interest in this experimental and applied scientific field [7, 8, 9, 10]. After a chemical pretreatment, initial toxic and/or non biodegradable compounds can be assimilated by biomass in a SBR obtaining a free of pollution effluent.

In the last decades, environmental awareness has increased in such a way that, apart from technical and financial aspects, environmental considerations play an increasingly important role in the selection of water treatment technologies [11].

The removal of Diuron and Linuron herbicides from water has been previously studied by our group [10]. These herbicides have been selected as a model of toxic and non biodegradable organic matter. Both phenylurea compounds act as inhibitors of photosynthesis, thus impeding weed growth and are used for selective control of germinating grass and broad-leaved weeds in many crops (e.g. cereals) [12].

The assessment, from an environmental point of view, of the different AOP combinations tested in the removal of Diuron and Linuroin is of practical interest. Life cycle assessment (LCA) has been chosen for this purpose. LCA is a systematic way to evaluate the environment impact of products or processes by following a *cradle-to-grave* approach according to ISO 14.040 standard methodology [13]. Using this tool three wastewater technologies will be analyzed in order to prove which of them is the most environmentally compatible. The three wastewater treatment technologies selected for this work are; (i) artificial light assisted photo-Fenton, (ii) artificial light assisted photo-Fenton coupled to a biological treatment and finally (iii) solar assisted photo-Fenton.

The literature on environmental performance of AOPs is limited [14-17]. As a consequence, it is important to perform an LCA of those different environmentally friendly wastewater treatments in order to prove their environmental compatibility.

2.Materials and methods

2.1.Preparation of initial wastewater

Diuron (98.5% Aragonesas Agro S.A. technical grade) and *Linuron* (92.6% Makhteshim Agan España, S.A.) were used as target compounds in the experiments. A unique solution of 42 $mg \cdot L^{-1}$ of Diuron and 75 $mg \cdot L^{-1}$ of Linuron was prepared in Mili-Q quality water. Those values correspond to the maximum solubility of both herbicides in water at 25 ^{o}C. A saturated initial solution was prepared and then filtrated by means of a 20 μm Nylon filter. The initial features of the filtered solution were as follow: pH=5.7, TOC=50±2 $mg \cdot L^{-1}$, COD=139±7 $mg \cdot L^{-1}$, BOD_5=≤5 $mg \cdot L^{-1}$, $BOD_5/COD \leq 0.033$. This initial solution was transparent and colorless. The solution was biorecalcitrant as seen by the Zahn-Wellens test [18]. Adsorption of TOC on the biomass was not observed after the 28 days of the test duration.

2.2. Photo-Fenton oxidation process

$FeSO_4 \cdot 7H_2O$ (Merck) and H_2O_2 (Panreac, 33% w/v) were used as photo-Fenton reagents. Oxidation experiments were conducted at 25±0.2 ^{o}C in a 0.25 L cylindrical Pyrex thermostatic cell equipped with a magnetic stirrer. A 6W Phillips black light was used as light source, providing a light intensity of 0.21 $mW \cdot cm^{-2}$. The illuminated reactor surface was 49.3 cm^2.

The experimental procedure was as follows: in each experiment the photo-reactor was charged with 0.250 L of solution to be photo-treated. The pH of the solution was always adjusted to 2.8 and the required amount of solid $FeSO_4 \cdot 7H_2O$ was added. Finally, the hydrogen peroxide was added to the solution and UV light was immediately switched on. Reagent dosage was different depending on the studied scenario.

2.3. Biological treatment

A sludge sample taken from the aerobic stage of an urban wastewater treatment plant in Manresa (Spain),with an initial volatile suspended solids (VSS) content around 5 $g \cdot L^{-1}$, was used

as inoculum in the SBR. A dilution was carried out to obtain a final VSS value of 0.6 $g \cdot L^{-1}$. The daily operation procedure was explained elsewhere [10]. The operating volume was 1.250 L and the hydraulic retention time (HRT) was two days. The biological experiment was carried out during 12 cycles (24 days) in order to obtain repetitive results (i.e. variation coefficients of TOC removal lower than 4%). Temperature remained stable at 20 ^oC (room temperature). pH and dissolved oxygen (DO) were controlled daily. pH was adjusted to 7 and DO was kept above 3 $mg \cdot L^{-1}$. Moreover, daily analysis of VSS and TOC were carried out.

2.4. Analytical Methods

TOC was analyzed with a Shimadzu TOC-V_{CSH} analyzer. COD was determined with a close reflux method [19], using 0-150 $mg \cdot L^{-1}$ range Aqualytic® vials. A HACH COD reactor and a HACH DR/2000 spectophotometer were used in the COD analyses. The accuracy of the COD measurements was checked by preparing a potassium hydrogen phthalate standard. Correction of hydrogen peroxide interference on the COD test was required [20]. The H_2O_2 was analyzed by a modified iodometric method [21] explained elsewhere [10]. At the end of the oxidation process, biochemical oxygen demand (BOD_5) was determined by means of a mercury-free WTW 2000 Oxytop thermostated at 20 ^oC. In those analysis, the measurement accuracy was checked with a standard mixture of 150 $mg \cdot L^{-1}$ glucose and 150 $mg \cdot L^{-1}$ glutamic acid. Ammonium ion concentration was determined by the Nessler colorimetric assay [19] using a Helios Gamma UV-Visible spectrometer from Thermo Electron Corporation. Nitrate ion concentration was analyzed by means of ionic chromatography. The IC system included a LC-10AT VP pump (Shimatzu) and a 656-Conductimetric Detector Metrohm. A 10% in volume acetone solution containing 5 mM phtalic acid (pH=5) was used as mobile phase, finally a PRP-100 from Hamilton was used as stationary phase. Gravimetrical determination of total suspended solids (TSS) and VSS was carried out according to Standard Methods [19].

3. Life Cycle Assessment Methodology

For the application of the LCA tool, the ISO 14040 Standard was used [13]. The study was undertaken in four main phases, namely: (1) Goal and scope, in which the purpose, scope, main hypothesis and type and quality of data are defined; (2) Inventory analysis, in which data are collected in order to quantify the inputs and the outputs of the system; (3) Impact assessment, in which the potential environmental impacts produced by the system under study are identified and characterized, and (4) Interpretation, in which the obtained results are discussed in terms of critical sources of impact in the whole process and the ways or opportunities to reduce these impacts.

3.1. Goal and scope

The environmental impact assessment was focused on the following small-scale wastewater treatment for the removal of Diuron and Linuron herbicides from water: artificial light assisted photo-Fenton process (scenario 1), artificial light assisted photo-Fenton process coupled to a biological treatment (scenario 2) and solar assisted photo-Fenton process (scenario 3).

This LCA study was intended to gain insight on the environmental impact of these three processes and to compare them from an environmental point of view.

In order to compare the three scenarios a functional unit was selected. The functional unit enables different systems to be treated as functionally equivalent and allows reference flows to be determined for each of them [22]. The functional unit was defined as “The removal of more than 80% TOC from a 1.25 L of Diuron and Linuron saturated effluent (TOC= 50 $mg \cdot L^{-1}$)”. The different scenarios are described as follows:

3.1.1. Scenario 1

Complete mineralization was achieved in a unique chemical step (i.e. photo-Fenton process). 15.9 mg·L^{-1} of $FeSO_4 \cdot 7H_2O$ and 415.2 mg·L^{-1} were required to reach the selected percentage on TOC removal (i.e. 83%). The UVA irradiation time needed was 8.5 hours.

Scenario 2

15.9 mg·L^{-1} of FeSO4·$7H_2O$ and 202 mg·L^{-1} of H_2O_2 were used in the chemical step. The photo-treatment time selected was 60 minutes. After this time, 36% of TOC removal was acquired and the photo-treated solution reached BOD_5/COD ratio close to 0.4. It is well-known that the wastewater BOD_5/COD ratio must reach the 0.4 value to consider it completely biodegradable [23]. At this point the solution was used to feed a biological sequencing batch reactor (SBR). Complete TOC elimination was achieved at the end of the biological treatment (i.e. 100% TOC removal). The remaining TOC concentration at the end of the biological treatment (i.e. 8.125 mg·L^{-1}) matched the concentration of the residual TOC due to the biomass metabolism [10].

Scenario 3

Since the main disadvantage of Advanced Oxidation Processes is the high electricity consumption, and taking into account that photo-Fenton process can work under natural solar light, a third scenario, using the same scenario 1 conditions but replacing the black light by sunlight, was also studied. Figure a1.2.1 shows the flow diagram of the system and boundaries considered in scenario 1. When scenario 3 is considered, production of electricity must be eliminated from scenario 1 flow diagram. Figure a1.2.2 shows the flow diagram of the system and boundaries considered in scenario 2.

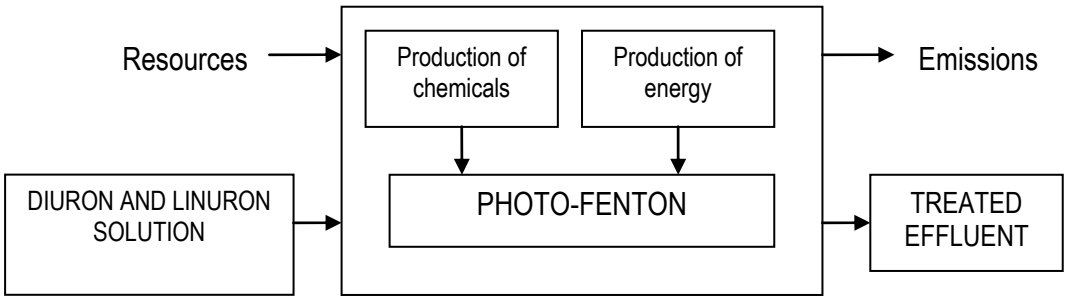

Figure a1.2.1. Simplified flow diagram and system boundaries for scenarios 1 and 3. When scenario 3 is considered electricity production must be eliminated from the diagram.

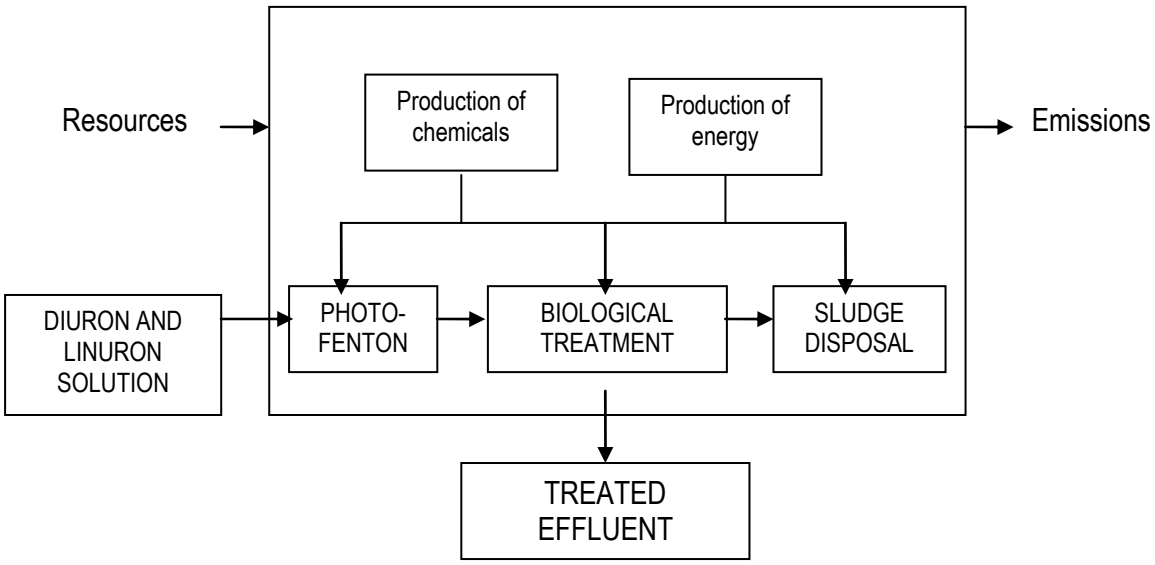

Figure a1.2.2. Simplified flow diagram and system boundaries for scenario 2.

3.2. Inventory analysis

The processes included in the inventory of the different studied treatments for the removal of Diuron and Linuron herbicides from water are: (i) production of consumed electricity, including extractions of resources, transport and electricity production, (ii) production of chemicals, including extraction of resources, production and transport, and (iii) air and water emissions generated through the considered scenarios. The construction and the end-of-life of the infrastructure needed in each case have not been considered. Table a1.2.1 summarizes the

sources and quality of the data used to perform the inventory analysis. This data was obtained from the Ecoinvent version 1.2 database [24].

Table a1.2.1. Data used in the Life Cycle Assessment inventory phase.

Topic	Reference
Iron sulphate, at plant/RER S	35
Hydrogen peroxide, 50% in H_2O, at plant/RER S	36
Acrylonitrile, at plant/RER S	37
Lime, hydrated, packed, at plant/CH S	38
Heat diesel B250	34
Transport, lorry 16t/RER S	39
Electricity, medium voltage, production UCTE, at gird/UCTE S	40

The main hypothesis and limitations assumed in the present work are published elsewhere [17] and can be summarized as follows:

-For the photo-Fenton process the energy used to run the UVA light has been assumed to be electricity delivered from the European grid. 100% efficiency has been considered in order to obtain operational conditions similar to those employed in a full-scale photochemical reactor. This assumption implies that all the photons emitted by the UVA lamp reach the solution. In fact, in the laboratory set-up used in this work a large fraction of photons were wasted. The light intensity coming from the black light is 0.21 $mW \cdot cm^{-2}$ and the reactor surface is 49.3 cm^2. Thus, the calculated efficiency of the 6W lamp is 0.17%.

-H_2O_2 and $FeSO_4$ have been assumed to be produced in Spain and delivered from the supplier to the site by 16 ton-trucks over a 50 km distance. It has been assumed that residual H_2O_2 is totally decomposed after each photo-Fenton process.

-Since iron emissions after the oxidation process are equivalent in the three considered scenarios, the removal of this residual has been excluded from this study.

-CO_2 emissions have been estimated according to the TOC mineralized in the chemical oxidation process. Residual TOC, COD, ammonium and nitrate ions content have been considered for final effluent impact assessment.

-The biological process has been modeled in the LCA assuming a conventional biological treatment process. A municipal WWTP with a 0.76 VSS/TSS ratio has been chosen as a model assuming an excess sludge production of 0.55 mg VSS per mg COD consumed [32]. External electricity consumption for mechanical aeration of 1.5 kg O_2/ kWh [33] has been considered. The oxygen required for organic matter oxidation has been determined from the removed COD in the SBR (i.e. 28.75 mg·L^{-1}) minus the COD fraction assimilated by the biomass (i.e. 24.04 mg·L^{-1}) quantified as 1.52 mg O_2 per mg VSS of sludge production, since sludge composition considered is $C_8H_{15}O_4N$ [34]. On the other hand, oxygen required for nitrification of ammonium has been also considered. The oxygen required for nitrification has been determined from the removed NH_4^+ in the SBR (i.e. 10.36 mg·L^{-1}) minus the NH_4^+ fraction assimilated by the biomass (i.e. 1.25 mg·L^{-1}), quantified as 0.074 mg NH_4^+ per mg VSS of sludge production, according to the sludge composition above defined.

-The CO_2 emissions at the end of the biological treatment have been determined by considering the COD eliminated in the SBR after the subtraction of the COD required for biomass grown. Residual TOC, COD, ammonium and nitrate ions content has been considered for final effluent impact assessment. Nitrate concentration has been estimated by considering that all the disappeared NH_4^+, minus the N fraction assimilated by the biomass for cells growth, was completely oxidized to NO_3^- through aerobic biodegradation.

-A subsequent sludge treatment system composed of several independent unit processes has been considered [35]: thickening, dewatering and stabilization process. By means of this treatment, a dewatered sludge with 31% final dry matter content (DM) is obtained. 50 kWh of electricity and 4 kg of polymers per ton of DM of sludge have been considered to be consumed at the thickening stage and, while 40 kWh and 5kg of polymer per ton of DM of sludge have been considered for the dewatering stage. On the other hand, 200kg of lime per ton of DM of sludge are needed for stabilization while 5kWh of electricity are consumed for pumping and mixing [35].

-It has been assumed that solid residues from excess sludge management are finally deposited in a landfill (i.e. 8.114×10^{-8} t). The main environmental emissions from the landfill (leachate and

landfill gas) have been calculated according to the ORWARE (Organic Waste Research) model [36, 37]. By means of this model, the air/water/land distribution of different elements deposited in a landfill can be obtained, considering a period of 100 years for biochemical stabilization after anaerobic sludge digestion. An input to the model is the amount of fresh sludge (without the lime and polyelectrolyte) (i.e. 7.679×10^{-8} t). This sludge is 27% in DM and the sludge chemical composition is $C_8H_{15}O_4N$, which is transformed according the following process [37]:

$$2\ C_8H_{15}O_4N \rightarrow 9\ CH_4 + 7\ CO_2 + 2\ NH_3 \qquad (a1.2.3)$$

-The model considers that the leachate generated at the landfill is treated biologically and that the recovered biogas (99% both CO_2 and CH_4 [38]) is totally burned in a torch. 50% capture efficiency for biogas [39] and 90% for leachate [40] have been assumed. The electricity consumption for biogas pumping is considered to be 0.013 $kW \cdot m^{-3}$as indirectly determined from the BUWAL 250 database [41], which gives 1.35 kWh per ton of residue that produces 200 m^3 of biogas. Fugitive biogas and leachate reach the atmosphere and aquatic media, respectively. The removal yields considered for the captured leachate treated in a subsequent biological reactor are 90% for both COD and BOD_7 [38] and 80% for $N\text{-}NH_4^+$ [39]. Atmosphere emissions and the management of the sludge generated during the leachate treatment have been excluded from the inventory.

-With regard to the energy requirements, 1.8 L of diesel consumption per ton of fresh sludge (considering also the lime and the polymer, i.e. 8.114×10^{-8} t)) have been considered for machinery operation at landfill [29]. The energy consumption (electricity) for leachate treatment has been quantified as a function of the BOD_7 and NH_4^+ eliminated, following the ORWARE methodology.

-All reagents used in the biological treatment have been supposed to be produced in Spain and delivered by 16 ton-trucks. The assumed distance for transport of the lime and the polymer employed in the biological sludge disposal process was 50 km. The average distance for the sludge transport between the municipal WWTP and the landfill site has also been considered to be 50 km. Table a1.2.2 summarizes data concerning energy, chemical consumption and generated emissions per functional unit in each considered scenario.

Table a1.2.2. Inventoried data per functional unit corresponding to scenarios 1, 2 and 3.

Inputs	Scenario1	Scenario 2	Scenario 3
Photo-Fenton treatment			
$FeSO_4$ (mg)	54.09	54.09	54.09
H_2O_2 (mg)	1038	505	1038
$FeSO_4$ transport (50km, 16 ton-truck)(tkm)	2.704×10^{-6}	2.704×10^{-6}	2.704×10^{-6}
H_2O_2 transport (50km, 16 ton-truck)(tkm)	5.189×10^{-5}	2.525×10^{-5}	5.189×10^{-5}
Energy required to run UVA light (kWh)	4.889×10^{-4}	5.752×10^{-5}	-
Biological treatment			
energy required for mechanical aeration (kWh)	-	2.474×10^{-5}	-
Biomass post-treatment			
sludge production (t)	-	2.081×10^{-8}	-
lime (t)	-	4.161×10^{-9}	-
acrylonitrile (t)	-	1.873×10^{-11}	-
lime transport (50km, 16 ton-truck)(tkm)	-	2.081×10^{-7}	-
polymer transport (50km, 16 ton-truck)(tkm)	-	9.363×10^{-9}	-
energy required for thickening, dewatering and stabilization process (kWh)	-	1.977×10^{-6}	-
Sludge disposal			
sludge transport to landfill (tkm)	-	4.057×10^{-6}	-
diesel for machinery operation at landfill (kg)	-	1.227×10^{-7}	-
energy required at landfill for biogas pumping and treatment of leacheated (kWh)	-	3.686×10^{-6}	-
Outputs	Scenario 1	Scenario 2	Scenario 3
Photo-Fenton treatment emissions			
emissions to air			
CO_2 (mg)	191.4	82.5	191.4
emissions to water			
NO_3^- (mg)	0.7563	-	0.7563
NH_4^+(mg)	13.43	-	13.43
COD (mg)	15	-	15
TOC (mg)	10.32	-	10.32
Biological treatment emissions			
emissions to air			
CO_2 (mg)	-	6.483	-
emissions to water			
NO_3^- (mg)	-	31.38	-
NH_4^+(mg)	-	3.066	-

COD (mg)	-	12.50	-
TOC (mg)	-	8.125	-
Sludge disposal emissions (ORWARE)			
emissions to air			
CH_4 (mg)	-	2.304	-
CO_2 (mg)	-	21.15	-
NH_3(mg)	-	6.144×10^{-3}	-
NO_x(mg)	-	7.679×10^{-2}	-
emissions to water			
COD (mg)	-	4.608×10^{-2}	-
NH_4^+(mg)	-	3.840×10^{-1}	-
NO_3^- (mg)	-	1.613	-

3.3. Impact assessment

Following the inventory analysis, the impact assessment phase for the removal of Diuron and Linuron herbicides from water was carried out. The inventoried data (i.e. Table a1.2.2) was classified considering the following potential environmental impact categories included in the CML 2 baseline 2000 2.03 method [22]: Abiotic resource depletion (ARD), that are natural resources (including energy resources) which are regarded as non-living; global warming potential (GWP), that refers to the impact of human emissions on the radiative forcing of the atmosphere; ozone depletion potential (ODP), that refers to the thinning of the stratospheric ozone layer as a result of anthropogenic emissions. Human toxicity potential (HTP), that covers the impacts on human health of toxic substances present in the environment; freshwater aquatic toxicity potential (FATP), marine aquatic ecotoxicity potential (MAEP) and terrestrial ecotoxicity potential (TEP) that refers to the impacts of toxic substances on freshwater aquatic ecosystem, marine aquatic ecosystem and terrestrial ecosystem respectively; photochemical oxidation potential (POP), that refers to the formation of photo-oxidants such as ozone by the action of sunlight on certain primary air pollutants; acidification potential (AP), that contains a wide variety of impacts on soil, groundwater, surface waters, biological organisms, ecosystems and materials due to acidifying pollutants as SO_2, NO_x and NH_x; finally, aquatic eutrophication potential (AEP), that covers all potential impacts of excessively high environmental levels of macronutrients, the most important

of which are nitrogen and phosphorous. Table a1.2.3 shows the environmental profile, that is, the characterization scores obtained for each scenario and impact categories.

Table a1.2.3. Environmental impact data characterization for scenarios 1, 2 and 3.

Environmental impacts categories	*unit*	*Scenario 1*	*Scenario 2*	*Scenario 3*
Abiotic Resource Depletion	kg Sb eq	1.15×10^{-5}	5.12×10^{-6}	9.78×10^{-6}
Global Warming Potential	kg CO_2 eq	1.62×10^{-3}	7.96×10^{-4}	1.38×10^{-3}
Ozone Depletion Potential	kg CFC-11 eq	1.20×10^{-10}	5.66×10^{-11}	1.10×10^{-10}
Human Toxicity Potential	kg 1,4-D* eq	3.86×10^{-3}	1.87×10^{-3}	3.81×10^{-3}
Freshwater Aquatic Toxicity Potential	kg 1,4-D* eq	2.70×10^{-4}	1.28×10^{-4}	2.56×10^{-4}
Marine Aquatic Ecotoxicity Potential	kg 1,4-D* eq	6.22×10^{-1}	2.58×10^{-1}	4.66×10^{-1}
Terrestrial Ecotoxicity Potential	kg 1,4-D* eq	9.25×10^{-6}	4.20×10^{-6}	8.17×10^{-6}
Photochemical Oxidation Potential	kg C_2H_4 eq	2.34×10^{-7}	1.14×10^{-7}	1.83×10^{-7}
Acidification Potential	kg SO_2 eq	5.36×10^{-6}	2.30×10^{-6}	4.07×10^{-6}
Aquatic Eutrophication Potential	kg PO_4^{3-} eq	5.30×10^{-6}	4.93×10^{-6}	5.23×10^{-6}

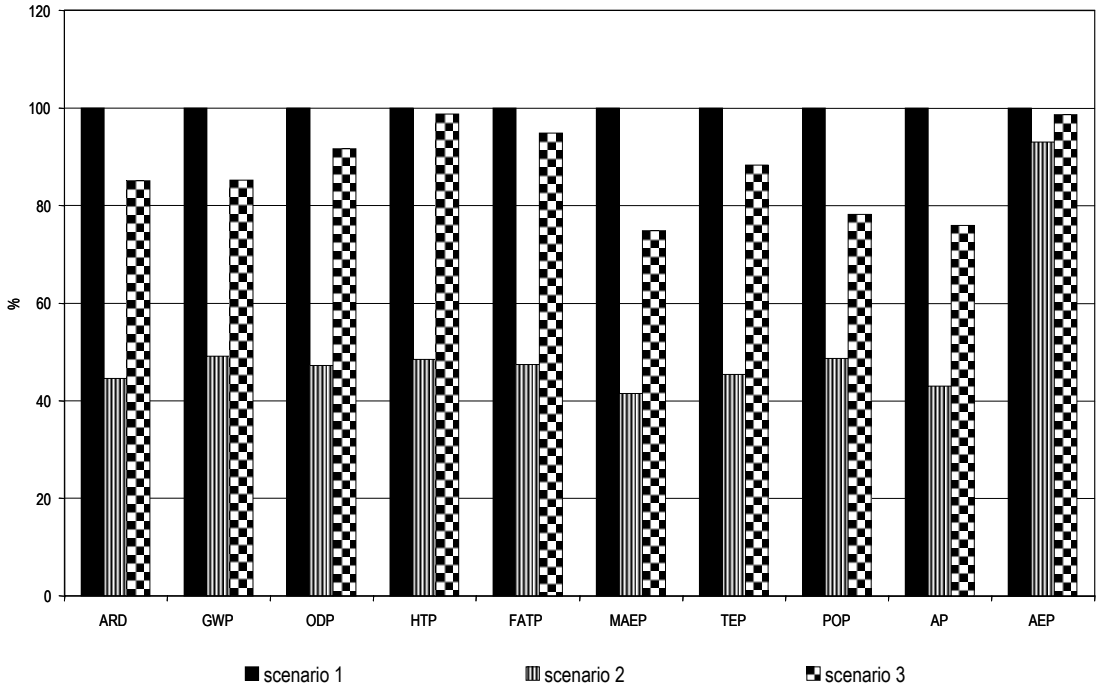

Figure a1.2.3. General environmental impact data for scenarios 1, 2 and 3.

3.4. Interpretation

From the environmental impact data summarized in Table a1.2.3 and graphically represented in Figure a1.2.3, it can be observed that the most environmentally friendly process for the treatment of wastewater polluted with Diuron and Linuron herbicides is the coupling of photo-Fenton and biological treatment (i.e. scenario 2). In Figure a1.2.3, the highest environmental impact (that always corresponds to scenario 1, i.e. artificial light assisted photo-Fenton) is set to 100% for each category and the impacts associated to scenario 2 and 3 are calculated according to this percentage.

These results show that the photo-Fenton and biological coupled treatment (i.e. scenario 2) exhibit the lowest environmental impact scores in all the studied categories, being the scores in all categories less than half of those related to the artificial light assisted photo-Fenton (except for aquatic eutrophication potential). For the aquatic eutrophication potential category, similar results can be observed for all the scenarios. When Diuron and Linuron are oxidized by means of an AOP, the urea group is attacked by the hydroxyl radical and nitrogen is liberated to the media mainly in form of ammonia ion. Later, in the biological treatment, ammonia ion is converted to nitrate ion due to the bacteria nitrification process, both ammonia and nitrate contribute to this environmental impact category.

With regard to solar assisted photo-Fenton a general reduction in all impact categories can be observed due to the elimination of electricity usage.

Despite the low impact score associated to the coupled chemical and biological treatment, a relatively high coefficient related to the marine aquatic ecotoxicity impact can be observed (see Table a1.2.3). At this point, and for a better understanding of these results, a contribution analysis for each scenario has been performed.

This individual analysis is aimed at identifying the critical subsystems for each treatment and impact category. For this purpose the characterization results are disaggregated so that the contribution of the chemical products, electricity, transport and emissions to air and water can be analyzed. Figures a1.2.4, a1.2.5 and a1.2.6 show (for scenario 1, 2 and 3 respectively) these relative contributions. Every impact indicator is expressed as 100%, being the contribution of a sub-system a fraction of the figure.

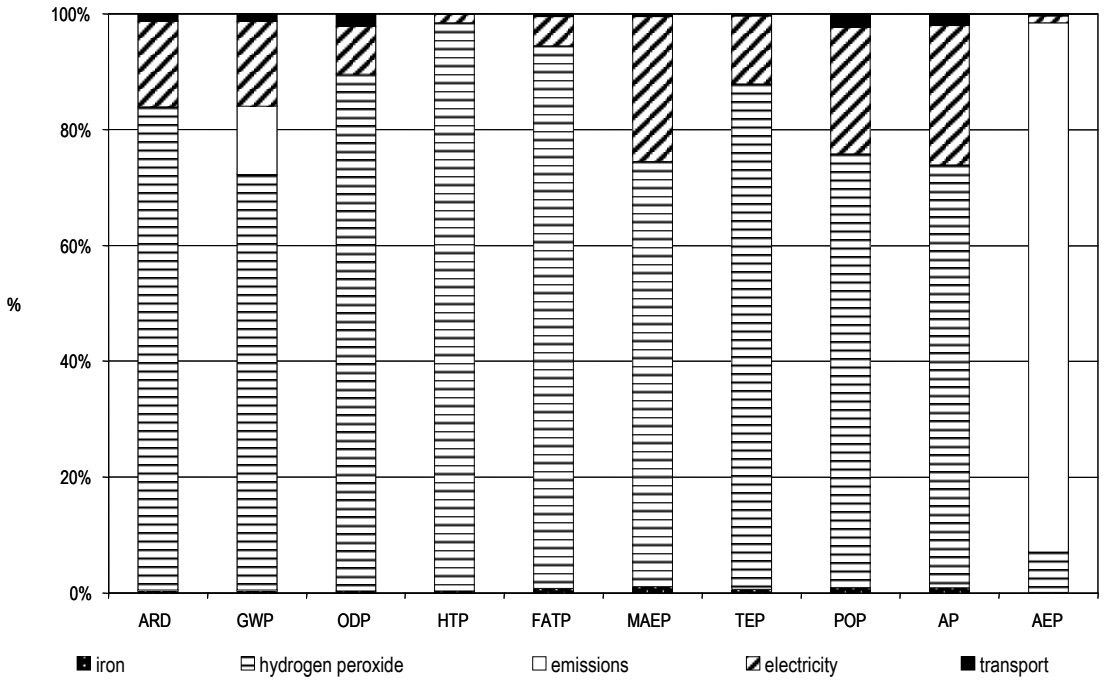

Figure a1.2.4. Relative contributions, due to the chemical products, electricity, transport and emissions to air and water, to different environmental impact categories for scenario 1.

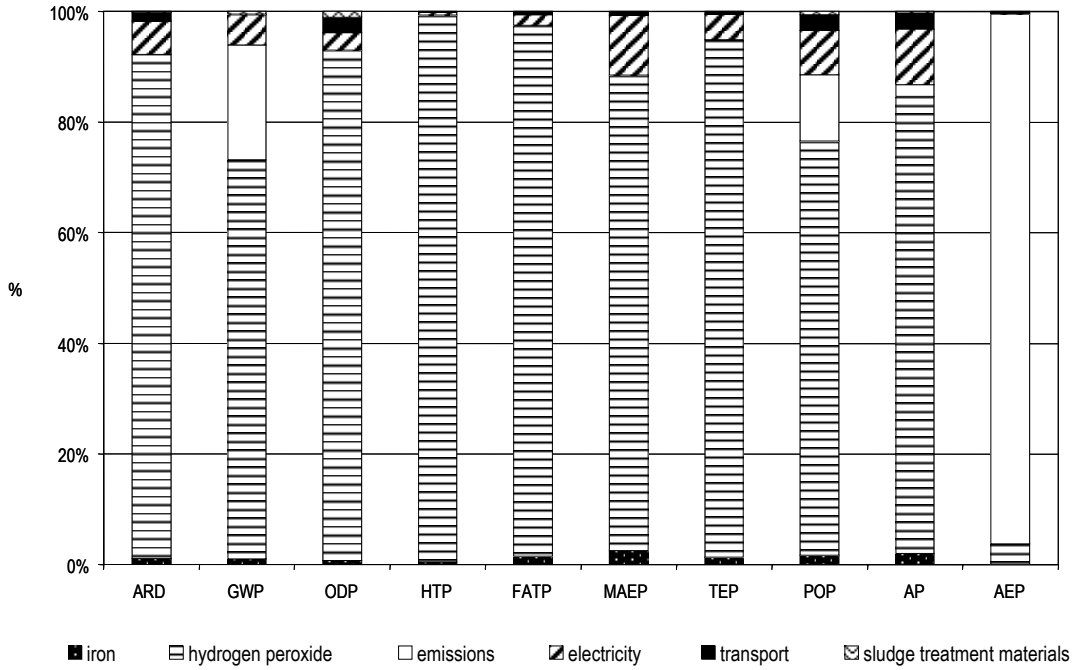

Figure a1.2.5. Relative contributions, due to the chemical products, electricity, transport and emissions to air and water, to different environmental impact categories for scenario 2.

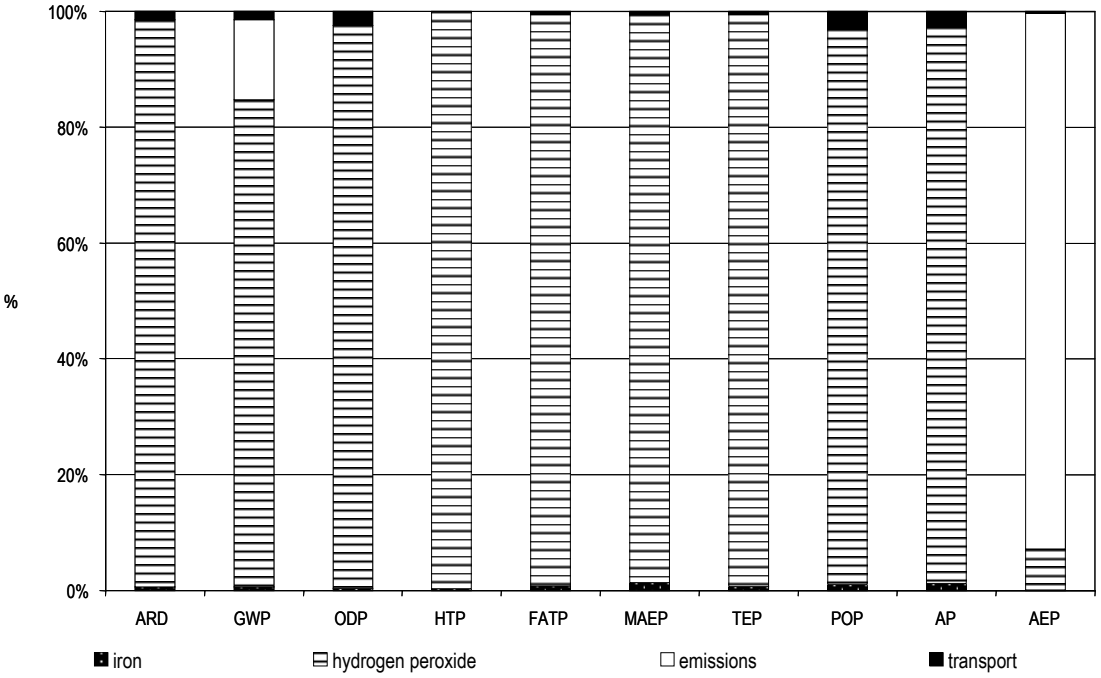

Figure a1.2.6. Relative contributions, due to the chemical products, electricity, transport and emissions to air and water, to different environmental impact categories for scenario 3.

In an attempt to facilitate the interpretation of the results, those processes inventoried by means of the same source of information (see Table a1.2.1) have been grouped in the figures; On one hand, transport of different materials (i.e. hydrogen peroxide, iron, lime, acrylonitrle, sludge transport to landfill) has been aggregated in one coefficient contribution named transport. Electricity for different processes has been also aggregated (i.e. electricity required to run UVA light, for mechanical aeration, for thickening, dewatering, stabilization and electricity required at landfill). On the other hand, impacts associated to COD, TOC, CO_2, NH_4^+, NH_3, NO_x and NO_3^- emissions have been also aggregated in one category named emissions (see Table a1.2.3 for concentration details). Finally materials used for sludge treatment (i.e. lime, acrylonitrile and diesel for machinery operation at landfill) have been also grouped for evaluation although they have been calculated using different sources of information (see Table a1.1.1).

From Figures a1.2.4, a1.2.5 and a1.2.6, the same trends can be observed for all studied scenarios. The main environmental impact is associated, by far, to hydrogen peroxide production. This impact accountes for at least 72% of the contribution to all impacts categories in all treatments, except for aquatic eutrophication potential. When this category is studied, the highest score is related to emissions due to the nitrogen emitted during both single photo-Fenton (artificial light or solar assisted) and photo-Fenton and biological coupled treatment, as explained above. If the composition of the initial contaminant to be oxidized by means of an AOP contains nitrogen, the contribution to the aquatic eutrophication potential impact will be always present. Emissions are also important in the global warming potential category of all scenarios, mainly due to the CO_2 produced in the mineralization process. Moreover, when the chemical and biological coupled treatment (i.e. scenario 2) is studied, a 12% impact contribution in photochemical oxidation potential can be observed due to the pollutants emitted mainly at landfill.

The relatively high environmental impact score related to hydrogen peroxide, that in some cases is responsible of almost 100% of the contribution, can be explained by its production process. On the other hand, environmental impact associated to $FeSO_4$ is negligible because this chemical is a by-product of the steel and iron manufactory and hence is charged with few environmental burdens [25]. The highest score associated to the production of this chemical is reflected in the marine aquatic ecotoxicity potential impact category when photo-Fenton and biological coupled treatment is studied (i.e. 3%). Other chemicals used in photo-Fenton and biological coupled treatment, named sludge treatment materials, imply less than 1% of the impact coefficients in all the studied categories.

Another important contribution to environmental impact categories is electricity production when scenario 1 and 2 are studied. This noticeable impact is caused by the energy characteristics of the UCTE mix for electricity production, which relies in a considerable extent on fossil fuels. In scenario 1 all the electricity is used to run UVA light while in scenario 2 electricity is used for different processes. If the overall contribution of electricity is disaggregated in this scenario, it can be observed that the major contribution to all the environmental impacts is due to the electricity required to run UVA light (i.e. 66%), followed by the electricity required to sludge aeration (i.e. 28%), the electricity required at landfill (i.e. 4%), and finally the electricity required to thickening, dewatering and stabilization process (i.e. 2%).

Finally, the chemicals transport to the wastewater plant as well as the sludge transport to the landfill does not imply an important environmental impact. The highest contribution implies a 3% of photochemical oxidation potential category when solar photo-Fenton treatment is studied.

4. Conclusions

A life cycle assessment for the removal of Diuron and Linuron herbicides from water using three environmentally friendly technologies has been performed. Artificial light assisted photo-Fenton, photo-Fenton and biological coupled treatment and solar assisted photo-Fenton have been selected as wastewater treatments for this study. The environmental analysis has been done classifying impacts due to different subsystems used in each scenario and in the categories used by the CML method [24].

The main environmental impact among the different categories is associated to hydrogen peroxide production for all studied scenarios, except for aquatic eutrophication potential category. The most important environmental impact for this category is attributed to nitrogen emitted during both the single photo-Fenton (artificial light or solar assisted) and photo-Fenton/biological coupled treatment. Electricity needed to run the UVA light is the second process with a highest impact contribution to all the categories when artificial light is used in the chemical treatment.

Comparing the three technologies from an environmental point of view, it can be concluded that the artificial light assisted photo-Fenton is the less preferable process. This process is greatly improved when artificial light is substituted by solar light, eliminating all the environmental impacts related to electricity production.

Finally it can be concluded that the most environmentally friendly process for the management of wastewaters polluted with Diuron and Linuron herbicides is the coupling of photo-Fenton and biological treatments. In this treatment, environmental impact scores in all the categories are less than half of those related to the artificial light assisted photo-Fenton.

As a final remark, from the obtained results, a great environmental improvement could be expected if solar assisted photo-Fenton coupled to a biological treatment would have been applied in Diuron and Linuron removal from water.

Acknowledgments

The authors wish to thank the Spanish Government (MEC project CTQ 2005-02808) for financial support.

REFERENCES TO ANNEXE 1.2

[1] Chiron S., Fernández-Alba A., Rodríguez A. and Garcia-Calvo, E. (2000). Pesticides chemical oxidation: State of the art. Water Res. 34, 366-377.

[2] Glaze W.H. (1987). Drinking water treatment with ozone. Environ. Sci. Technol. 21, 224-230.

[3] Mills A. and Le Hunte S. (1997). An overview of semiconductor photocatalysis. J. Photochem. Photobiol. A-Chem., 108, 1-35.

[4] Bauer R. and Fallmann H. (1997). The photo-Fenton oxidation, a cheap and efficient wastewater treatment method. Res. Chem. Intermed. 23, 341-354.

[5] Haber F. and Weiss J. (1934). The catalytic decomposition of H_2O_2 by iron salts. Proc. R. Soc. Series A. 147, 332-351.

[6] Pignatello J. (1992). Dark and photoassisted Fe3+-catalyzed degradation of chlorophenoxy herbicides by hydrogen peroxide. Environ. Sci. Technol. 26, 944-951.

[7] Kotsou M., Kyriacou A., Lasaridi K. and Pilidis G. (2004). Integrated aerobic biological treatment and chemical oxidation with Fenton's reagent for the processing of green table olive wastewater. Process Biochem. 39, 1653-1660.

[8] Al Momani F., Gonzalez O., Sans C. and Esplugas S. (2004). Combining photo-Fenton process with biological sequencing batch reactor for 2,4-dichlorophenol degradation. Water Sci. Technol. 49, 293-298.

[9] Garcia-Montaño J., Torrades F., García-Hortal J.A., Doménech X. and Peral J. (2006). Degradation of Porcion Red H-E7B reactive dye by coupling a photo-Fenton system with a Sequencing batch reactor. J. Hazard. Mat.134, 220-229.

[10] Farré M.J., Domènech S. and Peral J. (2006). Assessment of photo-Fenton and biological treatment coupling for Diuron and Linuron removal from water. Water Res. 40, 2533-2540.

[11] Hospido A., Moreira M.T., Fernández-Couto M. and Feijoo G. (2004). Environmental performance of a municipal wastewater treatment plant. Int. J. Life Cycle Ass. 9, 261-271.

[12] Tixier C., Bogaerts P., Sancelme M., Bonnemoy F., Twagilimana L., Cuer A., Bohatier J. and Veschambre H. (2000). Fungal biodegradation of phenylurea herbicide, diuron: structure and toxicity of metabolites. Pest Manag Sci. 56, 455-462.

[13] ISO. (1997). Environmental Management –Life Cycle Assessment- Principles and dramework. ISO 14040, International Standardization Organism. Geneva, Switzerland.

[14] Nidjam D., Blom J. and Boere J.A. (1999). Environmental Life Cycle Assessment of two advanced wastewater treatment techniques. Stud. Surf. Sci. Catal. 12, 763-775.

[15] Muñoz I., Rieradevall J., Torrades F., Peral J. and Domènech X. (2005). Environmental assessment of different solar driven advanced oxidation processes. Sol. Energy. 79, 369-375.

[16] Muñoz I., Rieradevall J., Torrades F., Peral J. and Doménech X. (2006). Environmantal assessment of different advanced oxidation processes applied to bleaching Kraft mill effluent. Chemosphere. 62, 9-16.

[17] García-Montaño J., Ruiz N., Muñoz I., Domènech X., García-Hortal J.A., Torrades F. and Peral J. (2006). Environmental assessment of different photo-Fenton approaches for commercial reactive dye removal. J. Hazard. Mat. 138, 218-225.

[18] OECD. (1992). Inherent biodegradability modified Zahn Wellens test. Test Guideline 302B. Paris, France.

[19] APHA-AWWA-WEF (1992). Standard Methods for the examination of water and wastewater nº 5220D. (18th ed). American Public Health Association. Washington,USA.

[20] Kang I.W., Cho M.J. and Hwang K.I. (1998). Correction of hydrogen peroxide interference on standard chemical oxygen demand test. Water Res. 33, 1247-1251.

[21] Jeffery G.H., Basset J., Mendham J. and Denny R.C. (1989). Vogel´s Textbook of Quantitative Chemical Analysis. Longman. (5th ed). New York, USA.

[22] Guinée JB, Gorree M, Heijungs R, Huppes G, Kleijn R, Udo de Haes HA, Van der Voet E, Wrisberg M.N. (2002) Life Cycle Assessment. An operational guide to ISO standards. Vol 1, 2, 3. Centre of Environmental Science, Leiden University (CML), The Netherlands.

[23] Sarria V., Parra S., Adler N., Péringer P., Benítez N. and Pulgarín C. (2002). Recent developments in the coupling of photoassisted and aerobic biological processes for the treatment of biorecalcitrant compounds. Catal. Today. 76, 301-315.

[24] Ecoinvent www.ecoinvent.ch. Program SIMAPRO 7.0 database, (2006).

[25] Jungbluth N. (2006). Sachbilanzen von Energiesystemen: Grundlagen für den ökologischen Vergleich von Energiesystemen und den Einbezug von Energiesystemen in Ökobilanzen für die Schweiz, Dones R. (ed), Final report ecoinvent 2000 No. 6, Paul Scherrer Institut Villigen, Swiss Centre for Life Cycle Inventories., Duebendorf, Germany.

[26] Althaus H.-J., Chudacoff M., Hischier R., Jungbluth N., Primas A. and Osses M. (2004). Life Cycle Inventories of Chemicals. Final report ecoinvent 2000 No. 8, Swiss Centre for Life Cycle Inventories., Duebendorf, Germany.

[27] Hischier R. (2004). Life cycle inventories of packaging and graphical paper. Final report ecoinvent 2000. Volume: 11. Swiss Centre for LCI, EMPA-SG., Dübendorf, Germany.

[28] Kellenberger D., Althaus H.-J. and Jungbluth N. (2004). Life cycle inventories of building products. Final report ecoinvent 2000 No. 7, Swiss Centre for Life Cycle Inventories., Duebendorf, Germany.

[29] Habersatter K. (1996). Ökoinventare für Verpackungen. Bundesamt Für Umwelt, Wald, Und Landschaft (BUWAL). Schriftenreihe Umwelt 250. Bern, Germany.

[30] Spielmann M., Kägi T. and Tietje O. (2004). Life cycle inventories of transport services. Final report ecoinvent 2000 No. 14, Swiss Centre for Life Cycle Inventories., Duebendorf, Germany.

[31] Frischknecht R. and Faist Emmenegger M. (2003). Strommix und Stromnetz. Sachbilanzen von Energiesystemen. Final report No. 6 ecoinvent 2000. Dones R. (ed), Swiss Centre for LCI, PSI., Dübendorf and Villigen, Germany.

[32] Jiménez-González C., Overcash R.M. and Curzons A. (2001). Waste treatment modules – a partial life cycle inventory. J. Chem. Technol. Biot. 70, 707-716.

[33] Metcalf and Eddy, Inc. (1991) Wastewater Engineering: Treatment, Disposal and Reuse. Metcalf-Eddy (Ed) McGraw-Hill Inc. (3 ed). New York, USA.

[34] Tchobanoglous G., Theisen H. and Vigil S. (1993). Integrated solid waste management: Engineering principles and management issues. Macgraw Hill. New York, USA.

[35] Suh Y.J. and Rosseaux P. (2002). An LCA of alternative wastewater sludge treatment scenarios. Resour. Conserv. Recy. 35, 191-200.

[36] Mingarini K. (1996). Systems Analysis of Organic waste with Emphasis on Modelling of the Incineration and the Landfilling Process. Licentiate Thesis. Dept. of Environmental Technology and Work Science. Stockholm, Sweden.

[37] Dalemo M. (1997). The ORWARE simulation model. Anaerobic digestion and sewage plant sub-models. Licenthiate thesis. Swedish Institute of Agricultural Engineering, Swedish University of Agricultural Sciences. Uppsala, Sweden.

[38] Domènech X., Rieradevall J. and Fullana P. (1997). Application of Life Cycle Assessment to Landfilling. Int. J. Life Cycle Ass. 2, 141-144.

[39] Nielsen P. and Hauschild, M. (1998) Product specific emissions from municipal solid waste landfills. Part I: Landfill model. Int. J. Life Cycle Ass. 3, 158-168.

[40] Bez J., Goldhan G. and Heyde M. (1998). Waste treatment in product specific life cycle inventories. An approach of material-related modelling. Part II: Sanitary Landfill. Int. J. Life Cycle Ass. 3, 100-105.

ANNEXE 2

ADDITIONAL INFORMATION

a2.1. Experimental design

The following figures show the main effects and interaction effects of variables Fe^{2+} and H_2O_2 optimized as well as scaled and unscaled coefficients obtained by means of multivariate experimental design. ANOVA results also are included in this annexe. See chapter 2, section 3 for experimental details

Main effects

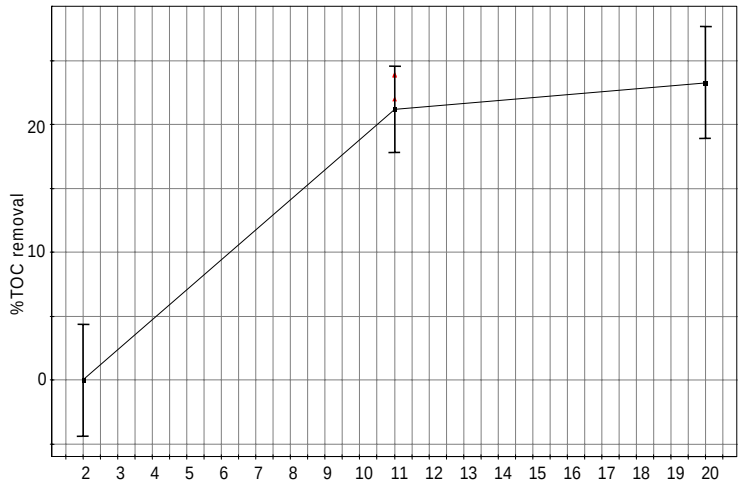

Figure a2.1. Main effect of iron to the experimental design

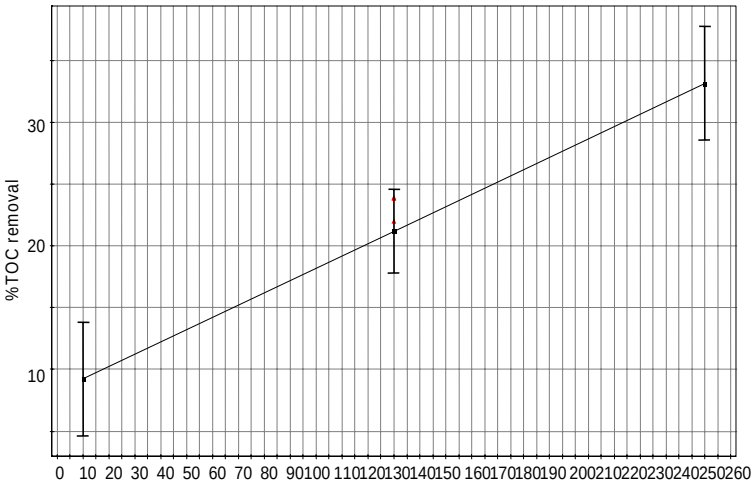

Figure a2.2. Main effect of hydrogen peroxide to the experimental design

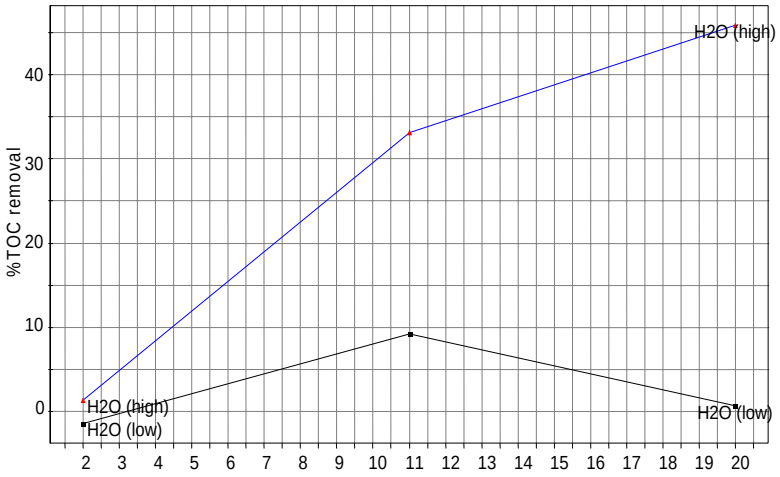

Figure a2.3. Main effect of interaction of iron with hydrogen peroxide to the experimental design

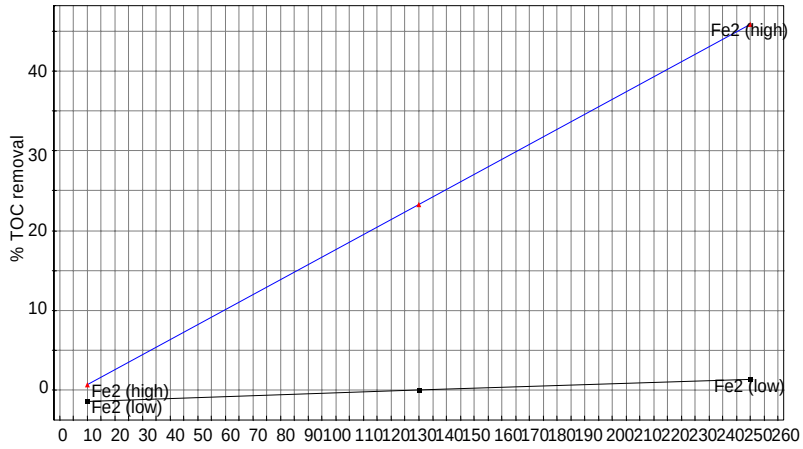

Figure a2.4. Main effect of interaction of hydrogen peroxide with iron to the experimental design

Coefficients

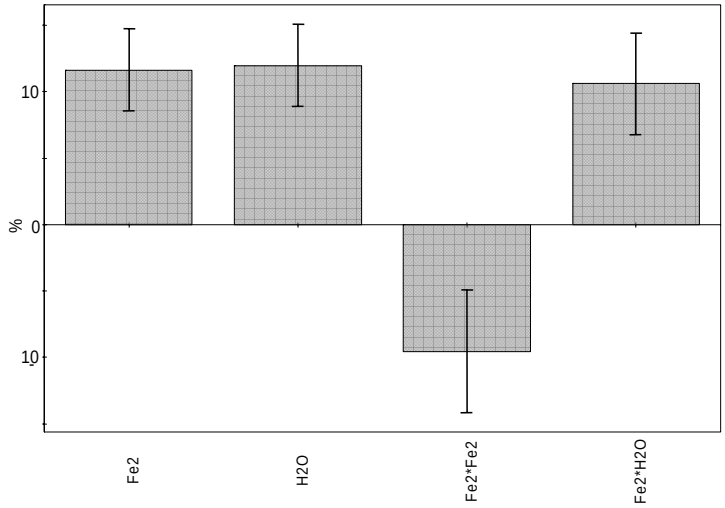

Figure a2.5. Centred and scaled coefficients to the experimental design

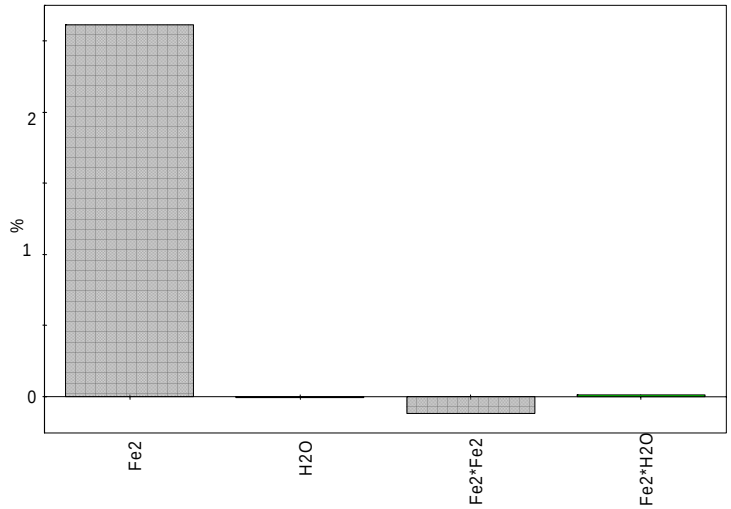

Figure a2.6. Centred and unscaled coefficients to the experimental design

ANOVA results

Table a2.1. ANOVA results for the experimental design

%TOC removal	DF	SS	MS (variance)	F	p	SD
Total	11	5234,95	475,904			
Constant	1	2808,64	2808,64			
Total Corrected	10	2426,3	242,63			15,5766
Regression	4	2368,38	592,094	61,329	0	24,333
Residual	6	57,9264	9,6544			3,10715
Lack of Fit (Model Error)	4	55,4413	13,8603	11,1549	0,084	3,72295
Pure Error (Replicate Error)	2	2,48506	1,24253			1,11469

N = 11	Q2 = 0,905	Cond. no. =2,7386
DF = 6	R2 =0,976	Y-miss =0
	R2 Adj. =0,96	RSD =3,1072

a2.2. Chromatographs and MS spectra

UPLC-MS

The following figures show the chromatogram as well as spectra obtained by means of UPLC-MS. See chapter 2, section 5.1.6.2. for experimental details.

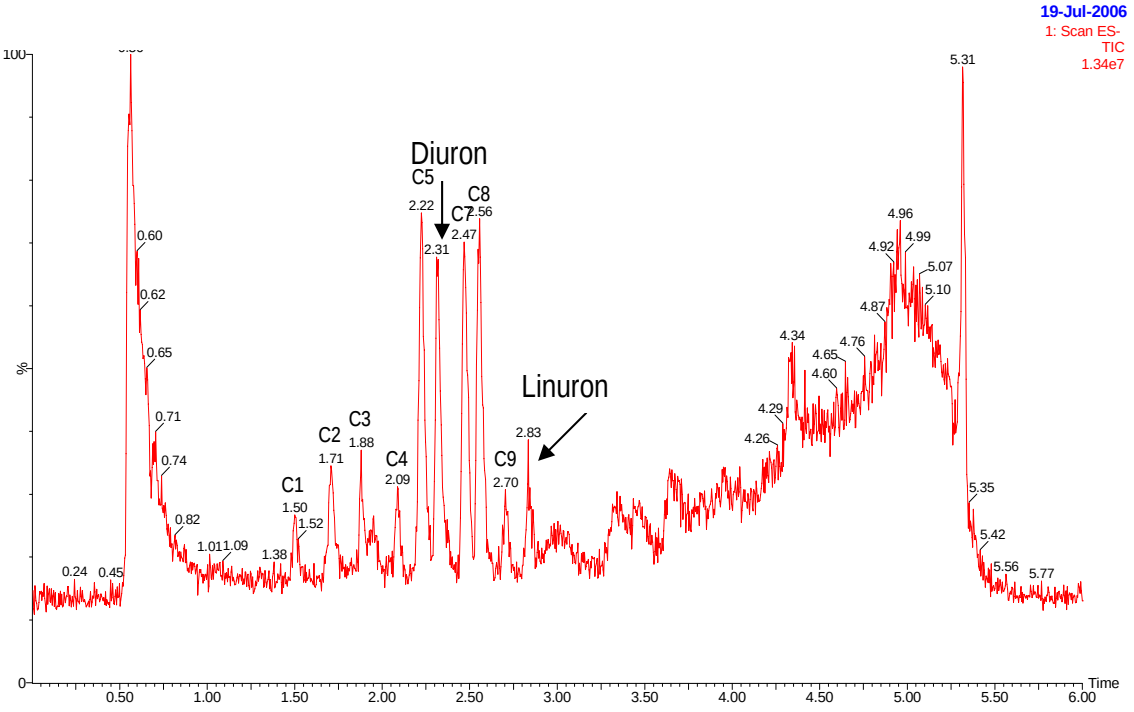

Figure a2.7. UPLC chromatogram corresponding to 15 minutes of an experiment of photo-Fenton with reactant dose [Fe(II)]=9.25 mg·L^{-1} and [H_2O_2]=97.1 mg·L^{-1}

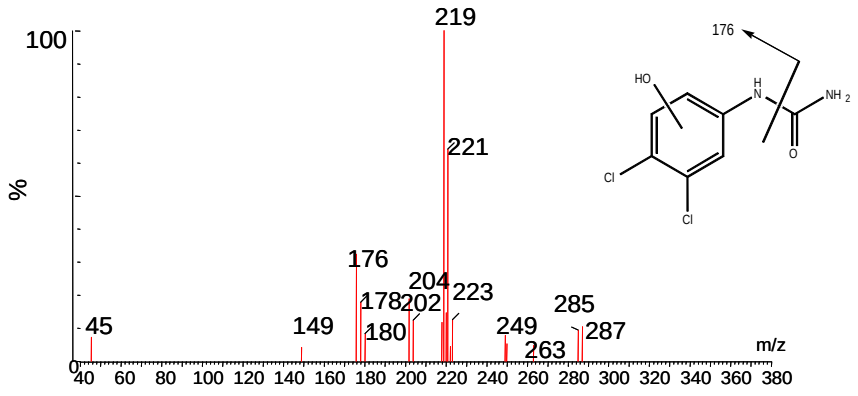

Figure a2.8. ESI-MS spectrum of compound 1obtained at 25 V and corresponding to 15 minutes of an experiment of photo-Fenton with reactant dose [Fe(II)]=9.25 mg·L^{-1} and [H_2O_2]=97.1 mg·L^{-1}.

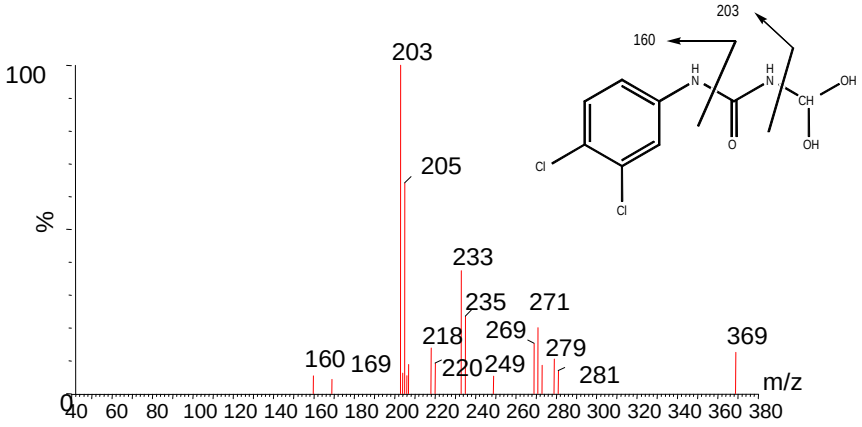

Figure a2.9. LC-ESI-MS spectrum of compound 2 obtained at 25 V and corresponding to 15 minutes of an experiment of photo-Fenton with reactant dose [Fe(II)]=9.25 mg·L^{-1} and [H_2O_2]=97.1 mg·L^{-1}.

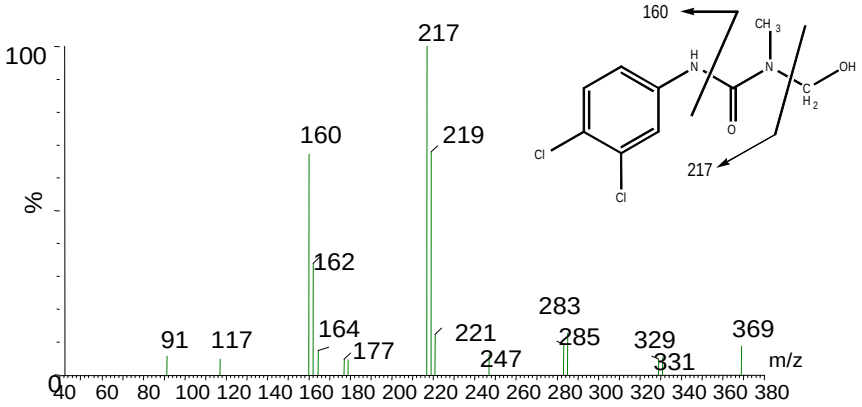

Figure a2.10. LC-ESI-MS spectrum of compound 3 obtained at 25 V and corresponding to 15 minutes of an experiment of photo-Fenton with reactant dose [Fe(II)]=9.25 mg·L^{-1} and [H_2O_2]=97.1 mg·L^{-1}.

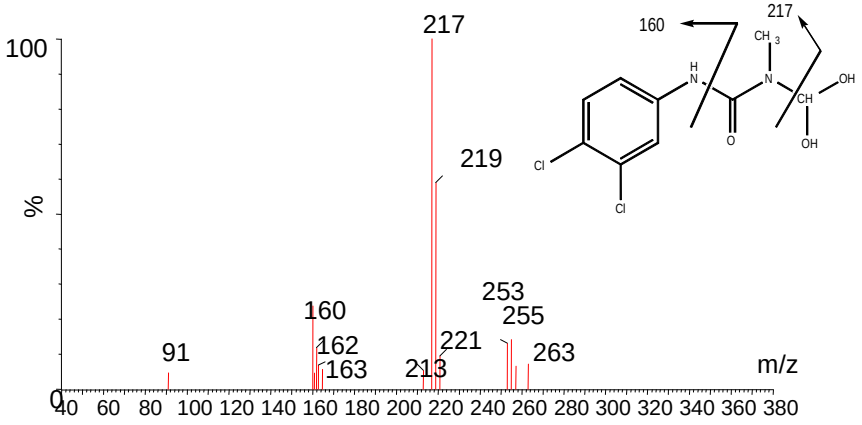

Figure a2.11. LC-ESI-MS spectrum of compound 4 obtained at 25 V and corresponding to 15 minutes of an experiment of photo-Fenton with reactant dose [Fe(II)]=9.25 mg·L^{-1} and [H_2O_2]=97.1 mg·L^{-1}.

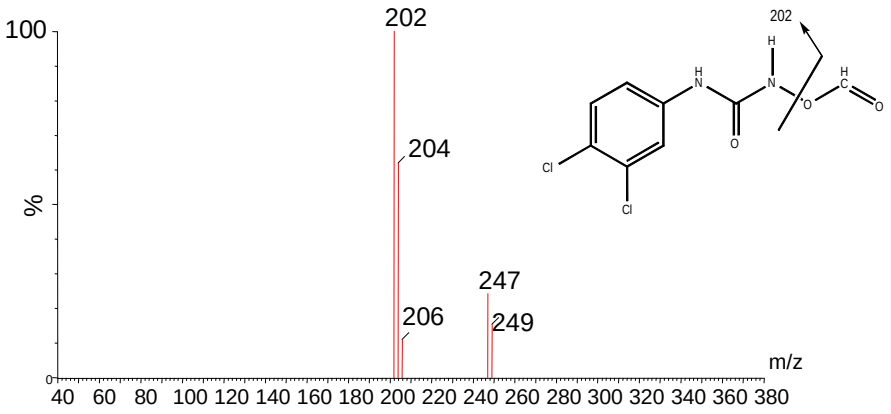

Figure a2.13. LC-ESI-MS spectrum of compound 5 obtained at 25 V and corresponding to 15 minutes of an experiment of photo-Fenton with reactant dose [Fe(II)]=9.25 mg·L^{-1} and [H_2O_2]=97.1 mg·L^{-1}.

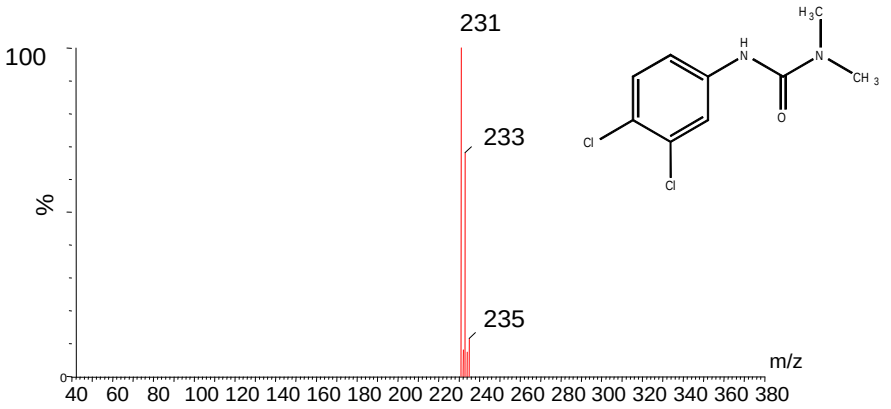

Figure a2.14. LC-ESI-MS spectrum of compound 6 obtained at 25 V and corresponding to 15 minutes of an experiment of photo-Fenton with reactant dose [Fe(II)]=9.25 mg·L^{-1} and [H_2O_2]=97.1 mg·L^{-1}.

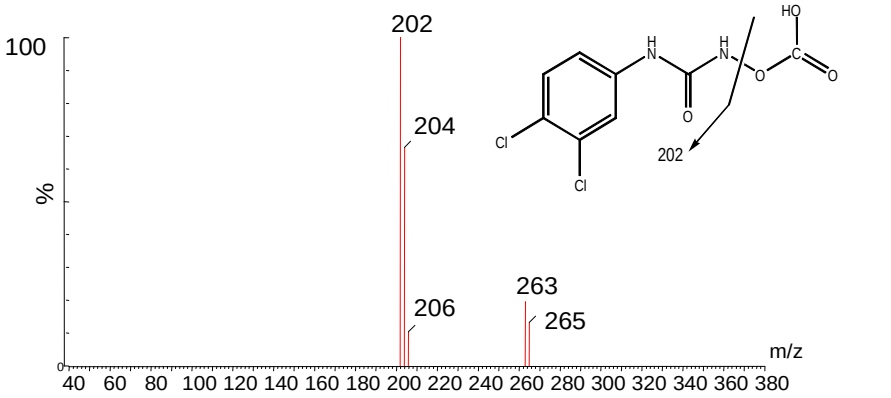

Figure a2.15. LC-ESI-MS spectrum of compound 7 and 8 obtained at 25 V and corresponding to 15 minutes of an experiment of photo-Fenton with reactant dose [Fe(II)]=9.25 mg·L^{-1} and [H_2O_2]=97.1 mg·L^{-1}.

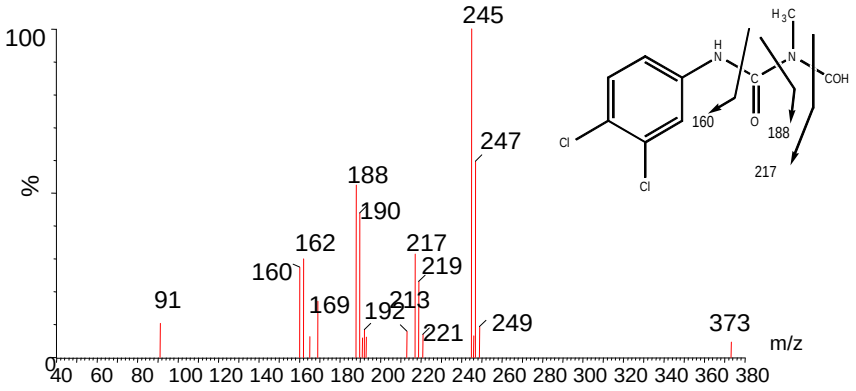

Figure a2.16. LC-ESI-MS spectrum of compound 9 obtained at 25 V and corresponding to 15 minutes of an experiment of photo-Fenton with reactant dose [Fe(II)]=9.25 mg·L^{-1} and [H_2O_2]=97.1 mg·L^{-1}.

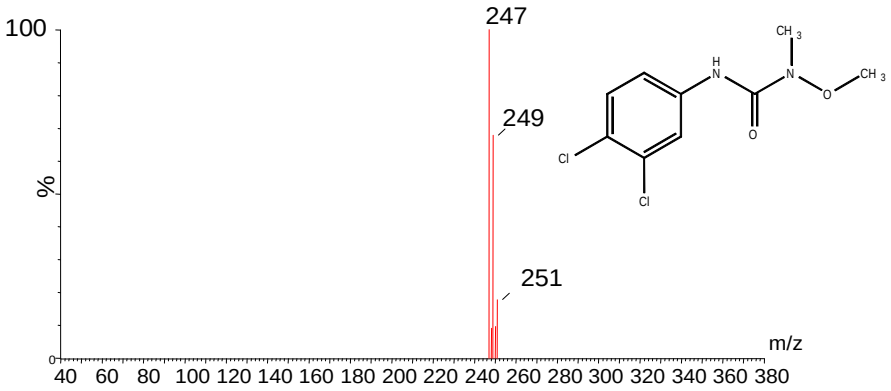

Figure a2.17. LC-ESI-MS spectrum of compound 10 obtained at 25 V and corresponding to 15 minutes of an experiment of photo-Fenton with reactant dose [Fe(II)]=9.25 mg·L^{-1} and [H_2O_2]=97.1 mg·L^{-1}.

HILIC-MS

The following figures show the chromatograms as well as spectra obtained by means of HILIC-MS. See chapter 2, section 5.1.6.3. for experimental details

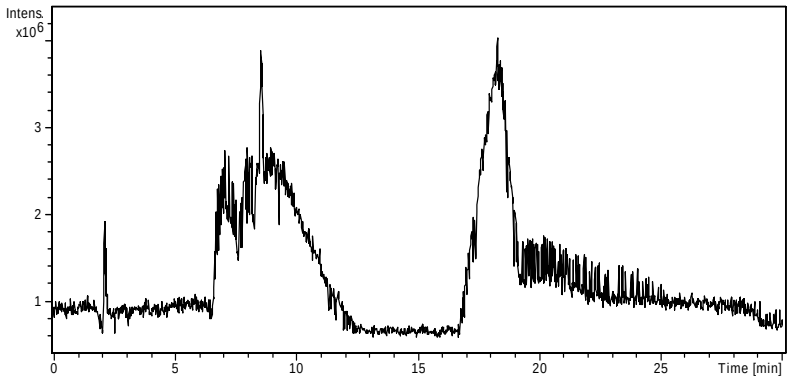

Figure a2.18. HILIC chromatogram in scan mode obtained at 5000 V and corresponding to 60 minutes of an experiment of photo-Fenton with reactant dose [Fe(II)]=9.25 mg·L^{-1} and [H_2O_2]=97.1 mg·L^{-1}

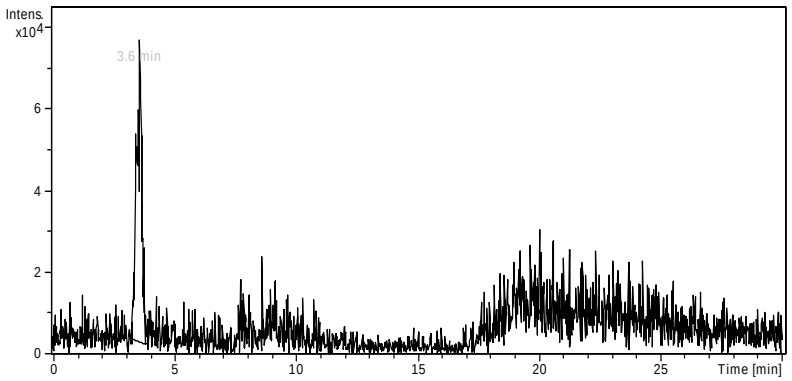

Figure a2.19. Spectrum ion chromatograph of ion m/z= 75 corresponding to 60 minutes of an experiment of photo-Fenton with reactant dose [Fe(II)]=9.25 mg·L^{-1} and [H_2O_2]=97.1 mg·L^{-1}

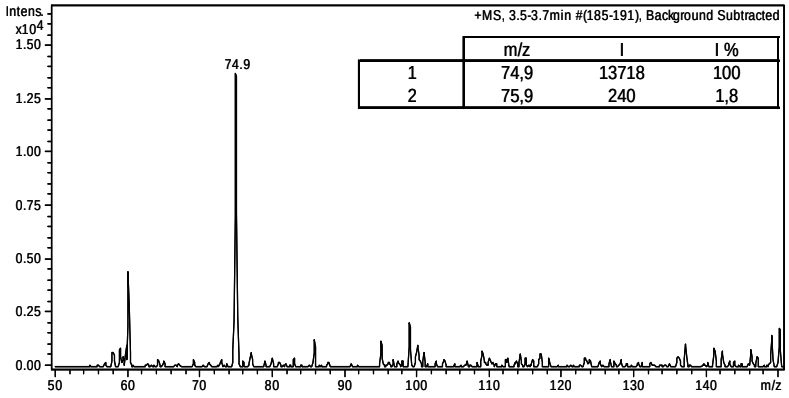

Figure a2.20. Mass spectrum and isotopic distribution of ion m/z=75

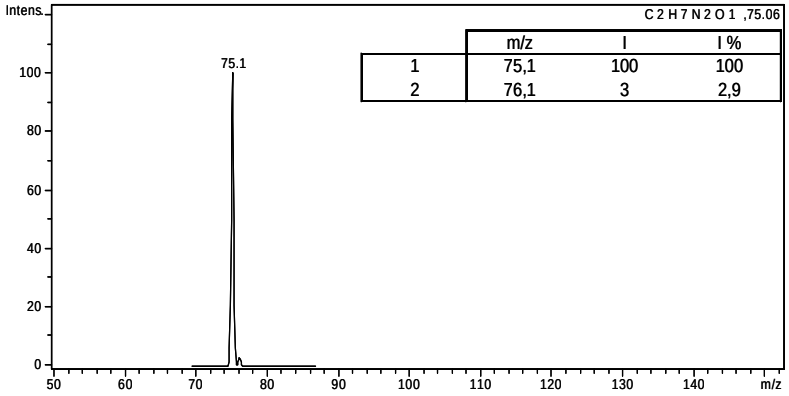

Figure a2.21. Methyllurea theoretical mass spectrum and isotopic distribution

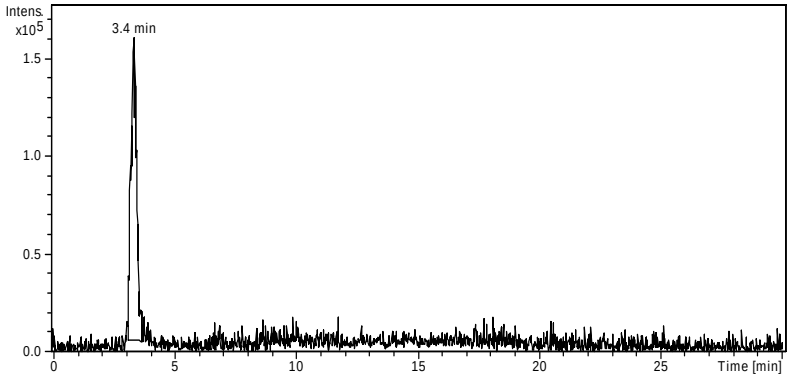

Figure a2.22. Spectrum ion chromatograph of ion m/z= 89 corresponding to 60 minutes of an experiment of photo-Fenton with reactant dose [Fe(II)]=9.25 mg·L^{-1} and [H_2O_2]=97.1 mg·L^{-1}

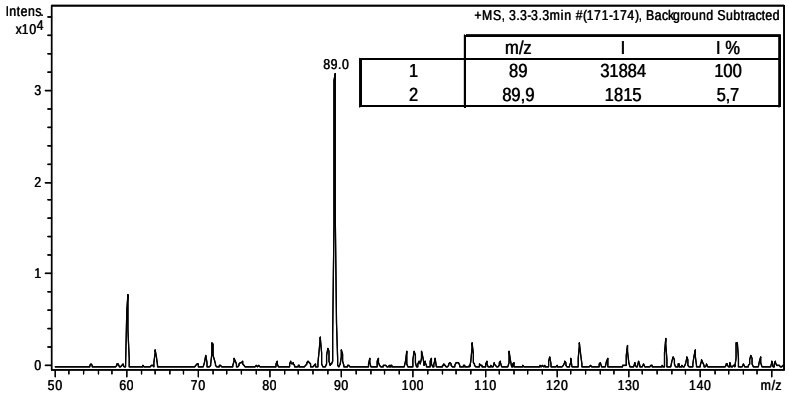

Figure a2.23. Mass spectrum and isotopic distribution of ion m/z=89

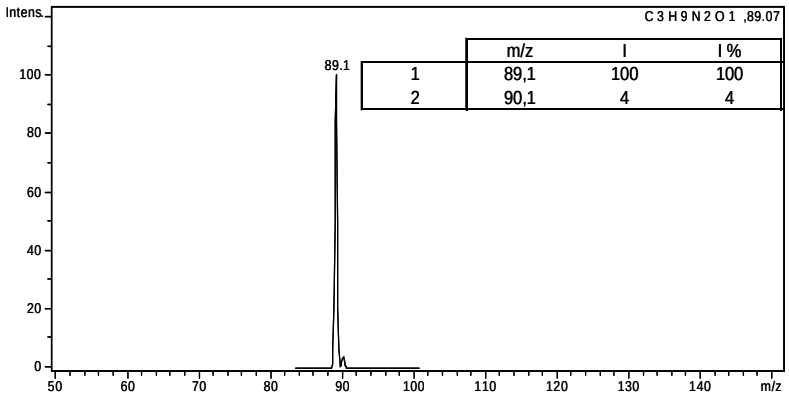

Figure a2.24. N-N´dimethyllurea theoretical mass spectrum and isotopic distribution

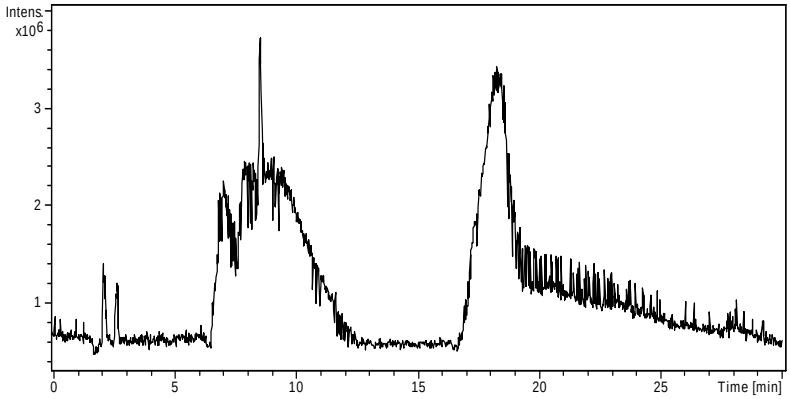

Figure a2.25. HILIC chromatogram in scan mode obtained at 5000 V and corresponding to 60 minutes of an experiment of photo-Fenton with reactant dose [Fe(II)]=9.25 mg·L^{-1} and [H_2O_2]=97.1 mg·L^{-1} and N,N´dimethylurea.

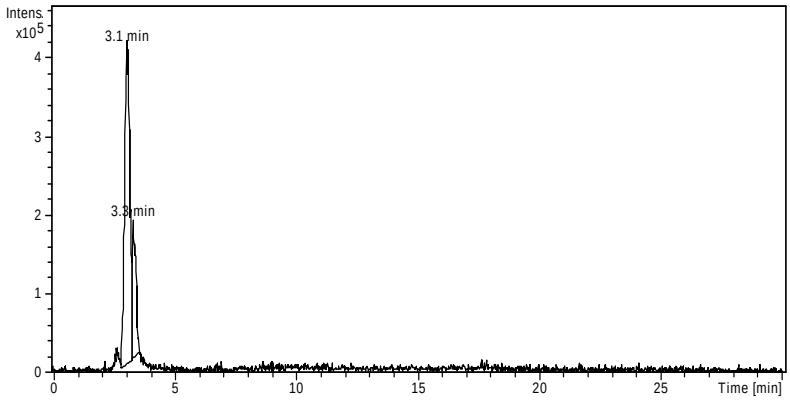

Figure a2.26. Spectrum ion chromatograph of ion m/z= 89 corresponding to 60 minutes of an experiment of photo-Fenton with reactant dose [Fe(II)]=9.25 mg·L^{-1} and [H_2O_2]=97.1 mg·L^{-1} and N,N´dimethylurea.

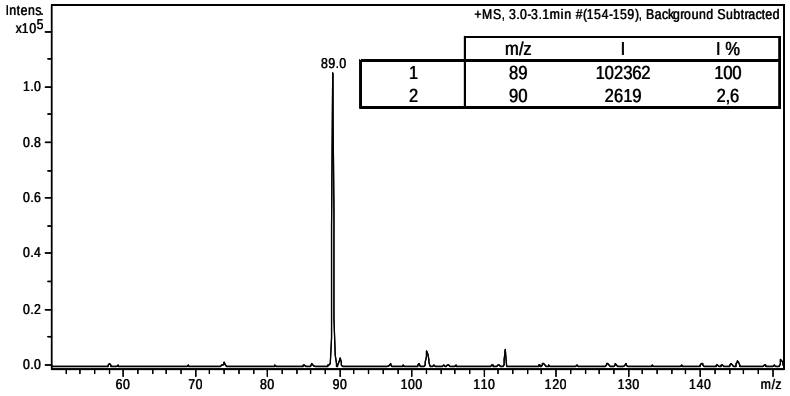

Figure a2.27. Mass spectrum and isotopic distribution of ion m/z=89 at retention time 3.1 min.

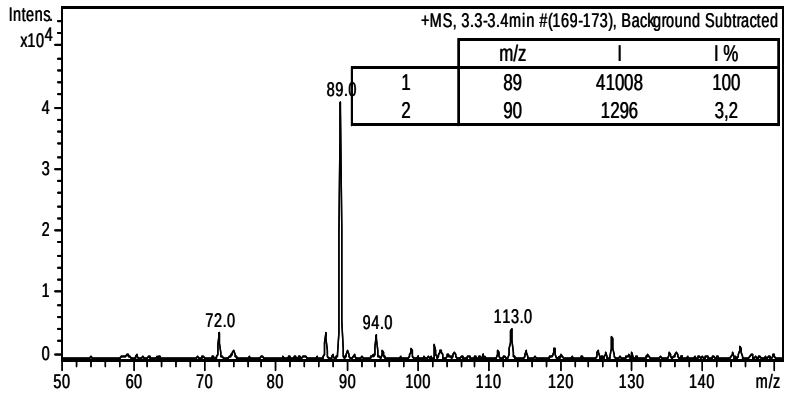

Figure a2.28. Mass spectrum and isotopic distribution of ion m/z=89 at retention time 3.4 min.

GS-MS

The following figures show the chromatogram as well as spectra obtained by means of GS-MS. See chapter 2, section 5.1.6.4. for experimental details.

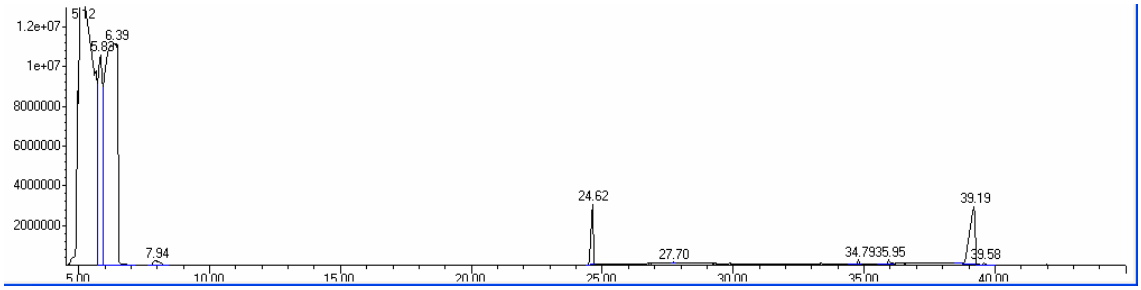

Figure a2.29. GS chromatogram in scan mode obtained at 70 eV and corresponding to 15 minutes of an Experiment of photo-Fenton with reactant dose [Fe(II)]=15.9 mg·L^{-1} and [H_2O_2]=202 mg·L^{-1}

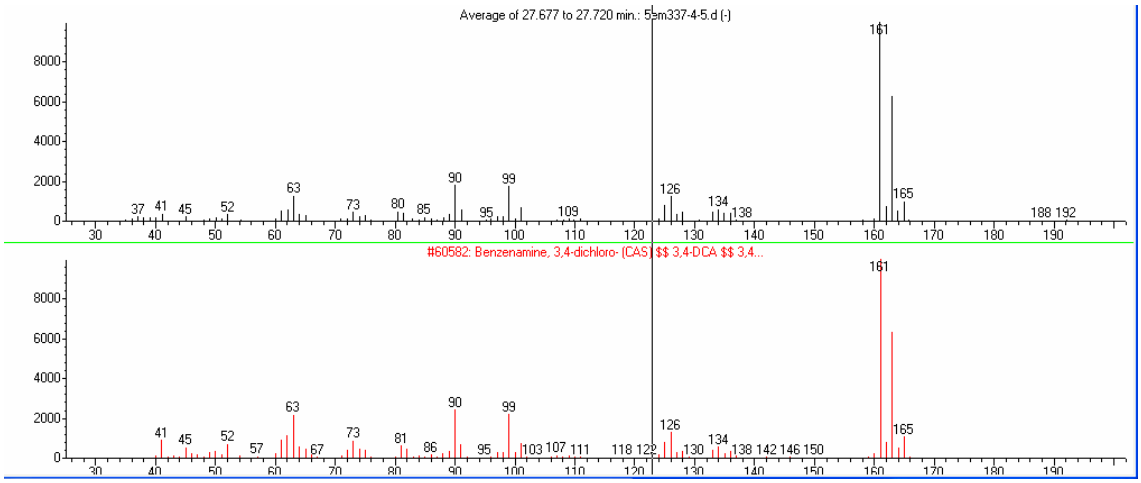

Figure a2.30. Empirical and theoretical MS spectra of peak at 27.7 min corresponding to 3,4- dichloroaniline

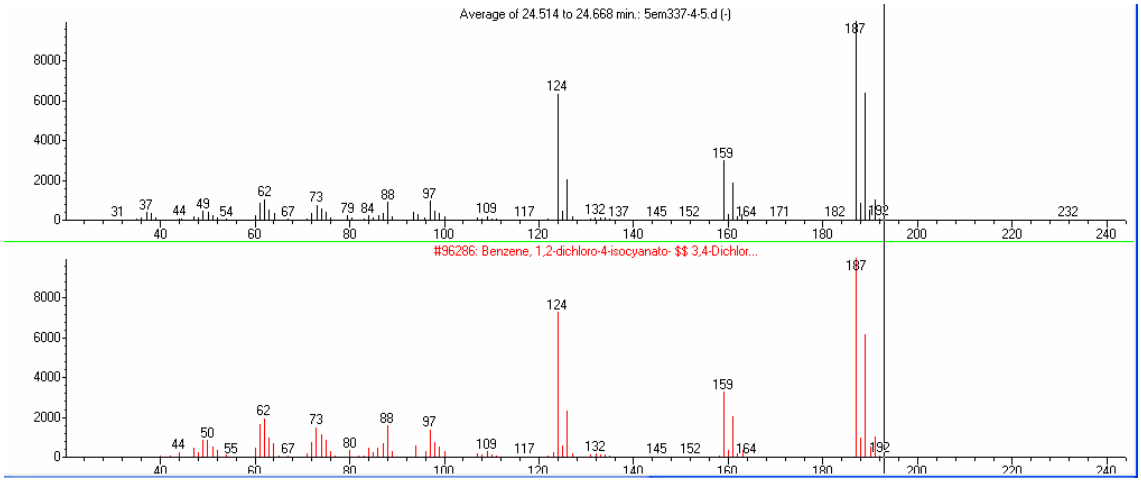

Figure a2.31. Empirical and theoretical MS spectra of peak at 24.4 min corresponding to 3,4- dichlorophenyl isocianate

a2.3. Life Cycle Impact Assessment tables

The following tables show the characterisation results for each alternative disaggregated by sub-systems.

Table a2.2. Characterisation results for artificial light assisted photo-Fenton.

Impact categories	Units	iron	hydrogen peroxide	emissions	electricity, medium voltage	transport
ARD	kg Sb eq	5,81E-08	9,58E-06	0	1,71E-06	1,39E-07
GWP	kg CO_2 eq	8,19E-06	0,00116	0,000191	0,000237	2,02E-05
ODP	kg CFC-11 eq	3,77E-13	1,07E-10	0	9,80E-12	2,68E-12
HTTP	kg 1,4-D* eq	9,87E-06	0,00379	0	5,27E-05	5,36E-06
FATP	kg 1,4-D* eq	1,99E-06	0,000253	0	1,38E-05	1,18E-06
MAEP	kg 1,4-D* eq	0,00644	0,456	0	0,156	2,75E-03
TEP	kg 1,4-D* eq	5,64E-08	8,07E-06	0	1,08E-06	3,74E-08
POP	kg C_2H_4 eq	2,01E-09	1,75E-07	0	5,10E-08	5,52E-09
AP	kg SO_2 eq	4,61E-08	3,91E-06	0	1,29E-06	1,10E-07
AEP	kg PO_4^{3-} eq	2,96E-09	3,72E-07	4,84E-06	6,25E-08	2,20E-08

*1,4-Dichlorobenzene

Table a2.3. Characterisation results for artificial light assisted photo-Fenton coupled to biological treatment.

Impact categories	Units	iron	hydrogen peroxide	emissions	electricity, medium voltage	transport	sludge treatment materials
ARD	kg Sb eq	5,81E-08	4,66E-06	0	3,07E-07	8,27E-08	1,09E-08
GWP	kg CO_2 eq	8,19E-06	0,000566	1,64E-04	4,25E-05	1,19E-06	3,71E-06
ODP	kg CFC-11 eq	3,77E-13	5,22E-11	0,00E+00	1,76E-12	1,58E-12	6,03E-13
HTTP	kg 1,4-D* eq	9,87E-06	0,00185	9,28E-08	9,48E-06	3,16E-06	1,90E-07
FATP	kg 1,4-D* eq	1,99E-06	0,000123	0	2,48E-06	6,95E-07	2,96E-08
MAEP	kg 1,4-D* eq	0,00644	0,222	0	0,02811	1,62E-03	9,53E-05
TEP	kg 1,4-D* eq	5,64E-08	3,93E-06	0	1,94E-07	2,21E-08	1,23E-09
POP	kg C_2H_4 eq	2,01E-09	8,54E-08	1,38E-08	9,17E-09	3,27E-09	6,62E-10
AP	kg SO_2 eq	4,61E-08	1,90E-06	4,82E-08	2,32E-07	6,53E-08	8,01E-09
AEP	kg PO_4^{3-} eq	2,96E-09	1,81E-07	4,72E-06	1,12E-08	1,30E-08	1,41E-09

*1,4-Dichlorobenzene

Table a2.4. Characterisation results for solar light assisted photo-Fenton

Impact categories	Units	iron	hydrogen peroxide	emissions	transport
ARD	kg Sb eq	5,81E-08	9,58E-06	0	1,39E-07
GWP	kg CO_2 eq	8,19E-06	0,00116	0,000191	2,02E-05
ODP	kg CFC-11 eq	3,77E-13	1,07E-10	0	2,68E-12
HTTP	kg 1,4-D* eq	9,87E-06	0,00379	0	5,36E-06
FATP	kg 1,4-D* eq	1,99E-06	0,000253	0	1,18E-06
MAEP	kg 1,4-D* eq	0,00644	0,456	0	2,75E-03
TEP	kg 1,4-D* eq	5,64E-08	8,07E-06	0	3,74E-08
POP	kg C_2H_4 eq	2,01E-09	1,75E-07	0	5,52E-09
AP	kg SO_2 eq	4,61E-08	3,91E-06	0	1,10E-07
AEP	kg PO_4^{3-} eq	2,96E-09	3,72E-07	4,84E-06	2,20E-08

* 1,4-Dichlorobenzene

Curriculum Vitae

Mª José Farré Olalla
Sabadell
☎ +34665607207
mariajose@klingon.uab.es
Fecha de nacimiento 3/6/1980

-FORMACIÓN ACADÉMICA REGLADA:

- 2003 - 2007. Doctora por la UAB en el Departamento de Química, area de conocimiento Química-Física. Tesis: "*Combination of Advanced Oxidation Processes with biological treatment for the remediation of water polluted with herbicides*".

- 2005. Diploma de Estudios Avanzados en Química, Universidad Autónoma de Barcelona. Tesina: "*Degradación y aumento de la biodegradabilidad de aguas contaminadas con herbicidas a través de Procesos Avanzados de Oxidación".*

- 2003 - 2004.Cursos de doctorado realizados, programa de doctorado en Química, Universidad Autónoma de Barcelona.
  - *Estaciones depuradoras de aguas residuales (EDAR)*
  - *Tratamiento biológico de aguas industriales*
  - *Fotoquímica avanzada*
  - *Ampliación de análisis instrumental y técnicas cromatográficas*
  - *Química de la contaminación*
  - *Membranas en procesos de separación*
  - *Riesgo en el laboratorio químico*

- 1998 - 2003. Licenciada en Química, Universidad Autónoma de Barcelona.

-IDIOMAS Y OTROS CONOCIMIENTOS:

- Catalán y castellano: lenguas maternas, uso habitual y cursado en la enseñanza reglada.

- Inglés: nivel bueno escrito, hablado y traducido.

- Ofimática: Usuaria avanzada de Internet, Word, Excel, Adobe Acrobat, Power Point, Modde 5.0, SimaPro 7.0…

-EXPERIÉNCIA LABORAL:

- 2006 - 2007. Profesora Ayudante en el Departamento de Química de la Universidad Autónoma de Barcelona. Área de Conocimiento: Química Física.

- 2005 - 2006. Profesora Asociada A4, 6. en el Departamento de Química de la Universidad Autónoma de Barcelona. Área de Conocimiento: Química Física.

- 2004 - 2005. Profesora Asociada A3, 6. en el Departamento de Química de la Universidad Autónoma de Barcelona. Área de Conocimiento: Química Física.

Docencia impartida:

- Licenciatura de Biología: 1er ciclo. Practicas de Química.
- Licenciatura de Química: 1er ciclo. Operaciones Básicas.
- Licenciatura de Ciencias Ambientales: 1er ciclo. Termodinámica y Cinética
- Licenciatura de Ingeniería Química: 1er ciclo. Experimentación Química.
- Licenciatura de Química: 2ndo ciclo. Laboratorio de Química Física.
- Licenciatura de Química: 1er ciclo. Laboratorio Integrado III.
- Licenciatura de Química: 1er ciclo. Estructura Atómica y Enlace.
- Licenciatura de Ciencias Ambientales: Técnicas Experimentales en Química.

- 2002. Realización de prácticas en empresa en la compañía KAO corporation S.A en funciones de formulación y evaluación de productos suavizantes y de higiene domestica.

-PARTICIPACIÓN EN PROYECTOS DE I+D:

- 2003 - 2004. Colaboradora del proyecto CADOX A coupled Advanced Oxidation-Biological Process for Recycling of Industrial Wastewater Containing Persistent Organic Contaminants con la Universidad Autónoma de Barcelona. www.psa.es/webeng/projects/cadox/ financiado por la Unión Europea.

- 2005- 2007. Colaboradora del proyecto Estudios de evolución y mejoría de los sistemas de tratamiento de aguas biorecalcitrantes basados en el acoplamineto de Procesos Avanzados de Oxidación y etapas biológicas. Financiado por el Ministerio de Educación y Ciencia dentro del Programa Nacional de Ciencias y Tecnologías Químicas.

-OTROS MÉRITOS PROFESIONALES:

- Acreditación otorgada por la Agència per la Qualitat del Sistema Universitari de Catalunya (AQU) para la contratación como Profesor Lector y Colaborador. num. expediente U1444/3806842-26

- Junio 2006 - agosto 2006. Estancia de investigación en el grupo de procesos de la Ecole Nationale Supérieure de Chimie de Rennes (Francia) bajo la supervisión del Dr. Stephan Brosillon.

- Octubre 2002 - marzo 2003. Finalización de la licenciatura con una beca erasmus disfrutada en el grupo de investigación de Procesos y Materiales Catalíticos en la facultad de ingeniería química en la Universidad de Twente (Holanda)

-PUBLICACIONES:

- Maria José Farré, Stephan Brosillon, Xavier Domènech and José Peral. Evaluation of the intermediates generated during the degradation of Diuron and Linuron herbicides by the photo-Fenton reaction. Aceptado para publicar en la revista *Photochemistry and Photobiology A: Chemistry.*

- Maria José Farré, Julia García-Montaño, Nilbia Ruiz, Ivan Muñoz, Xavier Doménech and José Peral. Life cycle assessment of the removal of Diuron and Linuron herbicides from water using three environmentally friendly Technologies. Aceptado para publicar en la revista *Environmental Technology.*

- Maria José Farré, Xavier Domènech and José Peral. Combined photo-Fenton and biological treatment for Diuron and Linuron removal from water containing humic acid. En prensa en la revista *Journal of Hazardous Materials*.

- Maria José Farré, Xavier Doménech and José Peral. Assessment of the coupling of photo-Fenton and biological treatment for Diuron and Linuron removal from water. *Water Research* (2006) 40, 2533-2540.

- Maria José Farré, Maria Isabel Franch, José Antonio Ayllón, José Peral and Xavier Doménech. Biodegradability of treated aqueous solutions of biorecalcitrant pesticide by means of photocatalytic ozonation. *Desalination* (2006) 211, 22-33.

- Maria José Farré, Maria Isabel Franch, Sixto Malato, José Antonio Ayllón, José Peral and Xavier Doménech. Degradation of some biorecalcitrant pesticides by Homogeneous and Heterogeneous Photocatalytic Ozonation. *Chemosphere* (2005) 58, 1127-1133.

-CONTRIBUCIONES A CONGRESOS:

- Maria José Farré, José Peral and Xavier Doménech. Assessment of the coupled photo-Fenton and biological treatment for Diuron and Linuron removal from water in the presence and absence of humic acid. *SPEA 4* (4rth European chemistry on solar Chemistry and photocatalysis: Environmental applications) (Las Palmas de Gran Canaria. 8, 9 y 10 Noviembre 2006).Comunicación en cartel.

- Maria José Farré, Maria Isabel Franch, José Antonio Ayllón, José Peral and Xavier Doménech. Degradation and biodegradability enhancement of phenylurea pesticides by homogeneous photocatalytic ozonation. *ChemPor 2005* (9th International Chemical Engineering Conference) (Coimbra. 21-23 setiembre 2005). Comunicación en cartel y artículo para el libro de resúmenes.

- Maria José Farré, Maria Isabel Franch, Sixto Malato, José Antonio Ayllón, José Peral and Xavier Doménech. Degradation of some biorecalcitrant pesticides by Homogeneous and Heterogeneous Photocatalytic Ozonation. *SPEA 3* (3rd European chemistry on solar Chemistry and photocatalysis: Environmental applications) (Barcelona. 30 Junio, 1-2, Julio 2004). Comunicación en cartel.
